CANKIRI KARATEKIN UNIVERSITY
GRADUATE SCHOOL OF NATURAL AND APPLIED SCIENCE

PhD THESIS

COMPARING SOIL THERMAL PROPERTIES UNDER DIFFERENT PLANT CANOPIES

Ahmet Sami EROL

FOREST ENGINEERING DEPARTMENT

CANKIRI
2016

TEZ ONAYI

Ahmet Sami EROL tarafından hazırlanan **"Comparing Soil Thermal Properties Under Different Plant Canopies *(Farklı Bitki Örtüleri Altında Toprak Termal Özelliklerinin Karşılaştırılması)*"** adlı tez çalışması 09/05/2016 tarihinde aşağıdaki jüri tarafından oy birliği ile Çankırı Karatekin Üniversitesi Fen Bilimleri Enstitüsü Orman Mühendisliği Anabilim Dalında **DOKTORA TEZİ** olarak kabul edilmiştir.

Danışman : **Prof. Dr. Sabit ERŞAHİN**

Jüri Üyeleri :

Başkan: Prof. Dr. Sabit ERŞAHİN

Üye: Prof. Dr. Evgeny SHEIN

Üye: Prof. Dr. Hasan Sabri ÖZTÜRK

Üye: Doç. Dr. Fariz MİKAİLSOY

Üye: Yrd. Doç. Dr. Gülay KARAHAN

Yukarıdaki sonucu onaylarım

Prof. Dr. Sezgin ÖZDEN

Enstitü Müdürü

09/05/2016

Kontrol edilmiştir.

Yunus Tuğberk SANALP

Bilgisayar İşletmeni

ABSTRACT

PhD THESIS

COMPARING SOIL THERMAL PROPERTIES UNDER DIFFERENT PLANT CANOPIES

Ahmet Sami EROL

Cankırı Karatekin University

Graduate School of Natural and Applied Sciences

Department of Forest Engineering

Supervisor: Prof. Dr. Sabit ERŞAHİN

Soil thermal properties have a significant control on soil processes and plant growth. This study was conducted to model diurnal and seasonal change of soil temperature in soil profiles under corn, sugar beets, and no crops in Kumar township of Konya (Dry-subhumid/Semiarid Continental Central Anatolian climate). Soil temperature was modeled at 0, 5, 10, 20, 30, 40, and 60 cm soil depths with layer, point1, and point2 methods. Point1 and point2 methods gave similar results compared to that given by layer method and one point1 and point2 methods outperformed layer method in all the cases. The layer method over predicted soil temperature in majority of the cases. The success of all three methods to predict soil temperature decreased consistently with depth. This decrease was more drastic beyond duping depth. Diurnal and seasonal soil temperature changes across the soil depths under corn were highly different from those of sugar beets and bare soils. Irrigation had a drastic influence on soil heat diffusivity and diurnal change of soil temperature in studied soil depths. The results suggested that that analytical solution and initial conditions used in models were important factors determining the performance of modeling. In this regard, the point2 method can be preferred to point1 and layer methods in modeling soil thermal properties. The results further showed that predications made in bare soil conditions cannot be applicable to cropped soils and that different canopies may affect soil thermal properties differently due to differences in canopy structure and in plant influence on soil water.

2016, 216 page

Key words: Heat diffusivity, heat conductivity, layer method, point method, soil volumetric heat content.

ÖZET

DOKTORA TEZİ

FARKLI BİTKİ ÖRTÜLERİ ALTINDA TOPRAK TERMAL ÖZELLİKLERİNİN KARŞILAŞTIRILMASI

Ahmet Sami EROL

Çankırı Karatekin Üniversitesi

Fen Bilimleri Enstitüsü

Orman Mühendisliği Anabilim Dalı

Danışman: Prof. Dr. Sabit ERŞAHİN

Toprak termal özellikleri, toprak süreçleri ve bitki gelişimi üzerinde önemli bir etkiye sahiptir. Bu çalışma, Konya Kumar ilçesinde (Kuru-yarı-nemli/yarı-kurak Karasal Orta Anadolu İklimi) şeker pancarı, mısır ve çıplak (kontrol) toprak yüzeyi koşullarında toprak profilinde sıcaklığın günlük ve mevsimlik değişiminin modellenmesi amacıyla yapılmıştır. Toprak sıcaklığı 0, 5, 10, 20, 30, 40 ve 60 cm toprak derinliklerinde katmansal, Noktasal1 ve Noktasal2 yöntemleri ile modellenmiştir. Noktasal1 ve Noktasal2 yöntemleri benzer sonuçlar vermiştir ve Noktasal1 ve Noktasal2 yöntemleri bütün durumlarda katmansal yönteminden daha başarılı tahminler yapmıştır. Katmansal yöntem, toprak sıcaklığını sistematik olarak gerçekte olduğundan daha yüksek tahmin etmiştir. Toprak sıcaklığını tahmin etmede her üç yöntemin başarısı derinlik ile giderek azalmıştır. Bu azalma sönme derinliği ötesinde daha belirgin olmuştur. Mısır parsellerinde günlük ve mevsimsel toprak sıcaklık değişimleri, şeker pancarı ve çıplak topraklara göre oldukça farklıdır. Çalışılan toprak derinliklerinde, sulamanın toprak ısı yayınımı ve toprak sıcaklığının mevsimsel değişimi üzerinde ciddi bir etkisi vardır. Sonuçlar, modellerde kullanılan analitik çözüm ve başlangıç koşullarının model performansını etkileyen önemli faktörler olduğunu göstermiştir. Bu bağlamda, toprak sıcaklığını tahmin etmede noktasal yöntemler Katmansal yönteme tercih edilebilir. Sonuçlar ayrıca çıplak toprak koşullarında yapılan tahminlerin üzerinde bitki bulunan topraklarda geçerli olmayacağını ve farklı kanopilerin, kanopi yapısı ve bitkinin toprak suyuna etkisindeki farklılıklar nedeni ile toprak termal özelliklerini etkileyebileceğini göstermiştir.

2016, 216 sayfa

Anahtar Kelimeler: Isı yayınımı, ısı iletimi, katmansal yöntem, noktasal yöntem, toprak hacimsel ısı içeriği

ACKNOWLEDGMENT

First of all, I would like to thank my supervisor Prof. Dr.Sabit Erşahin, for his diligent guidance throughout my graduate study. I listened his lectures with a great pleasure. Working with Prof. Erşahin was a privilege and in spite of his busy schedule he always found time to help me. I gained a broad scope of scientific knowledge under his supervision.

I am indepted to Prof. Dr. Evgeny Shein, who came from Moskow to Konya to join field studies in spite his busy schedule. I appreciate his hospitality, guidance, and help during my stay in Moscow Agricultural University for some of loboraroty analysis of this study.

I also would like to thank Prof. Dr. Fariz Mikayilsoy for his supporting me during my Ph.D work. I thank him for his help with data modeling, interpretaion, and thoughtful support. His encouragements and thoughtful support are deeply appreciated. I would like to thank Prof. Dr. Hasan Sabri Öztürk for his contribution and criticisms that improved quality of my mork. I sincerely thank Ass. Prof. Dr. Gülay Karahan, a devoted friend, for her assistance and eacouragements at every stages of my PhD study.

Thans are extended to Prof. Dr. Abdülreşit Brohi for directing me with his valuable advices during my study and to Prof. Dr. Yakov Pachepsky for giving direction to my studies with invaluable advices. I thank Prof. Dr. Evgeniy Y. Milanoskiy for his helping me with laboratory analysis in Moscow Agricultural University. I thank Assoc. Prof. Dr. Fatih Er for supplying me facilities, necessary laboratory equipment. His friendship and, supports, ecouragement ecouragements are deeply appreciated. I thank my collegues and students for their helping me with field and laboratory works of this study. Thanks are also extented to faculty and staff of Cankırı Karatekin University, Deparrment of Forest Engineering.

Finally, I thank my wife Zeliha Erol and my children who always supported me with tolerance, patience, and dedication during my studies. I dedicate this dissertation to my father and mother, Hasan Hüseyin and Şerife Erol who passed away during my Ph.D study.

Ahmet Sami EROL

Cankırı, May 2016

CONTENTS

LIST OF SYMBOLS AND ABBREVIATIONS

Symbol	Definition
A	Heat exchange between lower layers and the earth's surface
AIC	Akaike Information Criterion
BIC	Bayes Information Criterion
C	The confidence index
C	Heat capacity
Cp	Mallow Cp Criteria
C_m	Soil specific heat capacity
C_v	Volumetric heat capacity
C_{vs}	Volumetric heat capacity of solid phase
C_{vw}	Volumetric heat capacity of water phase
C_{va}	Volumetric heat capacity of air phase
D	Willmott's index of agreement
d	Damping depth
E	The amount of heat used to evaporate water.
E	Energy used evaporation from the soil and vegetation (condensation, liquefaction)
F	Fisher Criteria
f	Porosity (%)
f_a	The fractions of air phase
f_{min}	The fraction of mineral part
f_{org}	The fraction of the organic part
f_s	The fractions of solid phase
f_w	The fractions of water phase
G	Soil heat flux
h	Heat transfer coefficient by convection
h_{gr}	Heat convection coefficient
$h\ (\theta)$	Such as the matric potential versus water content relationship,
HQC	Hannan-Quinn Criterion
$K(\theta)$	The hydraulic conductivity versus water content relationship
k	The number of variable coefficients of model
L	Specific heat of evaporation
LE	The portion used for evaporation
LT	The portion used for transpiration
M	The part of the energy used in photosynthesis and transpiration
m	Mass
M_t	The weight of moist soil

M_s	The weight of the oven dry soil
M_w	The amount of water
N	Sample number
n	The number of the used data
P	The turbulent heat exchange (the warm air near the earth's surface);
Pv	Water volumetric fraction
R	Earth's radiation balance-Radiation (heat balance)
R_{air}	The other part of the solar radiation after being held by the gases, powders,
R_{atm}	Long-wave radiation from the atmosphere is a portion of the vertical solar radiation
R_{sol}	The vertical short-wave solar radiation
R^2	Coefficient of determination
$\bar{R}^2$	Adjusted R-square
SIC	Schwarz Information Criteria
t	Time
T_0	Average temperature at soil surface (daily, annual)
T_a	Wave amplitude
T_{air}	Air temperature
T_m	Measured temperature
T_p	Predicted temperature
Ts	The time series of surface temperature
T_{sur}	Soil surface temperature
U	Theil's Forecast Accuracy Coefficient
V	Volume
V_a	The air volume fraction
Vs	Volumetric solid fraction
Q_{CV}	Cross-validation Criterion
q	The heat source
Q	The shortwave radiant flux density from the sun and from hemisphere to the earth
Q_0	The long wavelength radiant flux density emitted by the surface;
Q_a	The heat flow density that are used in heating the air near the ground surface;
$Q^{\downarrow}_{CE}$	Convective heat flow between soil-air boundary layer and ground surface (occurring by conduction) heat-exchanger
$Q_{heat\ low}$	Heat flow to the soil surface;
Q_i	The density of the heat transmitted to the soil;
Q_s	total heat energy of short wavelength solar radiation
$Q^{\downarrow}_{SR}$	The solar radiation absorbed by soil surface

$Q^{\uparrow}_{LR}$	The long-wave radiation emitted by the earth's surface (radiation) net flux density
$Q^{\uparrow}_{LE}$	The portion of heat which is used in vaporization
w	Water content

Greek Symbol

$\Phi_a(y,b)$-	The amplitude of the temperature in the soil at a specified depth
$\Phi_{min}(x)$	Minimum temperature x_1 and x_2 are depths
$\Phi_{max}(x)$	Maximum temperature x_1 and x_2 are depths
α	Albedo (reflectivity constants)
ε	Phase difference
$\bar{\varepsilon}$	MAPE: Mean absolute percentage error
γ	The specific weight of the water (1 g cm^{-3})
η or R	Correlation coefficient
$\varphi(t)$	Function expressing the temporal change in temperature at the soil surface.
κ	Heat diffusivity
λ	Heat (thermal) conductivity
θ	The volumetric water content
Θ	Theta Criteria
ρ	Dry density
ρ_b	The soil oven dry bulk density
ρ_s	The particle density (g / cm3)
ρ	Absorptivity constants
ρQ	Sum of absorbed radiation energy,
αQ	Reflected radiation energy
βQ	Transported radiation energy
σ	Transmissivity constants
$\sigma_{T/t}$	Standard deviation of mean
τ_0	Period or wave length
ω	Wave number or frequency (angular frequency)
$\psi(t)$	The algebraic sum of radiant flux at the soil surface
ANN	Artificial Neural Network
CL	clayed-loam
ECPC	the Scripps Experimental Climate Prediction Center
RSM	Regional Spectral Model
SHCP	the soil heat calculator program
SL	sandy-loam

LIST OF FIGURES

LIST OF TABLES

1. INTRODUCTION

Soil temperature is an important climate variable controlling plant growth. Soil physical, chemical, and biological processes are affected by soil temperature. In specific, soil temperature has a tremendous influence on seed germination, root formation, biological activities of soil microbes, and soil organic matter decomposition, water and nutrient uptake by plants, formation and development of plant diseases, soil aeration, and soil moisture release (García-Suárez and Butler 2006). Soil temperature, as a plant development and growth limiting factor, should be understood adequately for a successful soil management (Tenge *et al.* 1998).

Solar radiation is the main energy source of soil temperature. Heat flow in soils shows a nonlinear behavior. Specific heat capacity, heat conductivity, and heat diffusivity that depends on volume weight and moisture content of the soil, play key roles in this variation. Therefore, various methods have been derived to determine the soil temperature. Although the methods based on energy balance are reliable, their use is highly elaborate. Periodic sinusoidal wave models describe diurnal and annual temperature changes in soils more practically. However, many researchers stress that the periodic sinusoidal and cosinusodial wave models should be used carefully.

Soil temperature is an important parameter that directly affects the physical, chemical and biological processes such as seed germination, plant growth, soil moisture availability, soil aeration, soil structure formation, microbiological actions, availability of plant nutrients, and freeze-thaw events. Plants need a particular temperature to germinate and grow, which is called base temperature, the temperature under which plant growth stops (Baver *et al.* 1972, Kirhan and Powers 1972).

Temperature is a property, arising from function of energy existing in material things. It is measured with a thermometer, and its unit is $^{\circ}$C or ^{o}K. Heat is a form of energy, measured by calorimeter and its unit is calorie or Joule (1 cal = 4.18 Joule).

Knowledge on soil thermal properties provides important clues on ecological factors of plant growth. Many soil chemical and biological processes are controlled by soil temperature. For example, each 10 ^{o}C rise of temperature between 10 to 30 ^{o}C results in an 2.3 times increase in nitrogen mineralization (Q_{10}=2.3) in soils (Campbell and Norman 1998).

Soil temperature is a function of soil heat flow, volumetric heat capacity, and amount and partitioning of radiation on the soil surface. Diurnal soil temperature changes by depth and time. Diurnal changes are effective up to 50 cm soil depth, while annual temperature changes can be effective up to 6-8 m (Campbell and Norman 1998). Soil thermal properties as well as solar irradiation and its partitioning on the soil surface control temperature changes (Campbell and Norman 1998). Soil tillage may influence soil temperature via altering radiation partitioning on soil surface and changing soil thermal properties in tillage depth (Özbek 1990).

Numerous models have been developed to predict soil thermal properties and heat flow. These developed models have several limitations. Nature and accuracy of these models is closely dependent on the subject area and concepts used in modeling. In addition, model selection depends on data availability of soil physical and chemical properties as well as soil thermal properties such as heat capacity and thermal conductivity besides meteorological data (Yeşilsoy 1975, Hadas 1977, De Vries and Philip 1986, Nassar *et al.* 1992, Bristow *et al.* 1993).

Thermal properties of soils under different plant covers show differences and a complicated relations with plant cover type as plant cover affects both amount and partitioning of solar radiation on the soil surface and heat flow and storage in the soil profile (Campbell and Norman 1998). The vertical changes of air temperature, environmental moisture, wind, and radiation show substantial differences across different plant cover types. Therefore, most of the models developed for predicting soil thermal properties were applied to bare soil conditions. This study was carried out to model soil temperature under corn and sugar beets canopy and to compare the results with those found in bare soils.

2. LITERATURE REVIEW

Soil temperature is one the most important factor affecting physical, chemical, and biological characteristics and various processes in soils. Soil temperature influences processes such as seed germination, plant growth and development, soil water flow and availability to plants, aeration, structure formation, microbiological activity, decomposition of crop residues, availability of plant nutrients, and freeze-thaw cycles. In addition, soil temperature has a decisive influence on soil formation and processes such as transformation and translocations of matters in soil profile.

Soil temperature has a positive influence on root growth in a certain soil temperature range (Sarıyev *et al.* 1995). In a certain temperature range, water movement from the soil to the root zone and root metabolic activities decreased with a decreased soil temperature (Sarıyev *et al.* 1995, Steduto 2000). Buchan (1991) examined the temperature regime in soils. He stated that surface heat balance, calculated thermal conductivity and thermal properties were entirely related to the heat flow in the soil.

2.1 Factors Affecting Soil Thermal Properties

Soil thermal properties of specific heat capacity (C_m), volumetric heat capacity (C_v), heat conductivity (λ), heat diffusivity (κ), heat balance (Radiation) *(R),* and damping depth (d) have been studied extensively. Kertsen (1949) found that soil thermal conductivity increases with increased temperature and decreased with increased water content. Thermal conductivity was greatest in sand and gravel, medium in sandy loam, and lowest in silty and clayey soils. De Vries (1963) found that thermal conductivity, soil water content, bulk density, porosity, and the shape of soil aggregates were dependent on the soil parent material. Kohnke and Nakshabandi (1964) and Nassar *et al.* (1992) stated that thermal conductivity of the soil varies depending on soil mineralogical composition, texture, water content, organic matter content, grain shape, spatial arrangements of soil grains, aggregation, and pore geometry.

Heat content of soil constituents (air, water, mineral and organic matter) are different, thus the volumetric heat capacity of soils differs considerably depending on the proportion of each soil constituent in a whole (Baver *et al.* 1972). The effect of soil water content is the most prominent on C_m due to its high specific heat capacity (Hillel 1980, Campbell and Norman 1998). There are two main heat transfer types in soils. The first one is thermal conduction, and the second one is convection (Hadas 1977). Heat flow occurs from the surface to soil in the morning and noon, while it occurs from soil to surface in the late afternoon and evening.

Thermal diffusivity of soil is the most important heat transmission parameter that represents the temperature change depending on soil heat conductivity and volumetric heat capacity (Horton and Wieranga 1983). The thermal conductivity is a function of C_v and λ. Ghuman and Lal (1985) stated that λ raised with the rise of soil water content and that λ values of the studied clayey soils were always lower than that of sandy soils with a same water content. Besides water content, soil structural properties affects heat transfer in soils.

Effect of temperature on water flow in soil-water flow studies is generally neglected (Giakoumakis and Tsakiris 1991). However, experimental studies have shown that soil temperature has a strong effect on the soil water characteristics, such as on the matric potential - water content relations, ($h(\Theta)$), and on hydraulic conductivity versus water content relations ($K(\Theta)$).

Nassar *et al.* (1992), examined water and the passage of the solution at the porous medium. Three simultaneous equations have been used to describe the transition of the heat and fluid (heat, water and solvent) of solution in soil. Heat, water, and solution flow equations have been developed together. Each equation involves three diffusion coefficients. Diffusion coefficient depends on solution density, its temperature, and soil moisture.

Campbell *et al.*(1994) measured thermal conductivity of soil samples with different structure, bulk density, water content, and temperature and they modeled their data with

de Vries model. Their results showed that thermal conductivity increased in wetter soils significantly and results from Modified De Vries theory were consistent with the measured data at low temperature. Poulovassilis *et al.* (1998) calculated heat flux density in wet and dry soils by different methods. They found that soil structure, soil water content, and particle-size distribution affected soil temperature. Soil heat flux density values calculated by different methods were compared with the measured heat flux values. Their results revealed that all the methods used yielded adequate predictions.

According to Ekberli *et al.* (2005), temperature in the soil profile, varies on daily, monthly and annually. These changes are periodic forms, as one day or one year. Temperature changes in are greatest on the earth's surface, and it decreases by depth. Diurnal temperature changes show their effect up to 35-100 cm soil depth.

Rahimi *et al.* (2010) used numerical solution of heat conduction equation to estimate thermal diffusivity (κ) in different texture and moisture contents at different depths and times. Their results showed that the values of κ increased with increased moisture up to a critical point and then decreased versus further increases in water content. The maximum values for κ occurred at 15 and 10% moisture contents for silty clay and sandy soils, respectively. Wang and Bou-Zeid (2012) developed a novel model for estimation of the heat flux density in soils. Their results showed that the proposed method was robust in estimation of heat flux under in soils under various meteorological conditions.

Usowicz *et al.* (2013) conducted a study to evaluate spatial distribution of the soil thermal properties (thermal conductivity, heat capacity, and thermal diffusivity) in relation to soil wetness and bulk density in wetland soils of Polesie and Biebrza regions (Poland). They found that heat capacity of the soils was linearly dependent on the water content. Extremes of the thermal diffusivity are mainly due to the changes in the intensity of the thermal conductivity of the soils due to change in soil moisture content and density. The heat capacity of the soil increases linearly with increasing water content. The value of soil thermal diffusivity depends highly on quartz content. Thermal

diffusivity of the soil with the same moisture content was greater for the higher densities, and minimum or maximum thermal diffusivity tends to move toward the lower moisture content for higher densities (Usowicz *et al.* 2013).

2.1.1 Soil texture

Smith and Byers (1938) reported greater thermal conductivity for sandy soils than clay soils. Midttomme *et al.* (1988) found a reasonable correlation between grain size distributions and measured thermal conductivity of soil samples. In a study Abu-Hamdeh (2001), measured values of thermal conductivity ranged from 0.19 to 1.13 $Wm^{-1}K^{-1}$ for sandy loam and from 0.35 to 0.69 $Wm^{-1}K^{-1}$ for clay loam with bulk densities of 1.25 and 1.49 g cm^{-3} and water contents of 7.2 and 18.2%, respectively. They further reported that the sandy loam had higher values of thermal conductivity than the clay loam. Their results show that thermal conductivity varies with soil texture, water content, and bulk density. For the two soils studied, an increased bulk density at a given moisture content resulted in an increased thermal conductivity, and increased moisture content at a given bulk density resulted in an increased thermal conductivity. They also reported that their clay loam soil generally had lower thermal conductivity than sandy loam.

Connectivity of the water filled pores may influence the thermal conductivity. Kim *et al.* (2011) found higher values of thermal and electrical conductivity for hydrophilic sand at low saturation compared to hydrophobic sand, and they attributed that to the well-developed long-range connectivity of fluid phase in pore space and the formation of liquid bridges at inter-particle contacts in the hydrophilic sand.

2.1.2 Dry bulk density

Abu-Hamdeh (2003) conducted laboratory studies on effect of water content and bulk density on the specific heat, volumetric heat capacity, and thermal diffusivity of some sieved and repacked soils. They found greater volumetric heat capacity with greater moisture content and soil bulk density. Differences between the observed and predicted

values of the volumetric heat capacity and specific heat were very small. Their results also showed that thermal diffusivity varied with moisture content and soil texture. Sandy soils exhibited a thermal diffusivity peak at moisture contents different from that of clay soils.

Ekwue *et al.* (2006) found that adding peat in sandy loam, clay loam and clay soils and compacting resulted in clay soils had a significantly lower values of thermal conductivity (λ) and greater values of soil water content. They concluded that increased compaction results in increased λ and increased peat rate resulted in decreased λ in soils. In another study, Ekwue *et al.* (2011) measured λ of twelve soils in laboratory and field using a portable sensor and a probe. Their field measured λ values ranged from 0.90 to 1.55 W m^{-1} $^{o}C^{-1}$ and laboratory measure values ranged from 0.5 to 2.00 W $m^{-1}{}^{o}C^{-1}$. They found increased λ-values with increased water content and bulk density (ρ_b)**.** They also found that the λ was lower for the clay than for the sandy loam and the clay loam and that a unique linear relationship existed between ρ_b and λ for compacted soils.

2.1.3 Organic matter content

Zhou *et al.* (2007) found that application of turkey litter decreased the soil thermal diffusivity. Hamamoto *et al.* (2010) studied heat transport of peat soils at different saturated conditions. In general, the thermal conductivity and the heat capacity of peat soils increased linearly with increasing volumetric water content. Smith and Byers (1938) concluded that the soils containing high amounts organic matter had low thermal conductivity.

2.1.4 Soil water content

When air in the soil pores replaced with water, thermal conductivity increases Patten (1909) due to high heat conductivity of water. Therefore, κ increases with soil moisture content proportionally Gemant (1950). Increased soil water content results in increased κ up to a specific water content. However, further increases in water content results in κ to decrease due to high heat capacity of water. Relation between water content and κ

depends on soil texture too (Campbell and Norman 1998). Soil organic matter content, soil structure, soil porosity, and pore geometry also affect κ through their influence on θ (Kemp *et al.* 1992).

Moisture variations have a much greater effect on thermal conductivity of soils than bulk density and grain size. Nakshabandi and Kohnke (1965) found that mineral soils with different textures, containing the same amount of water, had very different thermal conductivities. However, when the soils were compared at the same moisture potential, their thermal conductivities were much similar. Thermal conductivity of dry soils increases with the bulk density (Kemp *et al.* 1992). Hanson *et al.* (2000) reported that thermal conductivity of peat was lower than the thermal conductivity of typical soils (sands and silts) as large voids in peats prevented the effective transfer of heat through. Soil temperature may affect direction and rate of soil water flow. According to Gönen (1978), water moves in the direction of temperature slope of soil water, from warmer region to colder region.

During the diurnal soil temperature variation, it was found that the surface temperature amplitude was higher in wet soils than in dry soils. Formation of a thin dry soil layer on soil surface may tend to thermally insulate the soil, causing the surface heat flux to fall and the surface temperature to rise. In unsaturated moist soils, the transport of heat is complicated by the fact that heat and mass transfer is a coupled process (Balghouthi *et al.* 2005). The calculated and measured results indicate that temperature and temperature gradient play an important role in moisture transport in soils. Studies showed that influence of temperature on liquid water transfer was strong and the effect of temperature gradient on vapor diffusion was obvious.

The needle probe and specific heat dual probe are used widely for determining thermal properties of materials with high water content (Hanson *et al.* 2000). Measured thermal conductivity of several materials was evaluated to understand effect of water content on κ in these materials. Duarte *et al.* (2007) studied thermal properties of unsaturated sandy-loam (*SL*) and clayed-loam (*CL)* in laboratory. They measured heat parameters, thermal conductivity, and heat capacity in both soils with a thermal needle. The change

in thermal conductivity showed an exponential relationship with the gravimetric water content. Rubio (2011) studied influence of hysteresis on heat transport in soils in laboratory. Their specific heat capacity and thermal conductivity showed a positive linear relation with soil volumetric water content. However, thermal diffusivity values behaved differently from specific heat capacity and thermal conductivity against changing soil water content.

In general, water content-thermal diffusivity relations are defined by parabolic curves. Thus, the approximation of the parameters makes it possible to quantitatively characterize soil water content- κ relations in different soils (Arkhangel'skaya and Umarova 2011).

2.1.5 Soil structure

Aggregate geometry and size may have paramount effect on heat conductivity. (Hadas 1977) reported that small-sized aggregates promoted heat conductivity, while larger-sized aggregates had the reverse effect and it was attributed to that increased aggregate-size resulted in increased gaps and weakened contact points between aggregates, decreasing thermal conductivity. Usowicz *et al.* (2013) studied effects of aggregate size on soil thermal conductivity λ, at different water contents. They found that λ was highest in non-aggregated soil and gradually decreased in 0.25–3 mm and 3–10 mm aggregates due to likely reduced contact area between heat-conductive solids and water films.

2.1.6 Porosity

Soil thermal properties depends on volumetric water fraction *(θ)*, volumetric solid fraction *(Vs)* and the air volume fraction *(Va)*. Ochsner *et al.* (2001) found that the effect of θ on soil thermal properties was more predominant than the other working parameters and that a linear increase occurred ($r^2 = 0.93$) between θ and soil thermal conductivity**.** Usowicz *et al.* (2006) reported that compared to water content, air filled porosity and penetration resistance described a greater variation in thermal conductivity.

Smits *et al.* (2009) studied thermal conductivity of sands under different water content and porosity. They found that thermal conductivity increased with increased water content and that tightly-packed sand showed consistently higher thermal conductivity values than loosely packed sand. The heat conductivity of air is 1/20 of the heat conductivity of water and 1/60 of the solid. Therefore, soil air functions as an insulator against heat conduction in soils (Bayraklı 1993).

2.1.7 Soil cultivation

Soil thermal conductivity determines how fast or slow soil warms or cools with exchange of energy by conduction, convection, and radiation (Abu-Hamdeh 2000). Soil cultivation generally reduces soil water at the cultivation depth and increases porosity, resulting in a decreased heat flow to the underlying layer (Van Wijk and De Vries 1966). This causes an increased temperature with sensible heat in the upper soil layer. Potter *et al.* (1985) reported a greater thermal conductivity in uncultivated soils than soils cultivated with a chisel and a mold board.

Different soil tillage systems may show their effects on soil thermal properties differently. Abu-Hamdeh (2000) showed that rotary tillage decreased soil thermal conductivity more than chisel tillage, compared to no-tilled plots. For the clay loam, thermal conductivity ranged from 0.33 to 0.72 W m^{-1} K^{-1} in chisel tilled treatments, from 0.30 to 0.48 W m^{-1} K^{-1} in rotary tilled treatments, and from 0.45 to 0.78 W m^{-1} K^{-1}in no-tilled treatments. For the loam, thermal conductivity ranged from 0.40 to 0.75 W m^{-1} K^{-1} in chisel tilled treatments, from 0.34 to 0.57 W m^{-1} K^{-1} in rotary tilled treatments, and from 0.50 to 0.79 W m^{-1} K^{-1} in no-tilled treatments. The clay loam generally had lower thermal conductivity than loam in all similar tillage treatments. On the other hand, Licht and Al-Kaisi (2005) found that strip tillage had a limited advantage over no-tillage in improving soil temperature in early spring. Soil temperatures associated with strip-tillage were comparable with chisel tillage, and their maximum soil temperatures were greater by 1.4–1.9 ˚C than those of no-tillage.

Lipiec *et al.* (2007) reported that the mean values of λ were generally greater under cultivated soils than grasslands in moist soils and the inverse was true in drier soils. In general, the spatial distributions of both λ and C_v were similar to those of water content. In a study Dec *et al.* (2009), it was found that λ and C_v were higher and thermal diffusivity was lower in undisturbed columns of moldboard tilled soils.

Mulches used in covering soil surface may have a decisive effect on thermal regime in topsoil. Kowsar *et al.* (1966) compared change in temperature and moisture content in soils covered and non-covered with petroleum mulch. Mulched soil surface was found 5 ^{0}C higher than that of non-mulched soil.

2.2 Soil Thermal Properties under Different Plant Covers

Plants may affect partitioning of solar radiation on the soil surface and water status of soils, influencing soil thermal properties. Horton *et al.* (1984) developed a two-dimensional soil heat conduction model to calculate soil temperature distribution at plant under where soil surface remain partially shaded. They observed a large difference in soil temperature in surface and near-surface soils. They measured greater horizontal soil heat flux than the vertical at the top of the soil profile. Al-Kayssı *et al.* (1990) showed that increased water content decreased soil temperature differences between day-time and night-time, which provides protection to the plant root system against sharp and sudden changes of soil temperature. They also found that the absorbed solar energy increased as the water content increased, which provided a greater heat storage capacity at greater water contents.

The effect of plant cover on soil thermal properties is highly complicated due to relations between other soil properties influenced by plants and soil thermal properties. Usowicz *et al.* (1996) analyzed the spatial variability of soil thermal properties using classical statistics and geostatistics. Their results indicated a clear influence of soil water content and bulk density on the spatial variability of soil thermal properties. For particular soil thermal properties, this influence occurred differently, depending on soil water content. The spatial variability of soil thermal properties over cultivated fields is

mainly determined by soil water content and bulk density. Spatial autocorrelation of soil thermal properties for the sites containing different crops was reported over a broad range of soil water content values. For individual crops, spatial autocorrelation of soil thermal properties was related to soil water content. At water content close to or higher than field capacity, this range considerably decreased and was similar to the spatial autocorrelation range of soil bulk density (Usowicz *et al.* 1996).

Plant cover type and its spatial orientation can affect spatial distribution of soil thermal properties. Usowicz. *et al.* (2001) analyzed soil moisture and thermal properties in the surface layer on the fields with different crops. Analysis of soil moisture on particular cultivated fields showed that type and growth stage of vegetation were important factors, along with meteorological conditions (mainly frequency and amount of rainfall, as well as sunshine duration over a given period) determining the spatial distribution of soil thermal properties in the studied fields. They also reported that difference of soil moisture between examined fields was influenced by differences in intercepted amount of precipitation and in intensity of evaporation from soil surface and transpiration by plants. In the wheat field, because of greater rainwater retention by a dense plant canopy and evapotranspiration, the soil moisture and its changes were lower in comparison to those in the fields with incomplete plant of sugar beet and corn. They found that the soil compaction had both direct and indirect effect on soil heat flow, increasing the contact points of particles in the former and influencing vigor of plant cover on soil surface in the later.

Dalmago *et al.* (2004) evaluated differences in soil temperature in corn cropped no-tillage and conventional tillage systems. They reported that at the beginning of plant growth, the highest soil temperatures occurred in the conventional system in all soil layers. However, after 30 days from plant emergence, the highest temperatures occurred in the no-tillage system. However, variations among the cropping systems decreased as the plants covered the soil surface.

2.3 Mathematical Models of Heat Flow in Soil

Soil thermal variables such as thermal conductivity, heat capacity, and thermal diffusivity may be measured and/or predicted from other soil variables using mathematical models (Yeşilsoy 1975, Hadas 1977, Horton 1982, De Vries and Philip 1986, Juri *et al.* 1991, Nassar *et al.* 1992). Mathematical models are widely used in predicating soil thermal variables. Liu *et al.* (2005) used a mathematical model for describing simultaneous heat and moisture transfer in a soil with a dry surface layer. They obtained an adequate agreement between their measured and predicted values.

Krishnan and Kushwaha (1972) applied harmonic analyses to weekly temperature means of sand and loamy sand with clay content of 6-8% at Jodhpur, India. They found that amplitudes for different depths varied between 4.8°C and 9.1°C for first harmonic, decrease sharply with higher order harmonics, and the values for fourth harmonic ranged from 0.12-0.64°C. Hadas and Fucs (1973) compared calculated thermal diffusivity values with measured values. Their measured and calculated values were close to each other in the subsurface layers, while calculated values were lower than measured values in the surface horizon.

Kanamaru and Kanamitsu (2008), evaluated night time minimum temperature warming in the California Central Valley during summer due to irrigation. They used the Scripps Experimental Climate Prediction Center (*ECPC*) Regional Spectral Model (*RSM*) to simulate climate in a natural vegetation and modern land use that includes irrigation and urbanization. In irrigated cropland, soil moisture was kept at field capacity, half of field capacity, and no addition of water. It was found that ground heat flux efficiently kept the surface warm under half of the field capacity during nighttime due to increased thermal diffusivity.

According to Yeşilsoy (1975), Hadas (1969) compared the calculated values of thermal conductivity with the experimentally measured values. They concluded that measured and calculated values in steady-state conditions were similar, while those found in unstable were inconsistent.

Kluitenberg and Horton (1990) developed a complete analytic solution of two-dimensional heat conduction in soils. They showed that temperature of the soil exhibited a sinusoidal wave over time. Numerous of models were developed to describe soil heat flow. Nassar and Horton (1990) suggested a new method where variance and Fourier analysis were applied to the measured soil temperature values. First, the temperature measurements were adapted to Fourier series, and then thermal diffusivity values for each harmonic were calculated for non-uniform soil conditions using soil heat conduction analysis (non-uniform soil heat-transfer analysis). Consequently, thermal diffusivity values were obtained for all soil layers. Sharratt *et al.* (1992) developed a method for estimating soil heat flux *(G)* by implicitly solving the finite-difference form of the transient heat flow equation for the apparent daily thermal conductivity. They used apparent thermal conductivity and soil temperature gradient with Fourier's law for estimating *G*. This method requires the measurement of soil bulk density and daily water content (for volumetric heat capacity) and hourly temperatures at three depths.

Sarıyev *et al.* (1998) modeled soil temperature change by depth and time. They calculated soil heat capacity and conductivity using initial soil water content values. Çelebi (2001) monitored soil temperature in columns in stable and unstable condition (at 4 different humidity level) both with sensors and mathematical models.

In a study Gülser and Ekberli (2004), diurnal soil temperature changes of a clay were modeled using the cosinesoidal harmonic equation. Soil thermal properties such as amplitude, heat dissipation, and damping depth were calculated for 0, 10, 20, 30, 40 and 50 cm soil depths. Droulia *et al.* (2009) predicted subsurface temperature profiles. They used an analytical model and developed semi-empirical models, replacing the steady state soil temperature with easily obtained daily average temperatures. They reported that their developed models predicted soil temperature fairly well.

Bilgili (2010) developed an artificial neural network model to predict the average soil temperature. He measured temperature in 5, 10, 20, 50 and 100 cm depths for creating feed-forward neural network with three-layer structure. His results proved that the

artificial neural network approach was highly suitable for predicting soil temperature. Özturk *et al.* (2011) obtained good agreement between artificial neural network *(ANN)*-estimated soil temperature values and measured soil temperature values with correlation coefficients of 98.91, 97.99, 99.03, 98.26, and 95.37% for the 5, 10, 20, 50, and 100 cm soil depths, respectively. They concluded that *ANN* modeling was a reliable method for predicting monthly mean soil temperature in regions of Turkey where soil temperature monitoring stations are not present. Their results showed that altitude, latitude, longitude, year, month, cumulative monthly solar radiation, cumulative monthly sunshine duration, and monthly mean air temperature could be used in *ANN* models to obtain reasonable estimates of monthly mean soil temperature at various depths.

Mikayilov and Shein (2010) used mathematical models for predicting heat transfer in soils. They proposed a number of equations for calculating κ on the basis of different boundary conditions and sine shaped diurnal and annual temperature cycles. They included algorithms of arctangents of amplitudes and the phase shift between the daily temperatures at two depths in the model they developed. They obtained a mean integral solution for the prediction of the average temperature in a specified soil layer. They further developed a number of methods starting from the analysis of the temperature dynamics on the basis of four daily observations at the same depth with six hour intervals, and they prepared nomograms for the rapid and simple calculation of the soil thermal diffusivity at a given depth. They concluded that developed methods could be used for assessing the soil thermal diffusivity under natural conditions, which should improve the reliability, accuracy, and adequacy and expand the application range of predictive mathematical models for the thermal regime of soils.

Adeniyi and Oshunsanya (2012) concluded that the amplitude decay algorithm yielded the most reliable values of the soil thermal properties among compared prediction methods. They stated that the Arctangent algorithm gave the most deviated values of soil thermal properties with relative maximum error (*RME*) of 156.83% for soil thermal conductivity. Valipour *et al.* (2012) showed that the soil heat calculator program (*SHCP*) was an appropriate tool for calculating soil heat flux.

Danelichen (2013) evaluated soil thermal diffusivity of a Gleyic Solonetz soil in the Brazilian Pantanal by the amplitude, logarithmic, arctangent, and the phase methods between 0.01 and 0.03 m, 0.01 and 0.07 m and 0.01 and 0.15 m soil depths. The soil thermal diffusivity estimated by the four methods showed significant differences and varied over the study period as a function of volumetric soil water content. The soil thermal diffusivity estimated by logarithmic method showed better performance at different depths, followed by the method of phase.

Özgener *et al.* (2013) predicted daily soil temperature differences by depth and time Measured and predicted soil temperature values at depths of 5, 10, 20, and 300 cm were compared with measured values to validate the accuracy of their method. For an annual cycle; at 5, 10, 20, and 300 cm depths, the average maximum percentage of errors were 10.78%, 10%, 10.26%, and 14.95%, respectively.

Arkhangelskaya (2014) showed that lateral variability of soil thermal diffusivity could fully explain lateral temperature differentiation within the studied soil complexes. Ekberli and Sarılar (2014) compared theoretical soil temperature values obtained from the solution of thermal conductivity equation to experimental soil temperature values in a grassland and in a peach orchard. Their results showed that the initial unconditional solution of the heat conductivity equation in a short period ($\leq$ 3 days) gives much better periodic thermal changes on the soil surface and in soil layers.

Nowamooz *et al.* (2015) determined the heat distribution throughout the profile of unsaturated multilayered soil using finite difference method as its thermal diffusivity varies with time and depth. A comparison of the numerical results with the results of in-situ thermal probe measurements showed that the model could estimate heat distribution adequately within a multilayered soil.

Verhoef (2004) applied Fourier series analysis to the time series of surface temperature (T_0) and used Fourier series constants together with the remote estimate of thermal inertia to calculate diurnal estimates of the soil heat flux (G). Remote estimates of C_h

and $\sqrt{\kappa}$ and model predicted values of G compared well with values measured with in situ sensors.

Baladi *et al.* (1980) measured and predicted temperature variations at soil surface under a heat source. Their results showed that the numerical solution of the exact formulation agreed to their measured values well and the closed-form solutions deviated somewhat from the measurements, while they were shown to be useful for obtaining approximate predictions in a simple manner. They further concluded that: 1) For a given soil, energy transport was facilitated by higher moisture content, thus yielding lower temperatures in comparison with the same soil with a lower moisture content. 2) The numerical solution characterizing the complete formulation of the problem predicted the transient thermal response of soils reasonably well. 3) For well-graded moist soils, such as loam, the energy conduction model yielded approximate predictions that are adequate for many engineering applications. 4) For porous moist soils, such as saturated sand, convective transport of thermal energy due to mass migration is appreciable. For this situation, predictions based on the energy conduction model yielded considerable amount of error. Use of the numerical solution procedure was recommended for these cases when higher accuracy is desired. 5) For initially dry soils, the pure heat conduction model provided accurate predictions. For moist soils, this simplified procedure yielded approximate predictions only, with errors that are generally greater than those associated with the energy conduction model. 6) Simplified models over-predicted the transient temperature rise.

In addition to above mentioned studies many other studies have been conducted on modeling and predicting soil thermal parameters (Yeşilsoy 1975, Hadas 1977, Kurtener and Chudnovskii 1979, Horton 1982, Gerayzade 1982, De Vries and Philip 1986, Gerayzade 1989, Juri *et al.* 1991, Nassar *et al.* 1992, Marinova 1993, Sarıyev *et al.* 1995, Sarıyev and Gülüt 1995, Mihalakakou *et al.* 1997, Sarıyev *et al.* 1998, Barik 2002, Mihalakakou 2002, Ekberli *et al.* 2002, Gülser and Ekberli 2004, Ekberli *et al.* 2005, Shein 2005, Shein and Goncharov 2006, Ekberli 2006, Shein 2007, Mikayilov and Shein 2008, Yılmaz 2008, Mikayilov 2009, Mikayilov and Shein 2010, Şımarmaz 2010).

3. MODELING

3.1 Mathematical Modeling of Heat Transfer in Soils

3.1.1 The model concept

A model is a simplified form of a complex natural system based on assumptions (Lesh and Doerr 2003). Modeling is not an alternative to observation, while it may be a powerful tool in understanding observations and in developing and testing theory in certain conditions (Wainwright and Mulligan 2004). Modeling in agricultural sciences has grown significantly as a response to increased need to study systems in an integrated manner, and an increased demand for extrapolation in space and time. Modeling provides a unique advantage for researchers to better understand feedbacks and interactions between the environment, ecosystems, and human and animal populations.

Mathematical models, ranging from simple equations to complex software codes, are commonly used to describe states and rates of change in systems by formally expressed mathematical rules. The mathematical models may be defined into different types, while most mathematical models are mixtures of many types (Wainwright and Mulligan 2004).

3.1.2 Classification of models

The models are different depending on systems being represented and knowledge and scientific background of the modelers. A general classification of the models is shown in Figure 3.1.

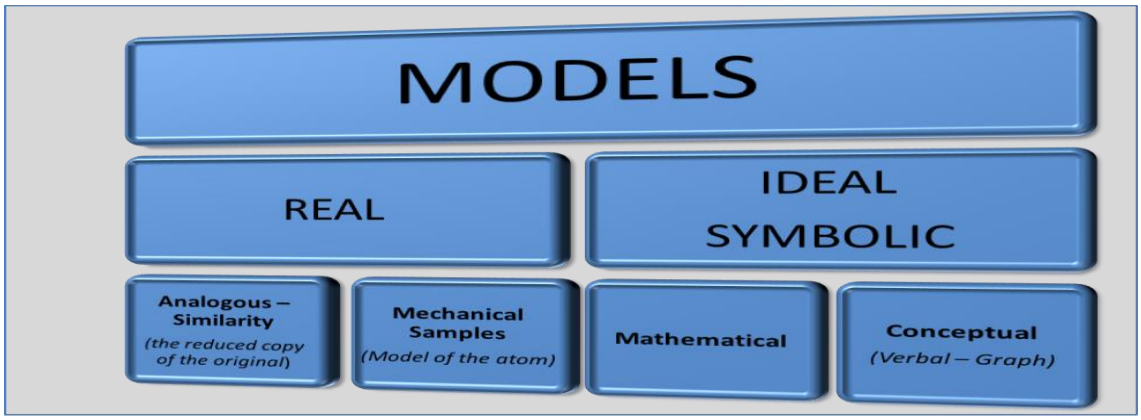

Figure 3.1 General classification of the models (Şımarmaz 2010)

Real models are small-scale of original systems and embrace many features of the original systems. Because the degree of similarity to the original scale of these models is not easy to determine, it creates difficulty in the implementation of the modeling results to original system. In addition, because there is no guarantee of similarity, it may not be able to eliminate the difficulties of implementation of technical considerations (Ekberli 2008).

Ideal (symbolic) model is different from the actual model, are the identification of the link with the original system with the help of Braille symbols and meaning of these symbols. Any set of words and phrases from the result of the expression (signs "language" cluster) is obtained. According to Poletayev (1966), when compared with actual models, symbolic models have larger facilities and their physical application limits can be controlled (Ekberli 2008).

3.1.3 Basic principles and mathematical models

Simulation models, which have been developed in recent years, have become main tools of analysis for complex systems. A simulation is a model creation which can represent a system. Simulation includes the artificially creation of a system of records and examination of artificial record for obtaining the results of the actual system (Banks and Carson 1984).

Mathematical models are built on the basis of the results, which depend on the outcomes of basic and/or applied research on complex systems and are applied to obtain the necessary information from the system. A mathematical model, in a braod sense, can be described as an equation or formula that expresses the main features of a process or any system with the mathematical terms and symbols.

Mathematical models can be shown as a functional relationship in the following format:

$$\mathbf{u} = f\ \mathbf{x}, \mathbf{y}, \boldsymbol{\sigma}, \mathbf{a} \tag{3.1}$$

Where;

$\mathbf{u} = u_1, u_2, ..., u_k$ – are the system's output variables;

$\mathbf{x} = (x_1, x_2, ..., x_n)$ – are system components;

$\mathbf{y} = (y_1, y_2, ..., y_m)$ – are the system's input variables;

$\boldsymbol{\sigma} = \sigma_1, \sigma_2, ..., \sigma_l$ – is the system's structure;

$\mathbf{a} = a_1, a_2, ..., a_p$ – are the parameters of the system.

As actual mathematical expression, Eq. (3.1) may be a simple algebraic relation or a very long complicated integro-differential equation units (Edwards *et al.* 2003, Ruan 2006). Mathematical models are classified in the following format in general (Figure 3.2).

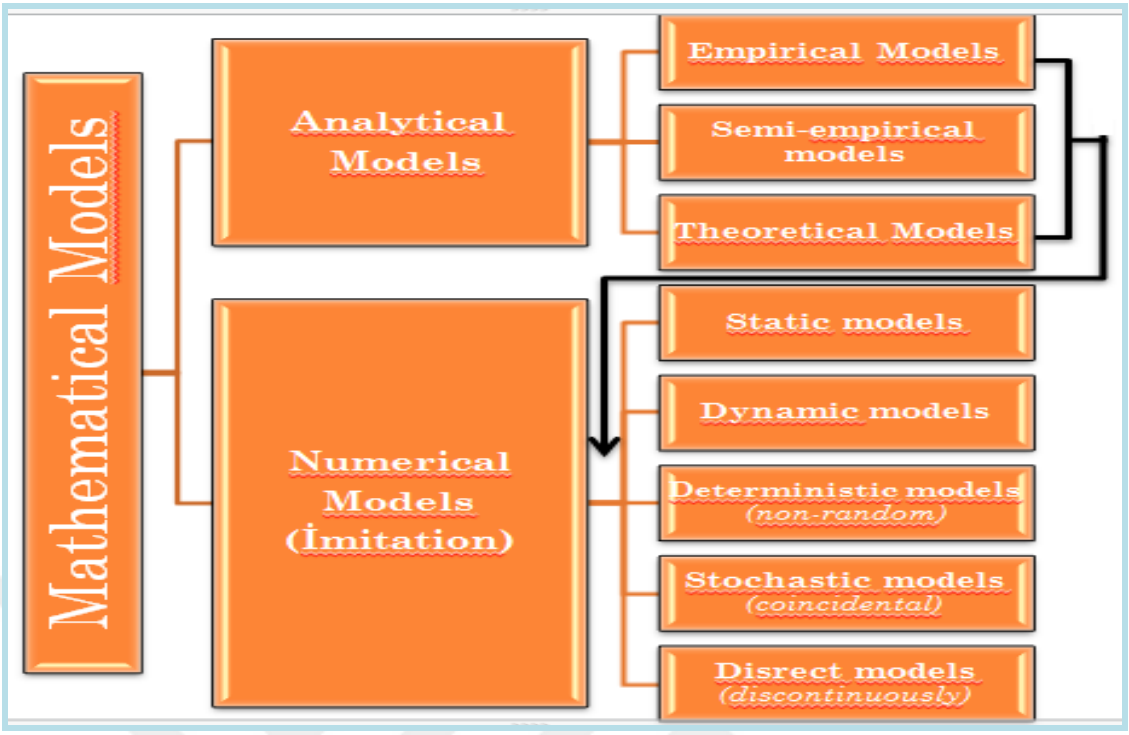

Figure 3.2 General classification of mathematical models (Şımarmaz 2010)

It is possible to collect mathematical models in specific categories in order to understand their nature. Berry and Haouston (1995), classified mathematical models in four categories: experimental models, theoretical models, simulation models, and spatial analysis models. On the other hand, Tedeschi *et al.* (2005) stated that mathematical models can be classified in five or more categories. Empirical models, semi-empirical models, and theoretical models will be discussed in detail in the following sections as we will use them in our study.

Empirical (regression) models are used in agricultural research as well as many other branches of science. Regression models are based on statistical analysis of data and they are generally called as experimental models (Bayraklı *et al.* 1999). In general, these models are the simplest functional models. Such models are used to determine errors in the experimental data and to solve (approximate) problem with a probability (Mikailsoy 2014).

One of the important aspects of the empirical model is determining the structure of the model by computer facilities (analytic expression) and making direct calculations. The

disadvantage of these models is impossibility to contain ecological hypothesis and cause-and-effect relationship between variables in the model (Mikailsoy 2014).

The experimental modeling starts with the detection of the most important factors influencing the system. Depending on the number of important factors, experimental models are divided into two classes as **single** and **multivariate models**.

Ecological facts show that the results arise from a large number of independent variables. Therefore ecological empirical models are often used with multiple numbers of independent variables. In these models, parameter prediction is generally made using the least squares method. Empirical Models are divided into 2 as single variable linear empirical models and multivariate curve empirical models. Determination of the structure of Empirical Models (linear, curvilinear etc.) and identifying and assessment of the degree of compliance with the experimental data are carried out according to certain criteria as described in the model selection section (3.1.4). Curve fitting, also known as regression analysis, is a general technique for modeling. The simplest use of the regression model summarizes the relationship observed in a particular system of data.

Semi-empirical models are composed of analytical expressions of mathematical/ statistical methods. Unlike empirical models, semi-empirical models are developed with mathematical theories, reflecting the fundamental laws of nature. Conservation of mass, the law of conservation of energy, the thermodynamic equations of chemical equilibrium, etc. are typical semi-empirical models (Pachepskii 1990). The semi-empirical models are used widely in soil science. The use of a single language of mathematics in solving various problems representing the different soil characteristics of the system can be investigated with this system of mathematical models.

Theoretical (conceptual) models provide information on the ecosystem components (chemical, physical, biological, etc.). Conceptual models include all the information that can be defined clearly and generally on the surveyed system. Advantages of conceptual

models such as universality, agility, the wealth of expression tools, etc. enable the models to be applied to various systems (Ekberli 2008).

Deterministic models have deterministic input variables and give the same result at each time. In such models, the alternative process is not in question approaching constant valuable is the basis. Deterministic models can be used in modeling controllable environmental, physical, and physiological approaches.

Stochastic models are based on one or more random variables. These models reveal the true behavior of the system only with a probability. Therefore, the model contains elements of probability. Stochastic models are generally applied to on the systems with components of which behavior is uncertain (Platonov and Çudnovski 1984, Zaslavskiy and Poluektov 1988).

Static models are not affected by time. Status of the model does not vary over time. The model which is created in vegetation period between the values of the various phases of plant growth model is a static model, but it can be used in the same period.

Dynamic models are affected by time. A simulation time is concerned. Dynamic models are expressed by difference equations or differential equations. They refer to ecosystem variables and feature of factors that evolve depending on time in dynamic models. To render a model dynamic, one needs to define the significant dynamic characteristics and parameters of the ecosystem. The majority of today's plant growth models are dynamic models.

Discrete (intermittent) models are applied to the data obtained by counting. Data are integers (for example the cells of a bacterium culture on i-th number).

Permanent models are applied to the measured data. These models show the time in a continuous manner (e.g. the lake's water temperature changes throughout the day).

3.1.4. Model selection

The model should be appropriate for the physical structure of the processes to be modeled. The selection of a proper model is based on the nature of the data. Applicability of the model depends on compatibility of the measured and predicted data (Ekberli 2008). Model complexity-scale relation is an important factor in model selection and evaluation. As scale increases, model complexity should be decreased. Application of model in a large area (i.e watershed scale) is highly difficult.

There are number of model selection criteria such as coefficient of determination (R^2**),** adjusted R-squared ($\bar{R}^2$), Akaike Information Criterion (AIC), Bayesian Information Criterion (BIC), Hannan-Quinn Criterion (HQC), Schwarz Information Criterion (SIC), Mallow's Cp Criterion, cross-validation , and many others. All these criteria are based on minimizing residual sum of squares (*RSS).* Detailed information on these criteria can be found in (Lin *et al.* 2011).

3.1.4.1 Model selection criteria

Model selection criteria are widely used in evaluating success of modeling results and ability of a model to repesent the subject system. Some of the widely used model selection criteria are:

1. Coefficient of determination (R^2**)**
2. Adjusted R-squared ($\bar{R}^2$)
3. Akaike Information Criterion (*AIC*)
4. Bayesian Information Criterion (*BIC*)
5. Hannan-Quinn Criterion (*HQC*)
6. Schwarz Information Criterion (*SIC*)
7. Mallow's Cp Criterion
8. Cross-Validation criterion

All these criteria are based on minimizing residual sum of square (*RSS)*. In addition, except R^2, all of them are rewarding to be "thrifty" (parsimonious-stinginess) in the number of explanatory variables.

Complying with the data of the most appropriate model and also success of prediction should be adequate. For the purpose of the comparison of the prediction success of the model, various evaluation criteria are used. Some of these criteria are; residual sum of square, estimate sum of square, total sum of square calculations.

1. Correlation coefficient *(η or r):*

Reliability means consistency and sensitivity in general. One of the most commonly used statistical techniques to determine the validity and reliability of the technique is the correlation coefficient.

Correlation coefficient is a measure of relationship between two or more variables. Correlation shows how the change in one varible is related to other associated variable. If there is a relationship, it enables us to determine the amount and direction of this relationship numerically. *Correlation coefficient* (η) is called the coefficient, which shows the compliance between the two variables (x_i and y_i). Values of the correlation coefficient as related to performance (The scale Cheddoka) are given in Table 3.1.

Table 3.1 Correlation coefficient values and related performance (The scale Cheddoka)

№	Correlation Coefficient	Performance
1	0.10 - 0.29	Poor- Weak
2	0.30 - 0.49	Moderate
3	0.50 - 0.69	Appreciable- Great
4	0.70 - 0.89	High- Strong
5	0.90 - 0.99	Very High- Very Strong

Following parameters are used in calculation (3.67) which is the fundamental theorem of dispersion analysis. These are residual sum of squares: $RSS = \sum_{i=1}^{n} \left(\tilde{y}_i - \bar{y} \right)^2$, Estimate sum of squares: $ESS = \sum_{i=1}^{n} \left(y_i - \tilde{y}_i \right)^2$ and Total sum of squares: $TSS = \sum_{i=1}^{n} \left(y_i - \bar{y} \right)^2$

From here, the following equation is applied for experimental models, which are linear in parameters.

$$\sum_{i=1}^{n} \left(y_i - \bar{y} \right)^2 = \sum_{i=1}^{n} \left(y_i - \tilde{y}_i \right)^2 + \sum_{i=1}^{n} \left(\tilde{y}_i - \bar{y} \right)^2 \qquad (3.2)$$

$$TSS \quad = \quad ESS \quad + \quad RSS$$

Using the equation (3.2), equation for correlation coefficient (3.3) (Pearson 1895) is

$$\eta = \sqrt{1 - \frac{\sum_{i=1}^{n} \left(y_i - \tilde{y}_i \right)^2}{\sum_{i=1}^{n} \left(y_i - \bar{y} \right)^2}} \quad , \ \mathbf{R^2} = \eta^2 \qquad (3.3)$$

Where $y_i -$ is observed values of dependent variable, $\tilde{y} -$ calculated values of the same dependent variable, $\bar{y} -$ is the mean value of the dependent variable.

1. Coefficient of determination (R^2)

Coefficient of determination (R^2) indicates percent of total variation in dependent variable described by the model. The coefficient of determination is a positive value between 0 and 1 and it is the square of the correlation coefficient (Efe *et al.* 2000). The coefficient of determination is calculated as follows:

$$R^2 = 1 - \frac{\sum_{i=1}^{n}(y_i - \tilde{y}_i)^2}{\sum_{i=1}^{n}(y_i - \bar{y})^2} \qquad (3.4)$$

Where $y_i -$ is observed values of dependent variable, $\tilde{y} -$ calculated values of the same dependent variable, $\bar{y} -$ is the mean value of the dependent variable.

The use of R^2 is well established in classical regression analysis (Rao 1973). The coefficients of determination is a measure of goodness of fit and a measure of precision in predictions for the general linear model as described by (Draper and Smith 1966).

When R^2 has been taken as a model selection criterion, we face with some problems (Gujarati 2003). 1). Even if they indicate how actual and predicted vaues are similar, it may not garantee the same resemblance in the future 2) In order to compare succses of different models by R^2, the functional structure of the model and estimators must be the same. For different model structures different R^2s can be used. Some of these are: Maddalena R^2, Gragg- Uh R^2, McFadden R^2, Estrella R^2, Pseudo R^2 (It is similar to McFadden but it is used in probit models). 3) R^2-value increases as the number of explanatory variables in the model increases. Maximum R^2 can be accessed with this method. However, this situation will lead to a rise in forecast error variance. In this case, the use of adjusted coefficient determination is more appropriate. Coefficient of determination and degree of freedom are scaled again since adjusted determination coefficient used mean of square instead of total square. Therefore, it is more appropriate to use the adjusted coefficient of determination in a nonlinear model (Costello and Sit 1994). In addition, in order to avoid difficulties in the interpretation of R^2, some researchers have preferred to use adjusted $\bar{R}^2$ (Haitovski 1969).

2. Adjusted R-squared ($\bar{R}^2$)

Expression for adjusted R-squared developed by Theil (1971) can be calculated as:

$$\bar{R}^2 = 1 - \frac{(n-1)\sum_{i=1}^{n}(y_i - \tilde{y}_i)^2}{(n-k-1)\sum_{i=1}^{n}(y_i - \bar{y})^2} \qquad n < 30$$

Or

$$\bar{R}^2 = 1 - (1 - R^2)\frac{n-1}{n-k-1} \tag{3.5}$$

Where *n*- is the number of the used data; *k*- is the number of variable coefficients of model, R^2 is Coefficient of determination.

The values for $\bar{R}^2$ is always smaller than R^2. The $\bar{R}^2$ is better in terms of comparisons between models, but it should not be forgotten that for a reasonable comparison dependent variable must be same (Ucal 2006).

In model comparisons, model with a greater $\bar{R}^2$ is always preferred. Maximum adjusted $\bar{R}^2$ is a selection criterion that it is identical to minimum residual variance criterion (Ebbler 1975). The adjusted $\bar{R}^2$ is used more in prediction with regressions with least squares. However, it's weak in the Bayesian approach (Burham and Anderson 1998).

3. Standard deviation of mean ($\sigma_{T/t}$)

$$\sigma_{y;x} = \sqrt{\frac{1}{n-m-1}\sum_{i=1}^{n}(y_i - \tilde{y}_i)^2} \Leftarrow (n \le 30)$$

$$\sigma_{y;x} = \sqrt{\frac{1}{n-m}\sum_{i=1}^{n}(y_i - \tilde{y}_i)^2} \Leftarrow (n > 30) \tag{3.6}$$

Where; y_i – is observed values of dependent variable, $\tilde{y}$ – calculated values of the same dependent variable, *n*— is the measuring number of x_i, *m*— is the number of parameters of the empirical model.

This statistic parameter is often used to test the validity of the model applied while several mathematical model is compared (Analla 1998). The Standard deviation of mean indicates how the model fails to estimate the measurements variability around the mean and measures the change in the estimated values around the measured values (Willmott and Matsuura 2005). The lower limit of Standard deviation of mean is 0, which means that there is full compliance between the model estimates and measurements.

4. Mean absolute percentage error, *MAPE* $(\bar{\varepsilon})$

Mean Percentage Error is considered as a basic measure of model performance. Mean Percentage Error is the percentage of the absolute value of the relative error. It shows the average of the absolute values deviation estimated from the measured value. It is stated as:

$$\bar{\varepsilon} = MAPE = \frac{100\%}{n}\sum_{i=1}^{n}\left|\frac{y_i - \tilde{y}_i}{y_i}\right| \tag{3.7}$$

Where y_i – is observed values of dependent variable, $\tilde{y}$ – calculated values of the same dependent variable, *n*- is the number of the data used.

The *MAPE* indicates the distance (deviation) of the mean mean of absolute values calculated as difference between predicted and measured values. Ideally, the *MAPE* and Standard deviation of mean values are near to zero (Willmott and Matsuura 2005). An ε value <10% indicates a good performance of the subject model, while an ε value >10% suggests that the model performance may not be adequate.

5. Agreement index (***Willmott's index of agreement:*** **D*)***

It shows the accuracy of the soil temperature related to measured values (Willmott and Wicks 1980, Willmott 1981, Willmott 1982, Willmott *et al.* 1985).

$$D = \mathbf{1} - \frac{\sum \left(y_i - \tilde{y}_i \right)^2}{\sum \left\{ \left| y_i - \bar{y} \right| + \left| \tilde{y}_i - \bar{y} \right| \right\}^2} \tag{3.8}$$

Where $y_i -$ is observed values of dependent variable, $\tilde{y} -$ calculated values of the same dependent variable, $\bar{y} -$ is the mean value of the dependent variable. The Willmott's Index varies between 0 and 1.0, 1.0 indicating the perfect fit.

6. The confidence index (C)

Confidence index *(C)* is obtained via multiplying compatibility index *(D)* by correlation coefficient *(η).*

$$C = \eta \cdot D \tag{3.9}$$

This index was used by Camargo and Sentelhas in (1997).

Table 3.2 Criterion for interpretation of the confidence index (C).

№	Confidence index	Performance	Symbol
1	> 0,85	Best	B
2	0,76 to 0,85	Very good	VG
3	0,66 to 0,75	Good	G
4	0,61 to 0,65	Fair	F
5	0,51 to 0,60	Bad	B
6	0,41 to 0,50	Very bad	VB
7	≤ 0,40	Worst	W

7. Theil's Forecast Accuracy Coefficient

In 1958, Henry Theil defined two error measures. The first measure (*U*1*)* was proposed in Theil (1958). The *U*1 compares the forecast with simple no-change model. *U*1 takes any value between 0 and 1. A value of 0 means perfect predictive performance, while 1 means that forecast is not better than just using last actual observation as a forecast. Bliemel (1973) analyzed *U*1 and concluded that it "has little or no value as an index to assess forecast accuracy". The value of 1 will be obtained only when a forecaster applies the simple no-change model. All other forecasts would lead to *U*1 value lower than 1, regardless of whether the forecast method led to better or worse performance than the naïve no-change model. Bliemel (1973) suggested applying later version of Theil's statistic *U*2.

Theil's U-statistic 1 is defined as:

$$U1 = \frac{\sqrt{\sum_{i=1}^{n}(y_i - \tilde{y}_i)^2}}{\sqrt{\sum_{i=1}^{n} y_i^2} + \sqrt{\sum_{i=1}^{n} \tilde{y}_i^2}}, \tag{3.10}$$

The second measure (*U*2) was proposed in Thiel (1966). The *U*2 shows whether the forecast is better than simple forecast, which is 0 all the time. For *U*2 holds that value equal to 0 confirms perfect forecast. Value lower than 1 means that forecast beat the naive forecast and value higher than 1 means that forecast is worse than naive forecast.

Theil's U-statistic 2 is given by the equation:

$$U2 = \frac{\sqrt{\sum_{i=1}^{n}(y_i - \tilde{y}_i)^2}}{\sqrt{\sum_{i=1}^{n} y_i^2}} \tag{3.11}$$

8. Akaike Information Criterion *(AIC)*

Akaike criterion (*AIC*) was developed by Hirotugu Akaike in 1974. There are multiple *AIC* definitions.

$$AIC = e^{2k/n\sum \hat{u}_i^2} / n = e^{2k/n} ESS / N \quad \text{or} \quad AIC = -2\ell\left(\hat{\theta}\right) + 2\left(k\right) \tag{3.12}$$

Where $\ell\left(\hat{\theta}\right)$, shows the possibility of most log which is a function of the parameter. *ESS* is estimate sum of square, *n*- is the number of the used data; *k*- is the number of variable coefficients of model, *N*- sample number.

The logarithmic form:

$$\ln AIC = \left(2k / n\right) + \ln\left(ESS / n\right)$$

Or

$$\mathbf{AIC} = \ln\left(\frac{ESS}{n}\right) + \frac{2m}{n} = \ln\left[\frac{1}{n}\sum_{i=1}^{n}\left(y_i - \tilde{y}_i\right)^2\right] + \frac{2m}{n} \tag{3.13}$$

Where *ESS* is estimate sum of square, y_i is observed values of dependent variable, $\tilde{y}$ calculated values of the same dependent variable, *n*- is the number of the used data; *k*- is the number of variable coefficients of model, *m*- is the number of parameters of the empirical model.

Zuchini (2000) developed *AICc* for small sample time-series regression model, which has the form:

$$AIC_c = AIC + 2k\left(k+1\right) / \left(n-k-1\right)$$

Or

$$\mathbf{AIC_c} = \ln\left[\frac{1}{n}\sum_{i=1}^{n}\left(y_i - \tilde{y}_i\right)^2\right] + \frac{2m(m+1)}{n-\left(m+1\right)} \ , \left(\frac{\mathbf{n}}{\mathbf{m}} < \mathbf{40}\right) \tag{3.14}$$

The smaller is the *AIC* the better is the suitability of the model. The biggest advantage of *AIC* criteria is its being able to use both inside and outside of the sample for comparing model the performance.

9. Bayesian Information Criterion *(BIC)*

The BIC has was described as follows (Akaike 1978; Schwarz, 1978):

$$BIC = -2\ell\left(\hat{\theta}\right) + k\,\mathbf{log}\,n \qquad \text{or} \qquad BIC = \ln\left[\frac{1}{n}\sum_{i=1}^{n}\left(y_i - \tilde{y}_i\right)^2\right] + \frac{m}{n}\ln n \tag{3. 15}$$

Where $\ell\left(\hat{\theta}\right)$ shows the possibility of most log which is a function of the parameter, y_i is observed values of dependent variable, $\tilde{y}$ calculated values of the same dependent variable, *n*- is the number of the used data; *k*- is the number of variable coefficients of model, *m*- is the number of parameters of the empirical model.

BIC differs from *AIC* in that second part depends on sample size on the right side of the equation. Despite close similarities between the *AIC* and *BIC*, later differs from the former in Bayesian structure (Raftery 1995, Weasserman 2000).

The *BIC* criterion is preferred when the number of parameters is low. Similar to *AIC*, a smaller *BIC* value indicates better model performance (Schwarz 1978, Alzahal *et al.* 2007).

10. Hannan-Quinn Criterion *(HQC)*

Another criterion, used in model selection, is HQC, which was recommended by Hanmam and Quinn (1979):

$$\mathbf{HQC} = \ln\left(\frac{ESS}{n}\right) + \frac{2p}{n}\cdot\left[\ln\left(\ln n\right)\right] = \ln\left[\frac{1}{n}\sum_{i=1}^{n}\left(y_i - \tilde{y}_i\right)^2\right] + \frac{2p}{n}\cdot\left[\ln\left(\ln n\right)\right] \tag{3.16}$$

Where *ESS* sum of square of residuals (predicted-measured values), y_i is observed values of dependent variable, $\tilde{y}$ calculated values of the same dependent variable, *n* is the number of the used data; *p* is the number of parameters.

Hannan and Quinn (1979) suggested that *HQC* is superior to its alternatives since it uses the iterative algorithm law. The *HQC* is common used as the other two criteria. Similar to *AIC* and *BIC* A smaller value for *HQC* indicates a better model performance.

11. Schwarz Information Criterion *(SIC)*

Schwarz Information Criteria (*SIC)* is similar to *AIC* and it's expressed as (Schwarz 1978):

$$SCI = n^{k/n}\frac{\sum \hat{u}^2}{n} = n^{k/n} ESS / n$$

In logarithmic form:

$$\boldsymbol{ln}\, SCI = \frac{k}{n}\boldsymbol{ln}\, n + \boldsymbol{ln}\left(ESS / n\right) \qquad (3.17)$$

Where *ESS* is estimate sum of square, *n*- is the number of the used data; *k*- is the number of variable coefficients of model. Compared to *AIC*, *SIC* is more sensitive to new variables included in the model and in the same conditions *SIC* always takes a lower value than *AIC*.

12. Mallow's *Cp* Criterion

Mallow model selection criteria (shortly Cp criterion) developed by Mallows (1973,1995) is:

$$C_P = \frac{ESS_p}{\hat{\sigma}^2} - \left(n - 2p\right) \qquad \text{Or} \qquad C_p = \frac{\sum_{i=1}^{n}\left(y_i - \tilde{y}_i\right)^2}{S^2} - \left(n - 2p\right) \qquad (3.18)$$

Where $\left(\hat{\sigma}^2\right)$ is the zero order estimator of the groundmass variance. *ESS* is estimate sum of square, y_i is observed values of dependent variable, $\tilde{y}$ calculated values of the same dependent variable, *n*- is the number of the used data; *p*- is the number of parameters.

If p explanatory variables are sufficient for an effective prediction, $\left(ESS_P\right)=\left(n-p\right)\sigma^2$. As a result,

$$E\left(C_P\right)\approx\frac{\left(n-p\right)\sigma^2}{\sigma^2}-\left(n-2p\right)\approx p \tag{3.19}$$

When models are compared within the parsimony principle under p<k, the model which gives the lowest *Cp* values is preferred (Gujarati 2003).

13. Cross-validation ***(Q_{CV})***

If square errors are going to be used, as a good left-one-outside-cross-validation estimator can be considered as a good estimator. This method may be used based on model performance (Saho 1993). The cross validation criterion has the following form:

$$Q_{CV}=\frac{1}{n}\sum_{j=1}^{n}L\left(y_j,\hat{y}_j\right)=\frac{PRESS}{n} \tag{3.20}$$

Where *PRESS* is prediction error sum of square, while expression $L\left(y_j,\hat{y}_j\right)$ can be explained by $L\left(y_j,\hat{y}_j\right)=\left(y_j-\hat{y}_j\right)$ (Banke and Drage 1984). Instead of coefficient, which located in regression model is going to predict only one time, it is repeated many times with left-outside-one.

Also, $Q_{CV}=\frac{1}{n}\sum_{j=1}^{n}L\left(y_j,\hat{y}_j\right)=\frac{PRESS}{n}$ can compare with $s^2 = ESS/(n-p)$

Where; N = number of observations, p = number of parameters including the constant term, and *ESS* = estimate sum of square. But Q_{CV} will always give greater value than s^2, while *PRESS* gives generally close results to s^2 (1 + p / n) (Hjorth 1994).

The sum of the squares of the difference between predicted and observed values gives the *PRESS* value for that model. *PRESS* criterion shows how explanatory variable and calculates as follows:

$$PRESS = \sum_{i}^{n} \left[y_i - \hat{y}_{i(i)} \right]^2$$

Where $\hat{y}_{i(i)}$ represents the estimated value of y_i.

14. Teta *(θ)*

Reliability of a linear and/or curvilinear model may be evaluated by the criterion θ which is calculated by (3.21).

$$\theta_\eta = \frac{\eta}{1-\eta^2}\sqrt{n} \qquad (3.21)$$

The θ is used to compare the different models for their performance and properness. A greater value for θ indicates a better performance of the model (Mirzadzhanzade and Shirinzade 1986).

15. Fisher Criterion

Fisher (1949) developed a procedure for making pairwise comparisons among a set of t population means. The procedure is called Fisher's least significant difference (LSD).

The α -level of Fisher's LSD is valid for a given comparison only if the LSD is used for independent (orthogonal) comparisons or for preplanned comparisons. However, since many people find Fisher's LSD easy to compute and hence use it for making all possible pairwise comparisons (particularly those that look ''interesting'' following the

completion of the experiment), researchers recommend applying Fisher's LSD only after the F- test for treatments has been shown to be significant. This adjusted approach is sometimes referred to as Fisher's protected LSD. Carmer and Swanson (1973) suggest that the error rate for the protected LSD is controlled on an experiment wise basis at a level approximately equal to the α -level for the F test (Ott and Longnecker 2001). The corredponded F-value is calculated as follows.

$$F = \frac{R^2}{1-R^2} \cdot \frac{n-k-1}{k} = \begin{cases} \frac{R^2}{1-R^2} \cdot (n-2) \leftarrow k = 1 \\ \frac{R^2}{1-R^2} \cdot \frac{n-3}{2} \leftarrow k = 2 \end{cases} \quad (3.22)$$

Where *n*- is the number of the used data; *k*- is the number of variable coefficients of model, R^2 is Coefficient of determination.

Several remarks should be made concerning the LSD method for pairwise comparisons. First, there is a possibility that the overall F-test in our analysis of variance is significant but that no pairwise differences are significant using the LSD procedure. Second, Fisher's LSD procedure can also be used to form a confidence interval for $\mu_i - \mu_j$ (Ott and Longnecker 2001).

Models should not be selected by only one criterion since inconsistencies can be observed between the criteria. For example, when we look at AIC and BIC, we may encounter with inconsistencies. In this case third or more selection criteria should be referred.

3.2. Soil Heat and Soil Temperature

3.2.1. Soil heat

Soil temperature is the average kinetic energy per calorie (C) or joule (J) (1C = 4.18 Joule) arising from vibration of molecules/atoms in soil elements. The main source of soil heat is the energy from the sun.

Radiation from the sun propagates through atmosphere before it reaches to the earth's surface (Fig. 3.3). Some of the incoming radiation is scattered while passing through the atmosphere. The thermal radiation is emitted and absorbed in atmosphere principally by water vapor and CO_2. The atmosphere acts almost like a blackbody in some wavebands, while in some other wavebands the absorptive and emissivity are low (Campbell and Norman 1998). Some of the radiation is reflected back from the atmosphere mainly by clouds (Fig. 3.3).

Some of the incoming radiation is absorbed in soil surface, rising temperature. From the heated soil surface, heat is transferred into soil due to the increased temperature differences between soil surfaces and under surface, and is emitted to atmosphere. Some of the heat stored in the soil is used in evaporation. Besides solar radiation, a limited amount of heat is released during the decomposition of organic matter in soil (Fırat 1998).

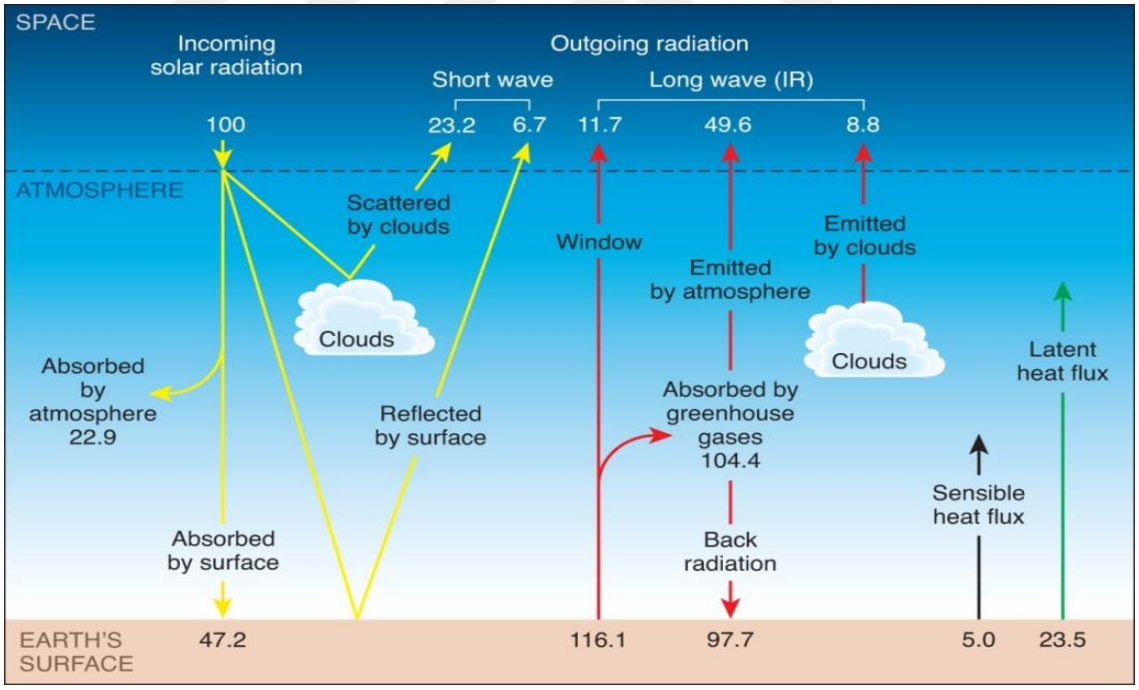

Figure 3.3 Distribution of incoming solar radiation
http://www.ametsoc.org/amsedu/ECS/extras/figure4-13.jpg

Altitude, time of the year, time of the day, weather conditions, and surface properties are important determinants of partitioning solar radiation on a soil surface. Heat is transferred into soil during the day and from soil to atmosphere during night. The rate of transfer is controlled by soil thermal properties and temperature difference between soil and soil surface (Campbell and Norman, 1998).

Temperature is an important factor controlling rates of physical, chemical and biological processes. Effect of temperature on the rate of soil microbiological processes is considerable, which in turn influence organic matter decomposition and nitrogen mineralization. Accumulation of organic matter in the soil is higher at low temperatures than high temperatures. In addition, soil temperature has a considerable influence on seed germination (Saatçı 1975).

3.2.2. Soil temperature

Soil temperature is a measure of heat content of the soil and its unit is degree. In other words, while heat expresses the total kinetic energy of all molecules of a substance; temperature is a function of the heat density (Lowry 1970). For example, although heat quantity of 3000 kg substance, which is at 10 ° C is higher than a 100 kg stove which is at 200 ° C, the stove is hotter (has a greater temperature). While heat is a capacity factors such as water content; temperature is a density factor such as water potential (Taylor and Ashcroft 1972). Soil temperature depends on irradiance as well as soil thermal properties (radiation, heat capacity, thermal conductivity, etc.) (Yeşilsoy and Aydın 1995).

3.3. Radiation and soil heat balance

According to the second law of thermodynamics, if the temperature difference is available between the two media, heat flows from a low temperature medium to a high-temperature medium. The heat transfer depends on the difference in ambient temperature as well as thermal properties of the media where transfer occurs (Kakaç 1998, Halıcı 2001).

Heat transfer occurs via four modes: Conduction, Convection, Radiation, and Adiabatic. When two substances with different temperatures are in contact, heat is transferred from the hotter one to colder one by conduction. Heat transferred by a moving fluid is called convection. In this mode of heat transfer the heat is transferred to a fluid by conduction and moving fluid transport the heat, stored in the fluid. In contrast to convection and conduction, radiative exchange does not require intervening molecules to transfer energy from one substance to another. A substance radiates energy depending on its temperature. Both the sun and earth emit radiation, but due to its far higher temperature, the Sun emits for greater radiation than the Earth. Much of the energy we receive from a hot stove is by radiation. Finally, to evaporate 1 g of water, 2450 joules energy is required. Evaporation of water from a surface needs energy and this energy is taken from the surface. The latent heat stored in the vapor is transferred away from the substance by convection (Campbell and Norman 1998).

3.3.1. Heat absorption of soil

Solar radiation received by an object is classified in three main categories as direct radiation, diffuse radiation, and reflected radiation. The direct radiation comes directly from the Sun, the diffuse radiation is first scattered by the clouds and then reaches to the object, and the reflected radiation first is reflected by terrestrial objects and the reaches to the object (Campbell and Norman 1998).

Heat stored in a soil is proportional to albedo, defined as ratio of incoming radiation to outgoing (reflected) radiation. Values of albedo Ratio between the reflected energy from the soil surface and the incoming energy ratio is called as "albedo" and in case of other features are equal, while albedo decreases, soil temperature increases. Albedo values in for different soil types and different vegetation are given in Table 3.3 and Figure 3.4.

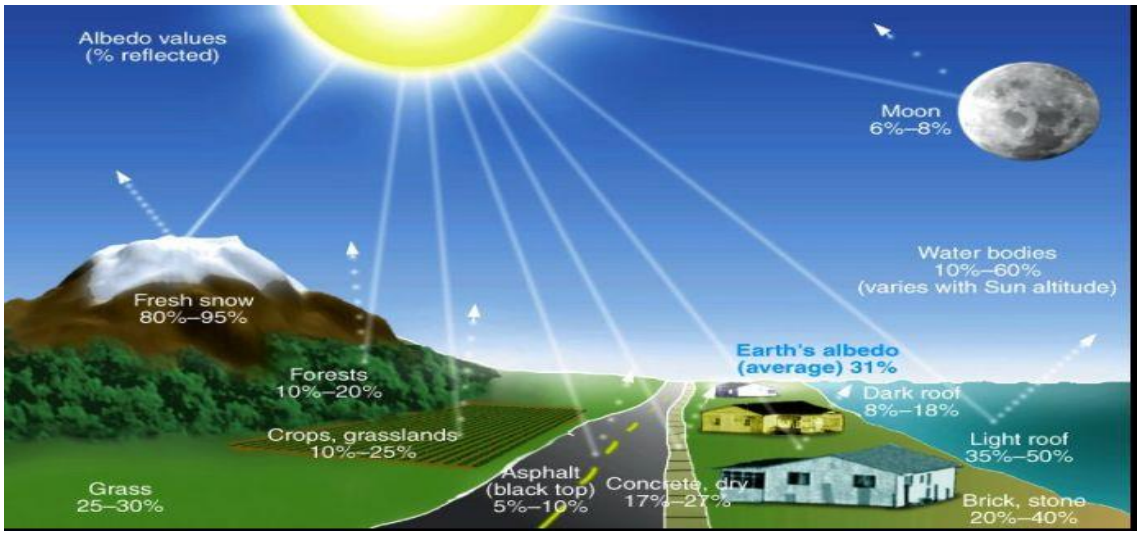

Figure 3.4 Some albedo values that the sun rays created on earth
http://regentsearth.com/ILLUSTRATED%20GLOSSARY/Glossary%20Pix/Albedo.jpg

Table 3.3 Values for albedo (α) for various surfaces (Van Wijk and De Vries 1966, Chudnovskii 1967)

Soils	**Albedo (α)**	**Vegetation**	**Albedo (α)**
Soil	0.05-0.40	Agricultural Crops	0.18-0.25
Dry Chernozem (Dark)	0.14	Grass (Dry- Green)	0.16-0.26
Humid Chernozem (Dark)	0.08	Cereal Field	0.10-0.25
Dry Serozem (Gri)	0.25-0.30	Cotton	0.20-0.22
Humid Serozem (Gri)	0.10-0.12	Rice	0.12
Humid Clay	0.23	Potato	0.19
Dry damp clay	0.16	Forest (Deciduous)	0.15-0.20
Dark damp clay	0.02-0.08	Forest (Coniferous)	0.05-0.15
Sand	0.15-0.45	Humid steppe	0.22
White and Yellow sand	0.34-0.40	Dry steppe	0.32
Quartz sand	0.35	Sawn area	0.15-0.17
Humid sand	0.09	Humid cultivated land	0.05-0.14
Lime	0.45	Water (Small Zenith Angle)	0.03-0.10
Dried salt	0.50	Water (Large Zenith Angle)	0.10-1.00
Tundra	0.18-0.25	Snow	0.40-0.95
Clouds (Thick)	0.60-0.90	Ice (Sea)	0.30-0.45
Clouds (Thin)	0.30-0.50	Ice (Glacier)	0.20-0.40

https://wattsupwiththat.files.wordpress.com/2012/05/table_11.jpg

The amount of solar radiation retained by the soil surface varies depending on location (geographical position and relief of region), time (day, month and year on) and atmosphere conditions (cloudiness).

The heat stored in soils during the day is released during night. The daily change of the soil temperature is sinusoidal (Özbek 1990). Average monthly change of soil temperature measured below 10 cm of soil is shown in Figure 3.5 (Davis 1986).

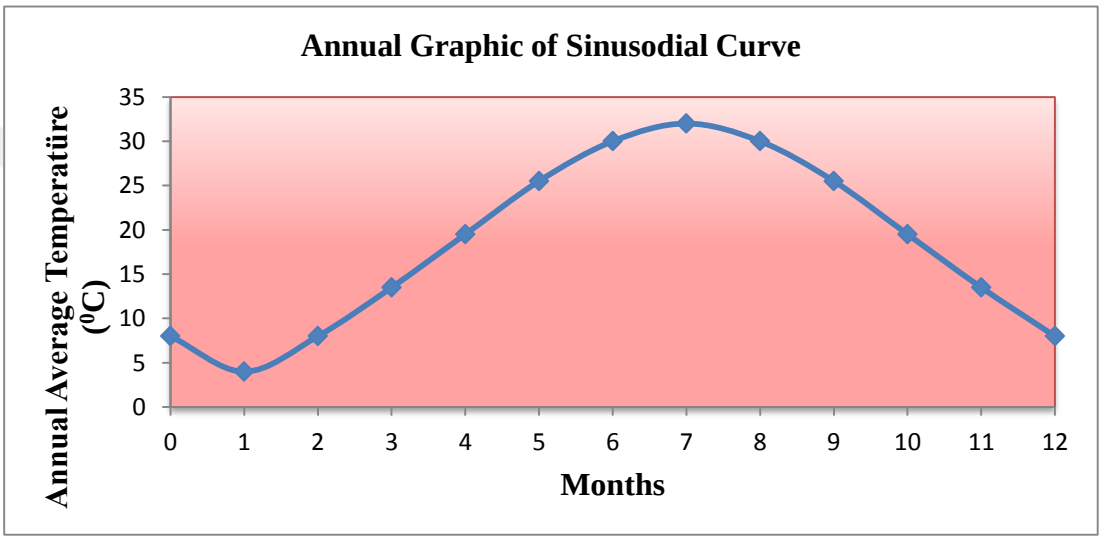

Figure 3.5 Soil sinusoidal curve of the change over 12 months measured temperature under 10 cm of soil (Davis 1986).

Heat resulting from chemical and biological processes in the soil may be concerned. However, their contribution to soil temperature is too low in comparison with the energy coming from the sun (Baver *et al.* 1972, Yeşilsoy 1975, Özkan 1985).

Spectral distribution of the radiation energy based on wavelength, which arrives in the atmosphere, is shown in Figure 3.6. The Sun emits radiation at 6000 °K, which is similar to the black body.

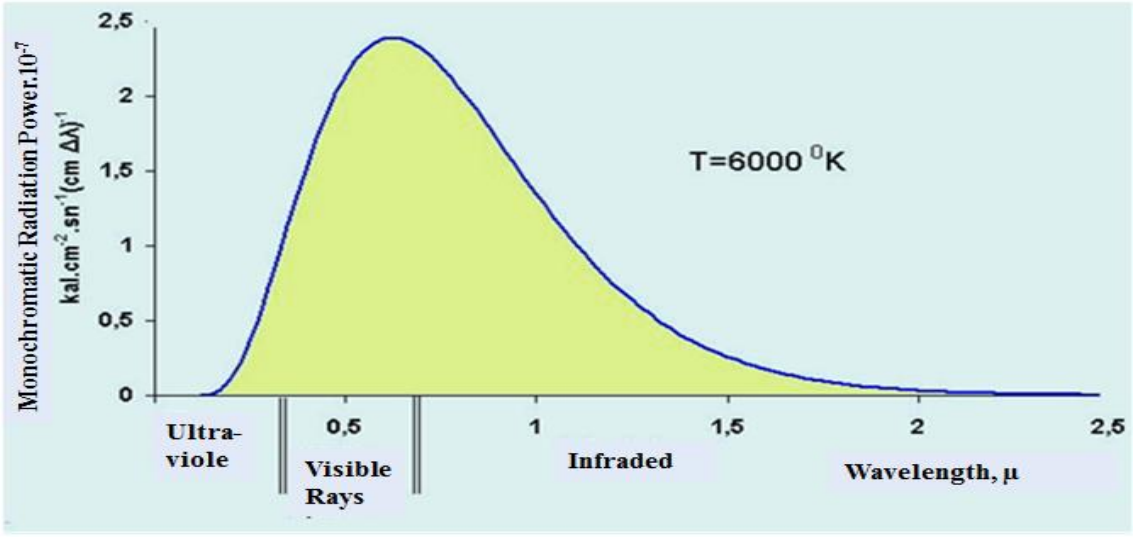

Figure 3.6 Distribution of radiation energy of a black body at the solar heat based on wave length (Rose 1979)

3.3.3 Soil Heat balance

The solar radiation and heat arising from chemical and biological reactions in soils are the source of soil temperature. The soil heat balance may be defined by Eq. (3.23):

$$R = A + P + M + LE + LT \tag{3.23}$$

Where R earth's radiation balance; A heat exchange between lower layers and the surface; P the turbulent heat exchange (the warm air near the earth's surface); M the part of the energy used in photosynthesis and transpiration; E energy used for evaporation from the soil (g.H_2O cm^{-2} day^{-1}); L specific heat of evaporation (approximately 2257 joule/gram= 540 g^{-1} cal H_2O); LE is the portion used for evaporation (525 cal cm^{-2} day^{-1}); LT is the portion used for transportation.

Balance of heat flow at soil surface may be described as follows (Kurtener and Chudnovskii 1979, Krarti *et al.* 1995):

$$Q^{\downarrow}_{heat\ flow}(t) = \underbrace{\left[Q^{\downarrow}_{SR}(t) + Q^{\downarrow}_{CE}(t)\right]}_{incoming\ heat\ flow} - \underbrace{\left[Q^{\uparrow}_{LR}(t) + Q^{\uparrow}_{LE}(t)\right]}_{outgoing\ heat\ flow} \tag{3.24}$$

Where; $Q^{\downarrow}_{heat\ flow}$ is directed heat flow to the soil surface; $Q^{\downarrow}_{SR}$ is the solar radiation absorbed by soil surface; $Q^{\downarrow}_{CE}$ is convective heat flow in the soil-air boundary layer; $Q^{\uparrow}_{LR}$ is the long-wave radiation emitted by the earth's surface; $Q^{\uparrow}_{LE}$ is the portion of heat which is used in vaporization.

Experimental values obtained for each component of heat flow function on the right hand side showed that the soil surface temperature T_{sur} found to be a function of time $f(t)$ and is generally illustrated as follows:

$$Q_i(t) = n_i(t)\mathrm{T}_{sur}(0,t) - f_i(t) \tag{3.25}$$

Where T_{sur} the soil surface temperature and i; SR, CE, LR, LE

All objects with above absolute zero emits heat by radiation, which is defined as thermal radiation.

According to the law of conservation of energy; sum of absorbed (ρQ), reflected (αQ) and transmitted (βQ) radiation energy is equal to total heat energy of short wavelength solar radiation (Q_S). According to the energy balance:

$$Q_S = \rho Q + \alpha Q + \sigma Q \tag{3.26}$$

Where ρ (absorptivity), α(reflectivity), and σ **(**transmissivity) are constants. The Eq. (3.26) shows that the heat energy which comes by radiation will be absorbed, reflected, and transmitted. If incoming radiation energy is unity, it can be written as:

$$1 = \rho + \alpha + \beta \tag{3.27}$$

As $\alpha = \dfrac{\alpha Q}{Q_S}$, then

$$\rho Q = (1-\alpha) Q_S \tag{3.28}$$

Thus absorbed energy, (ρQ) at per unit soil area, will be equal to the outgoing and stored net energy from unit area. Thus the following equation can be written for the earth's radiation balance:

$$\rho Q = (1-\alpha) Q = Q_0 + Q_a + Q_i + E \quad \text{Cal. cm}^{-2}\ \text{sn}^{-1} \tag{3.29}$$

Where; Q is the shortwave radiant flux density from the sun and from hemisphere to the earth; Q_0 is the long wavelength radiant flux density emitted by the surface; (The difference between the emitted and absorbed long wavelength radiation); Q_a is the heat flow density that is used in heating the air near the ground surface; Q_i is the density of the heat transmitted to the soil; *E* is the amount of heat used to evaporate water. Analytical solutions of the Eq. (3.29) were developed for various initial and boundary conditions (Crank 1956, Carslaw and Jaeger 1959).

3.4. Heat Conduction Equations in Soil

The soil is assumed uniform in heat conductivity and thermal conditions in applying mathematical definitions (Özkan 1985). Heat transfer may occur via one of any of four ways of conduction, convection, radiation, and adiabatic. These heat transfer forms can be found simultaneously in the same environment. As soil is a three-phase system, all four heat transfer modes can be found in soils (Kırda and Sarıyev 2002).

3.4.1. The general equation of heat conduction in a cartesian coordinate system

The concept of conservation of energy can be applied in developing a differential equation to define soil temperature change. In general, heat transfer in soil by conduction is the most important heat exchange parameter. As stated previously, heat transfer by convection of moving soil air and water may be important in some cases.

Fourier's transient equation can be obtained via applying the steady state equation with the principle of conservation of energy in a control volume as shown in Figure 3.7.

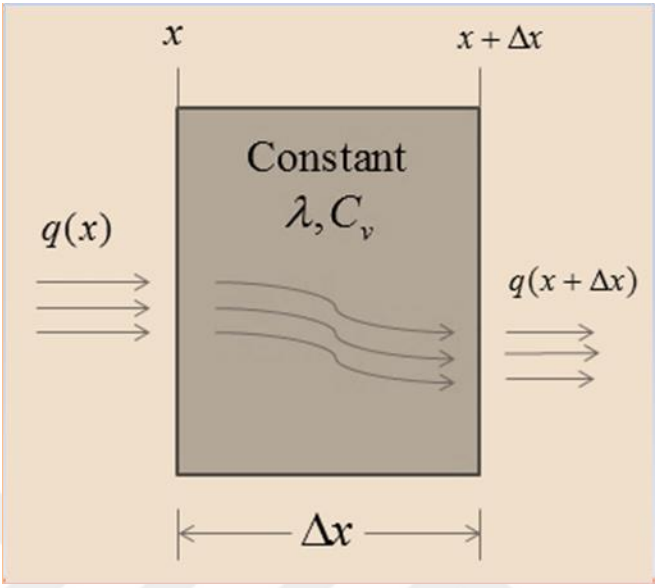

Figure 3.7 Schematic representation for the expression of differential equations of heat transfer (Kakaç 1998)

This control volume may be considered as heat flow with a perpendicular direction to the homogenous sheet surface with area of *A* and thickness of *Ax*. According to the law of conservation of energy, net heat flow at the exit of the control volume is a function of heat entering into the volume and heat stored in the volume.

Conservation of energy equation;

$$-\lambda A\frac{\partial T}{\partial x}(x) = -\lambda A\frac{\partial T}{\partial x}(x+\Delta x) + C_v A\Delta x\frac{\partial T}{\partial x} \tag{3.30}$$

Dividing control volume by *Ax*;

$$\lambda\left[\frac{\partial T}{\partial x}(x+\Delta x) - \frac{\partial T}{\partial x}(x)\right] / \Delta x = C_v\frac{\partial T}{\partial x} \tag{3.31}$$

When Δx approaches 0;

$$\lambda\frac{\partial^2 T}{\partial x^2} = C_v\frac{\partial T}{\partial t} \tag{3.32}$$

Hence, Equation (3.33) is widely used to describe one dimensional heat conduction in a homogenous soil where no heat is generated (Carslaw and Jaeger 1959, Kurtener and Chudnovskii 1979, Yeşilsoy and Aydın 1995).

$$\frac{\partial \mathrm{T}}{\partial t} = \kappa \frac{\partial^2 \mathrm{T}}{\partial x^2} \quad , \quad \left(\kappa = \frac{\lambda}{C_v} \right) \tag{3.33}$$

Where; κ is coefficient of heat diffusivity and $C_v = \rho_b C_m$ is volumetric heat capacity of soil. This equation is valid when λ and C_v is not dependent on space and time and soil conditions are uniform (Van Wijk and De Vries 1966, Koorevaar *et al.* 1975, Koorevaar *et al.* 1983).

Equations define heat conductivity in a three-dimensional homogenous-isotropic environment. The Equation (3.34) is a parabolic partial differential equation and it's called Fourier equation (Carslaw and Jaeger 1959):

$$\rho_b C_m \frac{\partial \mathrm{T}}{\partial t} = \frac{\partial}{\partial x}\left(\lambda \frac{\partial \mathrm{T}}{\partial x} \right) + \frac{\partial}{\partial y}\left(\lambda \frac{\partial \mathrm{T}}{\partial y} \right) + \frac{\partial}{\partial z}\left(\lambda \frac{\partial \mathrm{T}}{\partial z} \right) + q \tag{3.34}$$

Where; $\frac{\partial \mathrm{T}}{\partial x}$, $\frac{\partial \mathrm{T}}{\partial y}$, $\frac{\partial \mathrm{T}}{\partial z}$ is show temperature changes in the direction of the *ox*, *oy*, *oz* axis; $\frac{\partial \mathrm{T}}{\partial t}$ is the temperature change per unit time; C_m is specific heat capacity; ρ_b is bulk density; λ is heat conductivity of soil; and q is the heat, which is generated in soil (if any).

Since soil heat exchange is different in the day and night, summer and winter, temperature changes in the soil must be evaluated on a daily and annual basis. In both cases the soil temperature generally shows a sinusoidal variation (Davis 1986, Şımarmaz 2010).

3.5. Initial and Boundary Conditions of Heat Convection Model in Soils

To find a single solution of changes in the depth of a time-varying soil temperature as a result of the influence of various factors, analytical or numerical solution of (3.33) should be obtained. For this purpose initial and boundary conditions should be set.

3.5.1. Initial conditions

The initial conditions correspond to the state of the variable at the zero (initial) time moment. For the theoretical description of the quasistationary regime problem (e.g., the daily or annual variation of the soil temperature), the initial condition is available. Initial conditions for Equation (3.33) are defined as follows:

$$\mathrm{T}(x, t=0) = f(x) \tag{3.35}$$

3.5.2. 1st, 2nd, 3rd and 4th boundary conditions in soil surface

First type boundary condition: On soil surface, at $x = 0$, the temperature distribution can be fixed or be variable as a function of time.

If the surface temperature does not change, then the **first type boundary condition** is set as follows:

$$\mathrm{T}(x = 0, t) = \mathrm{T}_0 \tag{3.36}$$

Where; T_0 is temperature at the soil surface.

According to some authorities, the surface temperature may not be constant and they suggest Equation (3.37) be used instead:

$$\mathrm{T}(x = 0, t) = \varphi(t) \tag{3.37}$$

Where; $\varphi(t)$ is a function expressing the temporal change in temperature at the soil surface.

If temporal temperature change of the soil surface is sinusoidal (as analyzed by Fourier) the analytical solution of $\varphi(t)$ can be stated as follows (Van Wijk and De Vries 1966, Krarti *et al.* 1995, Verhoef 2004):

$$\varphi(t) = \mathrm{T}_0 + \mathrm{T}_a \cos\left(\omega t + \varepsilon\right) \quad \text{or} \quad \phi(t) = \mathrm{T}_0 + \mathrm{T}_a \sin\left(\omega t + \varepsilon\right) \qquad (3.38)$$

Where T_0 is average temperature at soil surface (daily, annual); T_a is expresses the maximum change of average temperature of the soil surface, wave amplitude; $\omega = 2\pi / \tau_0$ is angular frequency (ω is sometimes called as wave number or frequency). τ_0 is period or wave length; t is time (day, year); ε is phase difference, which adjusts the delay axis according to the sinusoidal curve of the abscissa (Figure 3.8).

In some cases (3.38) may be stated as follows, which is more practical.

$$\varphi(t) = \mathrm{T}_0 + A\cos\omega t + B\sin\omega t \qquad (3.39)$$

$$\text{Where}, \quad A = \mathrm{T}_A \cos\left(\varepsilon\right), \; B = -\mathrm{T}_A \sin\left(\varepsilon\right), \qquad \varepsilon = \arctan\left(-\frac{B}{A}\right) \qquad (3.40)$$

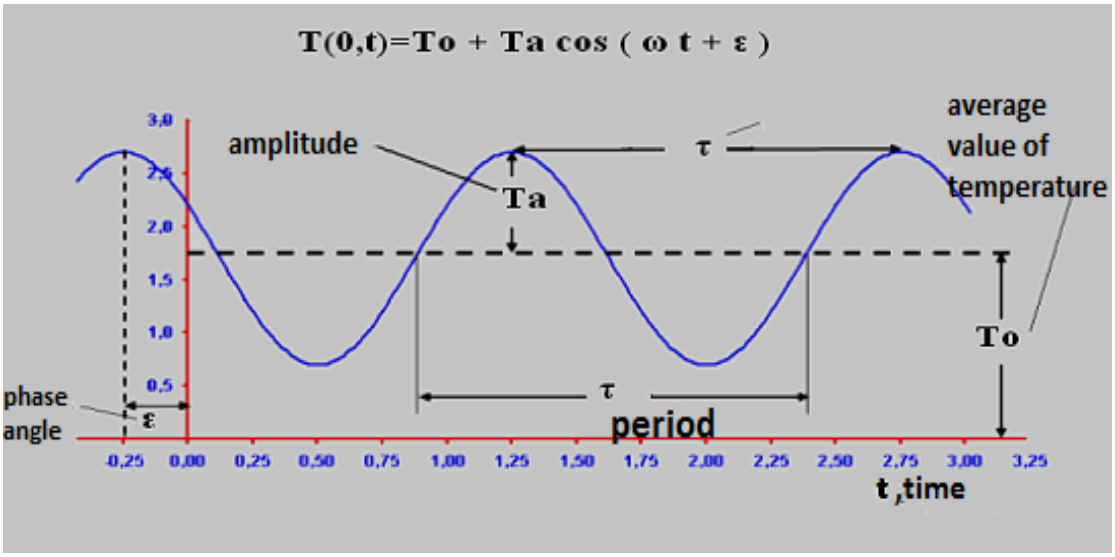

Figure 3.8 The curve for change of temperature on the soil surface (Şımarmaz 2010)

If soil surface temperature $\tau_0 = 2\pi/\omega$ is a periodical function, the function $\varphi(t)$ can be stated as a trigonometric polynomial (Carslaw and Jaeger 1959, Chudnovskii 1976, Mikayilov and Shein 2010):

$$\varphi(t) = \mathrm{T}_0 + C_1 \cos\left(\omega t + \varepsilon_1\right) + C_2 \cos\left(2\omega t + \varepsilon_2\right) + \ldots = \mathrm{T}_0 + \sum_{n=1}^{m} C_n \cdot \cos\left(n\omega t + \varepsilon_n\right) \qquad (3.41)$$

Or
$$\varphi(t) = \mathrm{T}_0 + \sum_{n=1}^{m} \left[A_n \cos\left(n\omega t\right) + B_n \sin\left(n\omega t\right) \right] \qquad (3.42)$$

Where

$$A_n = C_n \cos\left(\varepsilon\right), \quad B_n = -C_n \sin\left(\varepsilon\right), \quad C_n = \sqrt{A_n^2 + B_n^2}, \quad \varepsilon_n = \arctan\left(-\frac{B_n}{A_n}\right) \qquad (3.43)$$

Second type boundary condition: Heat flow per unit area of soil surface is constant. If heat flux density $Q(0,t)$ is known, the second type **boundary condition** is applied:

$$Q(0,t) = -\lambda \frac{\partial \mathrm{T}(0,t)}{\partial x} = \psi(t) \qquad (3.44)$$

Where; $\psi(t)$ is the algebraic sum of radiant flux at the soil surface.

Third type boundary condition: Second type boundary condition described above, cannot account for influence of changes in meteorological parameters on soil temperature.

Third type boundary condition is applied to vertical heat exchange between the soil surface and subsurface.

$$Q^{\uparrow}(0,t) = -\lambda \frac{\partial \mathrm{T}(0,t)}{\partial x} = h\left[\mathbf{T}_{air}\mathbf{(t)} - \mathbf{T(0,t)}\right] = Q^{\downarrow}(0,t) \qquad (3.45)$$

or $$\frac{\partial \mathrm{T}(0,t)}{\partial x} = \alpha\left[\mathbf{T(0,t)} - \mathbf{T}_{air}\mathbf{(t)}\right] \ , \ \alpha = \frac{h}{\lambda} \tag{3.46}$$

Here; λ is thermal conductivity coefficient; h is heat transfer coefficient by convection; and α is heat exchange coefficient.

If we assume that heat flow towards soil surface as positive and heat flux from surface to atmosphere is negative, **third type boundary condition** is stated as follows (Kurtener and Chudnovskii 1979, Krarti *et al.* 1995):

$$-\lambda \frac{\partial \mathrm{T}(0,t)}{\partial x} = Q^{\downarrow}_{heat\ flow}(t) = \underbrace{\left[Q^{\downarrow}_{SR}(t) + Q^{\downarrow}_{CE}(t) \right]}_{incoming\ heat\ flow} - \underbrace{\left[Q^{\uparrow}_{LR}(t) + Q^{\uparrow}_{LE}(t) \right]}_{outgoing\ heat\ flow} \tag{3.47}$$

Where $Q^{\downarrow}_{heat\ flow}$, $Q^{\downarrow}_{SR}$, $Q^{\downarrow}_{CE}$, $Q^{\uparrow}_{LR}$ and $Q^{\uparrow}_{LE}$ were expressed in Section 3.2.

The boundary condition which is represented by the heat balance equation (3.47) represents a typical summer day period. At night: sign of $Q^{\downarrow}_{SR} = 0$, $Q^{\uparrow}_{LE}$ and $Q^{\uparrow}_{LR}$ are positive. Depending on a variety of meteorological and soil conditions, the right hand side of the Equation (3.47) will take different values.

Experimental analysis showed that right hand side of Equation (3.47) was related to time function $f(t)$ and soil surface temperature (T_{sur}), which may be defined as follows:

$$\underbrace{\left[Q^{\downarrow}_{SR}(t) + Q^{\downarrow}_{CE}(t) \right]}_{incoming\ heat\ flow} - \underbrace{\left[Q^{\uparrow}_{LR}(t) + Q^{\uparrow}_{LE}(t) \right]}_{outgoing\ heat\ flow} = \Phi(t) - \mathrm{N}(t)\mathrm{T}_{sur}(0,t) \tag{3.48}$$

As a result, if heat balance equation of the soil surface with (3.48) is written: the following equation for heat flow through the soil surface is obtained:

$$\lambda \frac{\partial \mathrm{T}(0,t)}{\partial x} = \mathrm{N}(t)\left[\mathrm{T}_{sur}(0,t) - \mathrm{T}_{e}(t)\right] \tag{3.49}$$

(3.49) equation can be addressed as a **generalized third type boundary condition**.

Forth type boundary condition: The above-mentioned boundary conditions in practice are the most commonly used boundary conditions. In addition, if heat can be transferred by radiation from a border to its environment, in this case the boundary condition is written as follows:

$$\lambda \frac{\partial \mathrm{T}(0,t)}{\partial x} = \sigma \left[\mathbf{T}^4(\mathbf{0,t}) - \mathbf{T}^4{}_{sur}(\mathbf{t}) \right] \tag{3.50}$$

Such a boundary condition, unlike the above, is not linear, because on the right side of equation is determined by the fourth power of the temperature. This type of boundary condition is called **Stefan Banach boundary condition**.

This boundary condition corresponds to the emission in accordance with the Stefan–Boltzmann law from the soil surface into the environment with the temperature $T^4sur(t)$, where σ is the Stefan–Boltzmann constant (5.67×10^{-8} W/(m^2 degree^4) or 5.67×10^{-8} J/(m^2 degree^4)).

3.5.3. 1st, 2nd and 3rd type boundary conditions at a given soil depth

At a certain depth of soil similar to soil surface, 1, 2 and 3 boundary conditions can be defined. Oscillation of soil temperature waves vanishes while depth increases and temperature does not change after a certain depth.

This situation which is known as **first type boundary condition is**

$$\mathrm{T}(x = L, t) = \mathrm{T}_c = const \text{ or } \mathrm{T}(x \to \infty, t) = \mathrm{T}_c = const \tag{3.51}$$

Alternatively, it can be expressed with following equation which is known as **second type boundary condition**:

$$\frac{\partial \mathrm{T}(x=L,t)}{\partial x}=0 \text{ or } \frac{\partial \mathrm{T}(x\to\infty,t)}{\partial x}=0 \tag{3.52}$$

In practice, heat exchange may occur between a lower layer and an upper layer in a soil such as at $x=\ell$. The may be constant ($\mathrm{T}_0=const$) or variable ($\mathrm{T}_{gr}(t)$) .This condition is expressed with equation known as **third type boundary condition**:

$$\lambda\frac{\partial \mathrm{T}(\ell,t)}{\partial x}=h_{gr}\left[\mathrm{T}\left(\ell,t\right)-\mathrm{T}_{gr}\left(t\right)\right] \tag{3.53}$$

Where λ heat conductivity coefficient; $\mathrm{T}_{gr}\left(t\right)$ temperature of soil at $x=\ell$; h_{gr} heat convection coefficient.

3.5.4 Forth type boundary condition in a soil depth (interface of two soil layer)

When soil layers with different thermal properties are in contact, different boundary conditions may be applied. This condition is called as interface or forth type boundary condition as stated below:

$$\mathrm{T}(x,t)\big|_{x=l_i-0}=\mathrm{T}(x,t)\big|_{x=l_i+0} \text{ and } \lambda_i\frac{\partial \mathrm{T}(x,t)}{\partial x}\bigg|_{x=l_i-0}=\lambda_{i+1}\frac{\partial \mathrm{T}(x,t)}{\partial x}\bigg|_{x=l_i+0} \tag{3.54}$$

where *li* denotes the layer boundaries (i = 1, 2, 3, … n), and $li + 0$ and $li - 0$ are the upper and lower faces of the soil layers, respectively. The forth type boundary conditions should be used in modeling heat transfer in layered soils.

3.6. Analytical solutions of the thermal conductivity equation on the soil

A large proportion of the heat flow and the movement in soil occur by conduction. Problem of convection of heat waves on the soil, for the first time being examined by the French scientist Fourier is among the example of the mathematical theory of thermal conductivity, which is developed to explain a variety of natural events (Mikayilov and Shein 2010).

The Equation (3.39) should be solved using appropriate initial and boundary conditions to determine soil temperature in a specified soil depth and time. In practice, widely used solution of Equation (3.39) in homogeneous environment with a boundary condition in the soil surface defined as equation (3.38) with the cosine curve (Carslaw and Jaeger 1959):

$$\mathrm{T}(x,t) = \mathrm{T}_0 + \mathrm{T}_a \cdot e^{-x\sqrt{\frac{\omega}{2\kappa}}} \cos\left(\omega t - x\sqrt{\frac{\omega}{2\kappa}} + \varepsilon\right) \tag{3.55}$$

Where; T_0 is value of average temperature (daily or annual); $d = \sqrt{2\kappa/\omega}$ is dumping depth of heat wave. A dimensionless form of Equation (3.55) can be stated as follows:

$$\mathrm{T}(y,\tau) = \mathrm{T}_0 + \Phi_a(y,b) \cdot \cos\left[\bar{\omega}\tau + \varepsilon - \psi(y,b)\right] \tag{3.56}$$

Where; $y = x/L$, $\tau = \kappa t/L^2$, $\bar{\omega} = \omega L^2/\kappa$, $b = L\sqrt{\pi/\tau_0\kappa}$, $\psi(y,b) = b\,y$

$$\Phi_a(y,b) = \mathrm{T}_a \cdot e^{-by} \tag{3.57}$$

$\Phi_a(y,b)$ is the amplitude of the temperature in the soil at a specified depth (x).

The solution of Eq. (3.39) in dimensionless form obtained without the initial conditions and with initial conditions stated in Equations (3.38) and (3.53) is (Mikaiylov and Shein 2008):

$$\mathrm{T}(y,\tau) = \mathrm{T}_0 + \Phi_a(y,b) \cdot \cos\left[\bar{\omega}\tau + \varepsilon - \psi(y,b)\right] \tag{3.58}$$

Where; $y = x/L$, $\tau = \kappa t/L^2$, $\bar{\omega} = \omega L^2/\kappa$, $b = L\sqrt{\pi/\tau_0\kappa}$; and $\Phi_a(y,b)$, $\psi(y,b)$ are defined through.

$$\Phi(b,y)=\mathrm{T}_a\sqrt{\frac{\mathbf{ch}(d)+\cos(d)}{\mathbf{ch}(2b)+\cos(2b)}}\ ,\quad d=2b(1-y)$$

$$\psi(y,b)=\mathbf{arctan}\left[\frac{\mathbf{sh}\,(q)\sin(by)+\mathbf{sh}(by)\sin(q)}{\mathbf{ch}(q)\cos(by)+\mathbf{ch}(by)\cos(q)}\right],\ q=b(2-y) \tag{3.59}$$

$\mathbf{ch}(z)=\frac{1}{2}\left(e^{z}+e^{-z}\right)$ and $\mathbf{sh}(z)=\frac{1}{2}\left(e^{z}-e^{-z}\right)$ are the hyperbolic cosine and hyperbolic sine, respectively.

The study of the average soil temperature is also important as the average temperature of a specific soil layer (e.g., the 0 to 20 or 0 to 40 cm layer) varies to a lesser extent than the temperature at a specific depth (Mikayilov 2007, Mikayilov 2009).

Average integral solution of equation (3.39) has the form:

$$\overline{\mathrm{T}}(\tau,b)=\int_0^1\mathrm{T}(y,\tau)\,dy=\mathrm{T}_0+\mathrm{M}_a(b)\cdot\cos\left[\bar{\omega}\tau+\varepsilon-\hat{\psi}(b)\right] \tag{3.60}$$

Where; $M_a(b)$ and $\psi(b)$ have the forms at boundary conditions (3.38) and (3.53):

$$\mathrm{M}_a(b)=\mathrm{T}_a\sqrt{\frac{\mathbf{ch}(b)-\cos(b)}{b^2e^b}},\qquad \hat{\psi}(b)=\mathbf{arctan}\left\{\frac{1-e^{-b}\left[\sin(b)+\cos(b)\right]}{1+e^{-b}\left[\sin(b)-\cos(b)\right]}\right\} \tag{3.61}$$

and alternatively, they may be calculated using boundary conditions of (3.38) (3.53):

$$\mathrm{M}_a(b)=\mathrm{T}_a\frac{\sqrt{\mathbf{sh}^2(2b)+\sin^2(2b)}}{\sqrt{2}\,b\left[\mathbf{ch}(2b)+\cos(2b)\right]},\qquad \hat{\psi}(b)=\mathbf{arctan}\left[\frac{\sin(2b)-\mathbf{sh}(2b)}{\sin(2b)+\mathbf{sh}(2b)}\right] \tag{3.62}$$

3.7. Determination of Soil Thermal Properties

3.7.1. Calculation of volumetric and specific heat capacity

Another important factor affecting soil temperature is "specific heat capacity". Specific heat capacity is defined as the amount of heat required to increase temperature of 1 g of soil 1 ^{o}C and is indicated with C_m. Its unit is expressed with Cal $g^{-1}{}^{o}C^{-1}$ or J $g^{-1}{}^{o}C^{-1}$ (J $g^{-1}{}^{o}K^{-1}$).

The volumetric heat capacity *(Cv)* is heat required to increase temperature of a unit soil volume by 1 ^{o}C. Its unit is Cal $cm^{-3}\,{}^{o}C^{-1}$ or J $m^{-3}\,{}^{o}C^{-1}$ (J $m^{-3}\,{}^{o}K^{-1}$). If the specific heat capacity of any substance with an **m** and ***V*** is known, the heat capacity (*C*) of a substance is calculated as follows (Carslaw and Jaeger 1959, Yeşilsoy 1975, Juri *et al.* 1991):

$$C = m \cdot C_m = V \cdot C_v \tag{3.63}$$

The volumetric heat capacity of a soil is calculated as follows (Carslaw and Jaeger 1959, Yeşilsoy 1975, Juri *et al.* 1991):

$$C_v = \rho_b \cdot C_m \tag{3.64}$$

To find the soil heat capacity per unit volume, elements of different soil (solid, water and air phases) are required. To find the heat capacity per unit volume of humid soils, volumetric heat capacity of the soil constituents is required (Carslaw and Jaeger 1959, Yeşilsoy 1975, Juri *et al.* 1991):

$$C_v = f_s \cdot C_{vs} + f_w \cdot C_{vw} + f_a \cdot C_{va} \tag{3.65}$$

Where; f_s , f_w , f_a are fractions of solid, water and air phase, respectively ($f_s + f_w + f_a = 1$); C_{vs} , C_{vw} , C_{va} are volumetric heat capacity of solid, water, and air phase, respectively. Where;

$C_{vs} = 0,48\,cal/\left(cm^3 \cdot {}^0C\right)$, $C_{vw} = 1$, and $C_{va} = 0,003\ cal/\left(cm^3 \cdot {}^0C\right)$.

As the third term at the right side of the equation (3.65) is fairly small, it can be ignored. Therefore the equation (3.65) can be stated as follows:

$$C_v = f_s \cdot C_{vs} + f_w \cdot C_{vw} \tag{3.66}$$

Soil solid phase $\left(f_s\right)$ may be divided into mineral $\left(f_{\min}\right)$ and organic $\left(f_{org}\right)$ phases ($f_s = f_{\min} + f_{org}$)

Studies showed that in general, soil volumetric heat capacity can be defined by following equation (De Vries 1952, De Vries 1963, Hillel 1982, Juri *et al.* 1991, Shein and Goncharov 2006):

$$C_v = 0,48 \cdot f_{\min} + 0,60 \cdot f_{org} + f_w \tag{3.67}$$

Where; f_m is the fraction of mineral part f_{org} is the fraction of the organic part. Soil volumetric heat capacity is calculated with the following equation:

$$C_v = C_{m,solid\ phase} \cdot \rho_b + \theta \tag{3.68}$$

On the basis of research, mineral part in itself is divided into quartz, clay minerals, limestone, etc. Heat capacity for dry soils is considered as specific heat capacity of quartz and specific heat capacity of solid phase in unit volume of the soil is numerically $C_{m,solid\ phase} = 0.20\,cal/g \cdot {}^{\circ}C$. The volumetric heat capacity of the soil in dry conditions is calculated using Equation (3.69):

$$C_v = 0.20\rho_b + \theta \tag{3.69}$$

Here, ρ_b is bulk density; θ is the volumetric water content.

3.7.2. Determination of thermal diffusivity in soils

Heat diffusivity is the rate of heat conductivity of a material to its volumetric heat capacity. Its unit is expressed with $cm^2\ s^{-1}$ or $m^2\ s^{-1}$.

Soil heat diffusivity is determined in laboratory and field by monitoring the soil temperature. Commonly used methods for finding this parameter is based on via application of analytical and numerical solution of heat conduction equation to data from field trials. Based on solution (3.55) of the Equation (3.39) following methods are used to obtain thermal diffusivity (κ).

Amplitude Including Formula: This method is developed on the basis of Fourier's first law, which expresses decrease (extinction) of soil temperature amplitude by depth. In the case of equation (3.58) of the daily temperature change of the soil surface when solution (3.58) of equation (3.39) is examined, it is seen that $T_a(x) = T_a \cdot \exp(-x/d)$.

3.7.2.1. *'Layer'* methods

Many researchers Carslaw and Jaeger (1959), Gerayzade (1989), Horton (19829, Juri *et al.* (1991) used this method differently.

Method-1: This method is based on **Fourier's first law,** which expresses the solution of the heat diffusivity equation as follows.

$$\kappa = \frac{\pi\left(x_2 - x_1\right)^2}{\tau_0 \ln^2\left[\dfrac{\Phi_{\max}(x_1) - \Phi_{\min}(x_1)}{\Phi_{\max}(x_2) - \Phi_{\min}(x_2)}\right]} \tag{3.70}$$

Where; $\Phi_{min}\ (x)$ and $\Phi_{max}\ (x)$ minimum and maximum temperature x_1 and x_2 are depths and τ_0 heat wave period (e.g., 24 hours of daily observation)

Method-2 (Arctangent Containing Formula): Based on solution of the thermal conductivity equation, following equation has been developed to calculate heat diffusivity:

$$\kappa = \frac{\pi\left(x_2 - x_1\right)^2}{\tau_0 \cdot \arctan^2\left[\frac{\left(\mathrm{T}_1' - \mathrm{T}_3'\right)\left(\mathrm{T}_2'' - \mathrm{T}_4''\right) - \left(\mathrm{T}_2' - \mathrm{T}_4'\right)\left(\mathrm{T}_1'' - \mathrm{T}_3''\right)}{\left(\mathrm{T}_1' - \mathrm{T}_3'\right)\left(\mathrm{T}_1'' - \mathrm{T}_3''\right) + \left(\mathrm{T}_2' - \mathrm{T}_4'\right)\left(\mathrm{T}_2'' - \mathrm{T}_4''\right)}\right]} \tag{3.71}$$

Where; T_i' and T_i'' are temperatures at depths of $x = x_1$ and $x = x_2$ and at the times of $t_i = i \cdot \tau_0 / 4 \ (i = 1,2,3,4)$ (e.g, for $\tau_0 = 24$, **t_1=6, t_2=12, t_3=18** and **t_4=24** hours).

Method- 3 (Formula Containing Logarithms): Using the assumptions for method-2, Seemann (1979) obtained the following equation:

$$\kappa = \frac{4\pi\left(x_2 - x_1\right)^2}{\tau_0 \cdot \ln^2\left[\frac{\left(\mathrm{T}_1' - \mathrm{T}_3'\right)^2 + \left(\mathrm{T}_2' - \mathrm{T}_4'\right)^2}{\left(\mathrm{T}_1'' - \mathrm{T}_3''\right)^2 + \left(\mathrm{T}_2'' - \mathrm{T}_4''\right)^2}\right]} \tag{3.72}$$

Where; T_i' and T_i'' are temperatures at the depths of $x = x_1$ and $x = x_2$ at the time of $t_i = i \cdot \tau_0 / 4 \ (i = 1,2,3,4)$ (e.g, for $\tau_0 = 24$, t_1=6, t_2=12, t_3=18 and t_4=24 hours).

Method-4 (Containing phase shift of the heat wave formula): Another approach may be used to calculate the soil thermal diffusivity is based on measuring the required time difference for monitoring the maximum temperature at two different soil depths.

If time interval between maximum soil temperature in $x = x_1$ and $x = x_2$ depth is $\Delta t = t_2 - t_1$, a new phase formula is obtained from the solution of heat release equation:

$$\cos\left(\omega t_1 + \varepsilon - \frac{x_1}{d}\right) = \cos\left(\omega t_2 + \varepsilon - \frac{x_2}{d}\right) \text{ Or } \omega t_1 + \varepsilon - \frac{x_1}{d} = \omega t_2 + \varepsilon - \frac{x_2}{d}$$

Therefore, κ can be calculated as follows:

$$\kappa = \frac{1}{2\omega}\left(\frac{x_2 - x_1}{\Delta t}\right)^2 = \frac{\tau_0}{4\pi}\left(\frac{x_2 - x_1}{\Delta t}\right)^2 \text{ and } \kappa = \frac{\tau_0}{4\pi}\left(\frac{x_2 - x_1}{\Delta t}\right)^2 \tag{3.73}$$

All of the above equations for determination of the soil thermal diffusivity coefficient are based on analysis of soil temperature change in different depths and times, and all means periodic temperature change, or actual change in a certain time period. To apply calculation of thermal diffusivity coefficients, only soil temperature must be determined experimentally. However, this equation gives the mean value of the thermal diffusivity coefficient during considered duration and it is obtained with specified water content (θ) over the soil layer under the constant κ value. A suitable time period should be chosen to determine another κ in the same layer with different soil water content. Based on the obtained pair of κ and θ values, thermal diffusivity function (is the thermal diffusivity of a particular soil layer as a function of soil water content) κ (θ) can be determined.

3.7.2.2. *'Point'* methods

Some methods proposed for the determination of the κ from the experimental data on the soil temperature in separate soil layers, i.e. $T(x_i, t)$. These methods can be referred to as point (P) methods, because they determine the temperature of the soil at one depth, i.e., at one point of the soil space. Using the solution (3.56) with (3.57):

$$\mathrm{T}(y,\tau) = \mathrm{T}_0 + \Phi(y,b)\cdot\cos(\bar{\omega}\tau + \alpha) \tag{3.74}$$

Firstly, for an arbitrary dimensionless depth (y) and time $t_i = i\cdot\tau_0/4$ the following equations may be written:

$$\mathrm{T}(y,t_i) = \mathrm{T}_0 + \Phi(y,b)\cdot\cos\left(\frac{\pi}{2}i + \alpha\right),\ \left(i = \overline{1,4}\right) \tag{3.75}$$

As the following is the case,

$$\bar{\omega}\tau_i = \frac{\omega L^2}{\kappa}\cdot\frac{\kappa}{L^2}t_i = \omega t_i = \frac{2\pi}{\tau_0}\cdot i\cdot\frac{\tau_0}{4} = \frac{2\pi}{4}\cdot i \text{ and } \bar{\omega}\tau_i = \frac{2\pi}{8}\cdot i = \frac{\pi}{4}\cdot i,\ 2\bar{\omega}\tau_i = \frac{\pi}{2}\cdot i$$

Rearranging equation results in (3.75) (Mikayilov 2007):

$$\sum_{i=1}^{2}\left[\mathrm{T}\left(y,t_i\right)-\mathrm{T}\left(y,t_{i+4}\right)\right]^2 = 4\Phi^2\left(y,b\right) \tag{3.76}$$

Accounting for values of Equation (3.57) and (3.59) for the function $\Phi\left(y,b\right)$ in the equation (3.76), the following equations corresponding to the boundary conditions of (3.51) and (3.52), i.e. $\mathrm{T}\left(\infty,t\right)=\mathrm{T}_0$ and $\partial\mathrm{T}\left(L,t\right)/\partial x = 0$ are obtained.

$$\frac{\sum_{i=1}^{4}\left[\mathrm{T}\left(y,t_i\right)-\mathrm{T}\left(y,t_{i+4}\right)\right]^2}{4\mathrm{T}_1^2} = e^{-2by} \tag{3.77}$$

$$\frac{\sum_{i=1}^{4}\left[\mathrm{T}\left(y,t_i\right)-\mathrm{T}\left(y,t_{i+4}\right)\right]^2}{4\mathrm{T}_a^2} = \frac{\mathbf{ch}\left[2b\left(1-y\right)\right]+\cos\left[2b\left(1-y\right)\right]}{\mathbf{ch}\left(2b\right)+\cos(2b)} \tag{3.78}$$

To determine the thermal diffusivity coefficient κ (using the equations (3.77) and (3.78)), the following should be known: T_a the oscillation amplitude of soil active surface temperature; τ_0 the period (length) of a daily (yearly) wave expressed in days or years; $\mathrm{T}\left(y_*,t_i^*\right),\left(i=\overline{1,4}\right)$; is the temperature values of the soil layer $\left[0,L\right]$ at an arbitrary depth $y_* = y = x_*/L$ for *eight time points:* $t_i^* = i\cdot\tau_0^*/4\ \left(i=\overline{1,4}\right)$. For example, if $\tau_0^* = 24$ hours, then $t^* = 6,\ 12,18,\ 24$ hours.

Point method 1 (P1). *Determination of k at T* (∞, *t*) = *0.* First we calculate the differences: $\left[\mathrm{T}\left(y_*,t_i^*\right)-\mathrm{T}\left(y_*,t_{i+4}^*\right)\right]$ for all $i=\overline{1,4}$. Then from the equation (3.77) we obtain the value of thermal diffusivity coefficient at the depth $x_* = x$ by the equations:

$$\kappa^* = \frac{\pi}{\tau_0} \cdot \frac{\left(2x_*\right)^2}{\ln^2 \frac{\sum_{i=1}^{4}\left[\mathrm{T}\left(x_*, t_i^*\right) - \mathrm{T}\left(x_*, t_{i+4}^*\right)\right]^2}{4\mathrm{T}_a^2}} \tag{3.79}$$

Where;

$$y_* = \frac{x_*}{L},\ b = \sqrt{\frac{\bar{\omega}}{2}} = \sqrt{\frac{\omega L^2}{2\kappa}},\quad \omega = \frac{2\pi}{\tau_0},\qquad b = L\sqrt{\frac{\pi}{\tau_0}\cdot\frac{1}{\kappa}} \text{ and } 2by = 2x\sqrt{\frac{\pi}{\tau_0}\cdot\frac{1}{\kappa}}$$

Point method 2 (P2). *Determination of* κ *at* $\partial T(L, t)/\partial x = 0$. The determination of κ using the equation (3.78) is performed by fitting the values of b^* provided that the values of the left-hand side coincide with the right-hand side calculated from the given data, i.e. $\sum_{i=1}^{2}\left[\mathrm{T}\left(y_*, t_i^*\right) - \mathrm{T}\left(y_*, t_{i+4}^*\right)\right]^2 / 4\mathrm{T}_a^2$.

From the relation $b^* = \sqrt{\omega L^2 / 2\kappa}$ we find the value of the thermal diffusivity coefficient κ at the depth $x = x_*$, and it equals to

$$\kappa^* = \frac{\pi}{\tau_0} \cdot \left(\frac{L}{b_1^*}\right)^2 \tag{3.80}$$

3.7.3. Determination of thermal conductivity

The amount of heat that moves from a point to a certain distance in a porous media depends on the rate of conduction of the heat medium. Another important parameter for thermal phenomenon is heat conductivity.

Heat conductivity (λ) is the amount of heat passing a unit distance (e.g 1 cm) under a unit temperature difference (e.g. 1 ^oC) in a unit time (e.g. 1 s). Its commonly used units are Cal $cm^{-1}\,{}^oC^{-1}\,s^{-1}$ or J $cm^{-1}\,{}^oC^{-1}\,s^{-1}$ or Cal $cm^{-1}\,{}^oC^{-1}\,day^{-1}$ or J $cm^{-1}\,{}^oC^{-1}\,day^{-1}$.

When volumetric heat capacity and heat diffusivity are known, heat conductivity can be calculated from soil water content (θ) as follows:

$$\lambda(\theta) = \kappa \cdot C_v(\theta) \tag{3.81}$$

3.7.4. Determination of air temperature at soil surface

A periodic temporal variation of air temperature at soil-air boundary is formulated by $\mathrm{T}(x=0,t)=\varphi(t)$. Using hourly (N= 24) measured values, $\mathrm{T}(0,t_i)$, average temperature at soil-air boundary layer (T_0), heat waves amplitude $(\mathrm{T}_a)$and its phases ε values are found with the following formulae (Fadeev and Fadeeva 1963, Chapra and Canale 2010):

$$\mathrm{T}_0 = \frac{1}{\mathrm{N}}\sum_{i=1}^{\mathrm{N}} \mathrm{T}(0,t_i) \tag{3.82}$$

$$A = \frac{2}{\mathrm{N}}\sum_{i=1}^{\mathrm{N}} \mathrm{T}(0,t_i)\cos(\omega t_i) = \frac{2}{\mathrm{N}}\sum_{i=1}^{\mathrm{N}} \mathrm{T}(0,t_i)\cos\left(\frac{2\pi}{\tau_0}t_i\right) \tag{3.83}$$

$$B = \frac{2}{\mathrm{N}}\sum_{i=1}^{\mathrm{N}} \mathrm{T}(0,t_i)\sin(\omega t_i) = \frac{2}{\mathrm{N}}\sum_{i=1}^{\mathrm{N}} \mathrm{T}(0,t_i)\sin\left(\frac{2\pi}{\tau_0}t_i\right) \tag{3.84}$$

$$\mathrm{T}_a = \sqrt{A^2 + B^2} \tag{3.85}$$

$$\varepsilon = \arctan(-B/A) \text{ if } A>0 \text{ and } \varepsilon = \pi - \arctan(B/A) \text{ if } A<0 \tag{3.86}$$

Where; τ_0 – is period of heat wave (24 hours), t_i – is time of observation (t=0, 3, 6, 9, 15, 18, 21); N – is the number of observations (N=8); $\omega=2\pi/\tau_0$ is angular frequency (also called the wave number or frequency) and its value is calculated by $\omega=2\pi/\tau_0$=2x3.14/24 h or $2\pi/\tau_0$=2x3.14/24 h 84600 s.

3.7.5. Correlation between soil thermal properties and volumetric water content

Thermal diffusivity varies depending on the soil moisture content. Thermal diffusivity increases with increasing θ, and it then decreases with further increases with θ (Fragkogiannis *et al.* 2010).

De Vries (1975) described shape of mineral soil curve in terms of the microscopic properties of the soils. Heat diffusion is facilitated in very dry soils with contacting very small particles. Water is absorbed by soil particles in a higher moisture content and therefore κ increases. The increased water content results in a more contact with water rings and particles, increasing transmission area. A little increase in θ results in a considerable increase in κ (Clark 1983).

The thermal diffusivity of soils is κ divided by C, both largely dependent on the moisture content, the shape of the κ versus moisture content curve may be discussed in terms of these two parameters. Contradictory results have been found on the shape of the curve representing κ versus moisture content. Jackson and Kirkham (1958) found this curve to be continually increasing while others (Baver *et al.* 1972). Found it to decrease after a certain θ, the θ which depends on soil type.

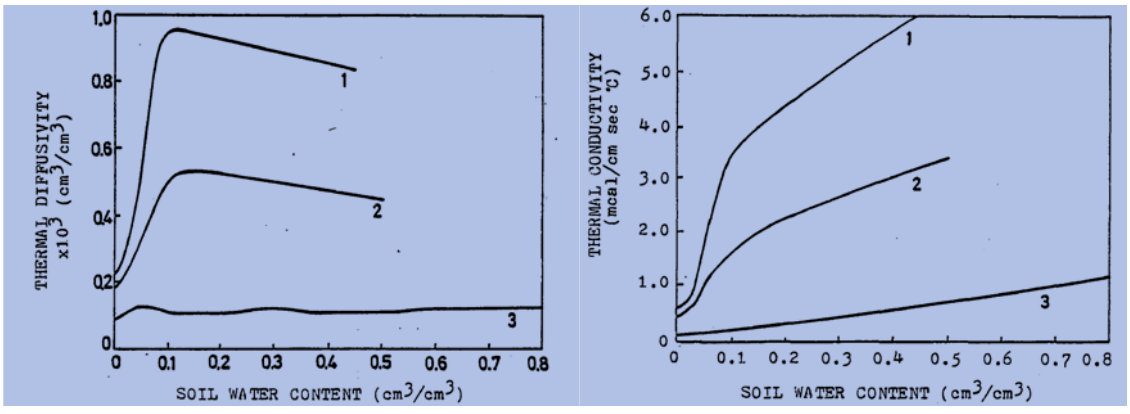

Figure 3.9 Values of thermal diffusivity for the soils and Thermal conductivity in relation to soil water content.
Curve 1: quartz sand with a porosity of 0.45. Curve 2: loam with a porosity of 0.5.
Curve 3. peat soil with a porosity of 0.8 (DeVries 1975)

Numerous studies have been conducted on the relation between κ and θ (Chudnovsky 1948,1959,1967,1976 Dimo 1948, Rollins *et al.* 1954, Chichua 1965, Tikhonov and Samarskiy 1966, Şirinov 1967, Gerayzade 1982, Chung and Horton 1987, Nabyev and Guseınov 1990, Tikhoravova 1991, Nabyev 1992, Rycheva 1994, Tikhonravova and Khitrov 2003, Arkhangel'skaya 2004, Shein *et al.* 2004, Shein 2005, 2007, Shein and Goncharov 2006, , Arkhangel'skaya and Umarova 2011,). Corresponding equations are given in Table 3.4.

Table 3.4 Regression models between volumetric soil moisture content and thermal diffusion coefficient

Kind characteristics	Number of Parameters	Equation	Source
power	4	$K = K_0 + a(\theta - \theta_0)^b$	Chudnovsky 1967
polynomial	4	$K = K_0 + a_1\theta + a_2\theta^2 + a_3\theta^5$	Tikhonravov, Khitrov, 2003
lognormal	4	$K = K_0 + a\exp\left[-0.5\left(\frac{\ln\left(\frac{\theta}{\theta_0}\right)}{b}\right)^2\right]$	Arkhangelskaya, 2004

K_0, Θ_0, a, b, a_1, a_2, a_3- parameters

The main objective in the establishment of regression models for $k = f(\theta)$ between the volumetric moisture and heat radiation and between other thermal parameters of soil and volumetric moisture $\lambda = \psi(\theta) = C_v \cdot \kappa = C_v f(\theta)$ is to determine analytical expressions for the relations between *k* and corresponding soil properties. The equation defined between the thermal conductivity of soil and volumetric moisture is as follows.

$$\lambda = \psi(\theta) = C_v \cdot \kappa = C_v f(\theta) = C_v(a + b\theta + c\theta^2) \quad (3.87)$$

Where; λ is the thermal conductivity (W/m·K); C_v volumetric heat capacity (Cal/cm^3.^{0}C); κ is thermal diffusivity (m^2/s); θ is volumetric moisture content (cm^3/cm^3); *a*,*b*,*c* are shows equation coefficient.

4. MATERIALS AND METHODS

4.1. Materials

4.2. Site Description of the Study Area

4.2.1. Geographical location of the study area

The study area is in Cumra, which is located between 37^0 - 38^0 North latitudes and 33^0 - 34^0 East longitudes (Fig.4.1). The Cumra region is surrounded by Karaman (province) and Karapınar (district) in the east, by Akören and Bozkır in the west, by Güneysınır and Bozkır in the south and by Konya, Meram and Karatay in the north. Located at 1013 m above sea level, the Cumra region covers approximately 2,330 km^2 flat terrain with varying topography (Anonymous 2014). Locations of the study plots are given in Table 4.1 and Fig.4.2.

Konya, where Cumra region is located within, is one of the most important agricultural areas in Turkey. Due to the favorable ecological aspect of the region, a wide variety of crops can be grown. Most of the soils are level. Approximately 70% of the total area of Cumra district is suitable for agriculture (Anonymous 2014).

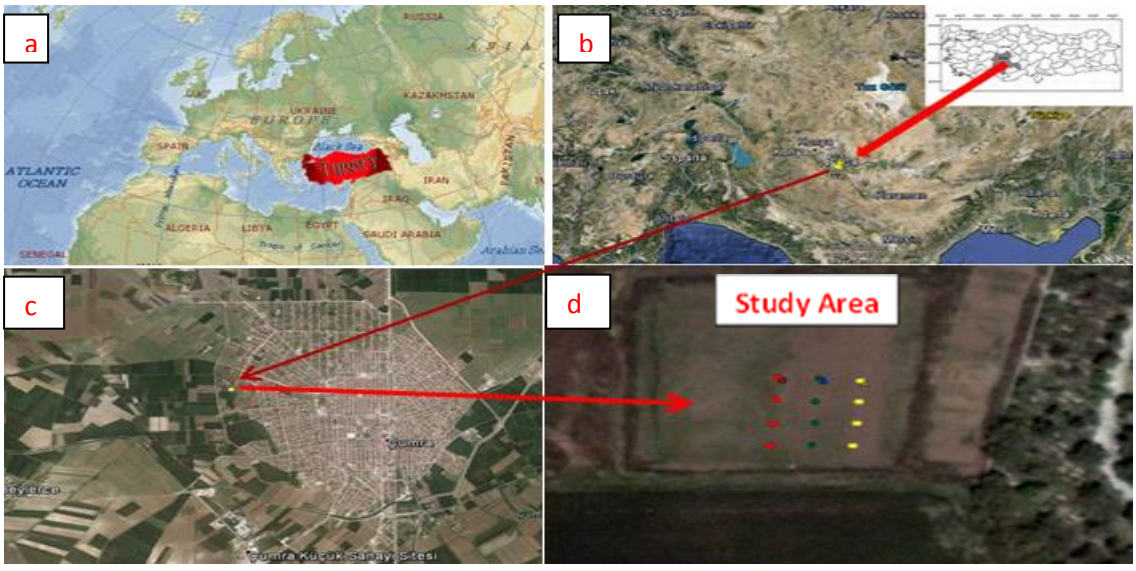

Figure 4.1 Location of study area in Cumra of Konya province in Central Anatolia of Turkey (www.google.com.tr/maps).

Table 4.1 Location of study plots at the experimental site

Crop	Code	Parcel	Latitude	Longitude	Altitude
Sugar beets	S1	1. block 1.plot	37° 33' 52.07"N	32° 45' 48.08"E	1047.80
Control	-	1. block 3.plot	37° 33' 51.79"N	32° 45' 48.42"E	1047.86
Corn	C1	1. block 4.plot	37° 33' 51.63"N	32° 45' 48.60"E	1047.86
Corn	C2	2. block 1.plot	37° 33' 51.90"N	32° 45' 47.85"E	1047.77
Sugar beets	S2	2. block 2.plot	37° 33' 51.75"N	32° 45' 48.03"E	1047.76
Control	Co	2. block 4.plot	37° 33' 51.46"N	32° 45' 48.38"E	1047.79
Control	-	3. block 2.plot	37° 33' 51.58"N	32° 45' 47.82"E	1047.61
Corn	C3	3. block 3.plot	37° 33' 51.44"N	32° 45' 47.98"E	1047.57
Sugar beets	S3	3. block 4.plot	37° 33' 51.28"N	32° 45' 48.18"E	1047.63

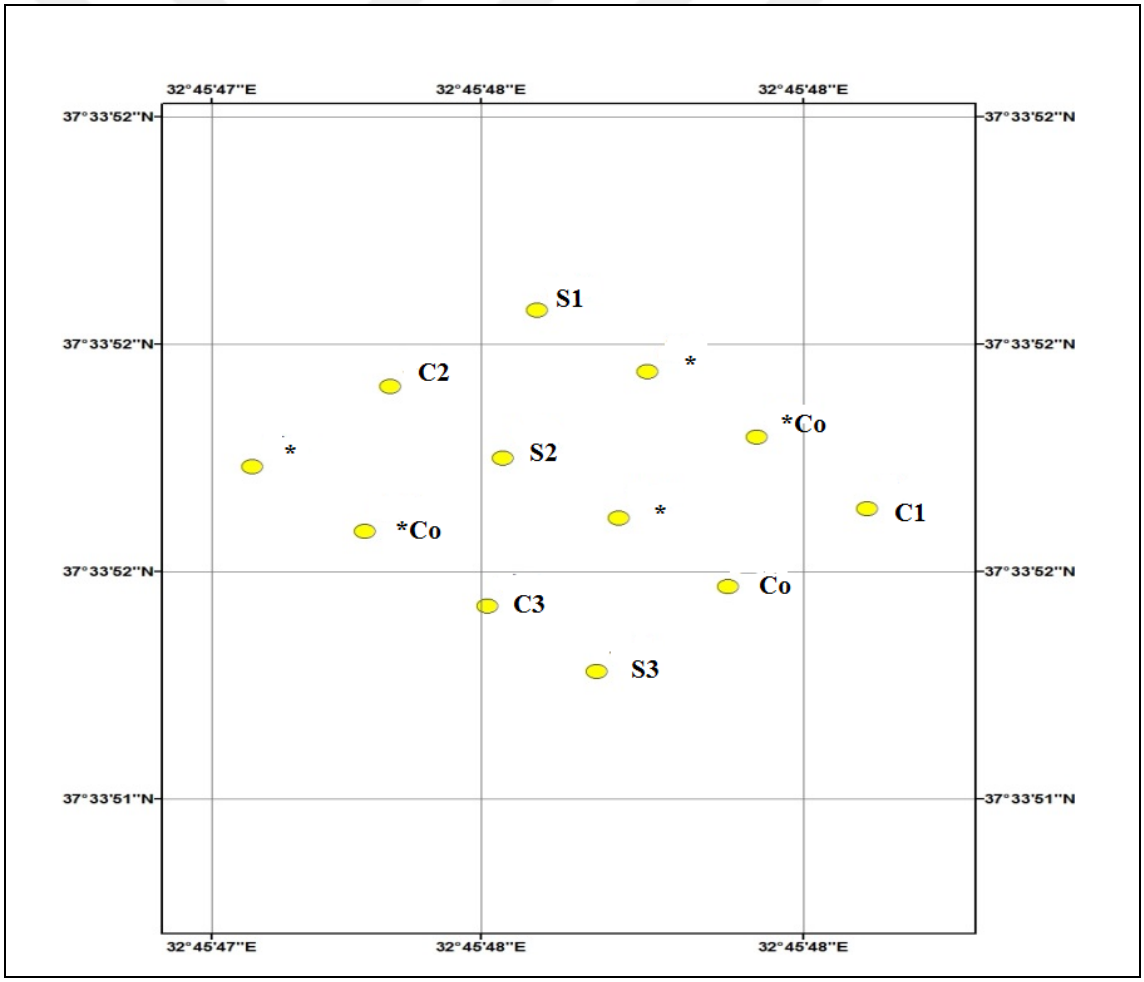

*The plot where measurements were not taken due to that the sensors malfunctioned

Figure 4.2 Location of the experimental plots in the study area

4.2.2. Climate of study area

Winters are cold and snowy, summers are hot and dry, falls and springs are rainy in the study area. Summer temperatures are favorable for growth of many crops (Akkuş 2000). While the average temperature increases in summer, humidity decreases.

The long term maximum temperature is 39.9 °C in July, minimum temperature is -26.3°C in February, and average temperature is 11.4 °C. Long term average yearly total precipitation is 318.9 mm. Total precipitation was 204.0 mm in 2013.

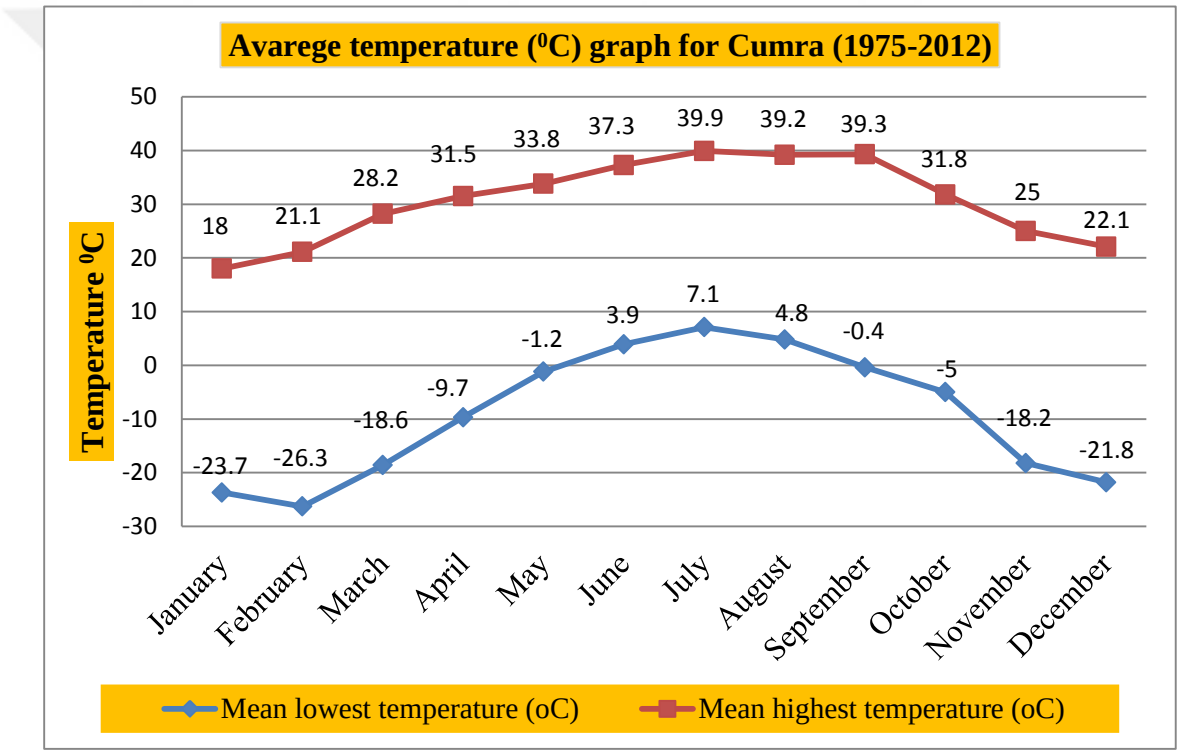

Figure 4.3 Long-term (1975-2012) climatic data for Çumra (Anonymous 2013)

Table 4.2 Long term (1975-2012) and 2013 climate data for Cumra (Anonymous 2013)

Variables	YEARS	January	February	March	April	May	June	July	August	September	October	November	December	Average
Maximum temperature (°C)	**1975-2012**	18.0	21.1	28.2	31.5	33.8	37.3	39.9	39.2	39.3	31.8	25.0	22.1	**30.6**
	2010	18.0	21.1	26.9	24.9	32.1	33.5	38.0	39.2	34.0	26.9	24.0	22.1	**28.4**
	2011	13.0	15.1	22.9	24.0	26.1	32.2	36.7	36.4	31.1	27.0	15.8	15.4	**24.6**
	2012	11.5	12.3	18.0	27.9	27.1	34.3	39.2	35.2	32.6	27.1	24.9	20.1	**25.9**
	2013	15.3	19.2	24.6	28.3	31.7	34.9	34.4	33.9	34.9	30.1	22.4	15.4	**27.1**
Minimum temperature (°C)	**1975-2012**	-23.7	-26.3	-18.6	-9.7	-1.2	3.9	7.1	4.8	-0.4	-5.0	-18.2	-21.8	**-9.1**
	2010	-12.0	-13.2	-6.0	0.4	4.8	9.7	13.0	12.5	9.5	-1.0	-1.3	-4.6	**1.0**
	2011	-6.0	-9.9	-8.7	-2.1	2.0	9.5	11.4	11.2	6.3	-2.3	-10.5	-9.1	**-0.7**
	2012	-20.3	-21.5	-7.8	0.6	4.9	9.2	10.7	11.9	7.2	5.4	-3.6	-6.5	**-0.8**
	2013	-13.5	-6.3	-6.2	3.0	7.2	9.0	10.6	12.5	4.8	-2.0	-2.5	-14.4	**0.2**
Mean temperature (°C)	**1975-2012**	0.1	1.1	5.7	11.2	15.7	20.0	23.0	22.3	17.9	12.2	6.0	1.9	**11.4**
	2010	3.7	6.1	8.8	11.4	17.7	20.9	25.7	26.1	21.0	12.6	9.8	6.2	**14.2**
	2011	1.6	2.3	5.4	9.7	14.3	19.5	24.9	22.5	18.6	10.3	1.8	1.9	**11.1**
	2012	-1.3	-1.9	4.3	14.0	16.4	22.3	25.1	23.3	20.1	14.7	7.9	4.5	**12.4**
	2013	2.3	5.3	7.8	12.1	18.5	21.0	22.5	22.5	18.0	10.1	8.1	-2.4	**12.2**

(Table 4.2 continued)

Parameters	YEARS	January	February	March	April	May	June	July	August	September	October	November	December	Average
Mean humidity (%)	**1975-2012**	76.0	72.1	64.0	59.2	58.2	53.2	49.2	49.9	53.2	63.8	71.4	76.4	**62.2**
	2010	66.0	57.4	47.0	53.2	40.8	45.6	39.0	32.3	40.6	60.5	53.7	69.7	**50.5**
	2011	84.6	76.3	70.5	68.8	64.3	54.0	39.6	40.9	41.4	58.2	73.6	72.6	**62.1**
	2012	83.1	81.8	61.5	41.7	54.2	40.5	36.1	43.5	37.8	62.4	78.2	78.6	**58.3**
	2013	80.5	71.2	56.0	59.7	48.2	41.3	39.2	38.2	43.5	53.4	65.6	82.1	**56.6**
Mean Total precipitation (mm)	**1975-2012**	37.8	28.3	31.2	40.9	36.0	19.6	5.4	3.1	8.9	30.6	34.5	42.6	**26.6**
	2010	43.6	33.3	12.1	67.4	12.4	47.9	0.0	-	1.6	62.6	4.2	106.8	**35.6**
	2011	52.9	40.1	44.2	48.0	52.5	39.5	-	1.0	3.8	32.1	29.2	24.9	**33.5**
	2012	37.1	-	-	-	-	-	-	-	-	-	-	-	**37.1**
	2013	13.4	26.4	14.8	61.2	12.8	13.0	4.6	0.2	0.2	19.4	20.6	17.4	**17.0**
Mean wind speed ($m\ s^{-1}$)	**1975-2012**	0.9	1.1	1.2	1.2	0.9	1.0	1.1	0.8	0.7	0.5	0.7	0.8	**0.9**
	2010	0.3	0.4	0.3	0.1	0.1	0.1	0.1	0.1	0.1	0.0	0.0	0.1	**0.1**
	2011	1.3	1.3	1.4	1.8	1.6	1.5	1.6	1.7	1.3	1.4	1.3	1.5	**1.5**
	2012	2.0	1.6	1.9	1.8	1.6	1.7	1.8	1.7	1.3	1.1	1.5	1.8	**1.6**
	2013	1.8	1.4	1.8	1.5	1.3	1.5	1.8	1.5	1.2	1.4	0.7	0.9	**1.4**

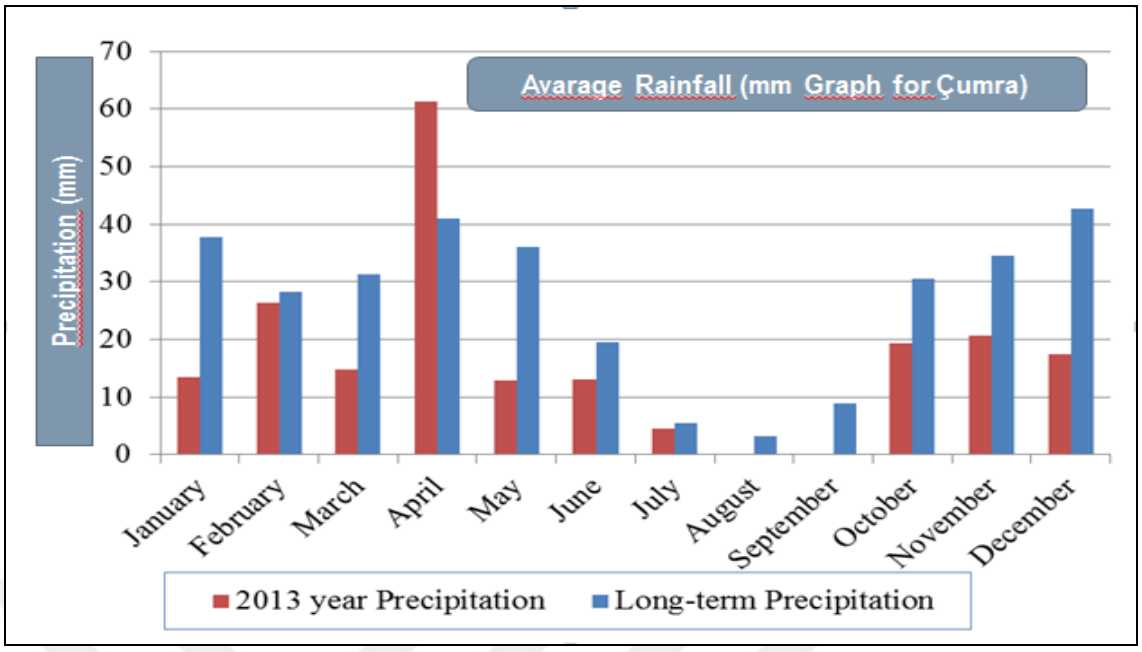

Figure 4.4 Long term (1975-2012) mean yearly total and 2013 total precipitation in Cumra (Anonymous 2013)

4.2.3. Soils

The soils of the experimental site are clay loam (*CL*) in texture. These soils are young alluvial soils with low organic matter content. Horizon boundaries of the soils are faint with slightly wavy structure.

The profile descriptions of the soils are given below.

A horizon: 0-24 cm; Dark yellowish brown (10 YR 4/4 moist), silty clay (SiC); weak medium subangular blocky structure; slightly sticky and moderately plastic when moist; common fine vesicular pores; very strongly effervescent with 0.1 M HCl; few, fine roots; abrupt, smooth boundaries

Bw horizon: 24-83 cm; Dark yellowish brown (7.5 YR 4/3 moist), silty clay (SiC); weak, coarse, subangular blocky structure; slightly sticky and slightly plastic when moist; common, fine, tubuler pores; strongly effervescent with 0.1 M HCl; few, very fine roots; very abrupt wavy boundary.

BC horizon: 83- cm; Dark brown (7.5 YR 3/3 moist), silty clay (SiC); weak, fine, subangular blocky structure; slightly sticky and slightly plastic when moist; common fine vesicular pores; very strongly effervescent with 0.1 M HCl; few, very fine roots.

4.3 Methods

The field experiment was designed based on completely randomized block design (Fig.4.5) at the experimental field of Cumra, Vocational School in Konya. Four treatments were repeated in three blocks (12 plots in total). The treatments were sugar beets (Beta vulgaris) and corn (Zea mays) and bare soil plots as control. A soil profile was open at each of the experimental plots. Thermal sensors were placed at the depths of 0, 5, 10, 20, 30, 40, 60 cm (Fig.4.6). In addition one sensor was placed above 1-2 m of the soil surface to measure air temperature. Overall, 12 sensors were located above the soil surface and 72 sensors in the soil profiles, summing to 84 in total. Disturbed soil samples were taken from the points where the sensors were placed. Each plot was 5.0 m wide and 5.60 m long, making 28 m^2.

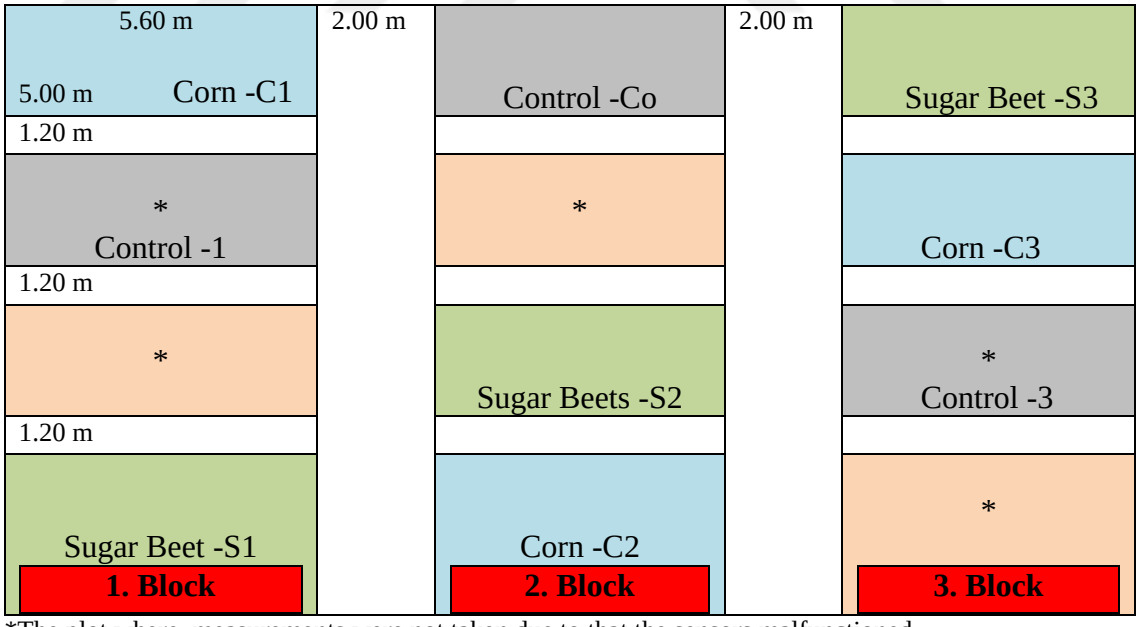

*The plot where measurements were not taken due to that the sensors malfunctioned

Figure 4.5 The experimental design of the field trial

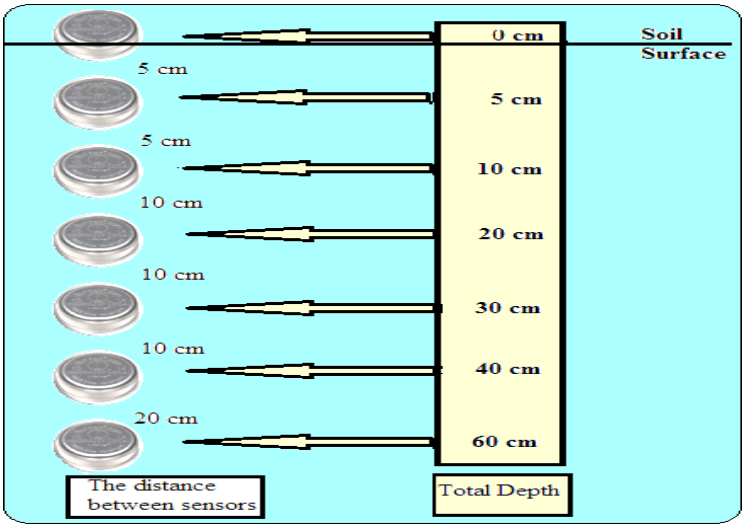

Figure 4.6 The locations of the sensors in a soil profile

Figure 4.7 Placing a sensor in a soil profile

During the experimentation, temperatures were recorded with three-hour interval at 0, 5, 10, 20, 30, 40 and 60 cm depths of each soil profile. The experiment; temperature recordings were started on 1 May 2013 and ended on 26 October 2013. Readings were stored in the memory of the inserted temperature sensors and removed from the profiles and processed with the computer program 'Termochron the iButton TMEX' (http://www.maxim-ic.com/products/ibutton/software/1wire/onewireviewer.cfm).

Drip irrigation was applied to all plots. Irrigation frequency and total amount of irrigation water applied to the plots are given in Table 4.1. Control and planted plots were saturated during the irrigations. After 12 hours following irrigation was stopped, disturbed soil samples were taken from the depths of 0-10, 10-20, 20-30, 30-40, 40-50, 50-60 cm from each plot to determine gravimetric water content.

Table 4.3 Irrigation frequency and total amount of irrigation water applied to the plots

Plant	Code	Plot no	Weekly (m^3)	Total (m^3)
Sugar beets	S1	1. block 1.plot	4.6	69.0
Corn	C1	1. block 4.plot	3.5	52.5
Corn	C2	2. block 1.plot	4.0	60.0
Sugar beets	S2	2. block 2.plot	5.0	75.0
Control	Co	2. block 4.plot	4.1	61.5
Corn	C3	3. block 3.plot	3.3	49.5
Sugar beets	S3	3. block 4.plot	4.6	69.0

All plots were watered on a weekly basis between 3 June 2013 and 9 October 2013. Irrigation was performed eight hours (from 17:00 to 24:00) on Monday of each week. Fieldwork was started on 21 March 2013 and completed on 18 November 2013. The following works were implemented throughout the fieldwork (table 4.3).

Table 4.4 Field research works and dates

Dates	Processes
March 21	Weeds were cleaned, soil was tilled and 750 kg/da manure was applied.
April 1	Research field plots were tilled.
12 April	The trial plots were prepared (Fig. 2.1). Herbicides were applied to sugar beets plots.
19 April	Sugar beets were seeded at 12 cm within row space and 45 cm between rows space. 1000 g of DAP was applied to each plot.
27 April	Soil profiles were open at each plot and temperature sensors were placed at 0, 5, 10, 20, 30, 40, 60 cm depths. The sensors were started to record temperature at 00:00 on May 01 2013. Disturbed and undisturbed soil samples were taken from 10, 20, 30, 40, 50, 60 cm soil depths.
30 April	Corn plots were prepared. Twenty cm of within row and 45 cm of between row spacing were applied at seeding (13 rows at each plot). Five hundred g of DAP was applied at the seeding. Corn was seeded at 20 cm in row spacing and 70 cm between the rows (9 rows at each plot). One thousand g of DAP was applied at seeding.
6 May	The sugar beets were germinated. All plots were sprinkler irrigated.
6 June	All the plots, except sugar beet plots, cleaned of weeds.
18 June	Sugar beet plots cleaned of weeds.
19 July	500 g of ammonium nitrate fertilizer was applied to all planted plots. Drip irrigation was applied for half an hour.
25 October	All the plants were harvested. Some visuals of crops at different stages are given in Fig.4.4.
18 November	Thermal sensors were removed from the soil profile and data were transferred to a computer.

Figure 4.8 Visuals of different crop growth stages

4.3.1. Determination of soil thermal properties

Soil volumetric heat capacity (C_v) was calculated with the Equation (3.64), heat diffusivity parameter of soil (κ) with the Equation (3.33), and soil thermal conductivity (λ) with the Equation (3.81).

4.3.1.2. Calculation of temperature parameters at the soil-air interception

φ(t) function, which is described in section 3, expresses diurnal change of surface temperature as:

$$T(0,t) = \varphi(t) = T_0 + T_a \cos(\omega t + \varepsilon) = T_0 + A\cos(\omega t) + B\sin(\omega t) \qquad (4.1)$$

where; T_0; the average temperature of the soil surface, T_a; amplitude of temperature wave and ε values of its phase. Temperature was measured at t = 0, 3, 6, 9, 15, 18, 21 with thermal sensors (*Thermochro the iButton DS1921G*). The parameters in Eq. (4.1) were approximated by equations (3.82-3.86) (Fadeev and Fadeeva 1963, Chapra and Canale 2010,) and values of *T(0,t)* were calculated by eq. (4.2).

4.3.1.3 Calculating thermal diffusivity of soils

In the semi-homogenous soil environment, in which no heat source is found, the one-dimensional equations describing heat change based on Fourier's law is:

$$\frac{\partial T}{\partial t} = \kappa \frac{\partial^2 T}{\partial x^2} \quad \left(\kappa = \frac{\lambda}{c_v}\right) \quad , \{0 < x < L \ ve \ \infty \ ; \ t > 0\} \qquad (4.2)$$

A variety of formula have been developed for calculating heat diffusivity with different boundary conditions (layer, point and average integral).

$$T(y,\tau) = T_0 + \Phi_a(y,b) \cdot \cos\left[\bar{\omega}\tau + \varepsilon - \psi(y,b)\right] \qquad (4.3)$$

Where; $y = \frac{x}{L}$, $\tau = \frac{\kappa t}{L^2}$, $\bar{\omega} = \omega \frac{L^2}{\kappa}$, $b = \sqrt{\frac{\bar{\omega}}{2}} = L\sqrt{\frac{\pi}{\tau_0 \kappa}}$

$\Phi_a(y,b)$ is amplitude of the temperature wave in a given soil depth, (x).

Heat diffusivity parameter (κ) is calculated with below described method based on equation (4.2) by numerical analysis.

4.3.1.3.1. 'Layer' methods

Method-1 (Containing heat wave amplitude formulae): The recommended method for the presence of heat diffusivity parameters is developed based on Fourier's 1. law, which expresses steadily decreasing soil temperature amplitude in by depth. In this study κ was calculated by Eq. (4.4).

$$\kappa = \frac{\pi \left(x_2 - x_1\right)^2}{\tau_0 \ln^2 \left[\frac{\Phi_{\max}(x_1) - \Phi_{\min}(x_1)}{\Phi_{\max}(x_2) - \Phi_{\min}(x_2)} \right]} \tag{4.4}$$

Where; $\Phi_{\min}(x)$ and $\Phi_{\max}(x)$ – are minimum and maximum temperature in depths x_1 and x_2; τ_0 – period of heat wave (e.g., 24 hours for daily observations).

4.3.1.3.2 'Point' Methods

Point methods were proposed for the determination of κ from the experimental soil temperature data in different soil layers, i.e., $T(x_i, t)$. These methods can be referred to as point (P) methods, because they determine the temperature of the soil at one point at a particular soil depth.

To determine the thermal diffusivity coefficient κ (using the equations (3.79) and (3.80), the following should be known: T_a the oscillation amplitude of soil active surface

temperature; τ_0 the period (length) of a daily or yearly wave expressed in days or years; $\mathrm{T}\left(y_*, t_i^*\right), \left(i = \overline{1,4}\right)$ – the temperature values of the soil layer $[0, L]$ at an arbitrary depth $y_* = y = x_* / L$ for *eight time points:* $t_i^* = i \cdot \tau_0^* / 4 \left(i = \overline{1,4}\right)$. For example, if $\tau_0^* = 24$ hours, then $t^* = 6, 12, 18, 24$ hours.

Point method 1 (P1): Determination of κ at T (∞, t) = 0. Having this data: x^*, τ_0, T_a, $\mathrm{T}\left(y_*, t_i^*\right)$ first we calculated the differences: $\left[\mathrm{T}\left(y_*, t_i^*\right) - \mathrm{T}\left(y_*, t_{i+4}^*\right)\right]$ for all $i = \overline{1,4}$. Then, the equation (3.79) is applied to calculate κ*:

$$\kappa^* = \frac{\pi}{\tau_0} \cdot \frac{\left(2x_*\right)^2}{\ln^2 \frac{\sum_{i=1}^{2}\left[\mathrm{T}\left(x_*, t_i^*\right) - \mathrm{T}\left(x_*, t_{i+4}^*\right)\right]^2}{4\mathrm{T}_a^2}} \tag{4.5}$$

Point method 2 (P2): Calculation of κ at ∂T (L, t)/∂x = 0. The determination of κ using the equation (3.78) is performed by fitting the values of b^* in Eq. (4.6)

$$\kappa^* = \frac{\pi}{\tau_0} \cdot \left(\frac{L}{b_1^*}\right)^2 \tag{4.6}$$

Where b* is defined in eq. (4.7)

$$\sum_{i=1}^{2}\left[\mathrm{T}\left(y_*, t_i^*\right) - \mathrm{T}\left(y_*, t_{i+4}^*\right)\right]^2 / 4\mathrm{T}_a^2 \tag{4.7}$$

4.3.1.4 Evaluation of model performance

Correlation coefficient *(r)* was used to evaluate similarity between measured and predicted values of modeled variables and coefficient of determination (R^2) was used to evaluate modeling success. Root mean squared error (RMSE) and mean absolute error

(MAE) were used along with r and R^2 to evaluate the accuracy of modeling results. Deal index (D) and confidence index (C) were calculated to evaluate accuracy of modeling results.

Akaikie *(AIC)* and Bayesian Information Criterion *(BIC)* are used to evaluate model appropriateness. As our number of observations is low, *AICc*, which is derived from *AIC* was used. Criterion θ was used for comparing success of two different models and *F* was used for making pairwise comparisons of population means.

4.3.1.5. Assessment of relations between soil thermal properties and soil water content

Numerous studies have been conducted on evaluation of relations between soil water content and heat diffusivity, $\kappa = f(\theta)$. The parabolic pattern has been applied first time by (Chudnovsky 1948) and then by (Gerayzade 1982, Nabyev 1992, Fragkogiannis *et al.* 2010).

In this study, Equation (4.8) was used to describe $\tilde{\kappa}$ as function soil volumetric water content.

$$\tilde{\kappa} = a + b\theta + c\theta^2 \tag{4.8}$$

Where; $\tilde{\kappa}$ is predicted heat diffusivity, θ is the volumetric soil water content, and *a, b* and *c* are the coefficients.

Measurement of soil water content by gravimetric method

Soil water content was measured gravimetrically. Disturbed and undisturbed soil samples were taken for bulk density and water content measurements. Disturbed and undisturbed soil samples were taken from the depths where temperature sensors were placed (Fig. 4.12). Soil samples from surface soils were taken with a shovel and from deeper soils with an auger. The soil samples were placed in plastic bags, taken to nearby

laboratory, and their gravimetric water contents were determined using standard procedure. The volumetric water content (θ) of the samples were calculated by equation 4.9:

$$\theta = w\rho_b / \gamma \quad (4.9)$$

Where; w is the gravimetric water content, ρ_b is the dry bulk density of the same soil sample, and (γ) is the specific weight of the water (1 g cm^{-3}) (Hillel 1982).

4.3.2. Measurement of soil thermal properties

Soil temperature was measured with a water-proof portable thermal Sensor (Thermochro the iButton DS1921G) (Fig. 4.9). The sensor measures temperature and stores values in its memory. Recorded temperature values can be downloaded from the memory after measurements are completed.

The portable thermal sensors have used widely for measuring temperature in food science, ecological studies, and aquatic environments (Gasvoda *et al.* 2003, Robert and Thompson 2003, Hubbart *et al.* 2005, Hartman and Oring 2006, Zangmeister *et al.* 2009, Lovegrove 2009, Roznik and Alford 2012).

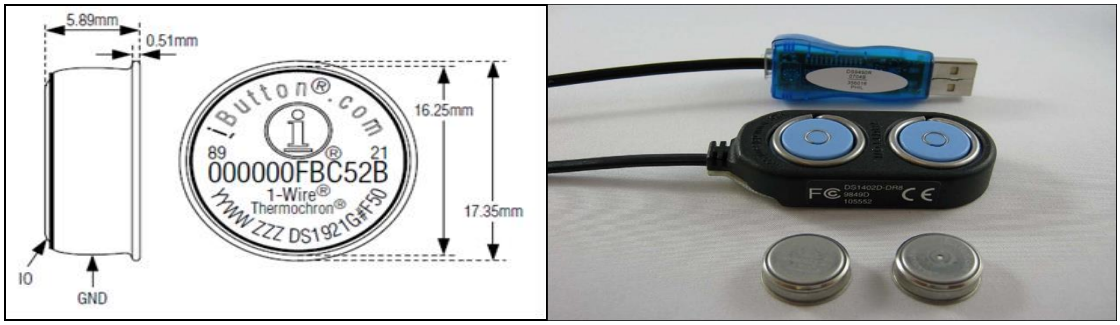

Figure 4.9 Thermochron iButton DS1921G thermal sensors and schematic diagram of Blue Dot™ receptor and USB adapter

A thermal sensor kit has four components (Fig 4.10):

1) A software and a personal computer 2) an iButton 3) a receptor 4) an adapter

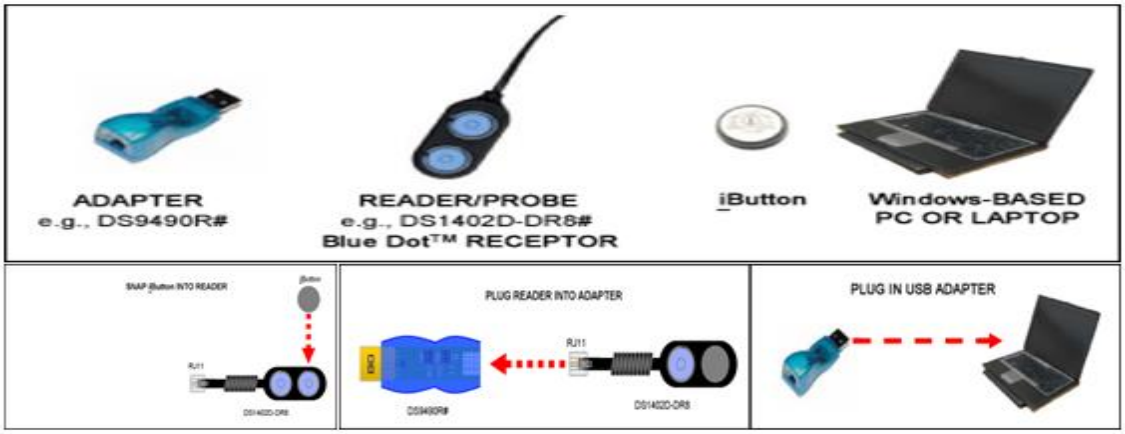

Figure 4.10 Components of a thermal sensor (iButton, Blue Dot™ receptor, USB adapter and personal computer) and the hardware diagram

Properties of Thermochron iButton Device used in this study (Maxim-Integrated 2013):

- Digital Thermometer. Measures temperature in 0.5°C increments.
- Accuracy ±1°C from -30°C to +70°C.
- Built-In Real-Time Clock (RTC) and Timer has accuracy of ±2 minutes per month from 0°C to +45°C.
- Water Resistant or Waterproof (up to 3 atm) if placed inside DS9107 iButton Capsule.
- Functions automatically and measures temperature at user-programmable intervals from 1 minute to 255 minutes.
- Logs consecutive temperature measurements in 2KB of Data-Log Memory.
- Records a long-term temperature histogram with 2.0°C resolution.
- Has programmable temperature high and temperature low alarm trip points.
- Records up to 24 timestamps and durations when temperature leaves the range specified by the trip points.
- 512 bytes of general-purpose battery-backed SRAM.
- Communicates to host with a single digital signal at 15.4kbps or 125 kbps using 1-wire protocol.

A kit is needed for installing thermal sensor and its software inside. Several versions of this software can be downloaded from the internet address

http://www.maximintegrated.com/en/products/ibutton/software/tmex/download_drivers.cfm according to the feature of computer used.

In our study, 8 temperature measurements were made in a day, making a sample range of 3 hours. Measurements were performed during 7 months, therefore, 8 x 30 x 7 = 1680 records were obtained. Sampling rate of 180 minutes was recorded. Recording was started on 1 May 2013 00:00 and ended on 26 October 2013 00:00.

Placing the thermal sensor in the profile, removing, and downloading the stored data

The thermal sensors were placed in 12 out of 36 trial plots. A soil profile was opened at the center of a plot (Fig.4.11a,b). To place a sensor, a horizontal hole was open on the wall of the soil profile normal to the vertical (Fig.4.11c), and the sensors were placed at 0, 5, 10, 20, 30, 40 and 60 cm depths (Fig.4.11d,e) and then supported using the soil taken out from the hole. After all the sensors were placed, the soil profile was filled with its original soil and its surface was leveled to plot surface (Fig.4.11f).

Figure 4.11 Placing thermal sensors in a soil profile

4.4 Laboratory Analysis

4.4.1 Soil physical properties

4.4.1.1 Soil texture

Particles size distribution was determined with a Laser Particle Sizer *analysette 22*. This device was tested in numerous of studies (Mccave *et al.* 1986, Matthews 1991, Konert and Vandenberghe 1997, Issmer 2000, Moerz and Wolf-Welling 2001, Vaasma 2010, Antinoro *et al.* 2012).

The Laser Particle Sizer *analysette 22* (Fig. 4.12) is an all-purpose measuring device that can be used to determine the particle-size distribution of solids in either fluids or gases (suspensions, aerosol) or in drops of liquid (emulsions) (Fritsch Gmbh 2004).

The *analysette 22* is controlled using the MaScontrol software. The exact measurement process is defined using SOPs (Standard Operating Procedures) which permit standardized performance of measurements for frequently recurring sample systems under identical analysis conditions (Fritsch Gmbh 2004).

Figure 4.12 The Laser Particle Device used to determine soil particle-size distribution (FRITSCH in Analyset 22 Comfort)

The analysis of the measurements as well as graphical display of the results can be predefined using templates and allowing standardized reports containing the specific values of interest to be generated as well. MaScontrol is a database-supported program. In other words, all measurements SOPs, directories and results folders or reports are saved in an SQL database that allows for simple, clear, and efficient access to all data (Fritsch Gmbh 2004). The principles of laser diffraction can be found in (Fritsch Gmbh 2004).

Soil Particle-size Analysis with "laser analysette 22"

The instrument includes: a laser system with a movable measuring cell, a unit wet dispersion comprising an ultrasonic bath (which is added directly to the sample) with a stirrer and a unit manual settings, and a computer software.

Sample preparation and carrying out measurements on «Analysette 22 comfort».
1. Preparation of the soil sample:

- The soil sample was sieved through a screen of 0.25 mm.
- From 100 to 130 mg of sieved soil sample was used.
- The sample was placed in a 50 ml plastic cup and the cap was filled with distilled water up to the mark indicating 50 ml.
- The suspension was treated with ultrasonic rod disperser BRANSON within 2 minutes at 60% power.
- The measurement was carried out following the procedure given in the Instruction manual.

2. After the measurement, the screen was prompted automatically to save, the name of the file was given and the results were saved.

4.4.1.2 Soil specific surface area

Soil thermal diffusivity is controlled by soil water content, particle size and specific surface area. Heat conduction occurs via the contact points of soil particles. While the

size of the soil particles gets smaller, specific surface area of particles increases. Increased specific surface area result in a greater contact area among soil particles and with soil water, affecting rate of the heat conduction. Specific surface area of the soils varies widely depending on the clay content and clay mineral type (Filgueira 1999, 2006).

The specific surface area and the porosity of the soil were measured with a sorptometer (Fig 4.13). Sorptometers are generally operated with helium or nitrogen gases. These gases can easily enter the small pores and enable to obtain more reliable results.

Figure 4.13 Sorptometer used in measurement of soil specific surface area

4.4.1.3 Soil bulk density

Oven dry bulk density was determined on undisturbed soil samples with a volume of 100 cm^3 taken with steel cylinders (Blake 1986).

4.4.1.4 Porosity

Soil porosity was calculated by the following equation.

$$f\% = [1- (\rho_b / \rho_s)]. 100 \quad (4.10)$$

Where; f: Porosity (%), ρ_b: oven dry bulk density (g / cm^3), ρ_b: The particle density (g / cm^3).

4.4.2 Soil chemical properties

4.4.2.1 Organic matter content

Soil organic matter content was measured using a modified Wakley-Black method (Page 1982).

4.4.2.2 Soil reaction (pH)

Soil pH was measured with a glass electrode in 1:1 soil water suspension (Mc Lean 1982).

4.4.2.3 Calcium carbonate (CaCO3)

Soil $CaCO_3$ content was measured from the Scheibler Calcimeter (Page, 1982).

4.4.2.4 Electrical conductivity (EC)

Soil electrical conductivity was measured in soil: water suspension (1:1) with a conductometer (Model 3200 Conductivity Instrument) (Rhoades, 1990).

5. RESULTS

5.1 Soils

5.1.1 Physical properties of study soils

5.1.1.1 Soil texture

Soil textural components of sand, silt and clay were highly uniform by depth (Table 5.1-5.4 and Figs 5.1 and 5.2). The overall soil texture across the treatments was clay loam (Table 5.4).

Table 5.1 Sand, silt and clay contents at the different depths of sugar beet parcels

	Size Class	**Clay %**	**Silt %**			**Sand %**	
Profile No	**Depth,** cm	<2 µm	2-5 µm	5-10 µm	10-50 µm	50-250 µm	250-2000 µm
S1	10	41.20	21.45	16.01	15.02	3.92	2.40
	20	41.18	21.66	16.65	16.22	1.57	2.72
	30	40.05	21.83	16.36	15.26	2.80	3.71
	40	41.29	23.67	17.20	14.61	0.26	2.97
	50	45.56	22.62	17.48	11.71	0.00	2.63
	60	41.78	22.08	16.69	14.03	1.46	3.97
	0-60	**41.84**	**22.22**	**16.73**	**14.47**	**1.67**	**3.06**
	Overall	**41.84**		**53.42**		**4.73**	
S2	10	36.28	18.82	14.71	21.55	5.25	3.40
	20	40.46	21.29	17.50	18.18	0.00	2.57
	30	39.05	20.52	15.46	18.28	3.10	3.58
	40	40.50	20.99	16.29	16.70	0.04	5.48
	50	41.48	21.89	16.49	16.26	0.22	3.65
	60	40.00	20.60	15.95	17.39	0.00	6.05
	0-60	**39.63**	**20.69**	**16.07**	**18.06**	**1.43**	**4.12**
	Overall	**39.63**		**54.82**		**5.55**	
S3	10	40.00	20.82	15.76	17.02	3.17	3.23
	20	40.33	21.16	16.30	17.71	0.84	3.66
	30	40.47	21.16	16.32	15.86	2.42	3.77
	40	41.59	22.67	17.27	15.01	0.57	2.89
	50	44.51	22.66	17.91	11.86	0.00	3.05
	60	43.35	22.77	17.39	11.71	0.73	4.05
	0-60	**41.71**	**21.87**	**16.82**	**14.86**	**1.29**	**3.44**
	Overall	**41.71**		**53.55**		**4.73**	

Table 5.2 Sand, silt, and clay contents at the different depths of corn plots

	Size Class	Clay %	Silt %			Sand %	
Profile	**Depht**	<2	2-5	5-10	10-50	50-250	250-2000
No	cm	µm	µm	µm	µm	µm	µm
C1	10	38.80	20.18	15.51	19.03	2.42	4.05
	20	39.48	20.66	15.94	19.21	0.11	4.60
	30	40.89	20.48	16.27	16.47	2.05	3.84
	40	41.88	21.68	17.34	15.42	0.87	2.81
	50	43.47	22.71	18.35	12.01	0.00	3.47
	60	44.92	23.46	18.08	9.40	0.00	4.14
	0-60	**41.57**	**21.53**	**16.92**	**15.26**	**0.91**	**3.82**
	Overall	**41.57**		**53.71**		**4.73**	
C2	10	38.31	19.00	14.80	20.62	3.19	4.08
	20	41.40	21.66	17.26	16.24	0.00	3.44
	30	40.45	20.54	15.82	17.02	2.06	4.12
	40	40.21	20.44	15.53	17.72	1.36	4.74
	50	39.57	19.99	15.45	18.05	0.55	6.38
	60	43.58	22.76	18.15	11.89	0.00	3.62
	0-60	**40.59**	**20.73**	**16.17**	**16.92**	**1.19**	**4.40**
	Overall	**40.59**		**53.82**		**5.59**	
C3	10	37.29	18.91	14.76	21.08	4.22	3.74
	20	40.93	21.48	17.38	17.21	0.00	3.01
	30	39.75	20.53	15.64	17.65	2.58	3.85
	40	40.36	20.72	15.91	17.21	0.70	5.11
	50	40.53	20.94	15.97	17.16	0.39	5.02
	60	41.79	21.68	17.05	14.64	0.00	4.84
	0-60	**40.11**	**20.71**	**16.12**	**17.49**	**1.31**	**4.26**
	Overall	**40.11**		**54.32**		**5.57**	

Table 5.3 Sand, silt and clay contents at the different depths of control plots

	Size Class	Clay %	Silt %			Sand %	
Profile	**Depht**	<2	2-5	5-10	10-50	50-250	250-2000
No	cm	µm	µm	µm	µm	µm	µm
Co	10	38.98	18.97	15.00	20.00	3.82	3.24
	20	39.88	20.13	16.36	18.84	0.10	4.69
	30	41.50	21.74	17.41	16.92	0.01	2.42
	40	40.48	21.18	16.41	18.19	0.05	3.69
	50	42.04	21.59	16.61	16.85	0.36	2.55
	60	40.64	20.68	16.15	15.48	1.64	5.40
	0-60	**40.59**	**20.72**	**16.32**	**17.71**	**1.00**	**3.67**
	Overall	**40.59**		**54.75**		**4.67**	

Table 5.4 Average sand, silt and clay contents at the different depths of all plots

Size Class	Clay	Silt			Sand	
Depht cm	<2 µm	2-5 µm	5-10 µm	10-50 µm	50-250 µm	250-2000 µm
10	38.69	19.74	15.22	19.19	3.71	3.45
20	40.52	21.15	16.77	17.66	0.38	3.53
30	40.31	20.97	16.18	16.78	2.14	3.61
40	40.90	21.62	16.57	16.41	0.55	3.95
50	42.45	21.77	16.90	14.84	0.22	3.82
60	42.29	22.00	17.07	13.51	0.55	4.58
0-60	**40.86**	**21.21**	**16.45**	**16.40**	**1.26**	**3.82**
Overall	**40.86**	**54.06**			**5.08**	

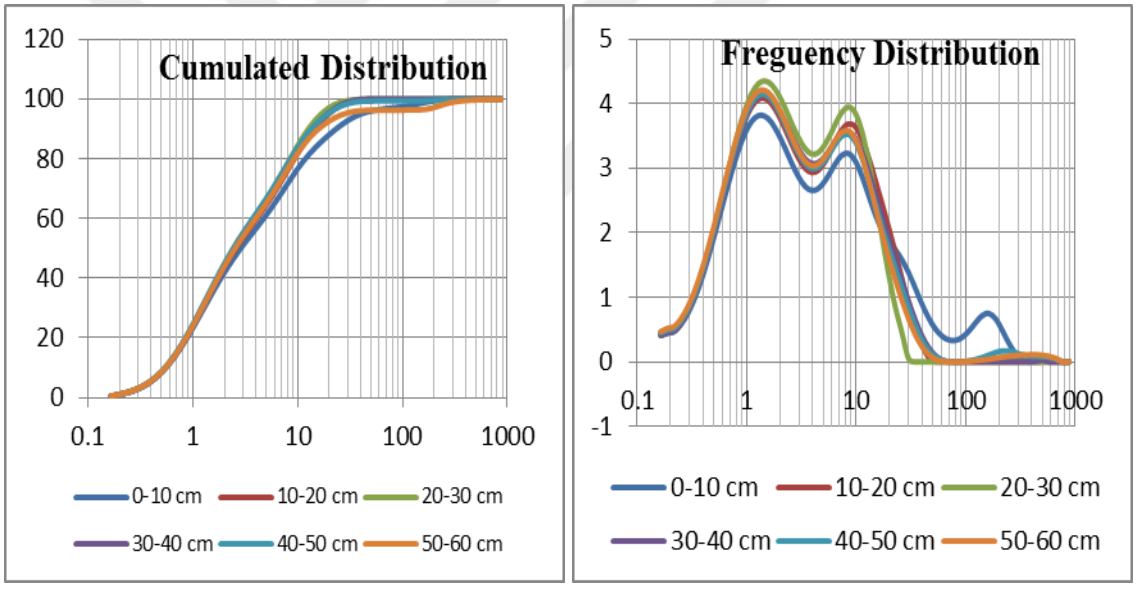

Figure 5.1 Cumulative and frequency distribution chart of sand, silt, and clay contents

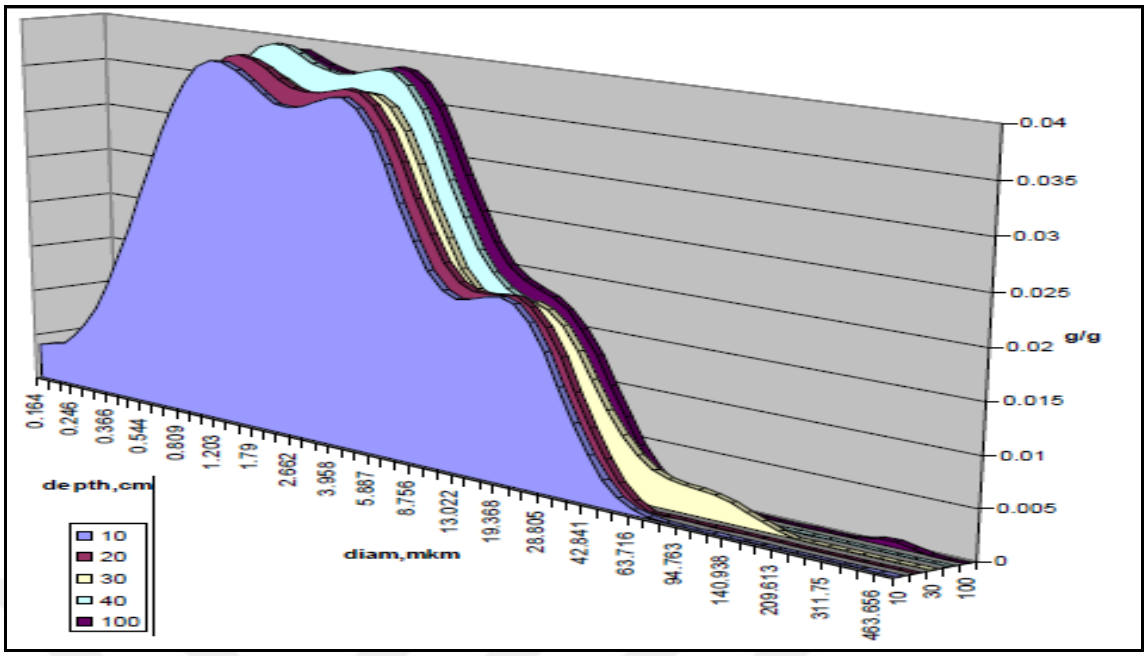

Figure 5.2 Particle size distribution (differential, g/g) of the study soils

5.1.1.2 Soil specific surface area

Soil specific surface area (SSA) was determined with sorbmeter and results obtained by the BET method are given in Table (5.5). Similar to soil particle size distribution, SSA was highly uniform with depth, which is expected since there is a close relationship between soil particle size distribution and SSA.

Table 5.5 Specific surface area of the studied soils

Vegetation	Depht (cm) / Profile No	0-10	10-20	20-30	30-40	40-50	50-60
		m^2/g					
Sugar Beet	S1	79.109	78.167	65.455	72.827	77.758	56.972
	S2	63.916	48.461	48.299	48.866	75.499	67.738
	S3	73.551	71.159	67.894	71.396	76.346	64.358
Corn	C1	67.992	64.151	70.333	69.964	74.933	71.744
	C2	69.850	66.749	66.033	47.492	54.976	52.802
	C3	66.883	57.605	57.166	48.179	65.238	60.270
Control	Co	70.963	71.931	62.256	65.023	69.011	61.625
	Mean	70.366	65.892	62.475	60.834	70.435	62.176

5.1.1.3 Soil particle density, bulk density, and porosity

The particle density (ρ_s: g/cm^3), bulk density (ρ_b: gr/cm^3) and porosity (f: %) values are given in Table (5.6). Mean value of particle density is 2.62 gr/cm^3, bulk density is 1.33 gr/cm^3, and porosity is % 49.203 (Table 5.6). All three variables are highly uniform by depth.

Table 5.6 Particle density, bulk density, and porosity of studied soils

Depth, cm	**Particle Density gr/cm^3**	**Bulk Density gr/cm^3**	**Porosity %**
10	2.636	1.201	54.427
20	2.632	1.299	50.646
30	2.619	1.362	47.995
40	2.612	1.392	46.708
50	2.608	1.349	48.275
60	2.602	1.378	47.041
Mean	**2.618**	**1.330**	**49.203**

5.1.2 Chemical properties of soils

Vertical change of soil pH, EC, $CaCO_3$, and nitrogen values of soil samples at sugar beet, corn, and control plots are given in Tables 5.7-5.10. In general, N content decreased, while C/N ratio increased with depth. In some plots (e.g. 1.block, 1. plot in Table 5.7) pH and EC are highly uniform, while at some other plots (e.g. Table 5.9 2.block, 4.plot) both variables somehow varied by depth.

Table 5.7 Soil pH, EC, $CaCO_3$, and nitrogen (N) contents at sugar beet plots

Profile No	**Depth,** cm	**pH** (1:1)	**EC** µS/cm (1:1)	**$CaCO_3$** %	**N** %	**C/N**
	0-10	7.56	817	2.40	0.14	6.3
	10-20	7.70	829	2.36	0.13	7.6
	20-30	7.64	850	2.35	0.13	5.3
S1	30-40	7.70	844	2.43	0.10	5.1
	40-50	7.80	652	2.49	0.07	6.0
	50-60	7.67	840	2.46	0.05	8.4
	0-60 Mean	**7.68**	**805**	**2.42**	**0.10**	**6.5**
	0-10	7.67	881	2.21	0.12	7.4
	10-20	7.61	928	2.22	0.12	5.7
	20-30	7.67	824	2.28	0.09	5.3
S2	30-40	7.69	716	2.27	0.09	4.8
	40-50	7.67	683	2.39	0.04	10.5
	50-60	7.65	640	2.46	0.05	7.0
	0-60 Mean	**7.66**	**779**	**2.31**	**0.09**	**6.8**
	0-10	7.60	801	2.38	0.14	6.1
	10-20	7.69	770	2.36	0.13	6.2
	20-30	7.65	837	2.37	0.12	5.0
S3	30-40	7.71	825	2.43	0.09	5.5
	40-50	7.74	731	2.45	0.06	7.2
	50-60	7.69	781	2.46	0.05	8.3
	0-60 Mean	**7.68**	**791**	**2.40**	**0.10**	**6.4**

Ph:Soil Reaction, EC: Elelctrical Conductivite, C: Carbon, N: Nitrogen

Except N, all other variables were highly uniform by depth.

Table 5.8 Soil pH, EC, $CaCO_3$, and nitrogen (N) contents values of corn plots

Profile No	Depth, cm	pH (1:1)	EC (1:1)	$CaCO_3$ %	N %	C/N
C1	0-10	7.64	785	2.35	0.14	5.8
	10-20	7.68	711	2.35	0.12	4.8
	20-30	7.66	823	2.38	0.11	4.6
	30-40	7.71	805	2.42	0.08	5.8
	40-50	7.68	810	2.40	0.05	8.4
	50-60	7.70	722	2.45	0.05	8.2
	0-60 Mean	**7.68**	**776**	**2.39**	**0.09**	**6.3**
C2	0-10	7.64	997	2.34	0.15	5.8
	10-20	7.65	890	2.42	0.12	6.0
	20-30	7.63	814	2.41	0.11	4.1
	30-40	7.56	714	2.43	0.09	4.0
	40-50	7.66	572	2.48	0.07	6.0
	50-60	7.71	561	2.51	0.05	8.6
	0-60 Mean	**7.64**	**758**	**2.43**	**0.10**	**5.8**
C3	0-10	7.66	939	2.28	0.14	6.6
	10-20	7.63	909	2.32	0.12	5.9
	20-30	7.65	819	2.35	0.10	4.7
	30-40	7.63	715	2.35	0.09	4.4
	40-50	7.67	628	2.44	0.06	8.3
	50-60	7.68	601	2.49	0.05	7.8
	0-60 Mean	**7.65**	**768**	**2.37**	**0.09**	**6.3**

Ph:Soil Reaction, EC: Electrical Conductivity, C: Carbon, N: Nitrogen

Table 5.9 Soil pH, EC, $CaCO_3$, and nitrogen (N) contents values at control plots

Profile No	Depth, cm	pH (1:1)	E.C (1:1)	$CaCO_3$ %	N %	C/N
Co	0-10	7.75	789	2.38	0.15	5.7
	10-20	7.71	745	2.39	0.13	6.2
	20-30	7.77	649	2.32	0.11	6.5
	30-40	7.75	649	2.32	0.08	7.7
	40-50	7.69	673	2.32	0.08	5.6
	50-60	7.91	726	2.39	0.03	15.0
	0-60 Mean	**7.76**	**705**	**2.35**	**0.10**	**7.8**

p^H: Soil Reaction, EC: Electrical conductivity, C: Carbon N: nitrogen

Table 5.10 Mean values of soil pH, EC, $CaCO_3$ and nitrogen (N) contents in all parcel

Depth, cm	**pH** (1:1)	**EC** (1:1)	**$CaCO_3$** %	**N** %	**C/N**
0-10	7.65	854	2.34	0.14	6.2
10-20	7.67	821	2.35	0.12	6.1
20-30	7.67	792	2.35	0.11	5.2
30-40	7.68	746	2.37	0.09	5.5
40-50	7.70	678	2.42	0.06	7.3
50-60	7.73	698	2.45	0.05	9.4
0-60 Mean	**7.68**	**765**	**2.38**	**0.10**	**6.6**

p^H: Soil Reaction, EC: Electrical conductivity, C: Carbon N: Nitrogen

5.2 Description of Research Area Soils

Exploratory statistics of soil properties according to average and different depths values were given in Table (5.11- 5.17).

Table 5.11 Exploratory statistics of soil properties at 0-10 cm

Parameters	**Min.**	**Max.**	**Mean**	**Std. Error**	**Std. Deviation**	**Variance**	**CV %**
Clay, (%)	36.280	41.200	38.694	0.618	1.634	2.671	4.224
Silt, (%)	52.480	55.080	54.146	0.336	0.889	0.791	1.643
Sand, (%)	6.320	8.650	7.161	0.332	0.880	0.774	12.282
SSA, (m^2/g)	63.916	79.109	70.323	1.868	4.942	24.427	7.028
BD, (gr/cm^3)	1.134	1.250	1.201	0.018	0.047	0.002	3.928
f, (%)	52.561	56.968	54.427	0.677	1.790	3.204	3.289
pH, (1:1)	7.560	7.750	7.645	0.022	0.059	0.004	0.775
EC, (µS/cm)	785.0	997.0	858.4	31.407	83.096	6904.9	9.680
C, (%)	2.210	2.400	2.334	0.025	0.067	0.005	2.883
N, (%)	0.120	0.150	0.140	0.004	0.010	0.000	7.143

SSA: Specific surface area, BD: Bulk density, f: Porosity, EC: Electrical conductivity, C: Carbon N: nitrogen, Min.: Minimum, Max.: Maximum, CV: Coefficient of variation

Table 5.12 Exploratory statistics of soil properties at 10-20 cm depth

Parameters	Min.	Max.	Mean	Std. Error	Std. Deviation	Variance	CV %
Clay, (%)	39.480	41.400	40.523	0.263	0.696	0.485	1.718
Silt, (%)	54.530	56.970	55.577	0.298	0.789	0.622	1.420
Sand, (%)	2.570	4.790	3.901	0.336	0.888	0.789	22.765
SSA, (m^2/g)	48.461	78.167	65.460	3.748	9.915	98.310	15.147
BD, (gr/cm^3)	1.268	1.357	1.299	0.012	0.032	0.001	2.438
f, (%)	48.447	51.825	50.642	0.455	1.203	1.448	2.376
pH, (1:1)	7.610	7.710	7.667	0.014	0.038	0.001	0.492
EC, (µS/cm)	711.0	928.0	826.0	32.484	85.946	7386.7	10.405
C, (%)	2.220	2.420	2.346	0.024	0.064	0.004	2.717
N, (%)	0.120	0.130	0.124	0.002	0.005	0.000	4.301

SSA: Specific surface area, BD: Bulk density, f: Porosity, EC: Electrical conductivity, C: Carbon N: nitrogen, Min.: Minimum, Max.: Maximum, CV: Coefficient of variation

Table 5.13 Exploratory statistics of soil properties at 20-30 cm

Parameters	Min.	Max.	Mean	Std. Error	Std. Deviation	Variance	CV %
Clay, (%)	39.050	41.500	40.309	0.299	0.792	0.628	1.966
Silt, (%)	53.220	56.070	53.934	0.381	1.007	1.014	1.867
Sand, (%)	2.430	6.680	5.759	0.563	1.490	2.221	25.879
SSA, (m^2/g)	48.299	70.333	62.491	2.853	7.548	56.974	12.079
BD, (gr/cm^3)	1.276	1.439	1.362	0.021	0.055	0.003	4.023
f, (%)	45.047	51.261	48.002	0.791	2.092	4.376	4.358
pH, (1:1)	7.630	7.770	7.667	0.018	0.047	0.002	0.615
EC, (µS/cm)	649.0	850.0	802.2	25.940	68.631	4710.2	8.555
C, (%)	2.280	2.410	2.351	0.016	0.042	0.002	1.795
N, (%)	0.090	0.130	0.110	0.005	0.013	0.000	11.736

SSA: Specific surface area, BD: Bulk density, f: Porosity, EC: Electrical conductivity, C: Carbon N: nitrogen, Min.: Minimum, Max.: Maximum, CV: Coefficient of variation

Table 5.14 Exploratory statistics of soil properties at 30-40 cm

Parameters	Min.	Max.	Mean	Std. Error	Std. Deviation	Variance	CV %
Clay, (%)	40.210	41.880	40.901	0.253	0.670	0.449	1.638
Silt, (%)	53.690	55.780	54.594	0.313	0.827	0.684	1.515
Sand, (%)	3.230	6.100	4.506	0.470	1.242	1.543	27.573
SSA, (m^2/g)	47.492	72.827	60.535	4.464	11.811	139.510	19.512
BD, (gr/cm^3)	1.368	1.468	1.392	0.013	0.035	0.001	2.542
f, (%)	43.811	47.615	46.696	0.512	1.355	1.835	2.901
pH, (1:1)	7.560	7.750	7.677	0.024	0.064	0.004	0.829
EC, (µS/cm)	649.0	844.0	752.5	27.275	72.164	5207.6	9.590
C, (%)	2.270	2.430	2.379	0.025	0.065	0.004	2.751
N, (%)	0.080	0.100	0.089	0.003	0.007	0.000	7.791

SSA: Specific surface area, BD: Bulk density, f: Porosity, EC: Electrical conductivity, C: Carbon N: nitrogen, Min.: Minimum, Max.: Maximum, CV: Coefficient of variation

Table 5.15 Exploratory statistics of soil properties at 40-50 cm

Parameters	Min.	Max.	Mean	Std. Error	Std. Deviation	Variance	CV %
Clay, (%)	39.570	45.560	42.451	0.817	2.162	4.674	5.093
Silt, (%)	51.810	55.050	53.509	0.442	1.170	1.369	2.186
Sand, (%)	2.630	6.930	4.039	0.594	1.572	2.471	38.926
SSA, (m^2/g)	54.976	77.758	70.537	3.095	8.189	67.064	11.610
BD, (gr/cm^3)	1.303	1.406	1.349	0.014	0.038	0.001	2.830
f, (%)	46.093	50.041	48.287	0.553	1.463	2.142	3.031
pH, (1:1)	7.660	7.800	7.701	0.019	0.051	0.003	0.667
EC, (µS/cm)	572.0	810.0	678.4	28.762	76.097	5790.7	11.218
C, (%)	2.320	2.490	2.424	0.022	0.059	0.003	2.439
N, (%)	0.040	0.080	0.061	0.005	0.013	0.000	21.898

SSA: Specific surface area, BD: Bulk density, f: Porosity, EC: Electrical conductivity, C: Carbon N: nitrogen, Min.: Minimum, Max.: Maximum, CV: Coefficient of variation

Table 5.16 Exploratory statistics of soil properties at 50-60 cm

Parameters	Min.	Max.	Mean	Std. Error	Std. Deviation	Variance	CV %
Clay, (%)	40.000	44.920	42.294	0.658	1.741	3.030	4.116
Silt, (%)	50.940	53.940	52.576	0.373	0.986	0.973	1.876
Sand, (%)	3.620	7.040	5.129	0.438	1.158	1.342	22.587
SSA, (m^2/g)	52.802	71.744	62.216	2.421	6.405	41.020	10.294
BD, (gr/cm^3)	1.304	1.464	1.378	0.021	0.056	0.003	4.043
f, (%)	43.746	49.881	47.030	0.809	2.141	4.586	4.553
pH, (1:1)	7.650	7.910	7.715	0.033	0.088	0.008	1.143
EC, (µS/cm)	561.0	840.0	695.8	37.802	100.015	10002.9	14.374
C, (%)	2.390	2.510	2.460	0.014	0.037	0.001	1.521
N, (%)	0.030	0.050	0.047	0.003	0.008	0.000	16.035

SSA: Specific surface area, BD: Bulk density, f: Porosity, EC: Electrical conductivity, C: Carbon N: nitrogen, Min.: Minimum, Max.: Maximum, CV: Coefficient of variation

In majority of cases, the soil properties exhibited low variations as indicated by their calculated CV values. However, in some cases sand content and content and SSA showed a medium variation. Greater variation of N at deeper depths was attributed to that N leached from upper soils accumulated to lower depths non uniformly depending on the magnitude of leaching that controlled by variations in water flow rates throughout the soil profile. Overall (0-60 cm depth), N was moderately variable and all the other soil properties were slightly variable (Table 5.17) suggesting that the soils could be deemed uniform to conduct a field trial.

Table 5.17 Exploratory statistics of soil properties at 0-60 cm

Parameters	Min.	Max.	Mean	Std. Error	Std. Deviation	Variance	CV %
Clay, (µm)	38.690	42.450	40.860	0.569	1.393	1.940	3.409
Silt, (µm)	53.120	57.860	55.310	0.703	1.722	2.964	3.113
Sand, (µm)	3.450	4.580	3.820	0.170	0.416	0.173	10.874
SSA, (m^2/g)	60.535	70.537	65.260	1.759	4.308	18.558	6.601
BD, (gr/cm^3)	1.201	1.392	1.330	0.029	0.071	0.005	5.326
f, (%)	46.700	54.430	49.180	1.192	2.921	8.531	5.939
pH, (1:1)	7.650	7.720	7.680	0.010	0.025	0.001	0.330
EC, (µS/cm)	678.4	858.4	768.8	29.551	72.386	5239.7	9.414
C, (%)	2.330	2.460	2.380	0.020	0.050	0.002	2.091
N, (%)	0.050	0.140	0.100	0.015	0.036	0.001	38.050

SSA: Specific surface area, BD: Bulk density, f: Porosity, EC: Electrical conductivity, C: Carbon N: nitrogen, Min.: Minimum, Max.: Maximum, CV: Coefficient of variation

5.3. Soil Thermal Properties

5.3.1. Volumetric heat capacity

Specific heat capacity of an oven dry soil is simply deemed equal to specific heat capacity of quars as given in Eq. (5.1).

$$C_{m,\,solid\,phase} = 0.20\ cal\ /\ g.\ ^{0}C \tag{5.1}$$

Calculation of volumetric heat capacity (C_v) is exemplified, giving the all the calculations for 0-5 cm depth at 2.block and 2. plot for sugar beet as: For 0-5 cm soil depth ρ_b=1.2187 and θ=0.3774. Using these values with Eqs. 3.64, 3.68, and 3.69; the related values for C_v was calculated as.

$$C_v = C_{m,solid\,phase}\cdot\rho_b + C_{vw}\cdot\theta = 0.20\frac{cal}{g\cdot{}^{o}C}\cdot 1.2187\frac{g}{cm^3} + 1\frac{cal}{cm^3\cdot{}^{o}C}\cdot 0.3774\frac{cm^3}{cm^3}$$

$$= 0.2436\frac{cal}{cm^3\cdot{}^{o}C} + 0.3774\frac{cal}{cm^3\cdot{}^{o}C} = 0.6211\frac{cal}{cm^3\cdot{}^{o}C} = 2.6\cdot 10^{6}\frac{J}{m^3\cdot{}^{o}C}$$

The variables θ, ρ_b, and C_v of studied soils are given in Table 5.18-5.20.

Table 5.18 Bulk density (ρ_b) gr/cm^3 of study soils

Crop	Profile No	0-5	5-10	10-20	20-30	30-40	40-50	50-60
Sugar beet	S1	1.159 ±0.04	1.209 ±0.05	1.320 ±0.03	1.327 ±0.04	1.375 ±0.00	1.406 ±0.05	1.368 ±0.02
	S2	1.218 ±0.04	1.268 ±0.05	1.279 ±0.01	1.276 ±0.04	1.369 ±0.00	1.331 ±0.02	1.364 ±0.01
	S3	1.142 ±0.04	1.167 ±0.05	1.269 ±0.02	1.348 ±0.02	1.368 ±0.00	1.307 ±0.02	1.336 ±0.03
Mean		1.173	1.215	1.290	1.317	1.371	1.348	1.356
Corn	C1	1.223 ±0.04	1.273 ±0.03	1.301 ±0.02	1.348 ±0.03	1.377 ±0.01	1.303 ±0.04	1.304 ±0.07
	C2	1.236 ±0.03	1.266 ±0.02	1.268 ±0.02	1.415 ±0.02	1.404 ±0.01	1.383 ±0.02	1.439 ±0.04
	C3	1.169 ±0.05	1.219 ±0.05	1.299 ±0.04	1.379 ±0.03	1.386 ±0.05	1.351 ±0.01	1.372 ±0.05
Mean		1.209	1.253	1.289	1.381	1.389	1.346	1.372
Control	Co	1.109	1.159	1.357	1.439	1.468	1.360	1.464
Grand mean		1.180	1.223	1.299	1.362	1.392	1.349	1.378

Table 5.19 Volumetric water content θ (cm^3/cm^3) of study soils

Crop	Profile No	0-5	5-10	10-20	20-30	30-40	40-50	50-60
Sugar beet	S1	0.372 ±0.01	0.391 ±0.01	0.422 ±0.01	0.410 ±0.02	0.405 ±0.01	0.415 ±0.01	0.399 ±0.01
	S2	**0.377** ±0.00	0.401 ±0.00	0.415 ±0.01	0.408 ±0.01	0.420 ±0.00	0.402 ±0.00	0.409 ±0.01
	S3	0.385 ±0.01	0.409 ±0.01	0.439 ±0.01	0.429 ±0.01	0.423 ±0.01	0.396 ±0.01	0.394 ±0.01
Mean		0.378	0.400	0.425	0.416	0.416	0.404	0.401
Corn	C1	0.373 ±0.02	0.396 ±0.01	0.428 ±0.00	0.422 ±0.01	0.412 ±0.00	0.384 ±0.02	0.380 ±0.02
	C2	0.409 ±0.01	0.422 ±0.01	0.435 ±0.00	0.433 ±0.00	0.420 ±0.00	0.416 ±0.01	0.425 ±0.01
	C3	0.393 ±0.00	0.412 ±0.00	0.435 ±0.01	0.422 ±0.01	0.417 ±0.01	0.401 ±0.01	0.402 ±0.01
Mean		0.392	0.410	0.432	0.426	0.416	0.401	0.402
Control	Co	0.386	0.418	0.446	0.441	0.441	0.413	0.423
Grand mean		0.385	0.407	0.431	0.423	0.420	0.404	0.405

Table 5.20 Volumetric heat capacity C_v (Cal/cm^3 ^{0}C) of study soils

Crop	Profile No	0-5	5-10	10-20	20-30	30-40	40-50	50-60
Sugar beet	S1	0.604 ±0.01	0.633 ±0.01	0.686 ±0.01	0.675 ±0.02	0.680 ±0.01	0.697 ±0.02	0.672 ±0.01
	S2	0.621 ±0.00	0.654 ±0.01	0.671 ±0.01	0.663 ±0.02	0.693 ±0.01	0.668 ±0.01	0.682 ±0.01
	S3	0.614 ±0.00	0.642 ±0.00	0.693 ±0.00	0.698 ±0.01	0.697 ±0.00	0.657 ±0.01	0.661 ±0.02
Mean		0.613	0.643	0.683	0.679	0.690	0.674	0.672
Corn	C1	0.618 ±0.02	0.650 ±0.01	0.688 ±0.00	0.691 ±0.01	0.687 ±0.01	0.645 ±0.02	0.641 ±0.04
	C2	0.656 ±0.02	0.675 ±0.01	0.689 ±0.00	0.716 ±0.01	0.700 ±0.00	0.693 ±0.01	0.713 ±0.02
	C3	0.627 ±0.01	0.656 ±0.01	0.694 ±0.01	0.697 ±0.02	0.694 ±0.02	0.671 ±0.01	0.676 ±0.02
Mean		0.634	0.660	0.690	0.702	0.694	0.670	0.677
Control	Co	0.608	0.650	0.718	0.729	0.735	0.685	0.715
Grand mean		0.622	0.652	0.690	0.695	0.697	0.673	0.679

The study plots were fairly uniform in ρ_b, θ, and C_v (Tables 5.18-5.20) by depth across the treatments of corn, sugar beets and control.

5.3.2 Soil surface thermal properties

We predicted soil thermal properties at soil surface by Eqs. (3.39-3.42). The calculations were exemplified using the variables obtained at a sugar beet plot (S2) on 20.08.2013. Taking initial parameters π=3.1416 and 25 h, the value for ω is calculates as follows:

$$\omega = \frac{2\pi}{\tau_0} = \frac{2\pi}{24h} = \frac{2 \cdot 3.1416}{24 \cdot 3600} = \frac{6.283185}{86400\,\mathrm{s}} = 7.2722.10^{-5}$$

Taking the t_1=0, $\omega t = 0 \cdot 7,2722 \cdot 10^{-5} = 0,00$. Using these values with Eqs. (3.39-3.42), the related parameters are calculated as follows:

$$T_i \cos(\omega t_i) = 16 * \cos(0,00) = 16 \text{ and } \quad T_i \sin(\omega t_i) = 16 * \sin(0,00) = 0,00$$

$$\mathrm{T}_0 = \frac{1}{8}\sum_{i=1}^{8} \mathrm{T}(0,t_i) = \frac{16.0+12.5+12.5+17.5+30.5+38.0+28.5+17.5}{8} = 21.75$$

$$A = \frac{2}{\mathrm{N}}\sum_{i=1}^{\mathrm{N}} \mathrm{T}(0,t_i)\cos(\omega t_i) = \frac{2}{8}\cdot(-31.8241) = -7.9560$$

$$B = \frac{2}{\mathrm{N}}\sum_{i=1}^{\mathrm{N}} \mathrm{T}(0,t_i)\sin(\omega t_i) = \frac{2}{8}\cdot(-33.3241) = -8.3310$$

$$T_a = \sqrt{A^2 + B^2} = \sqrt{(-7.956)^2 + (-8.331)^2} = 11.5197$$

$$\varepsilon = \pi - \arctan\left(\frac{B_1}{A_1}\right) = \pi - \arctan\left(\frac{-8.331}{-7.956}\right) = \pi - \arctan(1.047134) =$$
$$= \pi - 0.808419 = 2.333174$$

$$\tilde{\mathrm{T}}(0,t) = \mathrm{T}_0 + \mathrm{T}_a \cos(\omega t + \varepsilon) = 21.75 + 11.5197\cos(0.00 + 2.3332 = 13.79$$

The calculations for this plot (sugar beet; S2) are given in Table 5.21. These calculations were made all the studied plots once in a week during 16 weeks. The results are given in Tables 5.22-5.24.

Table 5.21 Values for T_0, T_a, ε on soil surface

t_i Time	**T_i ^{0}C**	**ωt**	**$T_i\cos(\omega t_i)$**	**$T_i\sin(\omega t_i)$**	**T_0 ^{0}C**
0	16.0	0.0000	16.0000	0.0000	13.794
3	13.5	0.7854	9.5459	9.5459	10.233
6	12.5	1.5708	0.0000	12.5000	13.419
9	17.5	2.3562	-12.3744	12.3744	21.485
12	30.5	3.1416	-30.5000	0.0000	29.706
15	38.0	3.9270	-26.8701	-26.8701	33.267
18	28.5	4.7124	0.0000	-28.5000	30.081
21	17.5	5.4978	12.3744	-12.3744	22.015
Tort	**21.75**		**-31.8241**	**-33.3241**	**21.7500**
ε	2.3332		**A** -7.9560	**B** -8.3310	
T_a	11.5972				

Table. 5.22 Measured (T_0 and T_a) and calculated (ω) parameters and corresponding goodness of fit parameters calculated for control plot for 16 weeks of study period.

		Parameters at the soil surface			**Parameters for goodness of fit**							
Weeks	**Date**	T_0	T_a	ε	η	R^2	R^2_{adj}	D	C=ηD	*UI*	*HQC*	**F*
1	06.06.2013	22.31	16.4732	2.9305	0.8542	0.7297	0.6216	0.9165	0.7830	0.1381	4.4661	6.75
2	21.06.2013	21.31	13.8764	2.4261	0.9677	0.9365	0.9111	0.9833	0.9516	0.0543	2.4256	36.85
3	24.06.2013	25.75	17.8594	2.5527	0.9767	0.9539	0.9355	0.9881	0.9650	0.0483	2.5913	51.72
4	02.07.2013	20.25	9.8583	2.5928	0.9497	0.9020	0.8627	0.9735	0.9246	0.0535	2.2135	23.00
5	09.07.2013	22.37	10.9298	2.2915	0.9767	0.9540	0.9356	0.9881	0.9651	0.0358	1.6067	51.86
6	15.07.2013	24.25	7.5238	2.6273	0.9261	0.8577	0.8008	0.9602	0.8892	0.0436	2.0958	15.07
7	23.01.2013	20.75	10.7584	2.2836	0.9623	0.9259	0.8963	0.9805	0.9435	0.0486	2.0813	31.26
8	14.08.2013	24.94	17.0271	2.3929	0.9581	0.9180	0.8853	0.9782	0.9373	0.0647	3.1095	28.00
9	20.08.2013	21.25	11.5972	2.4674	0.9690	0.9389	0.9144	0.9840	0.9534	0.0458	2.0256	38.40
10	27.08.2013	22.81	14.4219	2.5549	0.9658	0.9327	0.9058	0.9823	0.9487	0.0546	2.5641	34.66
11	04.09.2013	19.06	9.4036	2.7456	0.8849	0.7830	0.6962	0.9353	0.8276	0.0860	3.0547	9.02
12	10.09.2013	16.50	10.8255	2.3922	0.9707	0.9422	0.9191	0.9849	0.9561	0.0520	1.8277	40.78
13	25.09.2013	15.75	12.0459	2.4045	0.9252	0.8561	0.7985	0.9598	0.8881	0.0966	3.0503	14.87
14	01.10.2013	15.44	6.5578	2.3720	0.9167	0.8403	0.7764	0.9547	0.8751	0.0625	1.9570	13.15
15	08.10.2013	6.69	9.9864	2.3556	0.9292	0.8635	0.8089	0.9620	0.8939	0.1415	2.6137	15.81
16	22.10.2013	7.56	11.8192	2.3451	0.9179	0.8425	0.7795	0.9554	0.8769	0.1564	3.1183	13.37

T_0: Average Temperature at soil Surface, T_a: Wave amplitude, ε: Phase angle, η: Correlation coefficient, R^2: Coefficient of determination, R^2_{adj}: Adjusted R^2, *D:* Agreement index, *c*: The confidence index, *UI:* Theil's Forecast accuracy coefficient, *HQC*; Hannan-Quinn criteria, *F:* Fisher criteria.
* for α=0,01: **F_{tabl}=13.27;** for α=0,05: **F_{tabl}=5.79**

Table. 5.23 Mean measured (T_0, T_a) and calculated (ω) parameters and corredponding goodnes of fit parameters calculated for plots S1,S2,and S3 plots for 16 weeks of study period

		Parameters at the soil surface			Parameters for goodness of fit							
Weeks	**Date**	T_0	T_a	ε	η	R^2	R^2_{adj}	**D**	**C=ηD**	*UI*	*HQC*	***F**
1	06.06.2013	20.54	13.3128	2.1892	0.9199	0.8481	0.7874	0.9560	0.8806	0.088	3.174	18.06
2	21.06.2013	21.40	13.3258	2.6656	0.9507	0.9040	0.8656	0.9741	0.9262	0.064	2.737	25.16
3	24.06.2013	29.02	19.2036	2.7388	0.9100	0.8319	0.7647	0.9498	0.8665	0.089	3.963	18.91
4	02.07.2013	21.33	12.6144	2.0266	0.9101	0.8289	0.7605	0.9509	0.8658	0.085	3.224	13.55
5	09.07.2013	25.54	14.8419	2.1329	0.9353	0.8764	0.8270	0.9650	0.9035	0.069	3.116	25.84
6	15.07.2013	22.48	7.3288	2.1334	0.9045	0.8214	0.7500	0.9455	0.8572	0.043	1.882	15.85
7	23.07.2013	21.27	11.1859	2.1397	0.9351	0.8755	0.8257	0.9652	0.9032	0.065	2.506	21.77
8	14.08.2013	25.15	15.6729	2.1297	0.9077	0.8242	0.7539	0.9499	0.8624	0.092	3.788	12.07
9	20.08.2013	22.60	14.0112	2.1204	0.9062	0.8221	0.7509	0.9484	0.8600	0.093	3.543	12.78
10	27.08.2013	21.94	11.8937	2.0767	0.9419	0.8880	0.8432	0.9691	0.9132	0.063	2.584	24.89
11	04.09.2013	17.40	10.4806	2.2470	0.9096	0.8283	0.7596	0.9505	0.8651	0.087	2.665	14.32
12	10.09.2013	18.10	12.1089	2.1744	0.9334	0.8732	0.8225	0.9639	0.9008	0.080	2.559	29.28
13	25.09.2013	17.15	13.2037	2.2211	0.9286	0.8640	0.8097	0.9612	0.8935	0.091	2.965	22.21
14	01.10.2013	14.33	7.4695	2.3989	0.8401	0.7096	0.5935	0.9066	0.7640	0.098	2.476	8.01
15	08.10.2013	9.77	12.1654	2.2762	0.9301	0.8654	0.8115	0.9626	0.8955	0.126	2.924	16.80
16	22.10.2013	9.67	14.0050	2.3095	0.9280	0.8615	0.8060	0.9613	0.8923	0.138	3.147	16.86

T_0: Average Temperature at soil Surface, *T_a:* Wave amplitude, ε: Phase angle, η: Correlation coefficient, R^2: Coefficient of determination, R^2_{adj}: Adjusted R^2, *D:* Agreement index, *c*: The confidence index, *UI:* Theil's Forecast accuracy coefficient, *HQC*; Hannan-Quinn criteria, *F:* Fisher criteria.
* for α=0,01: **F_{tabl}=13.27;** for α=0,05: **F_{tabl}=5.79**

Table. 5.24 Mean measured (T_0, T_a) and calculated (ω) parameters and corredponding goodnes of fit parameters calculated for plots C1,C2,and C3 plots for 16 weeks of study period

		The parameters of the soil surface			**Statistical parameters of approximation**							
Weeks	**Date**	T_0	T_a	ε	η	R^2	R^2_{adj}	D	C=ηD	*UI*	*HQC*	**F*
1	06.06.2013	20.54	11.9894	2.7940	0.8445	0.7163	0.6027	0.9083	0.7692	0.1144	3.7988	7.1133
2	21.06.2013	20.48	10.8145	2.4540	0.9272	0.8618	0.8065	0.9600	0.8913	0.0682	2.3946	42.8600
3	24.06.2013	24.75	15.0494	2.5052	0.9462	0.8962	0.8547	0.9712	0.9195	0.0657	2.8443	40.5833
4	02.07.2013	19.50	6.8066	2.4397	0.9115	0.8325	0.7655	0.9511	0.8679	0.0545	2.0028	14.8533
5	09.07.2013	22.73	8.2535	2.3893	0.9402	0.8843	0.8381	0.9681	0.9105	0.0455	1.9570	20.6300
6	15.07.2013	24.35	7.0898	2.7846	0.8467	0.7224	0.6113	0.9072	0.7720	0.0625	2.5893	8.2767
7	23.07.2013	19.89	7.5413	2.4043	0.9348	0.8769	0.8277	0.9638	0.9027	0.0468	1.5700	37.1533
8	14.08.2013	21.69	8.0738	2.4138	0.9601	0.9221	0.8909	0.9792	0.9402	0.0371	1.4831	33.7067
9	20.08.2013	19.87	6.8830	2.3566	0.9563	0.9149	0.8809	0.9770	0.9346	0.0369	1.1641	33.5733
10	27.08.2013	20.04	6.8730	2.3447	0.9754	0.9515	0.9320	0.9874	0.9631	0.0265	0.7047	50.8200
11	04.09.2013	17.56	4.6065	2.6994	0.8610	0.7422	0.6391	0.9194	0.7922	0.0532	1.8039	7.6133
12	10.09.2013	15.58	7.6210	2.3636	0.9679	0.9370	0.9118	0.9835	0.9520	0.0424	1.1990	38.1033
13	25.09.2013	15.58	8.6490	2.4183	0.9477	0.8982	0.8575	0.9724	0.9216	0.0606	1.9460	22.8500
14	01.10.2013	17.96	7.1712	2.5093	0.9256	0.8569	0.7997	0.9597	0.8885	0.0537	1.9310	15.6833
15	08.10.2013	7.46	7.4987	2.4180	0.9622	0.9260	0.8964	0.9804	0.9434	0.0798	1.3247	31.8467
16	22.10.2013	7.25	8.1754	2.4497	0.9488	0.9004	0.8606	0.9731	0.9233	0.1021	1.7867	23.8933

T_0: Average Temperature at soil Surface, T_a: Wave amplitude, ε: Phase angle, η: Correlation coefficient, R^2: Coefficient of determination, R^2_{adj}: Adjusted R^2, *D:* Agreement index, *c*: The confidence index, *UI:* Theil's Forecast accuracy coefficient, *HQC*; Hannan-Quinn criteria, *F:* Fisher criteria.
* for α=0,01: **F_{tabl}=13.27;** for α=0,05: **F_{tabl}=5.79**

Tables 5.22-5.24 show that the thermal properties were predicted successfully as indicated by corresponding parameters for goodness of fit. Values for correlation coefficient were strong in majority of cases according to Cheddeka index (see Table 3.1). Similarly agreements index (D) were close to 1 in majority of the cases, indicating a successful prediction of the values at soil surface. However, for couple of weeks (weeks 11 and 14), the prediction successes was somehow poor as shown by Fisher index slightly greater than calculated values. On the other hand, the degree of prediction success was not consistent across the treatments (Sugar beet, corn, and control) as indicated by the calculated goodness of fit parameters (Tables 5.22-5.24).

Figs. 5.3-5.8 compare daily change of measured (T_m) and predicted (T_p) values obtained for one day in each week of 16-week study period. In the graph, each low-to-low represents the temperature change on the particular day on which measurements and predictions were made in that week. For example, the first low-to-low represents the diurnal changes in temperature on soil surface on the second day (Tuesday), in second week of June. The days of measurement were not consistent across the weeks. Adjustments were made regarding with the irrigation made since we wait the soil to reach field capacity after irrigation.

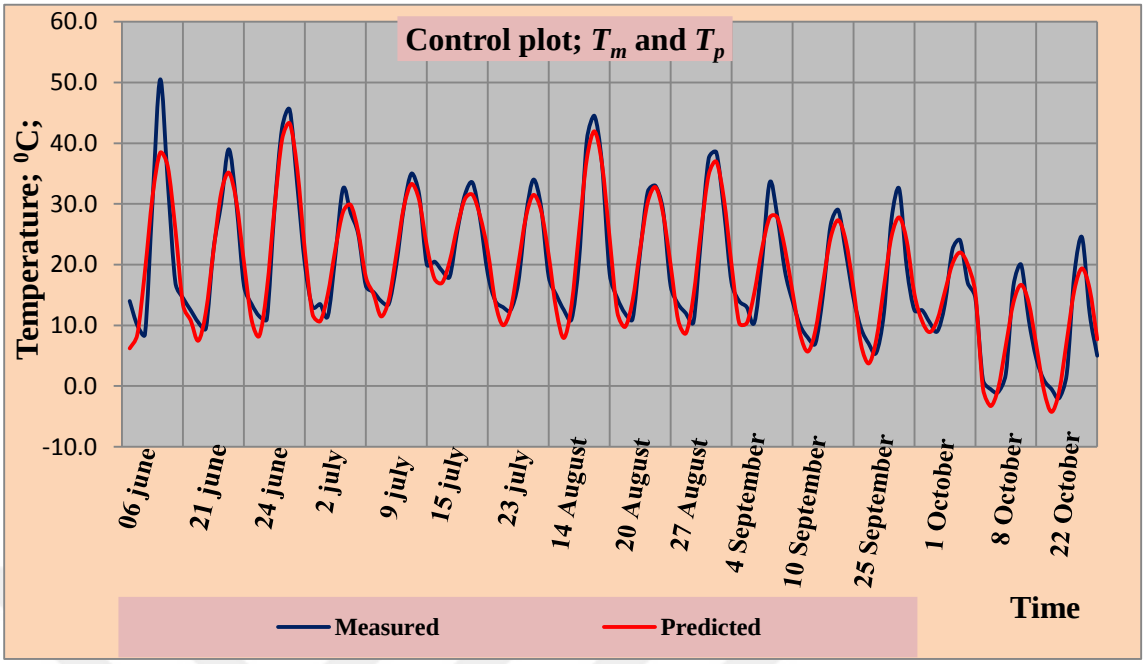

Figure 5.3 Diurnal changes of measured (T_m) and predicted (T_p) values obtained for control plot (Co) at selected dates during period. Each low to low represents diurnal temperature changes at soil surface on the day.

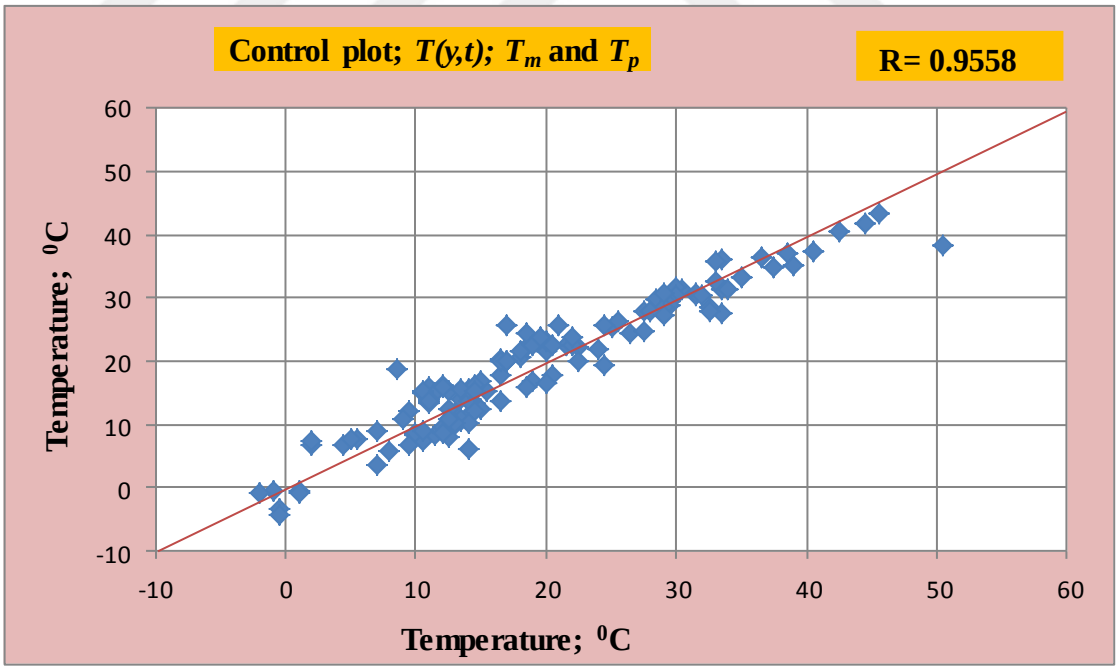

Figure 5.4 Comparing measured (T_m) and predicted (T_p) values obtained for control plot (Co) for 16 weeks of the study period (n= 16x8 = 128)

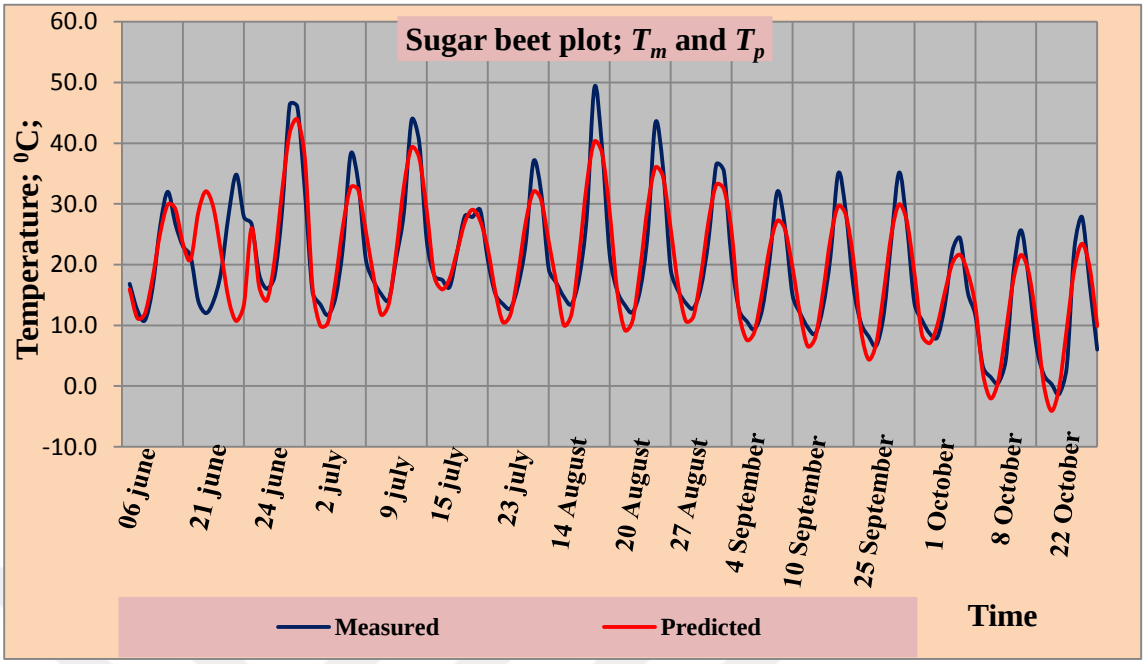

Figure 5.5 Diurnal changes of measured (T_m) and predicted (T_p) values obtained for sugar beet plots (S1, S2, S3) at selected dates during period. Each low to low represents diurnal temperature changes at soil surface on the day.

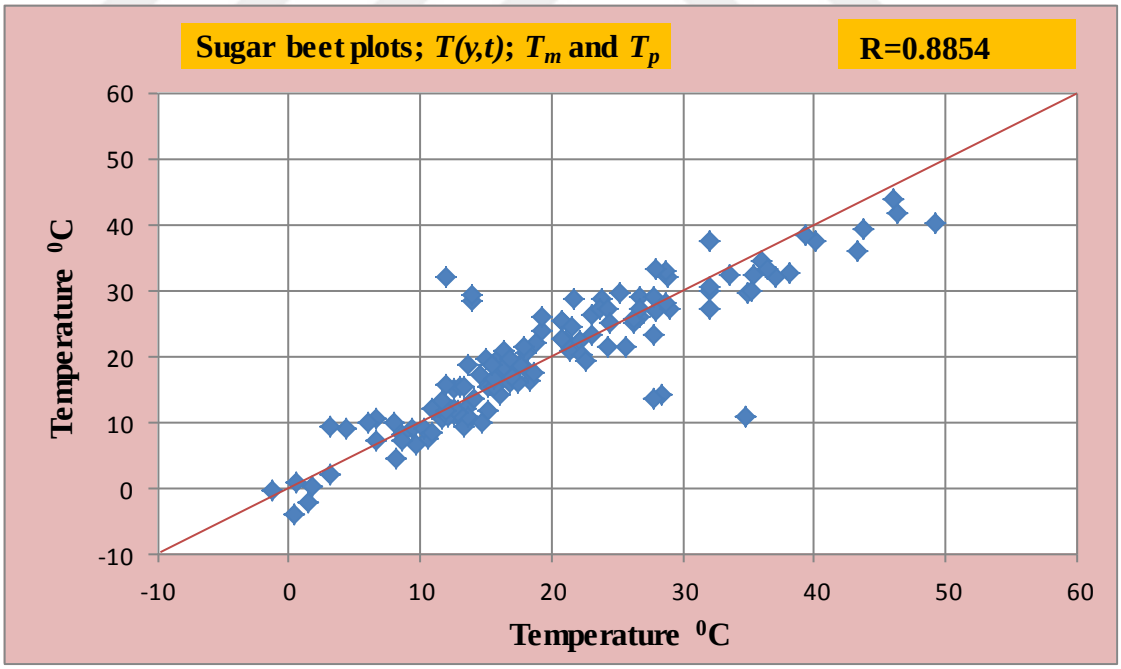

Figure 5.6 Comparing measured (T_m) and predicted (T_p) values obtained for sugar beet plots for 16 week of study period (n= 16x8 = 128). Each value is a mean of three plots (S1, S2, S3)

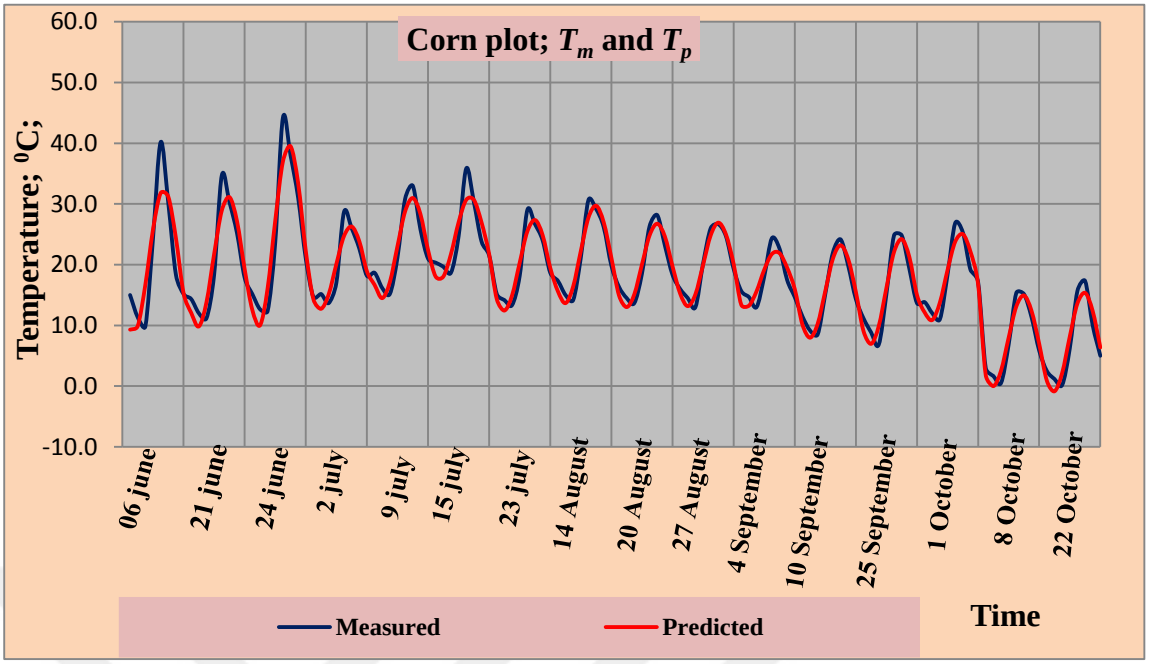

Figure 5.7 Diurnal changes of measured (T_m) and predicted (T_p) values obtained for corn plot (C1, C2, C3) at selected dates during period. Each low to low represents diurnal temperature changes at soil surface on the day

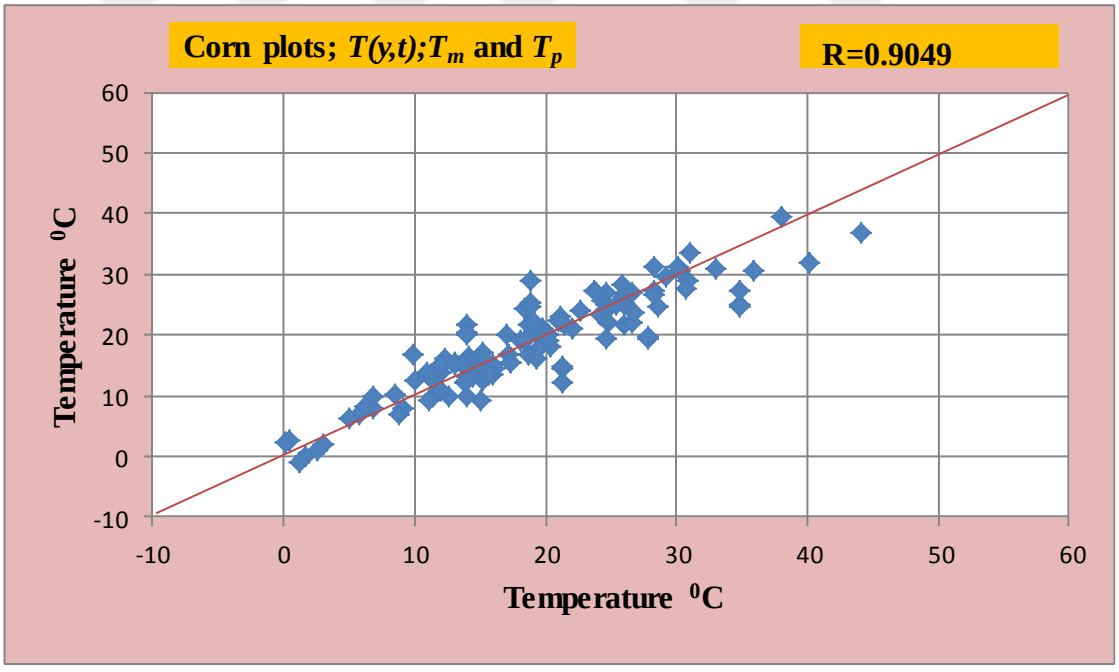

Figure 5.8 Coparing measured (T_m) and predicted (T_p) values obtained for corn plots (mean of C1, C2, and C3) for 16 weeks of study period (n= 16x8 = 128)

Diurnal changes in soil surface temperature were different across corn, sugar beets and control plots (Figs. 5.3, 5.5. and 5.7). Most drastic differences occurred between corn and the others. The soil surface temperature was predicted successfully in all the cases as indicated by thigh coalesces around the 1:1 lines and corresponding correlation coefficients given in the Figs of 3.4, 3.6 and 3.8.

The means of measured and predicted diurnal temperature changes once in every week for 16 weeks of study period for corn (C1, C2, C3), sugar beets (S1, S2, S3) and control (Co) plots are given in Fig. 5.9, 5.11, and 5.13; and corresponding 1:1-lines are given in Figs. 5.10, 5.12, and 4.14. Please note that the values for corn and sugar beet are means of three replicates (S1, S2, S3 for sugar beet; C1, C2, C3 for corn), while for control is a single plot (there is is no replicates for control since two of control plots were removed as the sensors placed at these plots did not function). These figs show that diurnal changes of temperature on the soil surface were predicted successfully in all the cases and the prediction success was highly uniform in correlation coefficient (R).

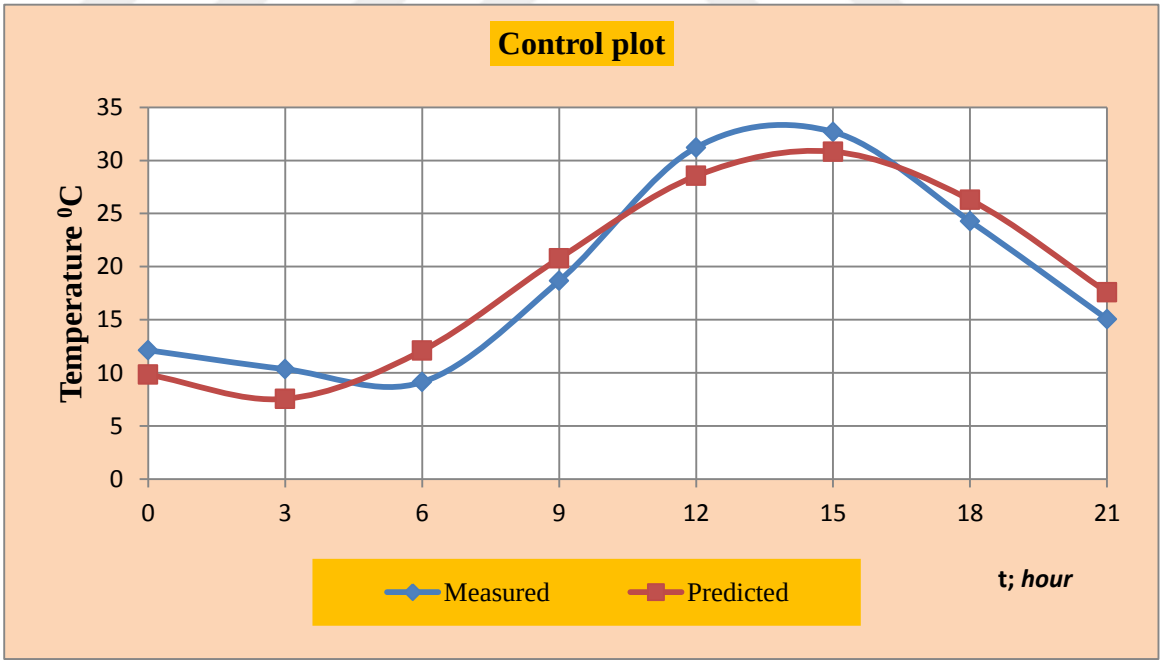

Figure 5.9 Diurnal changes of measured (T_m) and predicted (T_p) temperature at soil surface of control plot (Co). Each values represents mean of 16 data points obtained once in every week

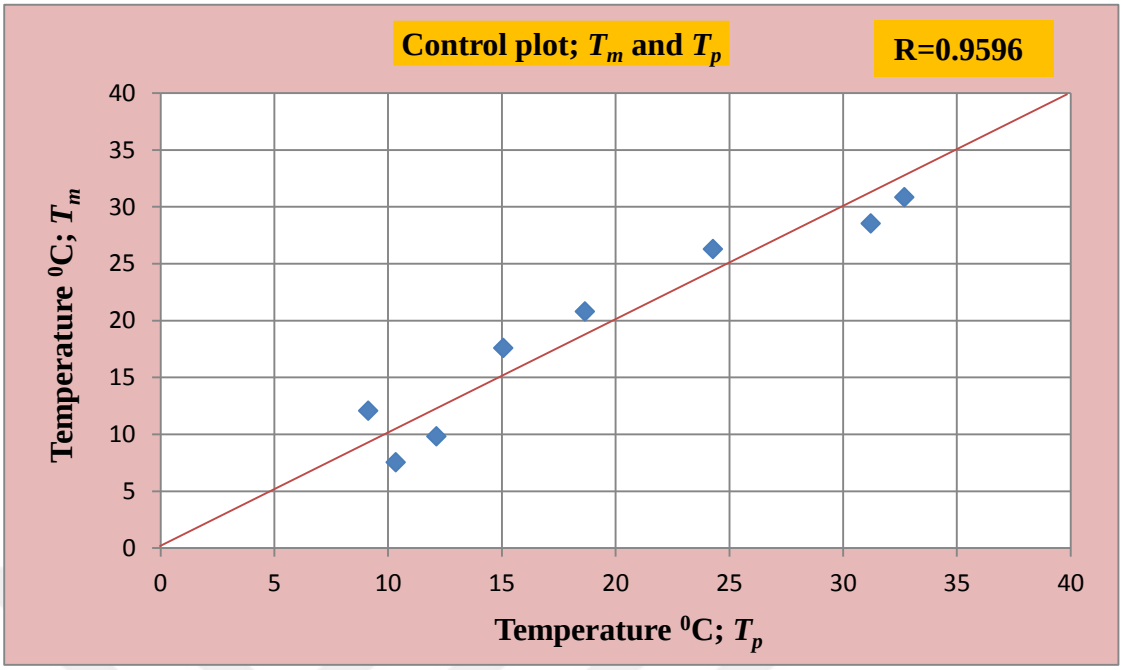

Figure 5.10 Compariment of measured (T_m) and predicted (T_p) values at the control plot (Co) during the study period. Each value represents mean of 16 values measured once in every week during 16 weeks of study period

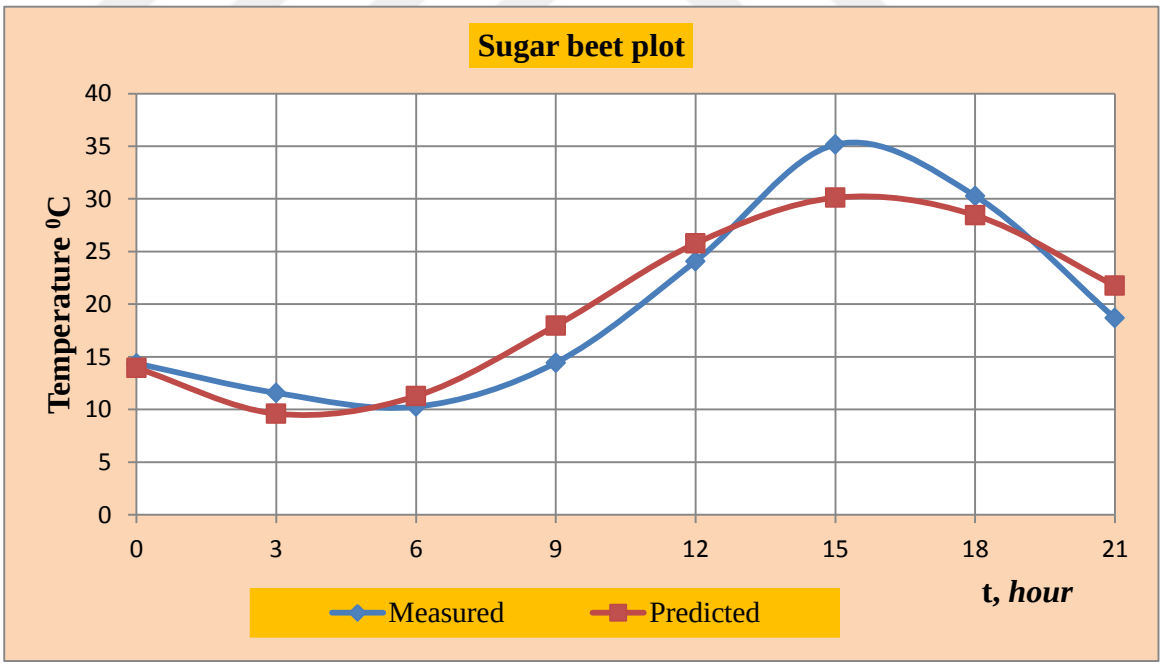

Figure 5.11 Diurnal changes of measured (T_m) and predicted (T_p) temperature at soil surface of sugar beet plots (S1, S2, S3). Each datum point represents mean of 16 values (as average of S1, S2, S3) obtained once in every week during 16 weeks of study period

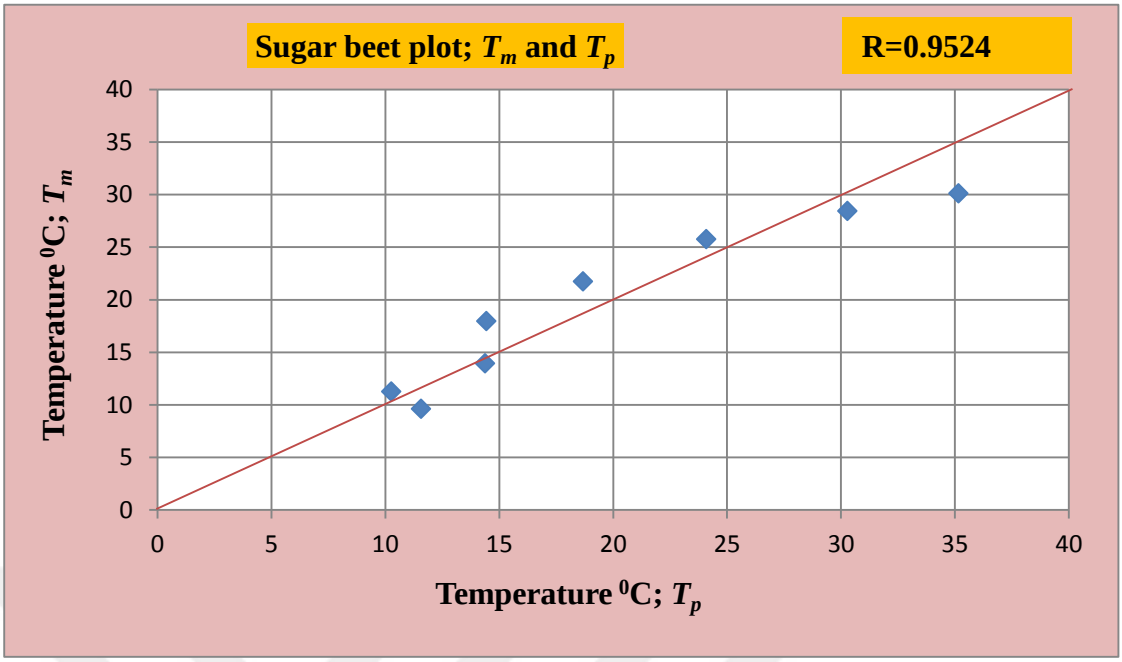

Figure 5.12 Comparisons of measured (T_m) and predicted (T_p) values at the sugar beet plots (S1, S2, S3) during the study period. Each value represents mean of 16 values (average of S1, S2, S3) measured once in every week during 16 weeks of study period

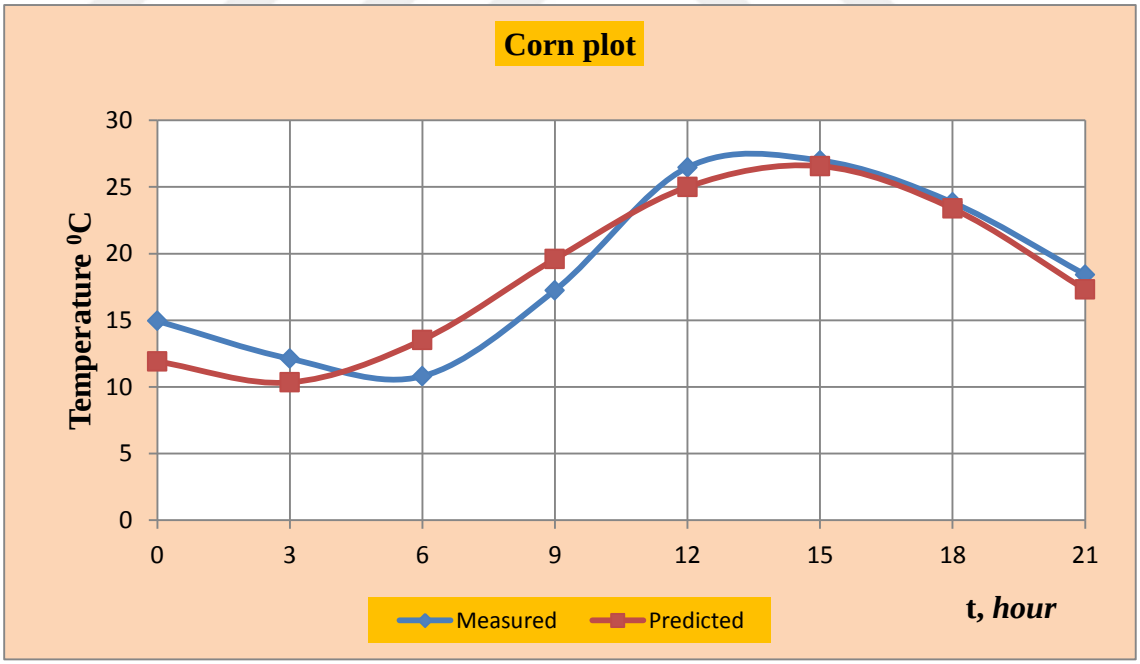

Figure 5.13 Diurnal changes of measured (T_m) and predicted (T_p) temperature at soil surface of corn plots (C1, C2, C3). Each values point represents mean of 16 values (as average of C1, C2, C3) obtained once in every week during 16 weeks of study period

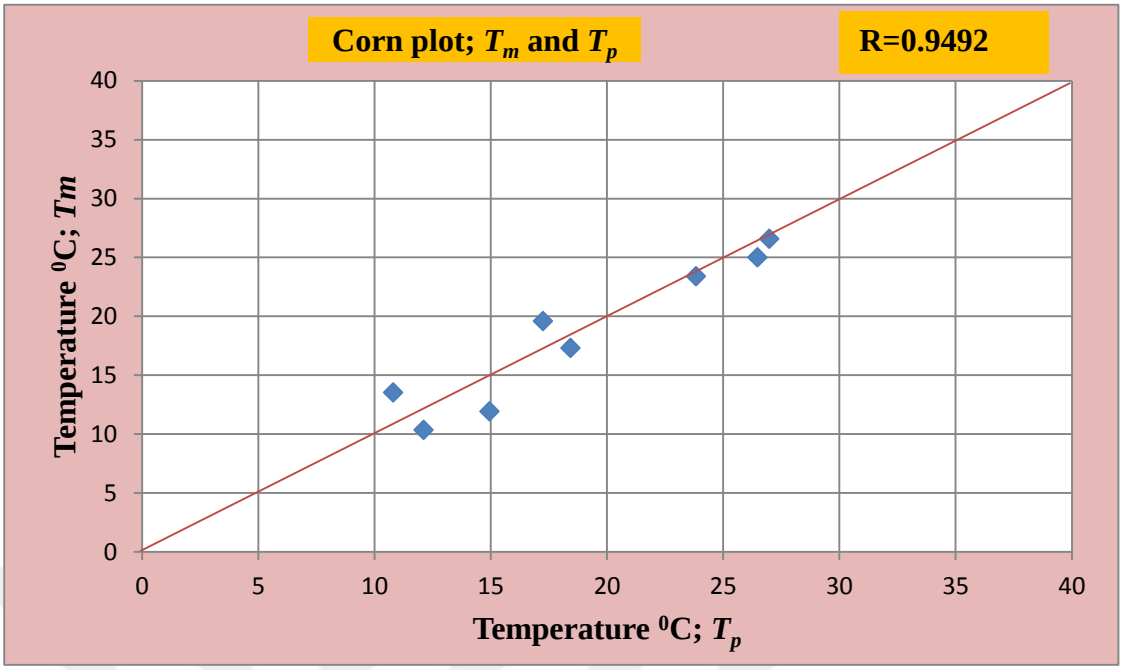

Figure 5.14 Comparisons of measured (T_m) and predicted (T_p) values at the corn plots (S1, S2, S3) during the study period. Each value represents mean of 16 values (as average of S1, S2, S3) measured once in every week during 16 weeks of study period

Figs 5.11, 5.13, and 5.15 show that the maximum temperature occurred at 15.00 at sugar beet plots, while it occurred at 12.00 at control and corn plots. In addition, both control and corn plots behaved similarly compared to sugar beet plots and this was attributed to canopy structure of sugar beets. The temperature at sugar beet plots behaved differently from those at control and corn plots as indicated by Figs 5.15 and 5.16. In majority of cases, temperature measured at sugar beet plots were greater than those measures at control and corn plots. On the other hand, the wave amplitude (*Ta*) behaved differently, the lowest wave amplitude occurred at corn plots, while those at sugar beet and control plots behaved similarly (Fig 5.16).

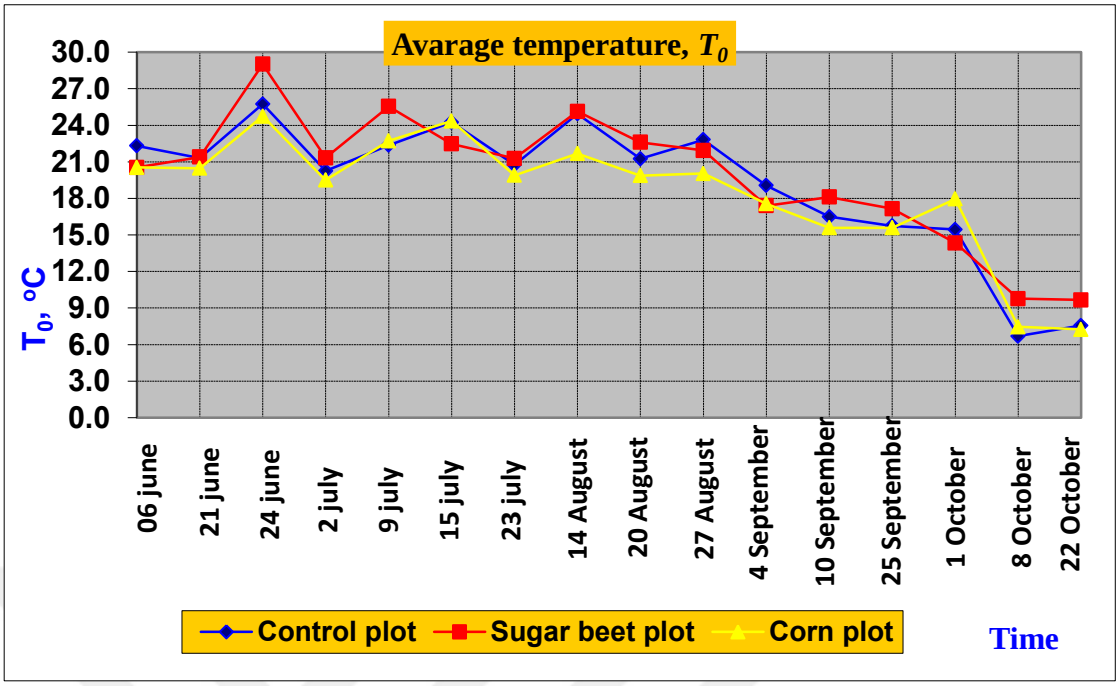

Figure 5.15 Diurnal soil surface air temperatures at the control, sugar beet, and corn plots. Values for corn and sugar beet are means of three replicates

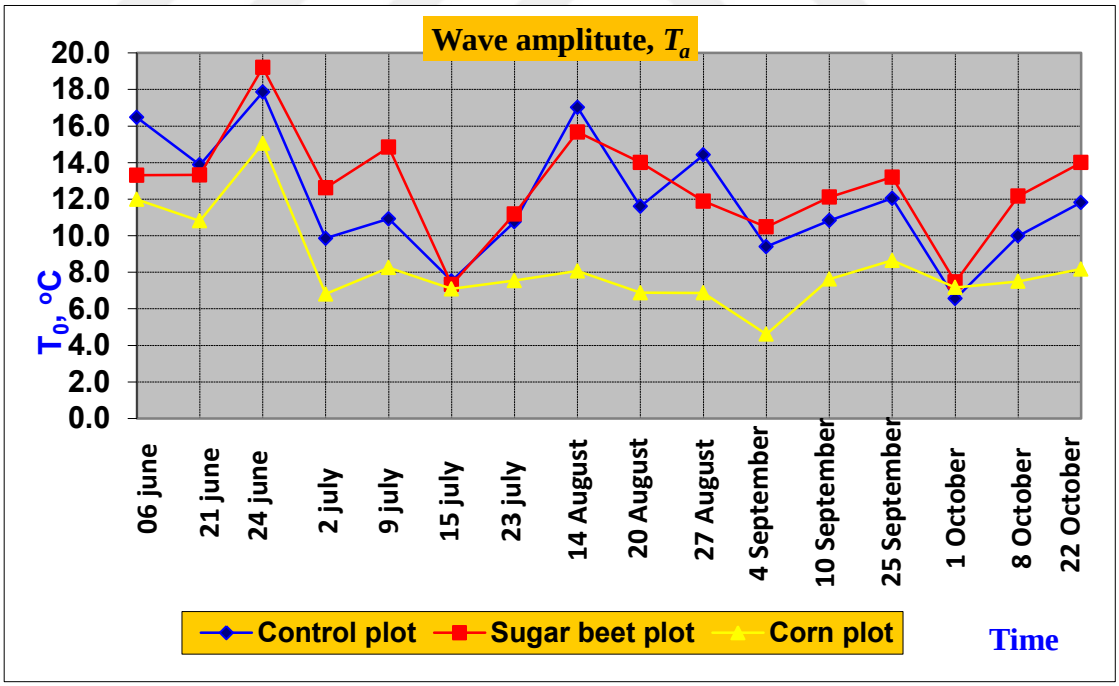

Figure 5.16 Change of amplitude (T_a) at control, sugar beet, and corn plots. Values for corn and sugar beet are mean of three replicates

Changes of relative humidity and air temperature over different heights are shown in Figs 5.17-5.22. Compared to control plot, maximum temperature occurred approximately 3 h later in sugar beet and corn plots. In control plots RH was always greater at 1 m above than 0 m of the soil surface (Table 5.25). The trend in RH was similar over control and sugar beet plots compared to corn plots and this was attributed to the canopy structure of corn. Interestingly, sugar beet plots behaved similar to control plots in change of RH.

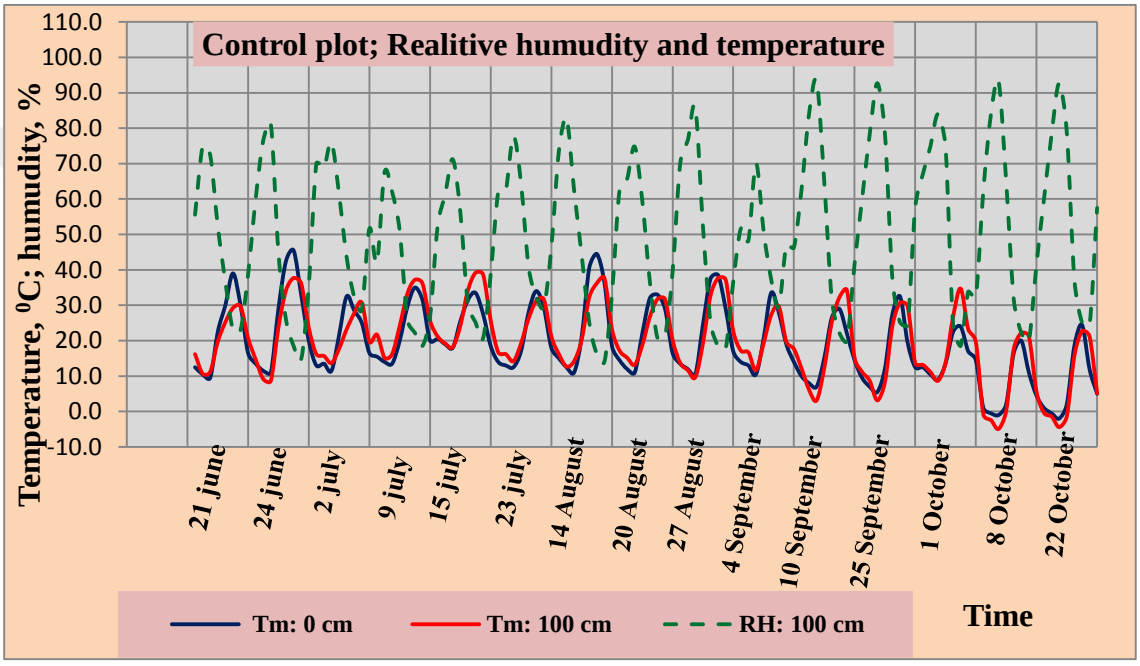

Figure 5.17 Changes of temperature and relative humidity (RH) at 0 and 100 cm heights over the control plot (Co) during study period

Table 5.25 Mean of temperature measurements taken at 0 and 100 cm above control plot (n= 15)

Time	0 cm	100 cm	
ti	T(y,ti)	T, ^{o}C	R.Humudity, %
0	12.00	13.75	65.09
3	10.37	10.98	75.12
6	9.17	9.10	80.81
9	17.87	15.92	63.44
12	29.93	26.98	33.56
15	32.63	32.00	23.78
18	24.77	30.60	23.95
21	15.10	18.67	43.41
Mean	**18.98**	**19.75**	**51.14**

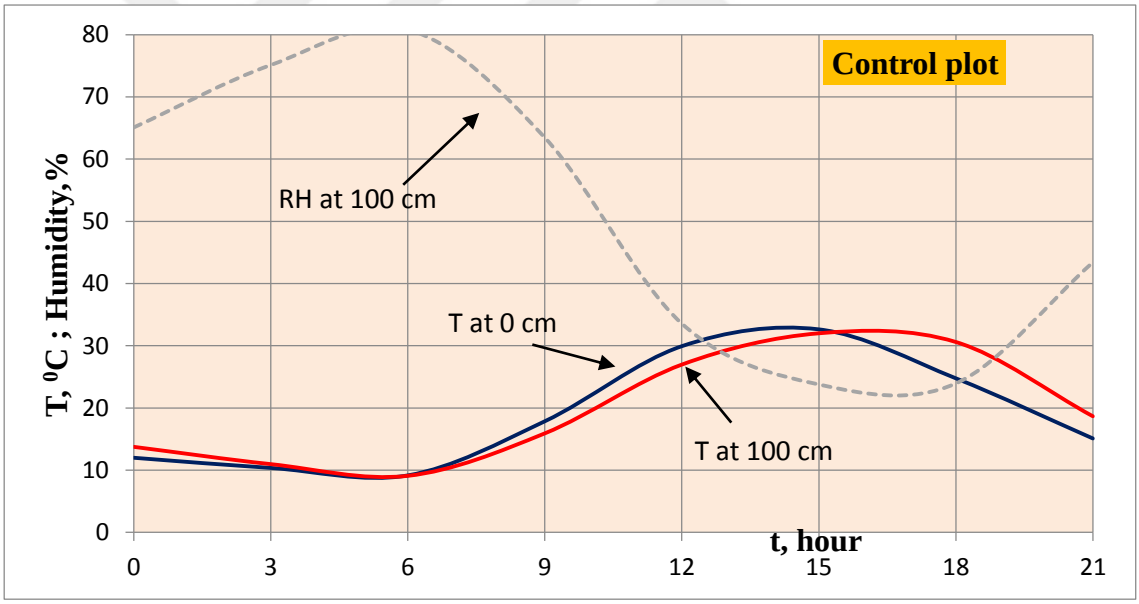

Figure 5.18 Diurnal changes of relative humidity (RH) and air temperature (*T*) at different heights over control plot

The time of maximum RH gradually delayed in the order of control, sugar beet and corn. The maximum RH occurred over control plot around 5 o'clock while it occurred around 6 over the corn plots. This delay was attributed to the delay at the time of minimum temperature, as maximum RH occurs at the minimum temperature (Campbell and Norman, 1998).

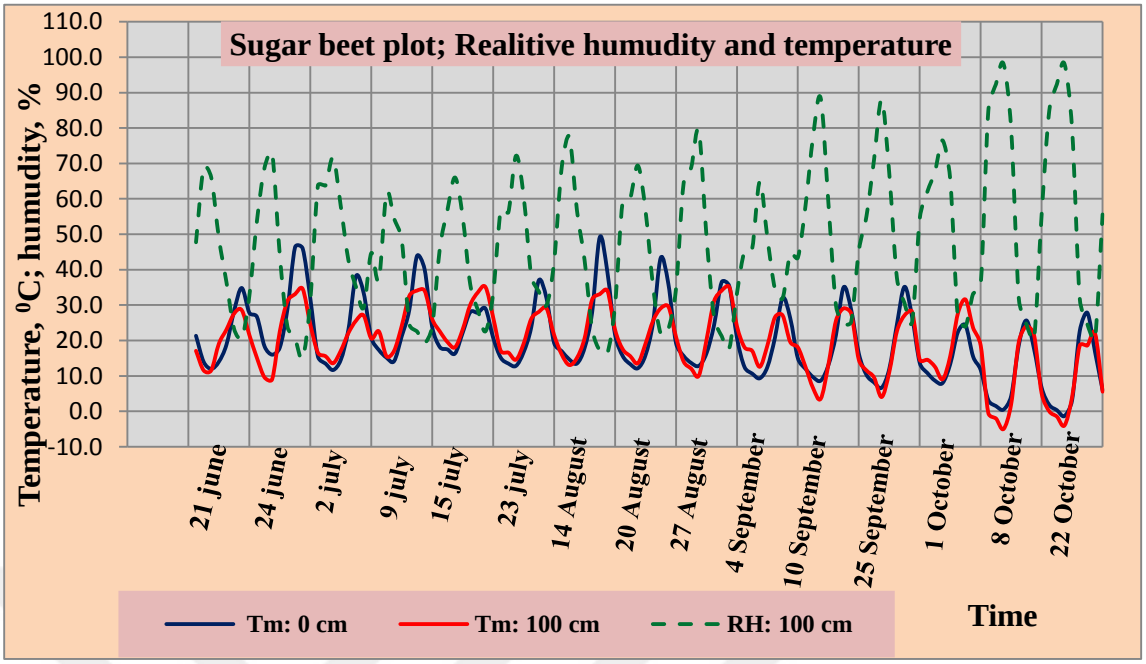

Figure 5.19 Changes of temperature and relative humidity (RH) at 0 and 100 cm heights over the S1, S2, and S3 on the specified days during study period. The values are mean of three replicates (S1, S2, S3)

Table 5.26 Mean of temperature measurements taken at 0 and 100 cm above S1, S2, S3 plots. The values are mean of S1, S2, S3 (n=15)

Time	**0 cm**	**100 cm**	
ti	T(y,ti), ºC	T(y,ti), ºC	R. Humidity, %
0	14.38	14.34	59.98
3	11.57	11.44	69.39
6	10.26	9.53	75.39
9	14.44	16.61	57.87
12	24.08	26.25	32.40
15	35.16	29.05	26.35
18	30.28	28.65	24.57
21	18.68	19.05	40.54
Mean	**19.86**	**19.37**	**48.31**

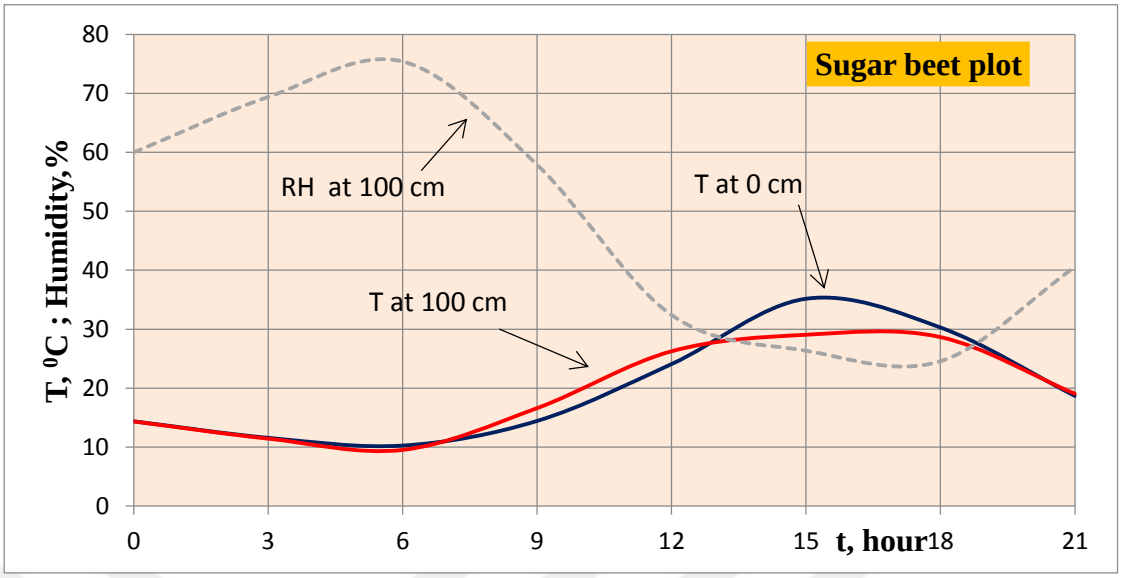

Figure 5.20 Diurnal changes of relative humidity (RH) and air temperature (*T*) at different heights over S1, S2, S3 plots. The values are means of S1, S2, and S3

Air temperature behaved differently over sugar beet plots than over corn and control plots. The maximum air temperature occurred 0 cm was greater than 100 cm over sugar beet plots (Fig.5.20), while reverse was true over control and corn plots (Figs 5.18 and 5.22). This was attributed to the fact that the heavy and dense canopy at sugar beet plots decreased latent heat loss by evaporation and convective heat loss by wind.

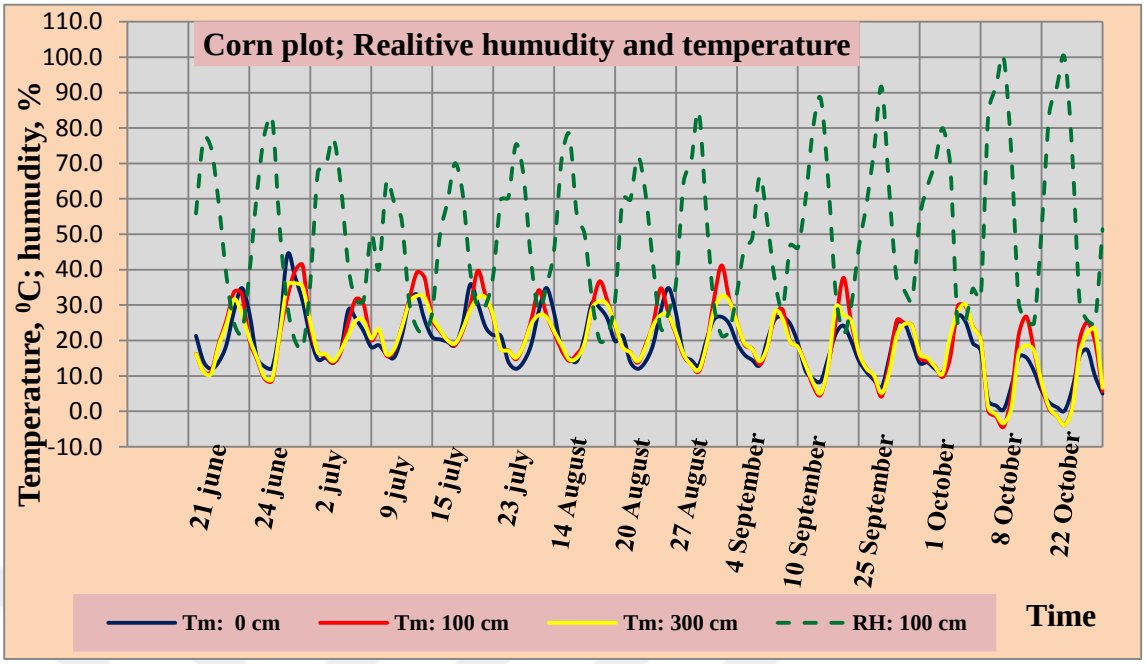

Figure 5.21 Diurnal changes of relative humidity (RH) and air temperature at 0 and 100 cm over corn plots on specified dates. The values are means of C1, C2, and C3 plots (replicates)

Table 5.27 Temperature measurements taken at 0, 100, and 300 cm above C1, C2, and C3 plots. The values are mean of C1, C2, and C3 (n=15)

Time	**0 cm**	**100 cm**		**300 cm**	
ti	T(y,ti)	T, ^{o}C	R.Humudity, %	T, ^{o}C	R.Humudity, %
0	14.94	15.10	57.49	14.75	62.67
3	12.17	12.07	66.37	11.87	72.36
6	10.87	10.30	72.71	9.93	78.96
9	16.78	16.27	59.11	16.35	62.68
12	25.56	25.91	32.85	27.13	34.91
15	26.78	28.34	25.98	33.59	26.09
18	24.20	26.74	26.38	28.19	28.85
21	18.64	20.04	37.27	19.56	42.55
Mean	**18.74**	**19.35**	**47.27**	**20.17**	**51.13**

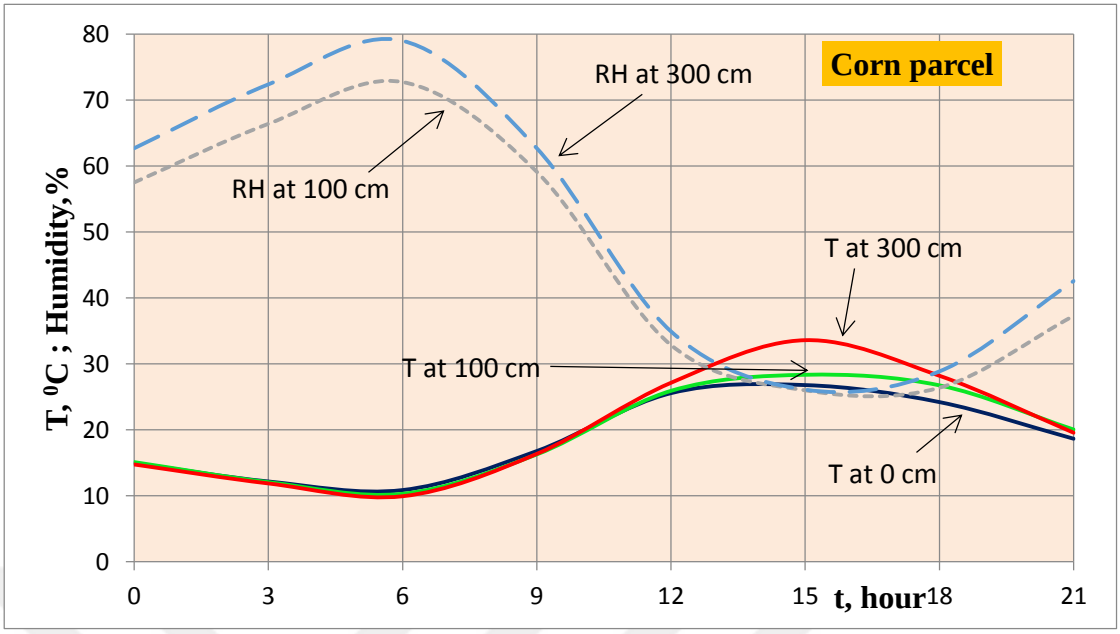

Figure 5.22 Diurnal changes of relative humidity (RH) and air temperature (T) over 0, 100, and 300 cm of the corn plots. The values are mean of C1, C2, and C3

5.3.3. Calculating heat diffusivity

5.3.3.1. According to the first type boundary conditions $T(\infty,t)=T_0$ 'layer' method

Soil temperatures at 0, 5, 10, 20 and 30 cm depths were calculated, using first type boundary conditions ($T(\infty, t) = T_0$) with Eqs. (4.2), (3.25), 4.4, and 4.5. The calculations were exemplified using the data for S2 on the day 20.08.2013 and the results are given in Table 5.28.

Table 5.28 Diurnal temperature (°C) change by depth in S2 on 20.08.2013

i	Time	Surface	Depths, x (cm)			
	t_i	0	5	10	20	30
1	0	16.0	20.5	22.5	23.0	23.0
2	3	13.5	19.0	21.0	22.5	23.0
3	6	12.5	17.5	20.0	22.0	22.5
4	9	17.5	17.0	19.0	21.5	22.5
5	12	30.5	21.5	20.0	21.0	22.0
6	15	38.0	26.0	23.0	21.5	21.5
7	18	28.5	27.0	25.0	22.0	22.0
8	21	17.5	23.5	24.0	23.0	22.0

Method-1 (Using the equation that includes amplitude of heat wave): The temperature values in Table 5.28, which were calculated for S2 were used with Eq. 4.5 and values in Table 5.29 were calculated. Then heat diffusivity values were calculated for the layers 0.0-0.05, 0.1-0.2, 0.2-0.3.

Table 5.29 Values for minimum temperature, maximum temperature, amplitude, and heat diffusivity coefficient for different soil layers

i	x_i	T_{min} (x_i)	T_{max} (x_i)	Φ (x_i)	$x_{i+1}-x_i$	Φ_i/Φ_{i+1}	$\ln(\Phi_i/\Phi_{i+1})$	$\kappa.10^{-7}$ m^2/s
1	0.00	12.5	38.0	**12.75**	0.05	2.5500	0.936093	**1.0374**
2	0.05	17.0	27.0	**5.00**	0.05	1.6667	0.510826	**3.4836**
3	0.10	19.0	25.0	**3.00**	0.10	3.0000	1.098612	**3.0126**
4	0.20	21.0	23.0	**1.00**	0.10	1.3333	0.287682	**43.9350**
5	0.30	21.5	23.0	**0.75**			**$\kappa_{mean}.10^{-7}$=**	**12.8672**

T_{min}: minimum temperature, T_{max}: maximum temperature, Φ:The amplitude of temperature

Using the minimum and maximum values for temperature and corresponding values for Φ in Table 5.29 the temperature wave was calculated as follows:

$$\Phi\left(x_1 = 0\ m\right) = \frac{1}{2}\left[T_{\max}\left(x_1\right) - T_{\min}\left(x_1\right)\right] = \frac{38.0 - 12.5}{2} = \frac{25.5}{2} = 12.75\ {}^{0}C$$

$$\Phi\left(x_2 = 0.05m\right) = \frac{1}{2}\left[T_{\max}\left(x_2\right) - T_{\min}\left(x_2\right)\right] = \frac{27 - 17.0}{2} = \frac{10.0}{2} = 5.0\ {}^{0}C$$

Using these calculated values for 0 and 0.05 m soil depths with Eq. (4.5) value for κ was calculated as follows:

$$\kappa = \frac{\pi}{24h} \cdot \left[\frac{0.05m - 0m}{\ln\left(12.75/5\right)}\right]^2 = 0.00003636 \cdot \left[\frac{0.05}{0.936093}\right]^2 \frac{m^2}{s} = 1.0374 \cdot 10^{-7}\ \frac{m^2}{s}$$

It should be noted that values of π =3.141593, τ_0 = 24 h = 86400 s and $\omega = \pi/\tau_0$ = 3.636x10^{-7} were used in calculating the κ. The mean value for S2 calculated for κ was 12.8672x10^{-7} m^2 s^{-1}.

5.3.3.2. Point methods

Method-2 (Mikayilov, 2009): **Point method depending on the First type boundary conditions** ($T(\infty,t)=T_0$)**.**

The calculations are exemplified for the plot S2. For calculating κ for S2, Eq.(4.3) was used with boundary conditions of (3.51) and (3.52) and then Eq. (3.77) was used. The parameter T (y, t_i) was calculated using the τ_0 = 24 h; t_1=6, t_2=12, t_3=18 and t_4=24 h. Then the parameter **M** (y,b) was calculated using T_a = 11.5197 and Eq.(3.76) as follows.

$$\mathbf{M}(y;b)=\frac{[26-19]^2+[23.5-17]^2}{4(11.5197)^2}=0.171905$$

In the Table 5.31; t_1=19,0 ^{0}C; t_2=17 ^{0}C; t_3=26 ^{0}C; ve t_4=23,5 ^{0}C are temperature values at 0.05 m soil depth.

The heat diffusivity values were calculated by Eq. (5.2) for all the layers (i = 1,2,3,4) and mean value for heat diffusivity was calculated for 0-30 m.

$$M(y;b)=e^{-2by} \tag{5.2}$$

Using the calculated values of M(y,b) with Eq. (3.78), the values for b_i was calculated as follows:

$b_i=-\frac{L}{2y_i}\ln[M(y,b)]=-\frac{0.3}{2\cdot 0.05}\ln[0.171905]=5.282447$. Finally κ was calculated by Eq. (3.79) as follows:

$$\kappa_i=\frac{3.141593}{86400}\cdot\frac{0.3^2}{5.282447^2}=1.172758\cdot 10^{-7}\ m^2/s$$

The calculated values of κ for the plot S2 are given in Table 5.30.

Table 5.30 Values of κ calculated by point2 method at S2 at 0.05, 0.1, 0.2 and 0.3 m depths and for 0-0.3 m layer (T_a= 11.5197, L= 0.3 m)

$T(y_i,t_i)$	t_i, ***hour***	**Depths,** $y = x/L$			
		y2=0.05	**y3=0.1**	**y4=0.2**	**y5=0.3**
$T(y_i,t_1)$	t_1=3	19.0	21.0	22.5	23.0
$T(y_i,t_2)$	t_1=9	17.0	19.0	21.5	22.5
$T(y_i,t_3)$	t_1=15	26.0	23.0	21.5	21.5
$T(y_i,t_4)$	t_1=21	23.5	24.0	23.0	22.0
T_a		11.5197	11.5197	11.5197	11.5197
M (y_i,b)		0.171905	0.054633	0.006123	0.004710
b_i		5.282447	4.360684	3.821823	2.679064
$K_i.10^{-7}$	m^2/s	1.172758	1.720954	2.240462	4.559450
κ_{mean} **.10^{-7}** m^2/s				**2.423406**	

Method-3 (Mikayilov, 2009): **Point method with Second type boundary conditions (($\partial T(L,t)/\partial x = 0$)).**

First, the parameter M (y,b) was calculated by Eq. (5.3) for all the soil depths and for 0-0.3 m soil layer.

$$M(y;b) = \frac{\sum_{i=1}^{4}\left[T(y,t_i) - T(y,t_{i+4})\right]^2}{4T_a^2} = \frac{\mathbf{ch}\left[2b(1-y)\right] + \cos\left[2b(1-y)\right]}{\mathbf{ch}(2b) + \cos(2b)} \qquad (5.3)$$

For example, using the values for S2 along with Ta= 11.5197 L=0.3 the value calculated for M ($y;b$).

$$\mathbf{M}(y;b) = \frac{[26-19]^2 + [23.5-17]^2}{4(11.5197)^2} = 0.171905$$

Then b_i was calculated as follows:

$$b_i = -\frac{L}{2y_i}\ln\left[M\left(y,b\right)\right] = -\frac{0.3}{2\cdot 0.05}\ln\left[0.171905\right] = 5.281764$$

Finally using these values, κ was calculated as follows:

$$\kappa_i = \frac{3.141593}{86400}\cdot\frac{0.3^2}{5.281764^2} = 1.173061\cdot 10^{-7}\ m^2/s$$

The values calculated for κ for S2 are given in Table 5.31. Values of κ calculated by point and layer methods are given in Tables 5.32-5.34.

Table 5.31 Values of κ calculated by Method-4 at S2 at 0.05, 0.1, 0.2 and 0.3 m depths and for 0-0.3 m layer (T_a= 11.5197, L= 0.3 m)

$T(y_i,t_i)$	t_i,	Depths, $y = x/L$			
	saat	**y_2=0.05**	**y3=0.1**	**y4=0.2**	**y5=0.3**
$T(y_i,t_1)$	t_1=3	19.0	21.0	22.5	23.0
$T(y_i,t_2)$	t_1=9	17.0	19.0	21.5	22.5
$T(y_i,t_3)$	t_1=15	26.0	23.0	21.5	21.5
$T(y_i,t_4)$	t_1=21	23.5	24.0	23.0	22.0
T_a		11.5197	11.5197	11.5197	11.5197
M (y_i,b)		0.171905	0.054633	0.006123	0.004710
b_i		5.281764	4.36897	3.721109	3.371071
$K_i.10^{-7}$	m^2/s	1.173061	1.714433	2.363382	2.879671
$\kappa_{mean}.10^{-7}$ m^2/s				**2.032637.10^{-7}**	

Table 5.32 Volumetric water content (θ) and calculated κ-values at control plot (C)

Dates	6.6.13	21.6.13	24.6.13	2.7.13	9.7.13	15.7.13	23.1.13	14.8.13	20.8.13	27.8.13	4.9.13	10.9.13	25.9.13	1.10.13	8.10.13	22.10.13	Mean
Depth, m	**θ, cm^3/cm^3**																
0.05	35.34	37.89	36.56	39.33	36.66	33.70	39.38	40.19	40.93	39.03	39.88	43.87	38.62	43.34	39.57	33.53	**38.61**
0.1	38.75	42.13	41.15	42.08	40.68	36.41	42.61	43.08	43.14	41.06	43.15	45.44	43.20	45.77	44.06	36.01	**41.80**
0.2	42.17	46.38	41.74	44.82	44.70	39.13	45.83	45.97	45.35	43.10	45.00	47.01	47.78	48.20	48.55	38.48	**44.64**
0.3	40.25	42.26	39.82	43.38	44.41	40.82	44.00	44.35	43.79	41.95	44.56	47.28	47.40	46.06	55.04	40.13	**44.09**
0-0.3	**39.13**	**42.17**	**39.82**	**42.40**	**41.61**	**37.52**	**42.96**	**43.40**	**43.30**	**41.28**	**43.15**	**45.90**	**44.25**	**45.85**	**46.80**	**37.04**	**42.29**
	$\kappa.10^{-7}$ (m^2/s) (calculated by layer method)																
0.05	0.4568	0.9108	0.8764	0.9603	1.2856	1.0923	1.1034	0.8050	1.0760	1.2251	0.7383	1.2512	0.9972	1.4037	1.3224	1.0170	**1.0326**
0.1	7.1956	2.3452	3.0126	5.1729	8.8729	7.5134	1.7101	2.2923	6.3433	1.8668	5.8951	8.8557	2.3884	5.3947	4.4452	2.3983	**4.7314**
0.2	13.9345	3.7796	22.1171	9.3856	16.4601	13.9345	2.3169	3.7796	11.6106	2.5084	13.9345	16.4601	3.7796	9.3856	7.5681	3.7796	**9.6709**
0.3	3.0126	3.0126	8.6687	13.9345	4.3308	3.0126	7.5681	3.0126	7.5681	22.1171	3.0126	4.3308	3.0126	4.3308	7.5681	22.1171	**7.5381**
0-0.3	**6.1499**	**2.5121**	**8.6687**	**7.3633**	**7.7374**	**6.3882**	**3.1746**	**2.4724**	**6.6495**	**6.9294**	**5.8951**	**7.7244**	**2.5445**	**5.1287**	**5.2259**	**7.3280**	**5.7433**
	$\kappa.10^{-7}$ (m^2/s) (calculated by point1 method)																
0.05	0.5024	0.9769	0.8473	0.8690	1.2722	0.5380	1.1025	0.7927	0.8810	1.1159	0.9105	1.2868	1.1376	1.0281	1.2128	1.1520	**0.9766**
0.1	1.5040	1.1934	1.2120	1.9530	1.6061	2.7016	1.8533	1.5385	1.9449	1.7040	1.7674	1.8203	1.4734	2.1387	1.9644	1.4929	**1.7417**
0.2	1.5772	1.4100	1.3958	2.1918	1.9400	2.8651	1.9626	1.6843	2.0163	1.8920	1.9351	2.3539	1.8092	2.2494	2.0746	1.8337	**1.9495**
0.3	1.8658	2.0286	1.5850	2.7136	2.4023	2.8236	2.8054	2.1799	2.5590	2.0976	2.0403	2.7263	2.6285	3.3979	2.4066	2.6571	**2.4323**
0-0.3	**1.3623**	**1.4022**	**1.2600**	**1.9319**	**1.8052**	**2.2321**	**1.9309**	**1.5489**	**1.8503**	**1.7024**	**1.6633**	**2.0468**	**1.7622**	**2.2035**	**1.9146**	**1.7839**	**1.7750**
	$\kappa.10^{-7}$ (m^2/s) (calculated by point2 method)																
0.05	0.5024	0.9768	0.8474	0.8691	1.2706	0.5380	1.1020	0.7929	0.8811	1.1154	0.9106	1.2851	1.1369	1.0279	1.2117	1.1513	**0.9762**
0.1	1.5067	1.2127	1.2346	1.9590	1.6516	1.9863	1.9580	1.5712	1.9499	1.7473	1.4560	1.8862	1.5124	2.2293	1.9636	1.5331	**1.7099**
0.2	1.6316	1.4485	1.3299	2.3100	2.0325	2.0345	2.0574	1.7496	2.1167	1.9793	1.7385	2.4872	1.8879	2.4307	2.1810	1.9149	**1.9581**
0.3	1.8374	2.0762	1.4373	2.9569	2.4353	2.4920	2.4939	1.9687	2.3584	2.1044	2.0725	2.8448	2.8361	3.2907	2.7057	2.8531	**2.4227**
0-0.3	**1.3695**	**1.4286**	**1.2123**	**2.0237**	**1.8475**	**1.7627**	**1.9028**	**1.5206**	**1.8265**	**1.7366**	**1.5444**	**2.1258**	**1.8433**	**2.2446**	**2.0155**	**1.8631**	**1.7667**

Table 5.33 Volumetric water content (θ) and calculated κ-values at sugar beet plots (S1, S2, S3). The values are means of three replicates (S1, S2, and S3)

Dates	**6.6.13**	**21.6.13**	**24.6.13**	**2.7.13**	**9.7.13**	**15.7.13**	**23.1.13**	**14.8.13**	**20.8.13**	**27.8.13**	**4.9.13**	**10.9.13**	**25.9.13**	**1.10.13**	**8.10.13**	**22.10.13**	**Mean**
Depth, m	**θ, cm^3/cm^3**																
0.05	36.42	36.12	35.88	38.30	40.87	37.22	39.16	38.30	39.43	38.86	38.70	39.30	36.14	40.40	39.20	30.66	**37.81**
0.1	38.78	38.61	37.90	41.53	42.28	39.35	41.51	41.26	41.94	41.23	40.82	41.92	38.40	39.23	41.95	33.56	**40.02**
0.2	42.18	42.53	40.44	41.67	43.81	40.37	42.58	44.39	44.39	41.67	44.29	43.07	42.74	44.25	45.15	36.99	**42.53**
0.3	41.15	40.01	39.74	41.75	43.31	41.28	43.00	41.74	43.98	40.44	43.58	41.58	39.87	42.40	43.96	37.15	**41.56**
0-0.3	**39.63**	**39.32**	**38.49**	**40.81**	**42.57**	**39.56**	**41.56**	**41.42**	**42.44**	**40.55**	**41.85**	**41.47**	**39.29**	**41.57**	**42.57**	**34.59**	**40.48**
	κ.10^{-7} (m^2/s) (calculated by layer method)																
0.05	0.7739	1.1687	0.7883	0.9194	1.1951	1.8750	1.8232	0.5590	0.3462	1.4105	0.9972	1.3448	0.8670	2.6106	0.9672	0.8671	**1.1571**
0.1	2.8155	2.5617	3.1662	3.8525	2.6651	2.9606	2.5739	2.9062	4.7886	4.2338	3.2720	3.1477	3.9809	3.7564	3.7133	3.4482	**3.3652**
0.2	3.5998	3.4520	2.7201	4.1576	4.6702	5.0772	2.5488	4.9832	9.1326	4.9775	3.1517	3.6171	3.3462	6.6554	3.2181	10.8993	**4.7629**
0.3	5.1083	3.7753	3.8584	7.7982	13.4608	11.0103	6.0496	2.5073	14.8426	8.7489	11.8123	9.0106	4.3378	9.6862	7.0926	5.2019	**7.7688**
0-0.3	**3.0744**	**2.7395**	**2.6333**	**4.1819**	**5.4978**	**5.2308**	**3.2489**	**2.7390**	**7.2775**	**4.8427**	**4.8083**	**4.2800**	**3.1330**	**5.6772**	**3.7478**	**5.1041**	**4.2635**
	κ.10^{-7} (m^2/s) (calculated by point1 method)																
0.05	0.6076	1.3959	0.8326	1.2198	1.0786	0.9177	1.0234	0.6622	0.6283	0.8059	0.8120	1.1933	0.7201	1.3423	0.9650	0.9792	**0.9490**
0.1	1.7371	2.0697	1.7652	2.1951	1.9671	1.9983	1.9726	1.8401	1.6443	2.0912	1.8986	1.8316	1.7369	2.1890	1.8623	1.8201	**1.9137**
0.2	1.9200	2.2284	2.0205	2.3887	2.2389	2.1302	2.3799	2.2705	1.8926	2.5982	2.3594	2.2709	2.1272	2.4260	2.1461	2.3164	**2.2321**
0.3	2.2417	2.6524	2.4211	2.8110	2.6853	2.5946	2.6762	2.6994	2.2876	2.8922	2.7798	2.5210	2.7789	2.9655	2.7428	2.6849	**2.6522**
0-0.3	**1.6266**	**2.0866**	**1.7599**	**2.1536**	**1.9925**	**1.9102**	**2.0130**	**1.8681**	**1.6132**	**2.0969**	**1.9624**	**1.9542**	**1.8408**	**2.2307**	**1.9291**	**1.9502**	**1.9367**
	κ.10^{-7} (m^2/s) (calculated by point2 method)																
0.05	0.6077	1.3904	0.8327	1.2183	1.0775	0.6767	1.0143	0.6623	0.6284	0.7991	0.8068	1.1875	0.7202	1.3090	0.9650	0.9774	**0.9296**
0.1	1.5567	2.0765	1.9163	2.1457	2.0701	1.9281	2.0020	1.8167	1.8612	2.1208	1.9092	1.8338	1.7467	2.1553	1.9871	1.8124	**1.9337**
0.2	1.9716	2.3479	2.1294	2.4511	2.2967	2.1584	2.4506	2.4315	1.9781	2.7118	2.5674	2.3863	2.2773	2.3745	2.4176	2.1214	**2.3170**
0.3	2.3835	2.6843	2.6502	2.7578	2.8021	2.7109	2.7809	2.7433	2.2921	3.0175	2.9032	2.7188	2.9316	2.9991	2.9210	2.7201	**2.7510**
0-0.3	**1.6299**	**2.1248**	**1.8822**	**2.1432**	**2.0616**	**1.8685**	**2.0619**	**1.9134**	**1.6899**	**2.1623**	**2.0467**	**2.0316**	**1.9189**	**2.2095**	**2.0726**	**1.9078**	**1.9828**

Table 5.34 Volumetric water content (θ) and calculated κ-values at corn plots (C1, C2, C3). The values are means of three replicates (C1, C2, and C3)

Dates	**6.6.13**	**21.6.13**	**24.6.13**	**2.7.13**	**9.7.13**	**15.7.13**	**23.1.13**	**14.8.13**	**20.8.13**	**27.8.13**	**4.9.13**	**10.9.13**	**25.9.13**	**1.10.13**	**8.10.13**	**22.10.13**	**Mean**
Depth, m	**θ, cm^3/cm^3**																
0.05	38.44	38.97	40.70	37.91	39.57	38.05	38.82	39.02	41.10	38.03	40.32	40.43	40.24	38.74	41.69	34.97	**39.19**
0.1	40.85	40.61	41.58	39.48	41.21	39.26	40.23	39.98	41.98	41.21	42.56	42.38	42.42	41.81	43.25	36.94	**40.98**
0.2	43.04	42.19	42.59	42.17	43.18	43.02	42.63	42.22	44.01	42.93	44.86	44.39	44.58	43.92	46.89	39.24	**43.24**
0.3	42.86	42.69	42.99	41.92	42.02	43.98	41.60	40.58	43.04	42.37	43.74	43.16	42.94	43.33	45.30	38.44	**42.56**
0-0.3	**41.30**	**41.12**	**41.97**	**40.37**	**41.49**	**41.08**	**40.82**	**40.45**	**42.53**	**41.14**	**42.87**	**42.59**	**42.54**	**41.95**	**44.28**	**37.40**	**41.49**
	$\kappa.10^{-7}$ (m^2/s) (calculated by layer method)																
0.05	0.3311	0.4753	0.4278	0.5439	0.5561	0.5582	0.4494	0.4072	0.4971	0.6365	0.4758	0.5069	0.4206	0.3685	0.4783	0.3986	**0.4707**
0.1	3.2910	2.1066	2.7374	9.9176	2.6421	4.7950	9.1034	4.2556	4.3953	9.1635	5.8950	2.8935	2.7399	8.5957	5.2878	3.3333	**5.0720**
0.2	6.2509	3.7380	3.9955	18.5401	6.7830	9.8688	5.7864	5.7656	8.2935	5.7039	6.4644	18.9053	5.7656	7.3049	17.2675	5.7864	**8.5137**
0.3	6.0496	6.0496	5.9572	10.9784	4.3426	6.9257	9.1449	5.7640	10.8993	9.9929	11.6404	4.7862	5.7051	7.5681	6.2009	6.8088	**7.4259**
0-0.3	**3.9806**	**3.0924**	**3.2795**	**9.9950**	**3.5809**	**5.5369**	**6.1210**	**4.0481**	**6.0213**	**6.3742**	**6.1189**	**6.7730**	**3.6578**	**5.9593**	**7.3086**	**4.0818**	**5.3706**
	$\kappa.10^{-7}$ (m^2/s) (calculated by point1 method)																
0.05	0.3014	0.5146	0.4552	0.5022	0.6180	0.3009	0.4179	0.4260	0.4083	0.6722	0.4419	0.5544	0.4660	0.3474	0.5110	0.3847	**0.4576**
0.1	1.2070	0.9559	0.9851	1.8666	1.4357	1.2329	1.1969	1.1820	1.4130	1.5150	1.1876	1.2668	0.9994	1.3571	1.2427	0.9822	**1.2516**
0.2	1.7607	1.3972	1.4574	2.3038	2.1022	1.5132	1.6794	1.5767	1.8548	2.1658	1.9333	1.7323	1.5243	2.6568	1.6673	1.7806	**1.8191**
0.3	2.2069	1.9301	1.7877	3.0498	2.1613	2.0402	2.2021	1.9760	2.3202	2.7933	2.4865	2.2510	2.3023	3.4816	2.2474	2.1137	**2.3344**
0-0.3	**1.3690**	**1.1995**	**1.1713**	**1.9306**	**1.5793**	**1.2718**	**1.3741**	**1.2902**	**1.4991**	**1.7866**	**1.5123**	**1.4511**	**1.3230**	**1.9607**	**1.4171**	**1.3153**	**1.4657**
	$\kappa.10^{-7}$ (m^2/s) (calculated by point2 method)																
0.05	0.3014	0.5146	0.4552	0.5023	0.6180	0.3009	0.4180	0.4260	0.4083	0.6726	0.4419	0.5544	0.4660	0.3474	0.5110	0.3847	**0.4577**
0.1	1.1365	0.9756	1.0016	1.9660	1.3981	1.1866	1.2489	1.2053	1.2326	1.5756	1.2331	1.2921	1.0206	1.1735	1.2881	0.9986	**1.2458**
0.2	1.6403	1.4365	1.4916	2.3958	1.8665	1.5951	1.5935	1.5445	1.8569	2.2420	2.0244	1.7016	1.5116	2.3436	1.7999	1.7811	**1.8016**
0.3	2.2265	1.8944	1.8557	2.9005	2.1405	2.1591	1.8039	2.0061	2.2991	2.5834	2.3702	2.0278	1.9684	2.9462	2.0654	2.2138	**2.2163**
0-0.3	**1.3262**	**1.2053**	**1.2010**	**1.9411**	**1.5058**	**1.3104**	**1.2661**	**1.2955**	**1.4492**	**1.7684**	**1.5174**	**1.3940**	**1.2416**	**1.7027**	**1.4161**	**1.3445**	**1.4303**

Compared to those calculated by layer method, point methods yielded greater values of κ (Tables 5.32-5.34). The values for κ calculated by point1 and point 2 methods were consistent. The values calculated by layer, point 1 and point 2 methods are shown in Figs. 5.23-5.25.

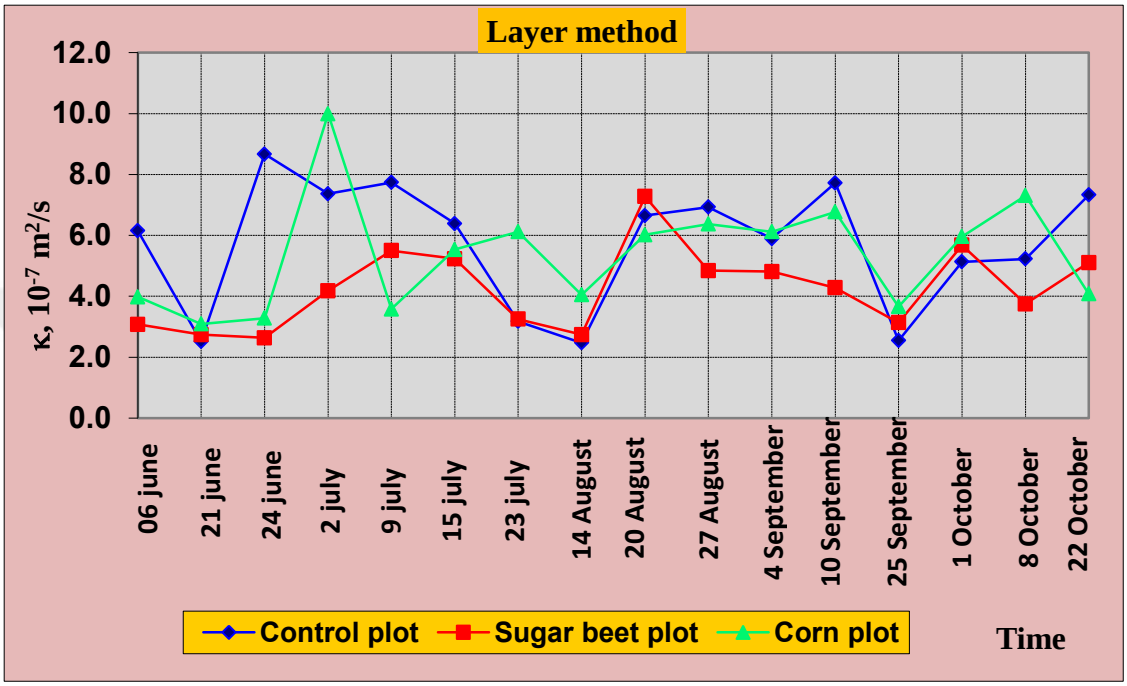

Figure 5.23 Changes of $\kappa.10^{-7}$ values calculated by layer method on selected days during the study. Values for corn and sugar beet are means of three replicates, while for control is a single value

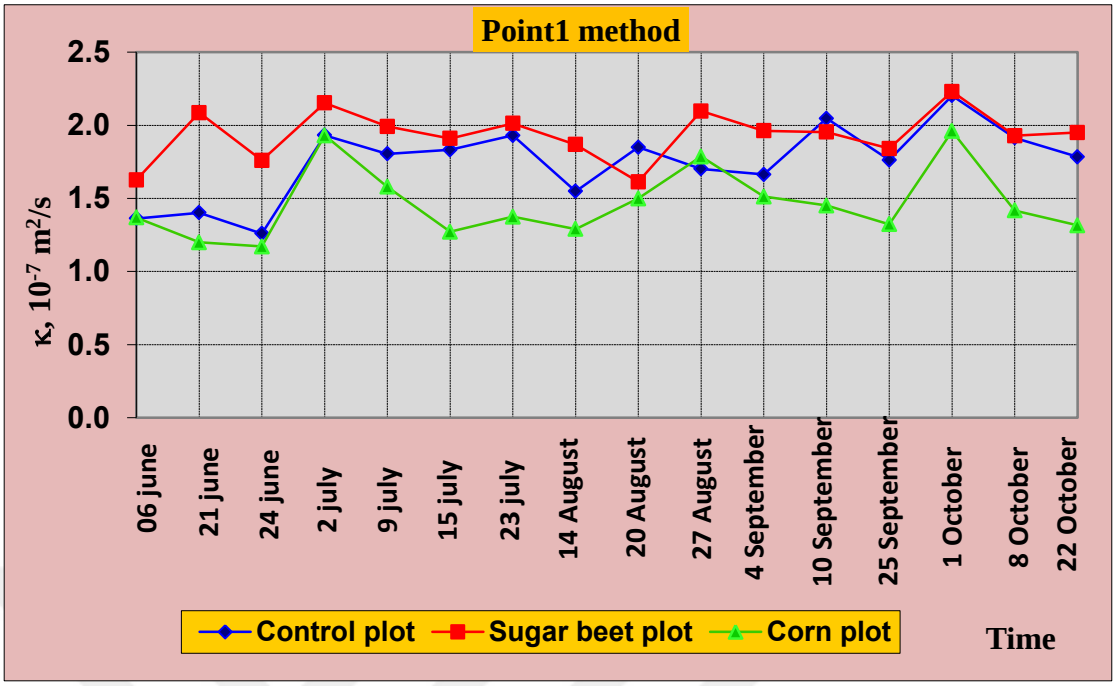

Figure 5.24 Changes of $\kappa.10^{-7}$ values calculated by point1 method on selected days during the study. Values for corn and sugar beet are means of three replicates, while for control is a single value

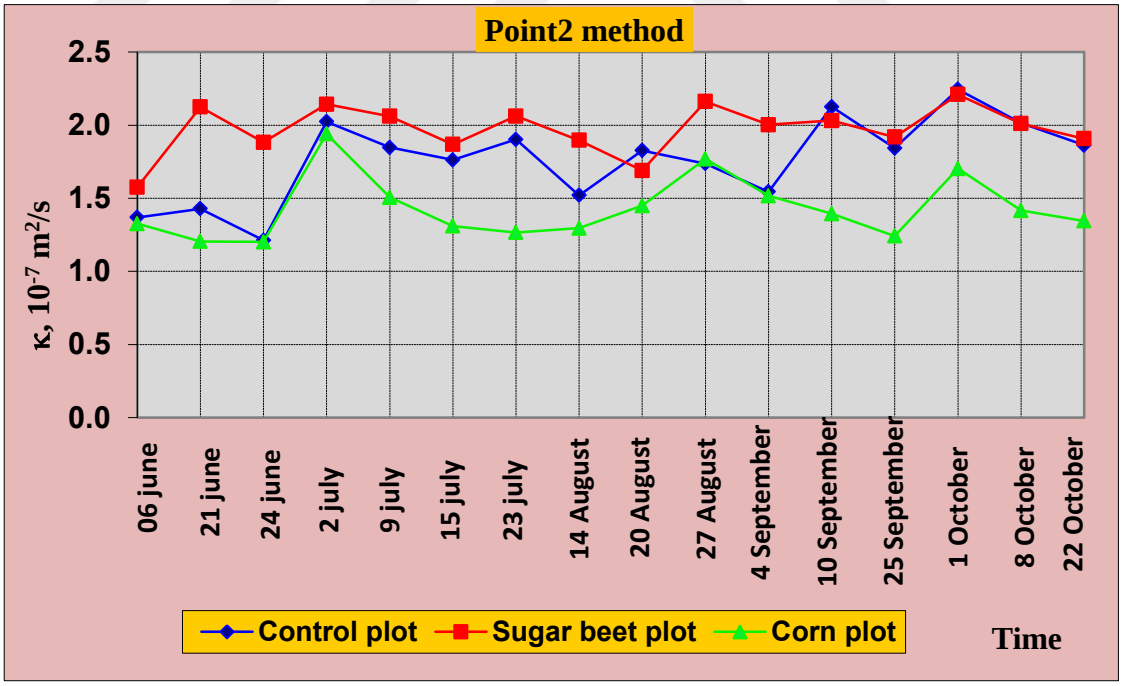

Figure 5.25 Changes of $\kappa.10^{-7}$ values calculated by point2 method on selected days during the study. Values for corn and sugar beet are means of three replicates, while for control is a single value

The predictions of point 1 and point 2 methods showed that the corn plots yielded lowest κ-values in all the cases, while calculations by layer methods showed a highly inconsistent behavior of the treatments during the study period. This suggested that point1 and point 2 methods were more reliable than layer method.

Mean values calculated for κ for 0-30 soil layer by pont1, point2, and layer methods are given in Table 5.35.

Table 5.35 Mean values calculated for κ for 0-30 soil layers of corn, sugar beet and control plots by point 1, point 2, and layer method

Treatments	**Co**	**S1**	**S2**	**S3**	**S1, S2, S3** (mean)	**C1**	C2	**C3**	**C1, C2, C3** (mean)
Depth,m					***θ, cm³/cm³***				
0.05	38.61	37.17	37.74	38.51	37.81	37.33	40.91	39.32	39.19
0.1	41.80	39.07	40.07	40.91	40.02	39.57	42.15	41.23	40.98
0.2	44.64	42.24	41.48	43.88	42.53	42.76	43.51	43.45	43.24
0.3	44.09	40.99	40.81	42.88	41.56	42.18	43.34	42.17	42.56
Mean	**42.29**	**39.87**	**40.03**	**41.54**	**40.48**	**40.46**	**42.48**	**41.54**	**41.49**
					Layer Method *κ.10⁻⁷ m²/s*				
0.05	1.0326	0.7368	1.1522	1.6255	1.1715	0.2609	0.4478	0.7034	0.4707
0.1	4.7314	2.7773	3.9722	3.2644	3.3380	2.7412	4.3911	8.0838	5.0720
0.2	9.6709	5.5570	3.3208	5.0284	4.6354	5.1035	9.3351	11.1026	8.5137
0.3	7.5381	8.1179	10.9526	6.0543	8.3749	6.0769	7.7515	8.4491	7.4259
Mean	**5.7433**	**4.2973**	**4.8495**	**3.9932**	**4.3800**	**3.5457**	**5.4814**	**7.0847**	**5.3706**
					Point1 method *κ.10⁻⁷ m²/s*				
0.05	0.9766	0.4087	1.0779	1.3604	0.9490	0.2748	0.4331	0.6650	0.4576
0.1	1.7417	1.7588	1.9316	2.0507	1.9137	0.9988	1.3265	1.4295	1.2516
0.2	1.9495	2.0678	2.2405	2.3881	2.2321	1.5807	1.8388	2.0379	1.8191
0.3	2.4323	2.4741	2.7258	2.7565	2.6522	2.1374	2.3773	2.4884	2.3344
Mean	**1.7750**	**1.6773**	**1.9940**	**2.1389**	**1.9367**	**1.2479**	**1.4939**	**1.6552**	**1.4657**
					Point2 method *κ.10⁻⁷ m²/s*				
0.05	0.9762	0.4036	1.0732	1.3119	0.9296	0.2749	0.4331	0.6650	0.4577
0.1	1.7099	1.7827	2.0248	1.9935	1.9337	1.0287	1.3508	1.3579	1.2458
0.2	1.9581	2.0779	2.3639	2.3768	2.2729	1.6416	1.8605	1.9026	1.8016
0.3	2.4227	2.5968	2.7836	2.8726	2.7510	2.0866	2.2343	2.3280	2.2163
Mean	**1.7667**	**1.7153**	**2.0614**	**2.1387**	**1.9718**	**1.2579**	**1.4697**	**1.5634**	**1.4303**

Vertical change of θ and κ calculated by layer, point 1 and point 2 methods are given in Figs 5.26-2.28. Values of κ calculated by layer method followed similar pattern as θ did for control and corn plots, but sugar beet plots. On the other hand, κ-values calculated by point 1 and point 2 methods followed different patterns than θ did (Figs 5.27 and 5.28).

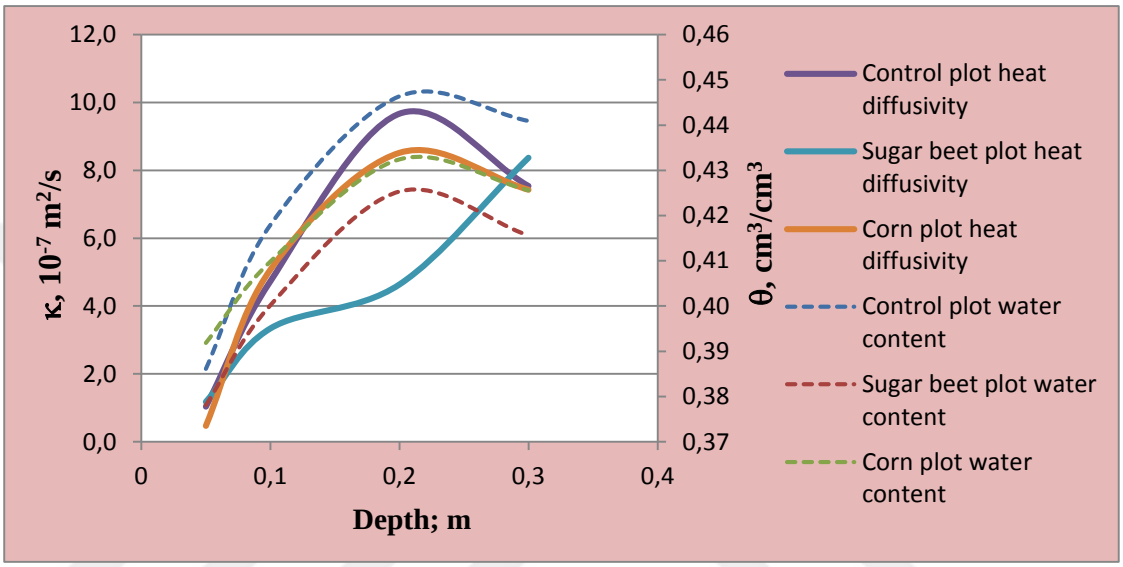

Figure 5.26 Vertical change of θ and κ calculated by layer method. Values for corn and sugar beet are mean of three replicates, while those for control are single values

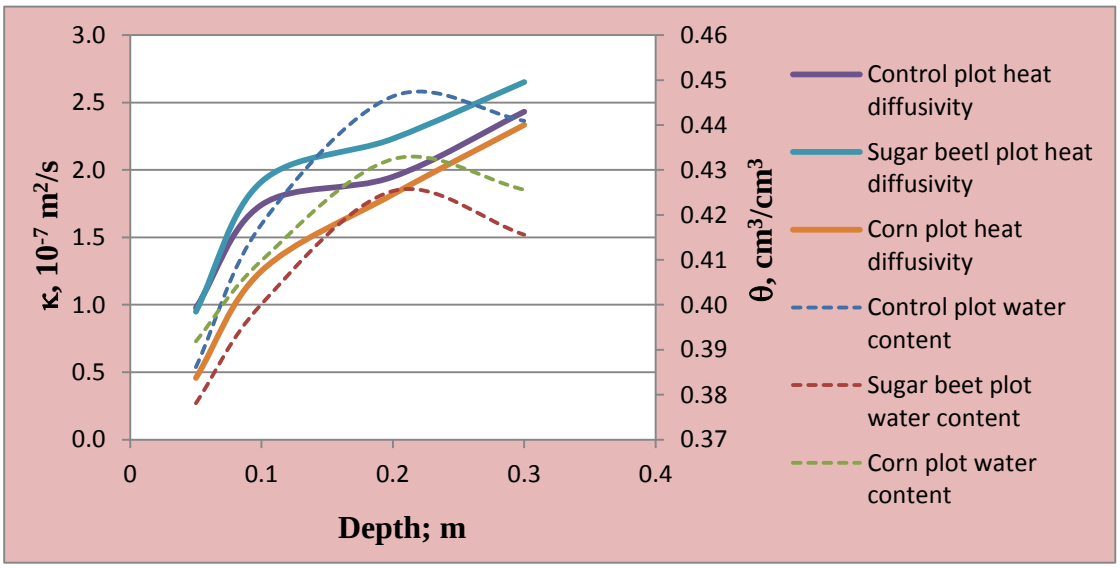

Figure 5.27 Vertical change of θ and κ calculated by point1 method. Values for corn and sugar beet are mean of three replicates, while those for control are single values

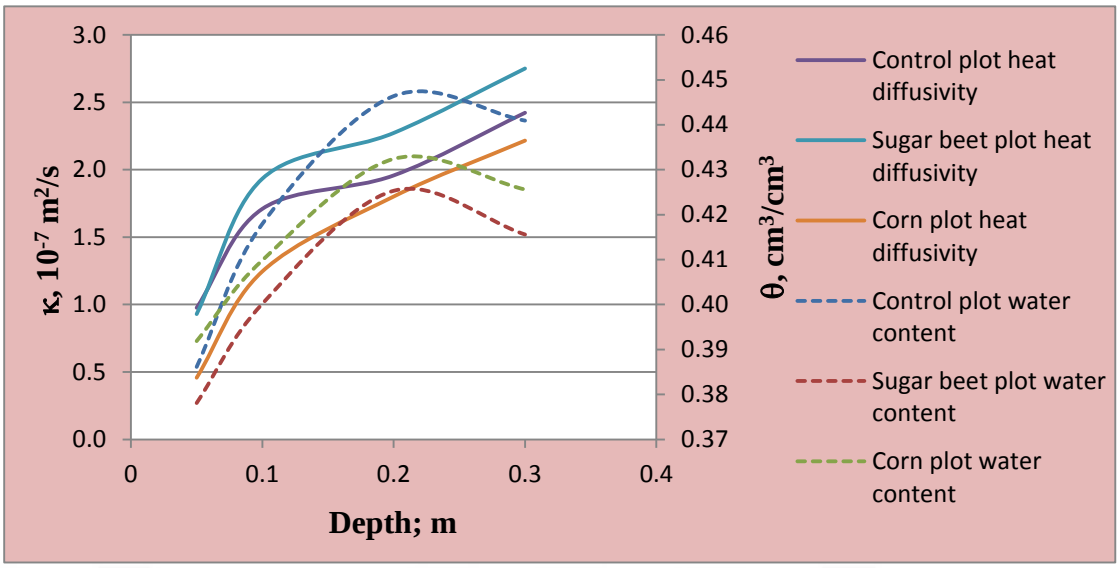

Figure 5.28 Vertical change of θ and κ calculated by point2 method. Values for corn and sugar beet are mean of three replicates, while those for control are single values

5.4 Heat conductivity

Heat conductivity (λ) was calculated by Eq. (4.2). For example, for S2, heat conductivity was calculated as follows:

$$\lambda = \kappa \cdot C_v = 4.2973 \cdot 10^{-7} \frac{m^2}{s} \cdot 0.6495 \frac{cal}{cm^3 \cdot {}^{\circ}C} = 2.8745.10^{-7} \cdot \frac{cal}{s \cdot cm \cdot {}^{\circ}C}$$

Calculated values of λ by layer, point1, and point2 methods and calculated values of volumetric heat capacity (C_v) are given in Table 5.36.

Table 5.36. Calculated values of λ by layer, point1, and point2 methods and calculated values of volumetric heat capacity (C_v)

Treatments	**Co**	**S1**	**S2**	**S3**	**S1, S2, S3** (mean)	**C1**	C2	**C3**	**C1, C2, C3** (mean)
Depth,m					***C_v, cal cm^{-3} ºC^{-1}***				
0.05	0.6080	0.6036	0.6211	0.6136	0.6127	0.6179	0.6562	0.6270	0.6337
0.1	0.6498	0.6326	0.6544	0.6425	0.6431	0.6504	0.6746	0.6562	0.6604
0.2	0.7178	0.6864	0.6706	0.6927	0.6832	0.6879	0.6887	0.6943	0.6903
0.3	0.7288	0.6753	0.6634	0.6984	0.6790	0.6914	0.7164	0.6975	0.7017
Mean	**0.6761**	**0.6495**	**0.6524**	**0.6618**	**0.6545**	**0.6619**	**0.6840**	**0.6687**	**0.6715**
					λ*, Layer method *cal cm^{-1} ºC^{-1} s^{-1}				
0.05	0.6278	0.4447	0.7156	0.9974	0.7192	0.1612	0.2938	0.4411	0.2987
0.1	3.0745	1.7569	2.5993	2.0973	2.1512	1.7828	2.9620	5.3044	3.3497
0.2	6.9414	3.8143	2.2271	3.4830	3.1748	3.5107	6.4290	7.7085	5.8827
0.3	5.4936	5.4822	7.2655	4.2282	5.6586	4.2015	5.5532	5.8929	5.2158
Mean	**4.0344**	**2.8745**	**3.2019**	**2.7015**	**2.9260**	**2.4140**	**3.8095**	**4.8367**	**3.6867**
					λ*, Point 1 method *cal cm^{-1} ºC^{-1} s^{-1}				
0.05	0.5938	0.2467	0.6695	0.8347	0.5836	0.1698	0.2842	0.4169	0.2903
0.1	1.1318	1.1126	1.2640	1.3176	1.2314	0.6496	0.8948	0.9380	0.8275
0.2	1.3992	1.4193	1.5026	1.6541	1.5253	1.0873	1.2664	1.4149	1.2562
0.3	1.7726	1.6708	1.8082	1.9251	1.8014	1.4778	1.7031	1.7355	1.6388
Mean	**1.2244**	**1.1123**	**1.3111**	**1.4329**	**1.2854**	**0.8461**	**1.0371**	**1.1263**	**1.0032**
					λ*, Point 2 method *cal cm^{-1} ºC^{-1} s^{-1}				
0.05	0.5935	0.2436	0.6665	0.8050	0.5717	0.1699	0.2842	0.4170	0.2904
0.1	1.1111	1.1277	1.3250	1.2808	1.2445	0.6690	0.9112	0.8910	0.8237
0.2	1.4055	1.4263	1.5854	1.6464	1.5527	1.1292	1.2813	1.3210	1.2438
0.3	1.7656	1.7537	1.8466	2.0062	1.8688	1.4427	1.6007	1.6236	1.5557
Mean	**1.2189**	**1.1378**	**1.3559**	**1.4346**	**1.3094**	**0.8527**	**1.0194**	**1.0631**	**0.9784**

The damping depth (d) was calculated as follows:

$$d = \sqrt{\frac{\tau_0 \kappa_{mean}}{\pi}} = \sqrt{\frac{84600\,s}{3.14} \cdot 4.2973.10^{-7}\,\frac{cm^2}{s}} \approx 10.76\,cm$$

The calculated values of *d* are given in Table 5.37.

Table 5. 37 Dumping depth (d)-values of treatment plots (cm)

Plants Grown Plot	Plots code	Damping Depth *d (cm)*
Control	**Co**	**12.44**
Sugar beet	S1	10.76
Sugar beet	S2	11.43
Sugar beet	S3	10.37
Sugar beet	**Mean**	**10.86**
Corn	C1	9.77
Corn	C2	12.15
Corn	C3	13.82
Corn	**Mean**	**12.03**

Dumping depth (*d*) was more variable at corn than sugar beet plots. On the other hand, the value of *d* calculated for corn was more similar to one calculated for Co. The *d* is a function of amplitude of temperature soil surface and soil water content. We believe that this difference between corn and others would be attributed to differences in water content and in temperature amplitudes on the soil surface under corn canopy.

5.5. Comparing Modeling Successes

Point1 and point2 methods out performed layer method as depicted by Figs 5.16-5.26. This success was attributed to that the point methods consider soil surface temperature parameters in calculating the values of κ, the value used in calculating soil temperature.

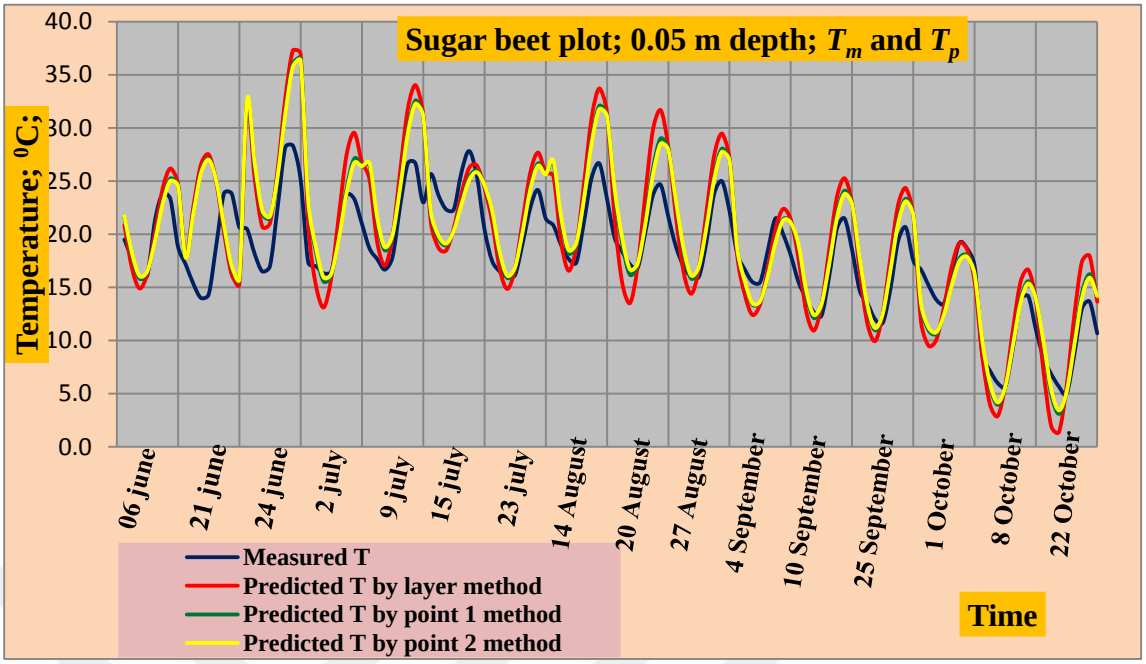

Figure 5.29 Measured and calculated temperature (T) values at 0.05 m depth of sugar beet plots (S1, S2, S3) on the selected days during the study period. The values are means of three replicates (S1, S2, and S3)

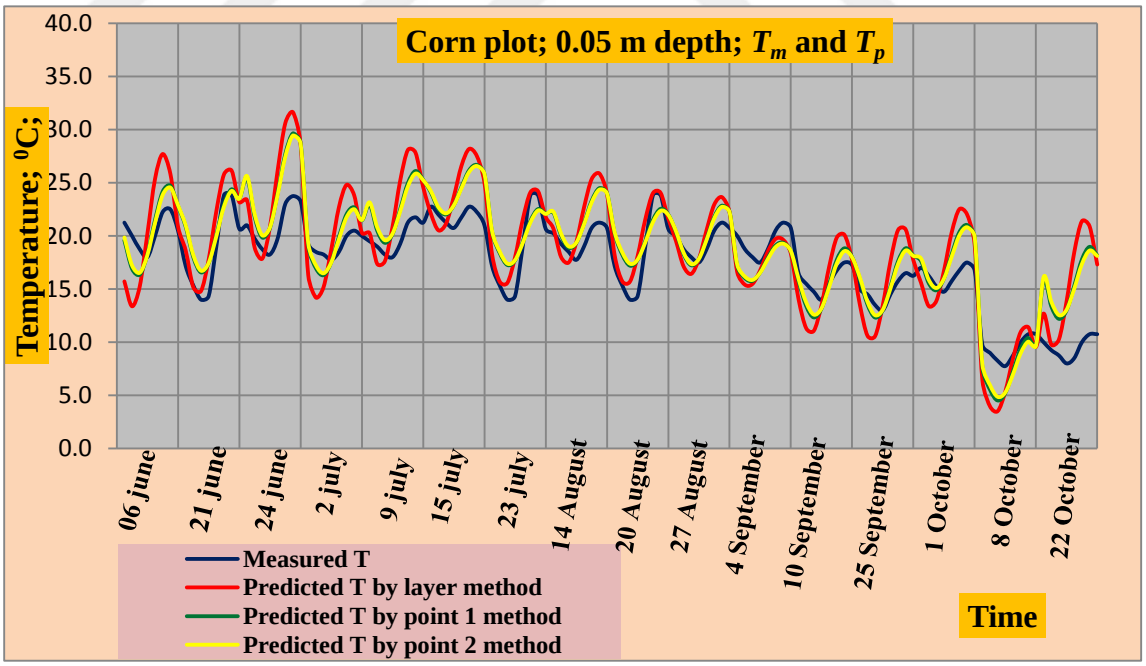

Figure 5.30 Measured and calculated temperature (T) values at 0.05 m depth of corn plots (C1, C2, C3) on the selected days during the study period. The values are means of three replicates (C1, C2, and C3)

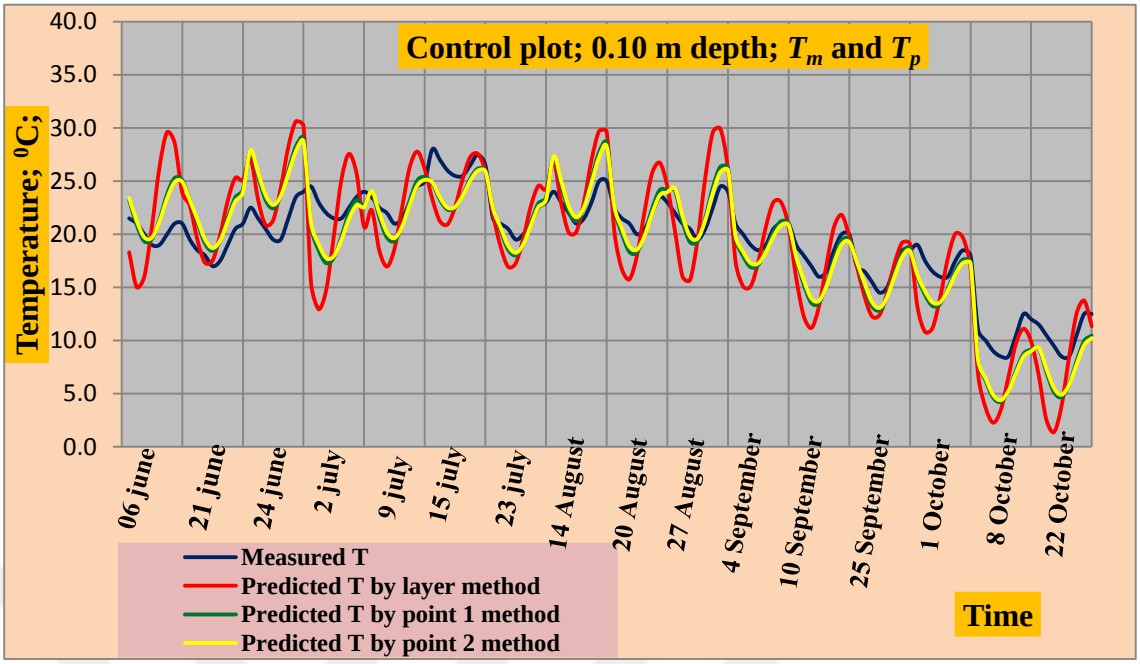

Figure 5.31 Measured and calculated temperature (T) values at 0.1 m depth of control plot (Co) on the selected days during the study period

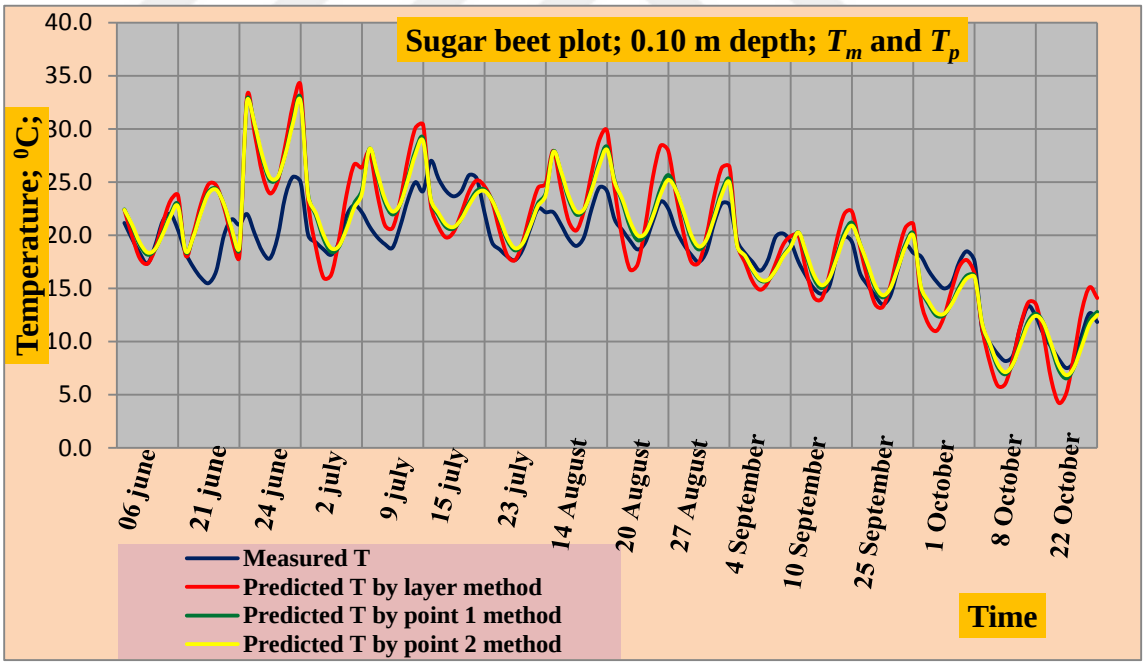

Figure 5.32 Measured and calculated temperature (T) values at 0.1 m depth of sugar beet plots (S1, S2, S3) on the selected days during the study period. The values are means of three replicates (S1, S2, and S3)

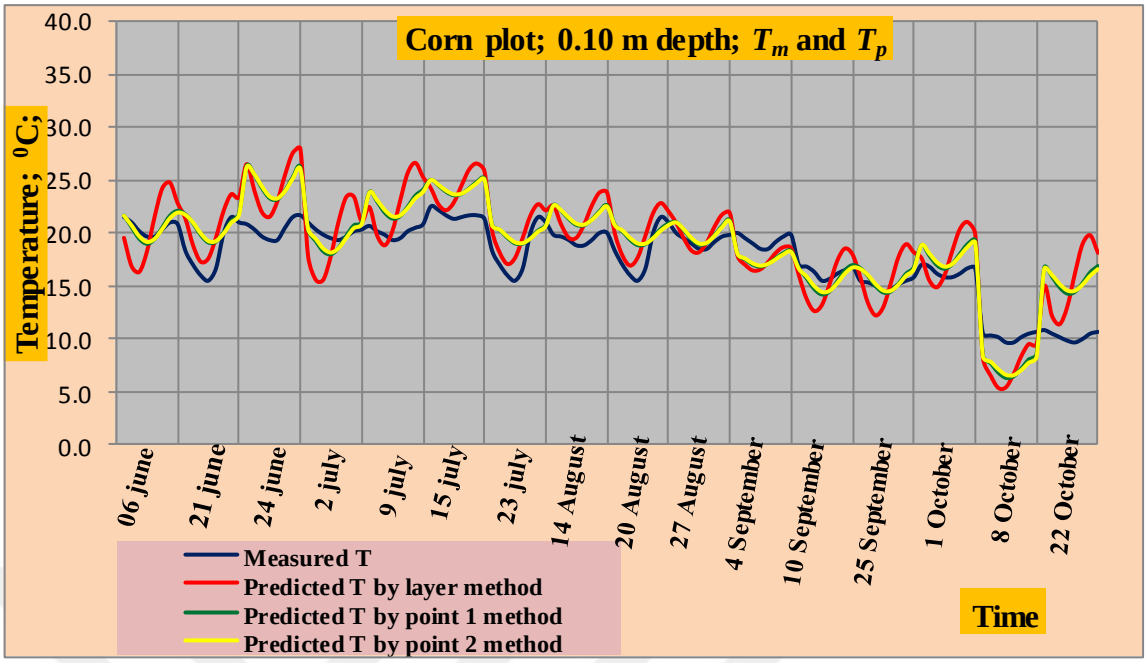

Figure 5.33 Measured and calculated temperature (T) values at 0.1 m depth of corn plots (C1, C2, C3) on the selected days during the study period. The values are means of three replicates (C1, C2, and C3)

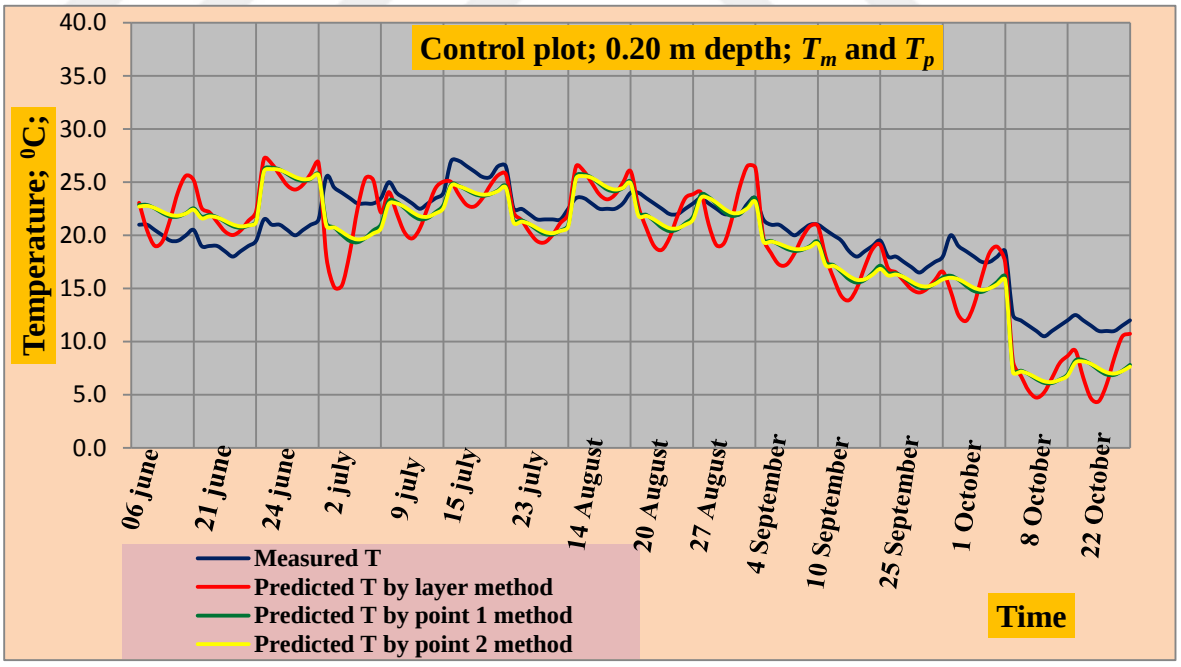

Figure 5.34 Measured and calculated temperature (T) values at 0.2 m depth of control plot (Co) on the selected days during the study period

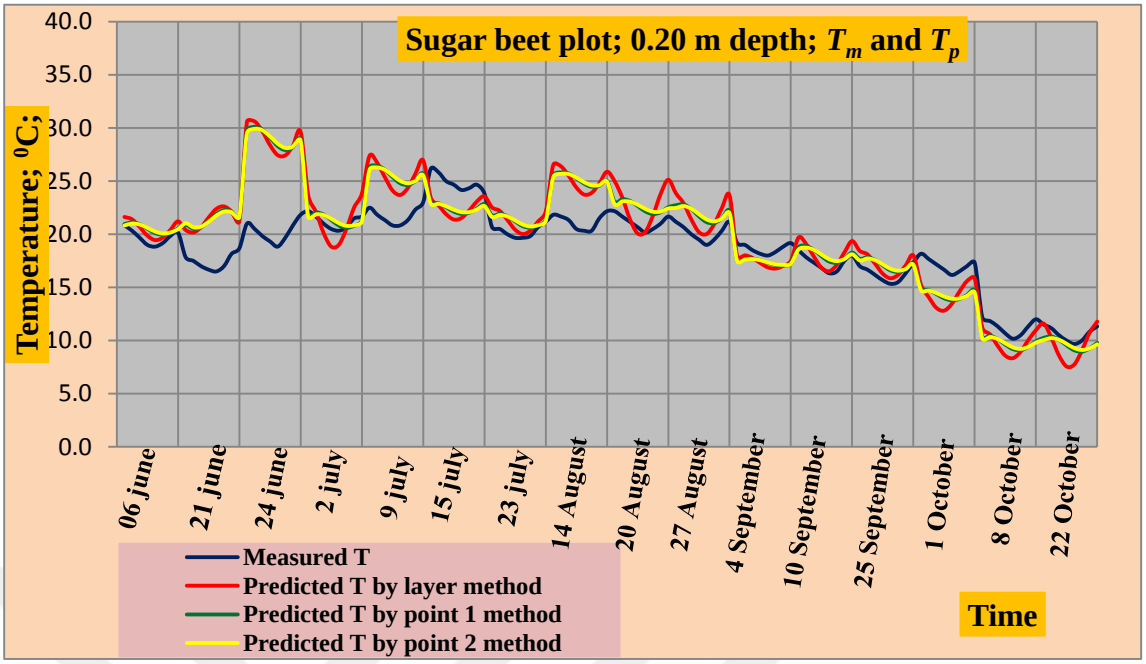

Figure 5.35 Measured and calculated temperature (T) values at 0.2 m depth of sugar beet plots (S1, S2, S3) on the selected days during the study period. The values are means of three replicates (S1, S2, and S3)

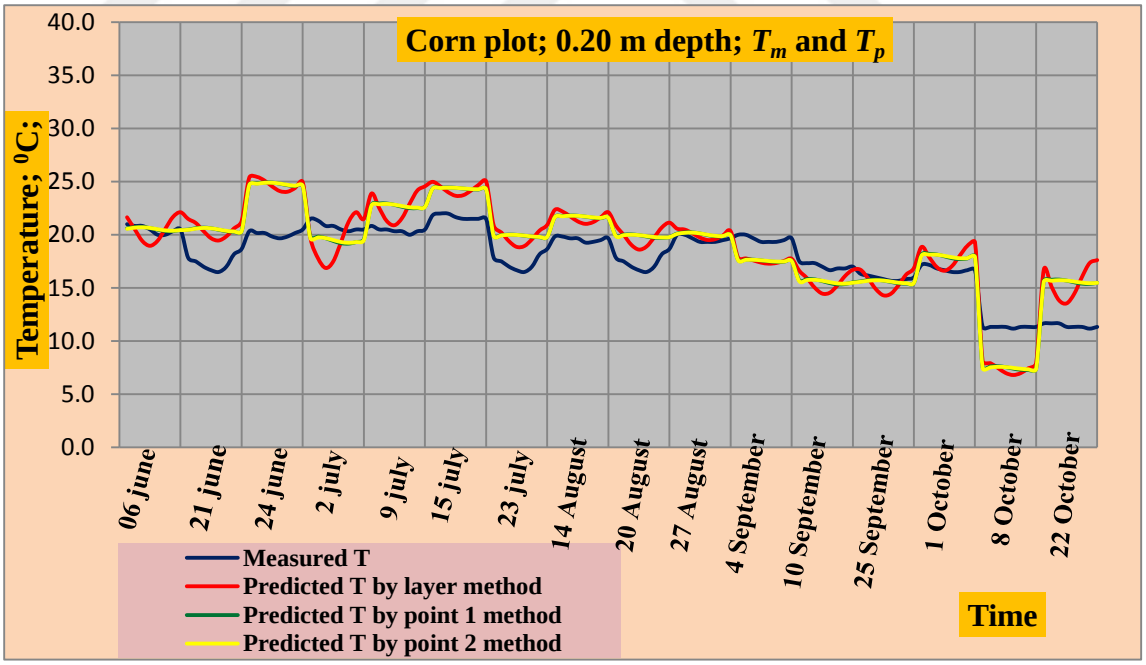

Figure 5.36 Measured and calculated temperature (T) values at 0.2 m depth of corn plots (C1, C2, C3) on the selected days during the study period. The values are means of three replicates (C1, C2, and C3)

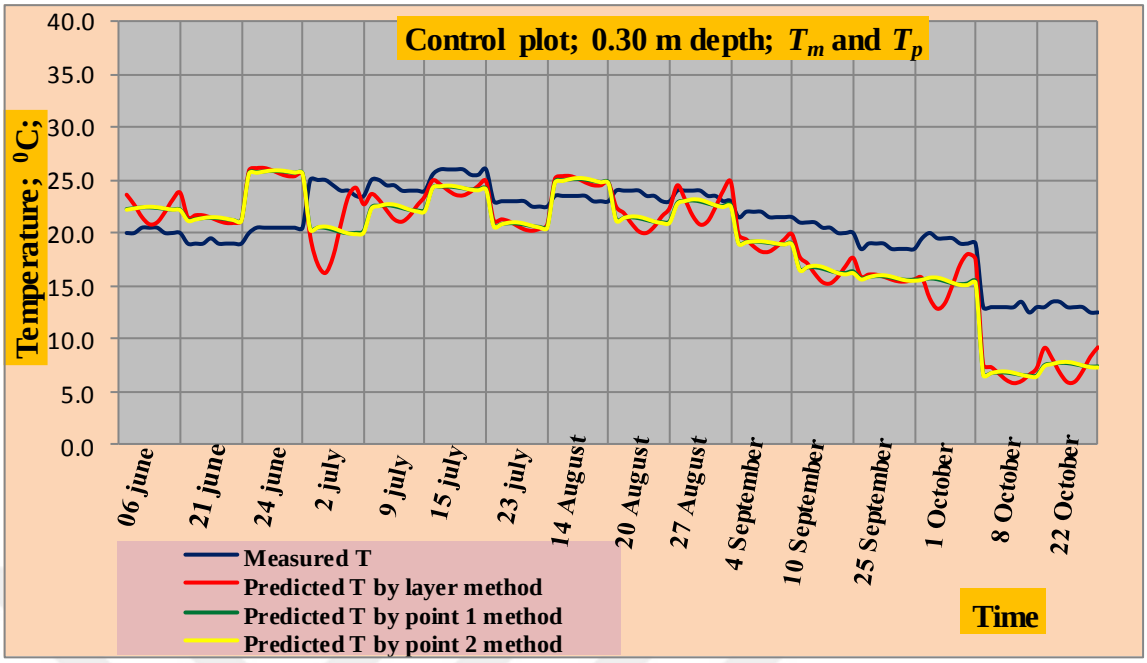

Figure 5.37 Measured and calculated temperature (T) values at 0.3 m depth of control plot (Co) on the selected days during the study period

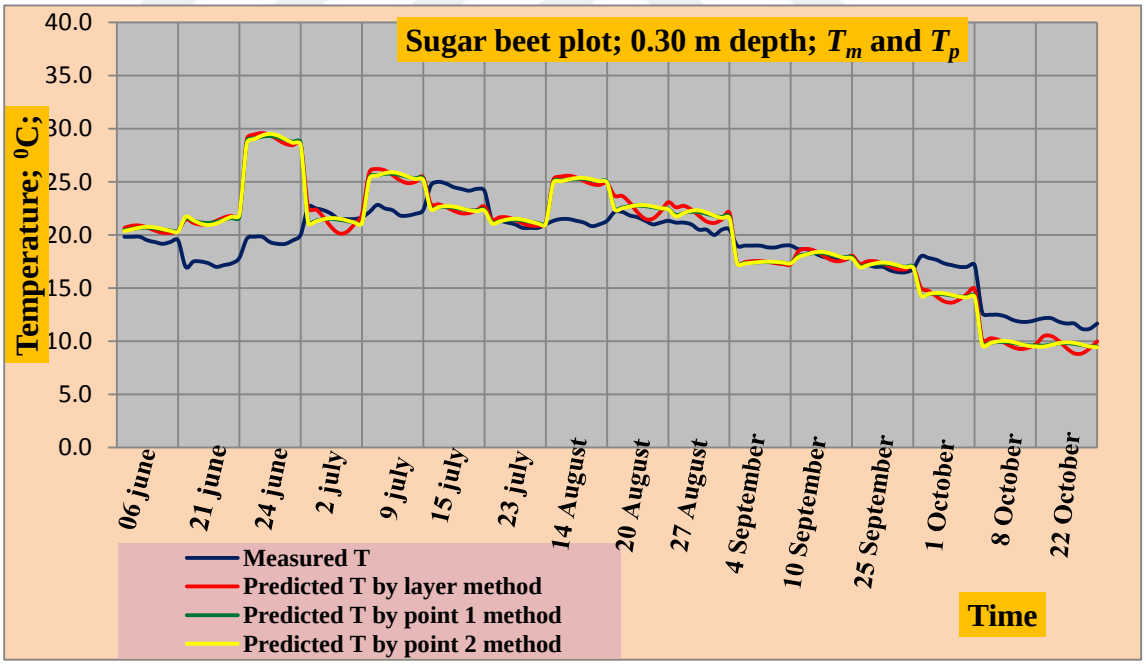

Figure 5.38 Measured and calculated temperature (T) values at 0.2 m depth of sugar beet plots (S1, S2, S3) on the selected days during the study period. The values are means of three replicates (S1, S2, and S3)

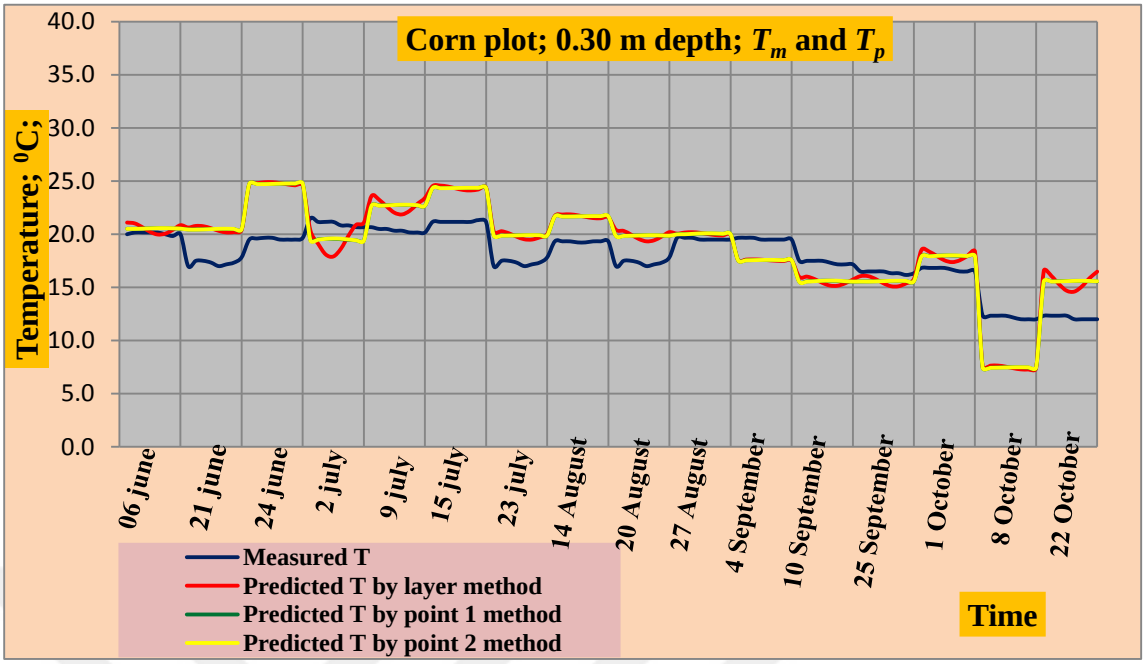

Figure 5.39 Measued and calculated temperature (T) values at 0.2 m depth of corn plots (C1, C2, C3) on the selected days during the study period. The values are means of three replicates (C1, C2, and C3)

Linear correlation analysis conducted between measured and calculated values of temperature at different depths are given in Table 5.38. Table 5.38 shows that all the methods predicted the temperature successfully at 0.05, 0.1, 0.2, and 0.3 cm depths of all the plots. However, the statistical parameters for goodness of fit show that the models were less successful at deeper depths (especially at 0.2 and 0.3 m) in predicting soil temperature, indicating that correlation analysis may not be used solely to evaluate the model performance. The correlation analysis measures if greater values matches with greater values, or vice versa. Some other measures should be used along with correlation analysis for a better evaluation of model performance.

Table 5.38 Linear correlation analysis conducted between measured and calculated values of temperature at different depths

Depth m	Control plot			Sugar beet plot			Corn plot		
	layer	**Point 1**	**Point 2**	**layer**	**Point 1**	**Point 2**	**layer**	**Point 1**	**Point 1**
0.05	-	-	-	0.8584	0.8589	0.8564	0.791	0.8499	0.8526
0.10	0.8247	0.9279	0.9320	0.8631	0.8609	0.8562	0.7968	0.8423	0.8415
0.20	0.8437	0.896	0.8945	0.8433	0.8399	0.8378	0.8083	0.8208	0.8204
0.30	0.8231	0.8503	0.8506	0.817	0.8144	0.8136	0.7911	0.7953	0.7952
Mean	0.8305	0.8914	**0.8924**	0.8455	0.8435	0.8410	0.7968	0.8271	**0.8274**

The predicted and measured values of temperature at 0.05, 0.1, 0.2, and 0.3 m depths of control, sugar beet and corn plots are given in tables 5.39, 5.41, 5.43, 5.45, 5.47, 5.49, 5.51, 5.43, and 5.55 and their corresponding statististical parameters for goodness of fit are given in 5.40, 5.42, 5.44, 5.46, 5.48, 5.50, 5.52, 5.54 and 5.56. In addition, measured and calculated temperature values at 0.05, 0.1, 0.2, and 0.3 m depths of control, sugar beet and corn plots are compared in the Figs. 5.40 thorough 5.47. These listed tables and figures show that the layer method generally poorly predicted the temperature in majority of the cases, while point1 and point2 methods successfully predicted the temperature at given depths. For example, Table 5.40 shows that the calculated F-values for layer method were lower than the corresponding standard table value, indicating that the layer method was not adequately predict the temperature at 0.1 m, while Table 5.42 and 5.44 show that the calculated F-values were greater than corresponding table value, suggesting that the point1 and point2 methods successfully predicted temperature at 0.1 m depth of control plot. Similarly, Fig. 5.40 shows that the line representing layer method-predicted temperature behaves differently from measured one, while those representing point1 and point2 predicted temperature values behave more consistently. In addition, behavior of lines for point1 and point2 methods are highly resemble.

Table 5.39 Measured and layer method-predicted values of temperature at different depths of control plot (n=16).

i	Time	0.10		0.20		0.3	
	t_i	T_m	T_p	T_m	T_p	T_m	T_p
1	0	20.5	18.5	21.1	20.1	21.0	19.9
2	3	19.5	15.2	20.7	18.5	21.2	19.3
3	6	18.7	14.3	20.3	17.3	21.1	18.6
4	9	17.8	16.2	19.8	17.2	21.1	18.3
5	12	18.2	19.9	19.4	18.2	20.8	18.5
6	15	19.7	23.2	19.6	19.8	20.7	19.1
7	18	21.2	24.1	20.1	21.1	20.5	19.7
8	21	21.2	22.1	20.6	21.2	20.6	20.1

Tm: Measured temperature ^{0}C; T_p: Predicted temperature ^{0}C

Table 5.40 Statistical parameters for comparing measured and layer method-predicted values of temperature at different depths of control plot (n=16).

x, m	R^2	R^2_{adj}	σ	ESS	RSS	TSS	F_C	F_T (1, 6)	
								α=0,01	α=0,05
0.10	0.392	0.291	1.1009	4.6890	7.2710	11.9600	3.87<	13.75	5.99
0.20	0.105	0.000	0.5984	0.2514	2.1486	2.4000	0.7<	13.75	5.99
0.30	0.221	0.091	0.2483	0.1051	0.3699	0.4750	1.7<	13.75	5.99

x: depts, R^2: Coefficient of determination, R^2_{adj}: Adjusted R^2, σ: Root Mean Squared Error, ESS: Estimate sum of square, RSS: Residual sum of squares, TSS: Total sum of square, F: Fisher Criteria, F_T: F- table, F_C: F-calculated

Table 5.41 Measured and point1 method-predicted values of temperature at different depths of control plot (n = 16)

i	Time	0.10		0.20		0.3	
	t_i	T_m	T_p	T_m	T_p	T_m	T_p
1	**0**	20.6	20.5	21.1	19.9	20.8	19.2
2	**3**	19.7	18.3	20.7	19.8	21.0	19.3
3	**6**	18.8	16.6	20.3	19.4	21.0	19.4
4	**9**	18.0	16.4	19.8	18.8	20.9	19.3
5	**12**	18.3	17.9	19.5	18.5	20.7	19.2
6	**15**	19.7	20.1	19.7	18.6	20.5	19.1
7	**18**	21.1	21.8	20.1	19.0	20.4	19.0
8	**21**	21.2	21.9	20.6	19.5	20.5	19.1

T_m: Measured temperature ^{0}C; T_p: Predicted temperature ^{0}C

Table 5.42 Statistical parameters for comparing measured and point 1 method-predicted values of temperature at different depths of control plot (N =16)

x, m	R^2	R^2_{adj}	σ	ESS	RSS	TSS	F	F_{table} (1,6)	
								α=0,01	α=0,05
0.10	0.990	0.883	0.4468	10.7620	1.1980	11.9600	53.92>	13.75	5.99
0.20	0.967	0.962	0.1147	2.3211	0.0789	2.4000	176.47>	13.75	5.99
0.30	0.849	0.824	0.1093	0.4033	0.0717	0.4750	33.77>	13.75	5.99

x: Depth, R^2: Determination coefficient, R^2_{adj}: Adjusted R^2, σ: Root mean squared Error, ESS: Estimate sum of square, RSS: Residual sum of squares, TSS: Total sum of square, F: Fisher Criteria

Table 5.43 Measured and point 2 method-predicted values of temperature at different depths of control plot (Nn=16)

i	Time	0.10		0.20		0.3	
	t_i	T_m	T_p	T_m	T_p	T_m	T_p
1	**0**	20.8	20.6	21.4	19.7	21.3	19.1
2	**3**	19.9	18.7	21.1	19.7	21.5	19.3
3	**6**	19.1	17.0	20.7	19.4	21.5	19.4
4	**9**	18.2	16.6	20.1	19.0	21.4	19.4
5	**12**	18.6	17.7	19.7	18.7	21.2	19.3
6	**15**	20.1	19.7	20.0	18.7	21.0	19.1
7	**18**	21.6	21.3	20.5	18.9	20.9	18.9
8	**21**	21.5	21.7	21.0	19.3	20.9	19.0

Tm: Measured temperature ^{0}C; T_p: Predicted temperature ^{0}C

Table 5.44 Statistical parameters for comparing measured and point 2 method-predicted values of temperature at different depths of control plot (n =16)

x, m	R^2	R^2_{adj}	σ	ESS	RSS	TSS	F	F_{table} (1,6)	
								α=0,01	α=0,05
0.10	0.948	0.939	0.3230	11.334	0.6260	11.9600	108.63>	13.75	5.99
0.20	0.874	0.853	0.2244	2.0978	0.3022	2.4000	41.65>	13.75	5.99
0.30	0.700	0.649	0.1542	0.3323	0.1427	0.4750	13.97>	13.75	5.99

x: Depth, R^2: Determination coefficient, R^2_{adj}: Adjusted R^2, σ: Root Mean Squared Error, ESS: Estimate sum of square, RSS: Residual sum of squares, TSS: Total sum of square, F: Fisher Criteria

Point2 method shows adequate for control plot soils due to values of R^2 ve R^2_{adj} are very high in x=10, 20, 30 cm depths and $F_{hes} > F_{tabl.}$

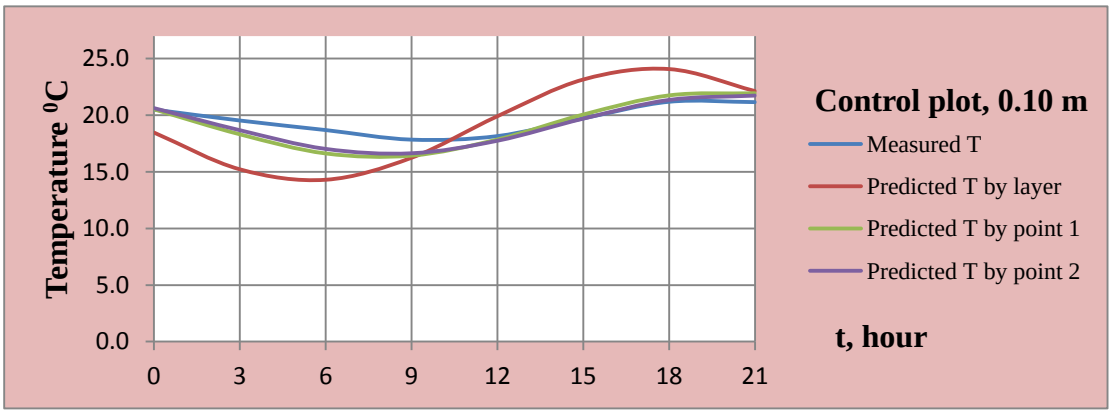

Figure 5.40 Measured vs calculated temperature values at 0.1 m depth of control plot (*N*=16)

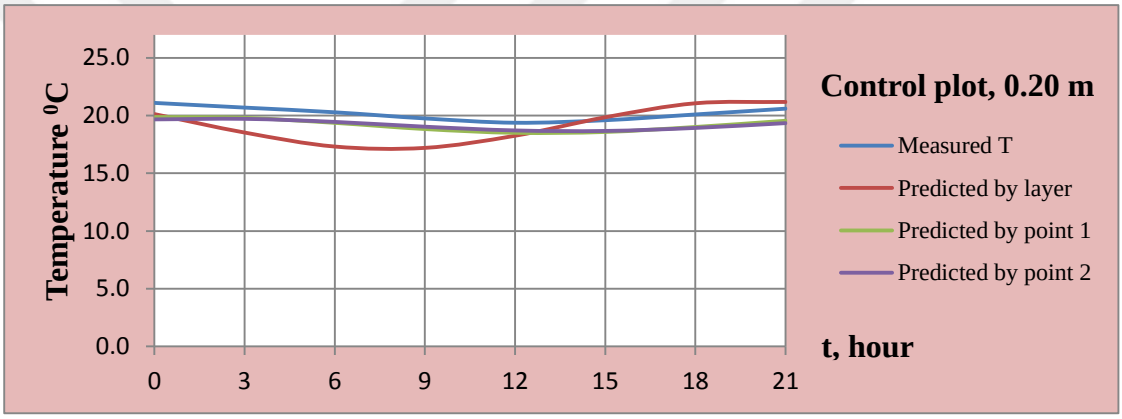

Figure 5.41 Measured vs calculated temperature values at 0.2 m depth of control plot (*n*=16)

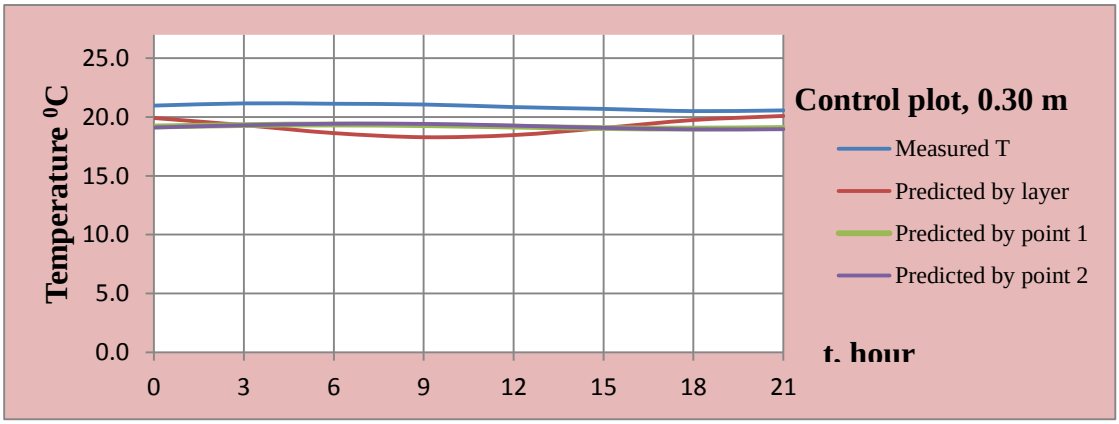

Figure 5.42 Measured vs calculated temperature values at 0.3 m depth of control plot (*n*=16)

Table 5.45 Measured and layer method-predicted values of temperature at different depths of sugar beet plots (n = 16). Values are means of three replicates (S1, S2, S3)

i	Time	0.05		0.1		0.2		0.3	
	t_i	T_m	T_p	T_m	T_p	T_m	T_p	T_m	T_p
1	0	17.4	19.2	19.1	21.3	19.6	21.2	19.4	20.3
2	3	15.9	15.0	17.9	18.4	19.1	20.6	19.4	20.4
3	6	14.6	13.6	16.9	16.3	18.6	19.5	19.3	20.2
4	9	14.6	15.9	16.2	16.4	18.1	18.7	19.1	19.8
5	12	18.4	20.5	17.2	18.4	17.8	18.5	18.8	19.4
6	15	22.3	24.7	19.7	21.3	18.1	19.2	18.7	19.4
7	18	22.5	26.1	21.2	23.4	18.9	20.2	18.8	19.6
8	21	19.4	23.8	20.3	23.3	19.4	21.0	19.0	19.9

Tm: Measured temperature ^{0}C; T_p: Predicted temperature ^{0}C

Table 5.46 Statistical parameters for comparing measured and layer method-predicted values of temperature at different depths of sugar beet plots (N =16)

x, m	R^2	R^2_{adj}	σ	*ESS*	*RSS*	*TSS*	*F*	F_{table} (1,6)	
								α=0,01	α=0,05
0.05	0.928	0.916	0.9094	63.6370	4.9620	68.5990	76.95>	13.75	5.99
0.10	0.949	0.940	0.4355	21.0610	1.1380	22.1990	111.03>	13.75	5.99
0.20	0.975	0.970	0.1136	2.9630	0.0770	3.0400	231.02>	13.75	5.99
0.30	0.950	0.942	0.0681	0.5309	0.0278	0.5587	114.66>	13.75	5.99

x: Depth, R^2: Determination coefficient, R^2_{adj}: Adjusted R^2, σ: Root mean squared Error, *ESS*: Estimate sum of square, *RSS*: Residual sum of squares, *TSS*: Total sum of square, *F*: Fisher Criteria

Table 5.47 Measured and point1 method-predicted values of temperature at different depths of sugar beet plots (n = 16). Values are means of three replicates (S1, S2, and S3)

i	Time	0.05		0.1		0.2		0.3	
	t_i	T_m	T_p	T_m	T_p	T_m	T_p	T_m	T_p
1	0	17.4	20.4	19.1	21.7	19.6	20.3	19.4	19.8
2	3	15.9	16.7	17.9	19.9	19.1	20.4	19.4	19.9
3	6	14.6	14.8	16.9	18.2	18.6	20.2	19.3	20.0
4	9	14.6	15.9	16.2	17.4	18.1	19.8	19.1	20.0
5	12	18.4	19.3	17.2	18.1	17.8	19.4	18.8	19.9
6	15	22.3	23.0	19.7	19.8	18.1	19.3	18.7	19.8
7	18	22.5	24.9	21.2	21.6	18.9	19.5	18.8	19.7
8	21	19.4	23.8	20.3	22.3	19.4	19.9	19.0	19.7

Tm: Measured temperature ^{0}C; T_p: Predicted temperature ^{0}C

Table 5.48 Statistical parameters for comparing measured and point1 method-predicted values of temperature at different depths of sugar beet plots (n =16)

x, cm	R^2	R^2_{adj}	σ	*ESS*	*RSS*	*TSS*	*F*	F_{table} (1,6)	
								α=0,01	α=0,05
5	0.874	0.853	1.1991	59.9720	8.6260	68.5990	41.71>	13.75	5.99
10	0.795	0.760	0.8718	17.6390	4.5600	22.1990	23.21>	13.75	5.99
20	0.455	0.364	0.5255	1.3829	1.6571	3.0400	5.01<	13.75	5.99
30	0.162	0.022	0.2794	0.0903	0.4685	0.5588	1,16<	13.75	5.99

x: Depth, R^2: Determination coefficient, R^2_{adj}: Adjusted R^2, σ: Root Mean squared error, *ESS*: Estimate sum of square, *RSS*: Residual sum of squares, *TSS*: Total sum of square, *F*: Fisher Criteria

Table 5.49 Measured and and point2 method-predicted values of temperature at different depths of sugar beet plots (N = 16). Values are means of three replicates (S1, S2, S3)

i	Time	0.05		0.1		0.2		0.3	
	t_i	T_m	T_p	T_m	T_p	T_m	T_p	T_m	T_p
1	0	17.4	20.6	19.1	21.6	19.6	20.2	19.4	19.7
2	3	15.9	17.0	17.9	20.1	19.1	20.3	19.4	19.9
3	6	14.6	15.0	16.9	18.4	18.6	20.2	19.3	20.0
4	9	14.6	15.9	16.2	17.6	18.1	19.9	19.1	20.1
5	12	18.4	19.1	17.2	18.1	17.8	19.5	18.8	20.0
6	15	22.3	22.7	19.7	19.6	18.1	19.4	18.7	19.8
7	18	22.5	24.7	21.2	21.3	18.9	19.5	18.8	19.7
8	21	19.4	23.8	20.3	22.1	19.4	19.8	19.0	19.6

Tm: Measured temperature, ^{0}C; T_p: Predicted temperature, ^{0}C

Table 5.50 Statistical parameters for comparing measured and point2 method-predicted values of temperature at different depths of sugar beet plots (n=16)

x, cm	R^2	R^2_{adj}	σ	*ESS*	*RSS*	*TSS*	*F*	F_{table} (1,6)	
								α=0.01	α=0.05
5	0.852	0.828	1.3000	58.4590	10.1400	68.5990	34.59>	13.75	5.99
10	0.736	0.692	0.9886	16.3350	5.8640	22.1990	16.71>	13.75	5.99
20	0.303	0.186	0.5944	0.9201	2.1199	3.0400	2.60<	13.75	5.99
30	0.016	0.000	0.3026	0.0092	0.5496	0.5588	0,10<	13.75	5.99

x: Depth, R^2: Determination coefficient, R^2_{adj}: Adjusted R^2, σ: Root mean squared Error, *ESS*: Estimate sum of square, *RSS*: Residual sum of squares, *TSS*: Total sum of square, *F*: Fisher Criteria

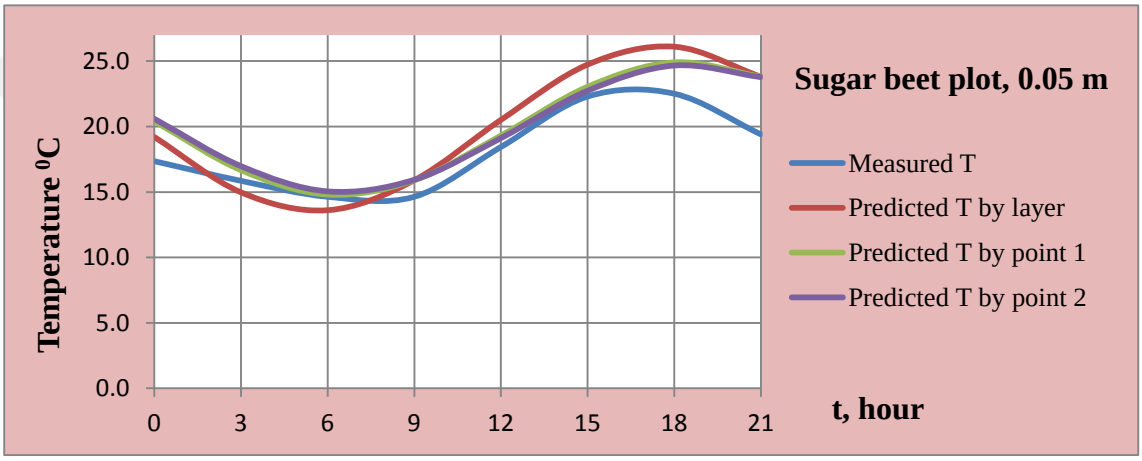

Figure 5.43 Mean measured vs predicted hourly temperature values at 0.05 m depth of sugar beet plots during the study period (n =16)

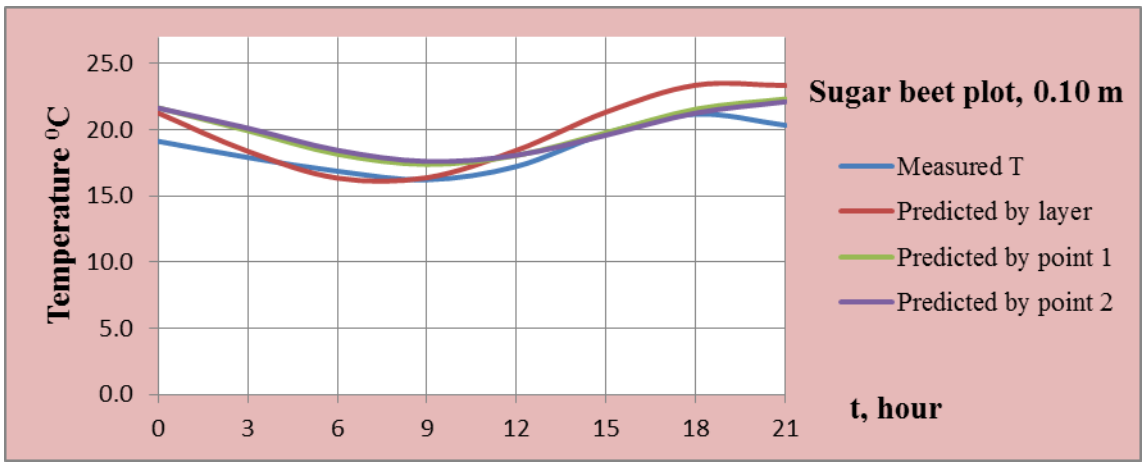

Figure 5.44 Mean measured vs predicted hourly temperature values at 0.1 m depth of sugar beet plots during the study period (n =16)

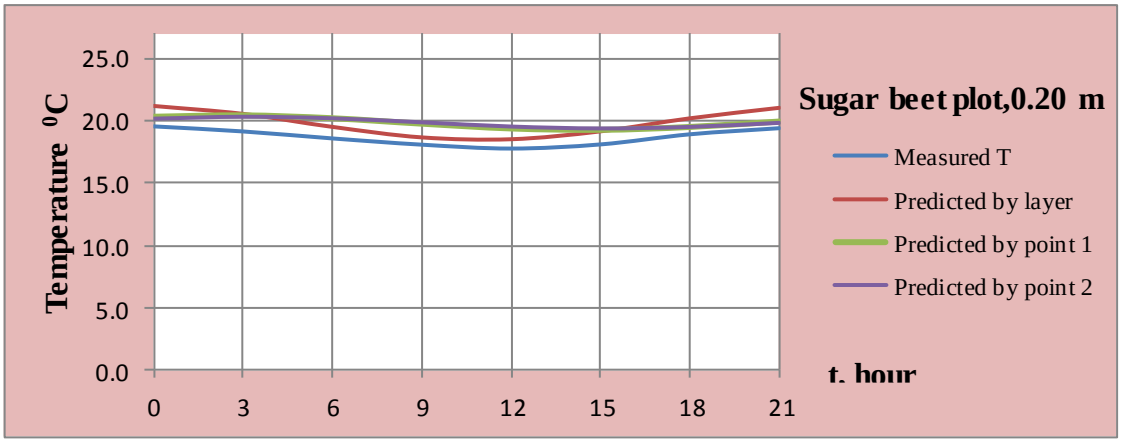

Figure 5.45 Mean measured vs predicted hourly temperature values at 0.2 m depth of sugar beet plots during the study period (n = 16)

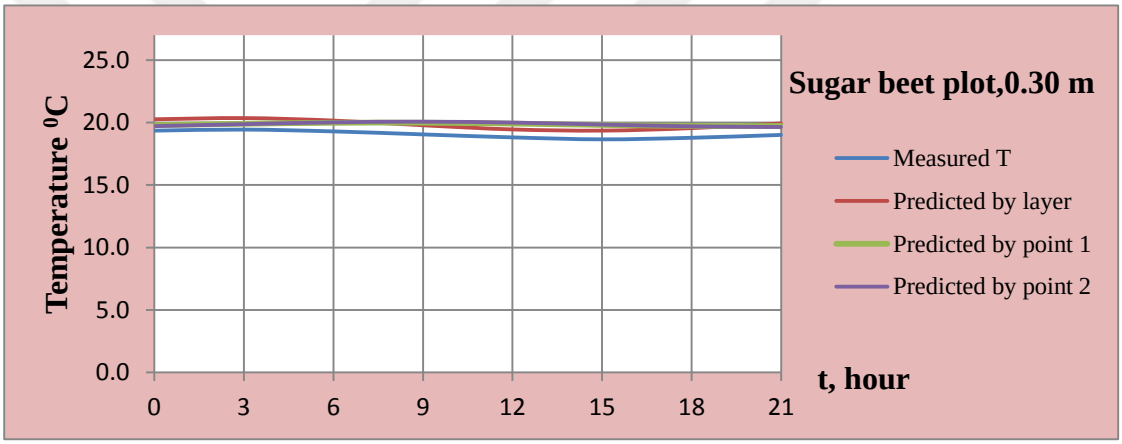

Figure 5.46 Mean measured vs predicted hourly temperature values at 0.3 m depth of sugar beet plots during the study period (n =16)

Table 5.51 Measured and layer method-predicted values of temperature at different depths of corn plots (n = 16). Values are means of three replicates (C1, C2, C3)

i	Time	0.05		0.1		0.2		0.3	
	t_i	T_m	T_p	T_m	T_p	T_m	T_p	T_m	T_p
1	0	17.7	17.0	18.3	19.1	18.3	19.8	18.0	19.4
2	3	16.7	14.4	17.7	17.0	18.2	19.1	18.1	19.2
3	6	15.8	14.5	17.1	16.1	18.0	18.3	18.1	19.0
4	9	15.4	17.2	16.7	16.8	17.7	17.9	18.0	18.7
5	12	17.2	20.9	16.9	18.8	17.5	18.2	17.9	18.6
6	15	19.5	23.5	18.0	20.9	17.6	18.9	17.8	18.7
7	18	19.9	23.5	18.6	21.9	18.0	19.6	17.9	19.0
8	21	18.9	20.8	18.6	21.2	18.2	20.0	18.0	19.2

Tm: Measured temperature ^{0}C; T_p: Predicted temperature ^{0}C

Table 5.52 Statistical parameters for comparing measured and layer method-predicted values of temperature at different depths of corn plots (n =16)

x, cm	R^2	R^2_{adj}	σ	*ESS*	*RSS*	*TSS*	*F*	F_{table} (1,6)	
								α=0,01	α=0,05
5	0.706	0.657	0.9806	13.8690	5.7700	19.6390	14.42>	13.75	5.99
10	0.628	0.566	0.5019	2.5473	1.5115	4.0587	10.11	13.75	5.99
20	0.533	0.455	0.2230	0.3404	0.2984	0.6388	6.84	13.75	5.99
30	0.307	0.191	0.0931	0.0230	0.0520	0.0750	2.65<	13.75	5.99

x: Depth, R^2: Determination coefficient, R^2_{adj}: Adjusted R^2, σ: Root Mean Squared Error, *ESS*: Estimate sum of square, *RSS*: Residual sum of squares, *TSS*: Total sum of square, *F*: Fisher Criteria

Table 5.53 Measured and point 1 method-predicted values of temperature at different depths of corn plots (n = 16). Values are means of three replicates (C1, C2, C3).

i	Time	0.05		0.1		0.2		0.3	
	t_i	T_m	T_p	T_m	T_p	T_m	T_p	T_m	T_p
1	0	17.7	19.1	18.3	20.0	18.3	19.0	18.0	18.9
2	3	16.7	16.8	17.7	19.2	18.2	19.1	18.1	19.0
3	6	15.8	15.8	17.1	18.3	18.0	19.1	18.1	19.0
4	9	15.4	16.7	16.7	17.8	17.7	19.1	18.0	19.0
5	12	17.2	18.9	16.9	18.0	17.5	18.9	17.9	19.0
6	15	19.5	21.1	18.0	18.7	17.6	18.8	17.8	19.0
7	18	19.9	22.1	18.6	19.7	18.0	18.8	17.9	19.0
8	21	18.9	21.3	18.6	20.2	18.2	18.9	18.0	19.0

Tm: Measured temperature ^{0}C; T_p: Predicted temperature ^{0}C

Table 5.54 Statistical parameters for comparing measured and point1 method-predicted values of temperature at different depths of corn plots (n =16)

x, *cm*	R^2	R^2_{adj}	σ	*ESS*	*RSS*	*TSS*	*F*	F_{table} (1,6)	
								α=0,01	α=0,05
5	0.933	0.922	0.4687	18.3210	1.3180	19.6390	83,41>	13.75	5.99
10	0.887	0.868	0.2763	3.6008	0.4579	4.0587	47,18>	13.75	5.99
20	0.087	0.000	0.3118	0.0556	0.5832	0.6388	0,57<	13.75	5.99
30	0.001	0.000	0.1113	0.0007	0.0743	0.0750	0,06<	13.75	5.99

x: Depth, R^2: Determination coefficient, R^2_{adj}: Adjusted R^2, σ: Root Mean Squared Error, *ESS*: Estimate sum of square, *RSS*: Residual sum of squares, *TSS*: Total sum of square, *F*: Fisher Criteria

Table 5.55 Measured and point 2 method-predicted values of temperature at different depths of corn plots (*N*=16). Values are means of three replicates (C1, C2, C3)

i	Time	0.05		0.1		0.2		0.3	
	t_i	T_m	T_p	T_m	T_p	T_m	T_p	T_m	T_p
1	0	17.7	19.3	18.3	19.9	18.3	19.0	18.0	18.9
2	3	16.7	17.1	17.7	19.3	18.2	19.1	18.1	18.9
3	6	15.8	16.0	17.1	18.5	18.0	19.1	18.1	19.0
4	9	15.4	16.7	16.7	17.9	17.7	19.1	18.0	19.0
5	12	17.2	18.7	16.9	18.0	17.5	19.0	17.9	19.0
6	15	19.5	20.9	18.0	18.6	17.6	18.9	17.8	19.0
7	18	19.9	21.9	18.6	19.5	18.0	18.8	17.9	19.0
8	21	18.9	21.3	18.6	20.0	18.2	18.9	18.0	19.0

Tm: Measured temperature ^{0}C; T_p: Predicted temperature ^{0}C

Table 5.56 Statistical parameters for comparing measured and point 2 method-predicted values of temperature at different depths of corn plots (*N* =16)

x, cm	R^2	R^2_{adj}	σ	*ESS*	*RSS*	*TSS*	*F*	F_{table} (1,6)	
								α=0,01	α=0,05
5	0.943	0.933	0.4338	18.5100	1.1290	19.6390	98.38>	13.75	5.99
10	0.821	0.791	0.3483	3.3308	0.7280	4.0587	27,45>	13.75	5.99
20	0.000	0.000	0.3263	0.0002	0.6386	0.6387	0<	13.75	5.99
30	0.020	0.067	0.1000	0.01500	0.0600	0.0750	1,50<	13.75	5.99

x: Depth R^2: Determination coefficient, R^2_{adj}: Adjusted R^2, σ: Root Mean Squared Error, *ESS*: Estimate sum of square, *RSS*: Residual sum of squares, *TSS*: Total sum of square, *F*: Fisher Criteria

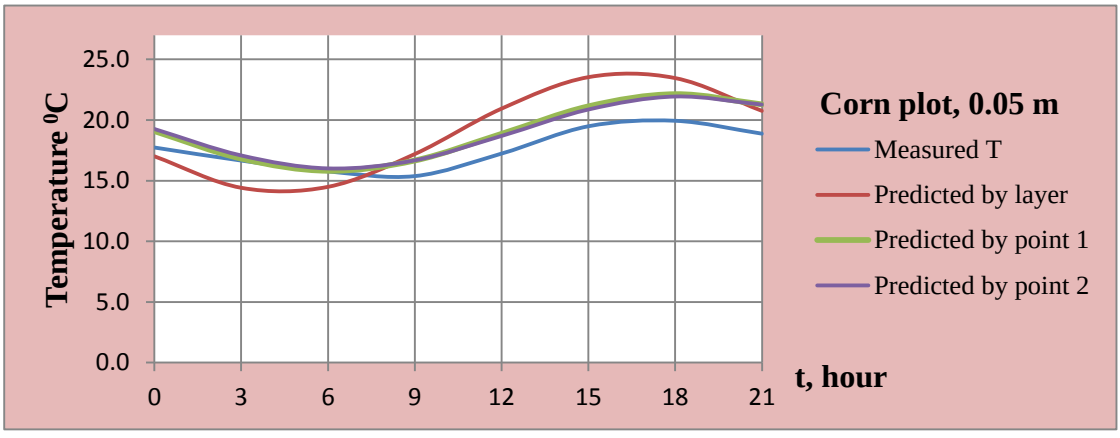

Figure 5.47 Mean measured vs predicted hourly temperature values at 0.05 m depth of corn plots during the study period (*n* =16)

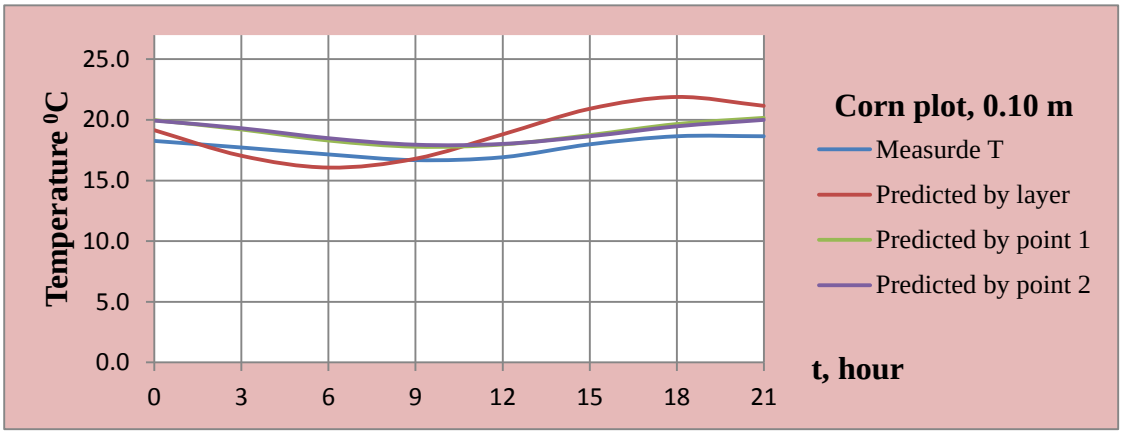

Figure 5.48 Mean measured vs predicted hourly temperature values at 0.1 m depth of corn plots during the study period (*n* =16)

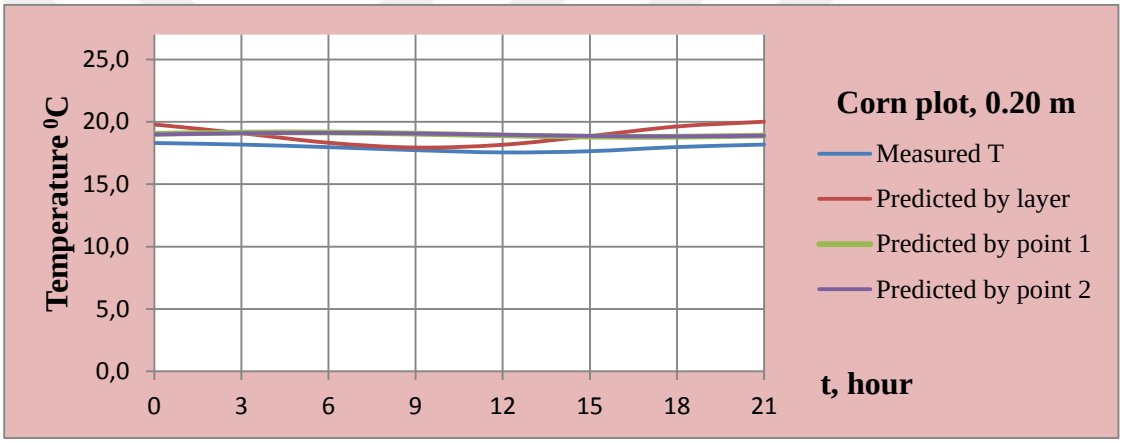

Figure 5.49 Mean measured vs predicted hourly temperature values at 0.2 m depth of corn plots during the study period (*n* =16)

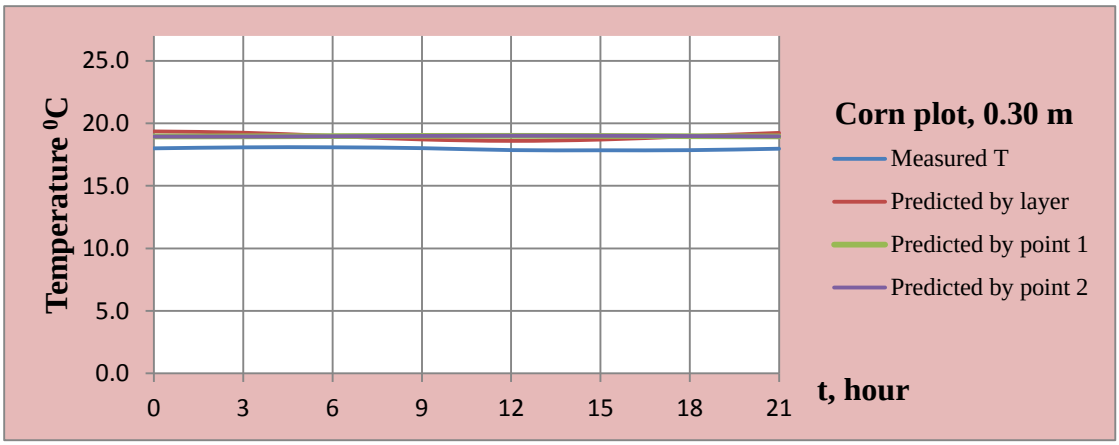

Figure 5.50 Mean measured vs predicted hourly temperature values at 0.3 m depth of corn plots during the study period (*n* =16)

6. DISCUSSION AND CONCLUSIONS

Soil thermal properties directly affect soil productivity. Soil thermal properties are influenced by soil texture, soil bulk density, soil organic matter content, and soil water content. Time of planting and harvesting are directly controlled to soil thermal properties. Soil thermal properties differ under different plant covers. In this study, soil thermal properties were modeled under different plant covers using three different models and the results were compared with measured values. In this regard, the specific targets were: 1. Determining aerodynamics of soil surface temperature differences under different crop canopies and discuss the likely reasons behind those differences, 2. Modeling the soil temperature and heat flow diffusivity at different soil depths under different plant canopies, and 3) Comparing the performance of different methods to model heat diffusivity and soil temperature at different depths under different crop canopies.

Plants are expected to influence the soil thermal properties by two major means: 1. they control the partitioning of the solar radiation reaching to earth surface, 2. they affect dynamics of heat flow from surface to soil, and 3. they control heat flow in soils indirectly, altering the soil structure, affecting soil water content, and altering the soil water flow. Most of the models developed for predicting soil thermal properties have been based on bare soil conditions as predicting soil thermal properties under plant cover requires accounting to additional factors that complicates the modeling process. In this study, we modeled heat flow under sugar beet and corn canopies and compared the results to those found under bare soil conditions.

The soils of the experimental site are clay loam (*CL*). These soils are young alluvial soils with low organic matter content. Horizon boundaries of the soils are faint with slightly wavy structure. Mean value of particle density is 2.62 gr/cm^3, bulk density is 1.33 gr/cm^3, and porosity is % 49.203. The specific surface area of the soils is 65.4 m^{2}g^{-1}, which is typical for a loam. Soil specific area differs depending on clay mineralogy and soil texture (Filgueira *et al.* 2006).

In this study, greatest soil surface air temperature occurred under sugar beet canopy, followed by bare soil and corn canopy. This was attributed to heavy and dense canopy of sugar beet that worked as an insulator for temperature on the soil surface, decreasing convective heat loss by wind and latent heat loss by evaporation. On the other hand, relatively light corn canopy and bare soil surface allowed wind flow that resulted in heat loss by convection and by evaporation from the soil surface. In addition, vertical distribution of light in corn canopy resulted in less light reaches to the soil surface, resulted in slightly cooler air at soil-air interface. Our results were consistent with those found by others (Grupta *et al.* 1982, Kowsar *et al.* 1966, Baver 1966 ve Streck *et al*. 1996). These researchers evaluated soil thermal properties under different mulches.

Soils under plant cover heat slower and cool slower. The soil thermal diffusivity is highly different under different plant covers. One of the main aims of this study was determine these differences under corn and sugar beet crops by modeling heat diffusivity and soil temperature at predetermined depths. The methodology of monitoring soil temperature and water content and modeling approach used in this study made it possible to evaluate effect of these crops on soil thermal properties during an entire growing season and compare the results with those found in bare soil conditions.

Measured and predicted values of air temperature at soil surface of control, sugar beet, and corn plots were highly similar as indicated by strong correlation coefficients (η = 0.96, 0.89, and 0.91 for control, sugar beet and corn plots, respectively). Amplitudes of temperature on the soil surface were 12.7 for sugar beet, 11.94 for control and 8.32 ^{o}C for corn, suggesting that corn plots warmed and cooled more slowly than control and sugar beet plots. Our results were consistent with those reported by Streck (1996) and Gülser and Ekberli (2004). This difference between corn and sugar beet plots was attributed to differences in plant canopies that controlled the vertical distribution of light in the canopy and heat loss from the soil during heating and cooling times.

Greatest coefficient of heat diffusivity (κ) calculated by point2 method (as point2 method outperformed point1 and layer methods we considered its predictions in comparison) occurred in sugar beet ($1.9718.10^{-7}$ m^2/s) followed by control ($1.7667.10^{-7}$

m^2/s) and corn ($1.4303.10^{-7}$ m^2/s) plots, respectively. Interestingly this rank of κ was identical to the rank of temperature amplitude for sugar beet, control, and corn plots. This difference in κ would be attributed to differences in soil water content, soil water flow, and soil structure caused by plant root system and differences in soil bulk density resulted from growth of plant roots and tubers. Our calculated κ values for control plot agreed to those calculated by Gao *et al.* (2008), who calculated κ at 0.05, 0.1, 0.2, and 0.4 m depths of a bare loam and a clay and to those calculated by Otunla and Oladiran (2006), who calculated κ at 0.05 and 0.1 m soil depths between 3 and 12 June, 2005.

In this study, we modeled soil temperature and κ using three different methods, namely layer method, point1 method, and point2 method. The layer method poorly described soil temperature and even some cases it failed. Contrary to layer method, the point1 and point2 methods successfully predicted the temperature in studied soil depths. The on the other hand, the point2 method outperformed point1 method in majority of the cases.

Performance of all the methods used in this study decreased in depth. Beyond 10 cm, the model's performance decreased sharply, which was attributed to the dumping depth. The damping depth (*d*) is an important factor determining the depth where temperature amplitude is effective. Beyond *d* the amplitude may not help to predict temperature change. In our soils, the *d* occurred at 12.44 cm for control, 12.03 cm corn, and 10.86 cm for sugar beet plots (Table 5.37). This explains why the modeling success decreased sharply at 0.2 and 0.3 m soil depths irrespective to soil surface conditions. Similar conclusions were made elsewhere (Andrade and Abreu 2002). Our results are consistent with those reported by Yılmaz (2008) and Şımarmaz (2010). In addition, our values for *d* agreed to those reported by De vries (1963) and Gülser and Ekberli (2004).

Several models have been developed to model soil thermal properties. Each of these models has their unique assumptions set by model developers. Therefore, the model structure and assumptions made should be considered carefully before employing these models for predicting the thermal properties (Yeşilsoy 1975, Hadas 1977, De Vries and Philip 1986, Nassar *et al*. 1992). Most of the models developed for predicting soil thermal properties are based the solutions derived from Cartesian and cylindrical

coordinate system. All these models are layer models, which use the initial conditions of $T(\infty,t)=T_0$. In this study, we used three models to predict κ. All three models have been developed based on Cartesian coordinate system.

Soil water content may have a decisive effect on heat flow and storage in soils. Lipiec *et al.* (2007) reported that the soil heat conductivity (λ) was generally greater under cultivated soils compared to grasslands in moist soils, while reverse was true in drier soils. Plants may affect soil heat flow, partitioning of solar radiation on the soil surface and water status of soils. Al-Kayssı *et al.* (1990) reported that increased θ resulted in decreased soil temperature differences between day-time and night-time. They further reported that increased θ resulted in an increased absorbed solar energy.

Plant covers have highly complicated effects on soil thermal properties due to multiple interactions among soil properties, plants, and soil thermal properties. Usowicz *et al.* (1996) studied spatial variability of soil thermal properties by classical statistics and geostatistics. Their results indicated a clear spatial relation between soil water content, bulk density, and spatial variability of soil thermal properties. The spatial relation was different for different soil properties depending on θ. For individual crops, spatial autocorrelation of soil thermal properties was related to soil water content. At water contents close to or higher than field capacity, this range decreased considerably, becoming more similar to the spatial autocorrelation range of soil bulk density (Usowicz *et al.* 1996)

Plant cover type and its spatial orientation can affect soil thermal properties. Usowicz *et al.* (2001) reported that soil moisture on particular cultivated fields showed that type and growth stage of vegetation and meteorological conditions (mainly frequency and amount of rainfall, as well as sunshine duration over a given period) were key factors affecting soil thermal properties in the studied fields. In addition, they also reported that difference in soil moisture between examined fields were influenced by variation in intercepted amount of precipitation and in amount of evaporation from soil surface and transpiration by plants.

Soil physical properties such as bulk density may have a control on soil thermal properties. Usowicz *et al.* (2001) found that the soil compaction had both direct and indirect effect on soil heat flow, increasing the contact points of particles in the former and influencing vigor of plant cover on soil surface in the later.

The soil tillage and cropping systems may influence soil thermal properties, while this effect may be different over the different periods in the growing season. Dalmago *et al.* (2004) compared soil temperature in corn-cropped no-tillage and conventional tillage systems. They reported that at the beginning of plant growth, the highest soil temperatures occurred in the conventional system in all soil layers. However, after 30 days from emergence, the highest temperatures occurred in the no-tillage system, and variations between the cropping systems decreased after the plants covered the soil surface. Rahimi *et al.* (2013) modeled κ in soil with different texture and θ. Their results showed initially increased then decreased behavior of κ against increasing θ, which were consistent with our findings.

Conclusions

We modeled soil temperature and thermal diffusivity (κ) in a clay loam during a growing season under sugar beet, corn, and bare soil conditions by three modeling approaches, namely layer, point 1 and point 2 methods. The following principal points were derived from the study.

1. Mean air temperature at soil surface was greatest under sugar beet and lowest under corn crop during entire of growing season. This was attributed to dense cover of the sugar beet that worked as insulator for temperature on the soil surface. On the other hand, relatively light corn canopy allowed wind flow that resulted in heat loss from the soil surface by convection. In addition, vertical distribution light in the corn canopy resulted in lower amount of solar radiation to reach on the soil surface.

2. Difference between measured and predicted temperature is greatest in sugar beet and lowest in corn plots. This variation in difference decreased by depth and by soil surface coverage of plants.

3. The point methods (point 1 and point 2 methods) outperformed the layer method in all the cases. The layer method over predicted the soil temperature in all depths under all the soil surface conditions. Point 1 and point 2 methods made more reasonable predications and their predications were consistent in majority of the cases. This success of the point methods were attributed to the initial conditions on soil surface that they employ. The layer method uses the initial conditions T(∞, t)=0, while the point methods use initial conditions $\partial \mathrm{T}(L,t)/\partial x = 0$. In addition, the analytical solutions used in point methods better account to the heat flow dynamics in soils.

4. The sugar beet plot always had lower θ than control and corn plots during the entire experimentation. This resulted in a greater κ in sugar beet plot soils.

5. Irrespective to soil surface conditions, at all the plots, the model success decreased by depth. After dumping depth, the predication success of the models decreased sharply. The predications made by layer method were even worsened.

6. The instruments (*Maxim iButton sensors*) used in this study made it possible to collect multiple measurements of temperature at multiple soil depths during the entire growing season. However, some sensors became inactive after they are installed in soil. This resulted in that we had to drop some of the plots and evaluated the rest of them. This should be considered in further studies. Some advanced types of these and other sensors may be used to ensure their functionality during the study. For example, some of these sensors that can communicate to computers and/or cellular phones can be installed in the soil and their functionality can be checked from time to time.

REFERENCES

Abu-Hamdeh, N.H. 2000. Effect of tillage treatments on soil thermal conductivity for some jordanian clay loam and loam soils. Soil & Tillage Research 56, 145-151.

Abu-Hamdeh, N. H. 2001. Measurement of the Thermal Conductivity of Sandy Loam and Clay Loam Soils using Single and Dual Probes. Journal of Agricultural Engineering Research 80, 209-216.

Abu-Hamdeh, N. H. 2003. Thermal Properties of Soils as affected by Density and Water Content. Biosystems Engineering 86, 97-102.

Adeniyi, M., and Oshunsanya, S. 2012. Validation of analytical algorithms for the estimation of soil thermal properties using de Vries model. American Journal of Scientific and Industrial Research 3, 103-114.

Akaike, H. 1974. A New Look at the Statistical Model Identification. IEEE Transactions on Automatic Control 19:716–723.

Akkuş, A. 2000. Cumra Çevresinin Fiziki Coğrafyası ve İnsan Çevre İliskisi 1.Uluslararası Çatal Höyükten Günümüze Cumra Kongresi, . Cumra Belediyesi Kültür Hizmetleri Yayınları, Cumra.

Al-Kayssı, A. W., Al-Karaghouli, A. A., Hasson, A. M., and Beker, S. A. 1990. Influence of Soil Moisture Content on Soil Temperature and Heat Storage under Greenhouse Conditions. J. agric. Engng Res. The British Society for Research in Agricultural Engineering 45, 241-252.

Alzahal, O., Kebreab, E., France, J., and Mcbride, B. W. 2007. A Mathematical Approach to Predicting Biological Values from Ruminal Ph Measurements. . J. Dairy Sci., 90:3777–3785.

Analla, M. 1998. Model validation through the linear regression fit to actual versus predicted values. Agricultural Systems 57, 115–119.

Anonymous 2013. Turkish State Meteorological Service.

Anonymous 2014. T.C Cumra kaymakamlığı. İlçe Tarım, Gıda ve Hayvancılık Müdürlüğü Haziran 2014 Yılı Brifing Raporu.

Antinoro, C., Bagarello, V., Ferro, V., Giordano, G., and Iovino, M. 2012. Testing the shape-similarity hypothesis between particle-size distribution and water retention for Sicilian soils. Journal of Agricultural Engineering 43.

Andrade, J. Abreu, F. 2002. Modelling daily and annual cycles of temperature in two types of soil. Transactions of 17th World Congress of Soil Science – Soil Science: confronting new realities in the 21th century

Arkhangel'skaya, T. A. 2004. "A New Empirical Formula for Estimating Thermal Diffusivity of Soils," in Proceedings of the Scientific Session on Fundamental Soil Science,. Moscow, Russia, pp. 45–46.

Arkhangel'skaya, T. A., and Umarova, A. B. 2011. Thermal diffusivity and temperature regime of soils in large lysimeters of the experimental soil station of Moscow State University. Eurasian Soil Science 41, 276-285.

Arkhangelskaya, T. A. 2014. Diversity of thermal conditions within the paleocryogenic soil complexes of the East European Plain: The discussion of key factors and mathematical modeling. Geoderma 213, 608-616.

B.S. Sharratt, G.S. Campbell, and D.M. Glenn 1992. Soil heat flux estimation based on the finite difference form of the transient heat flow equation. Agricultural and Forest Meteorology, 61 95-111.

Baladi, J. Y., Ayers, D. L., and Schoenhals, R. J. 1980. Transient Heat And Mass Transfer In Soils. Heat Mass Transfer 24, 449-458.

Balghouthi, M., Kooli, S., Farhat, A., Daghari, H., and Belghith, A. 2005. Experimental investigation of thermal and moisture behaviors of wet and dry soils with buried capillary heating system. Solar Energy 79, 669-681.

Banke, O., and Drage, B. 1984. Bootstrap and Cross-Validation Estimates of the Prediction Error for Linear Regression Models. The Annals of Statistics, 12, pp. 1400-1424.

Banks, J., and Carson, J. S. 1984. "Discrete event system simulation," Prentice Hall,Englewood Cliffs, NJ.

Barik, K. 2002. Toprakların Isısal Özelliklerinin Matematik Model İle Belirlenmesi Atatürk Üniversitesi Ziraat Fakültesi

Baver, L. D., Gardne, W. H., and Gardner, W. R. 1972. "Soil Aeration. In Soil physics. 4th ed. John Wiley & Sons, New York, USA."

Bayraklı, F. 1993. S.Ü. Ziraat Fakültesi Ders Notları; "Toprak Bilgisi", Ziraat Fakültesi Toprak Bölümü Konya, 148 s.

Bayraklı, F., Ekberli, İ. A., and Cülser, C. 1999. Azerbaycan Mil Ovası topraklarının verimlilik düzeylerinin Deneysel ve Matematiksel Olarak Değerlendirilmesi. . OMÜ Zir.Fak. Dergisi, 14 (2): 138-153.

Berry, J., and Haouston, K. 1995. Mathematical modelling. Bistrol:. J. W. Arrowsmith Ltd.

Bilgili, M. 2010. The use of artificial neural networks for forecasting the monthly mean soil temperatures in Adana, Turkey. Turk J. Agric. For. 35:83-93.

Blake, G. R., and Hartge, K. H. 1986. "Bulk Density In: Methods of Soil Analysis, Part 1, Physical and Mineralogical Methods."

Bliemel, F. W. 1973. Theil's forecast accuracy coefficient: A clarification,. Journal of Marketing Research, 10, 444-446.

Bristow, K. L., G.S., C., and C, C. 1993. Test of a heat-pulse probe for measuring changes in soil water content. Soil Science Society of America Journal 57, 930-934.

Buchan, G. D. 1991. "Soil Temperature Regime. Soil Analysis: Physical Methods, 551-612; 133 ref. New York.."

Burham, K. P., and Anderson, D. R. 1998. Model Selection an Inference: A Practical Information Theoric Approach, . Springer-Verlag, New York.

Campbell, G., Jungbauer Jr, J., Bidlake, W., and Hungerford, R. 1994. Predicting the effect of temperature on soil thermal conductivity. Soil Science 158, 307-313.

Campbell, G. S., and Norman, J. M. 1998. "An Introduction to Environmental Biophysics."

Carmer, S., and Swanson, M. 1973. An evaluation of ten pairwise multiple comparison procedures by Monte Carlo methods. Journal of the American Statistical Association 68, 66 –74.

Carslaw, H. S., and Jaeger, J. C. 1959. Conduction of Heat İn Solids, 2nd Edn. Oxford: Clarendon Pres, 1959. – 486p.

Chapra, S. C., and Canale, R. P. 2010. "Numerical methods forengineers."

Chichua, G. S. 1965. Gürcistan Sovyet Sosyalist ana toprak tiplerinin Termal özellikleri. Dis. 53.

Chudnovsky, A. F. 1948. Toprakta ısının Fiziği. M.; JL: G.ostehizdat, 220

Chudnovsky, A. F. 1959. Toprakta ısı transferi. Temel agrophysics. M:. Fizmatgiz, 455-519.
Chudnovskii, A. F. 1967. ‘’Fundamentals of Agrophysics.’’ Israel Prog.for Sc. Translations, Jerusalem,166 p.
Chudnovskii, A. F. 1976. "Toprakların Isı Fiziği."
Chung, S. O., and Horton, R. 1987. Soil heat and water flow with a partial surface mulch,. Water Resour. Res., 2312, 2175-2186.
Clark, A. J. 1983. Temperature And Thermal Propertıes Of Selected Arızona Soıls The Unıversıty Of Arızona.
Costello, M. P., and Sit, V. 1994. Catalogue of Curves for Curve Fitting. Forest Science Research Branch, England.110s.
Crank, J. 1956. The Mathematics of Diffusion. Oxford University Press, New York.
Çelebi, E. 2001. Toprak Kolonlarında Sıcaklık Dağılımlarının Farklı Nem Düzeylerinde Araştırılması. Ç.Ü. Fen Bilimleri Enstitüsü, Toprak Anabilim Dalı, Yüksek Lisans Tezi, 76 sayfa, Adana yayınlanmamış.
Dalmago, G. A., Bergamaschi, H., Comiran, F., Bianchi, C. A. M., Bergonci, J. I., and Heckler, B. M. M. 2004. Soil Temperature In Maize Crops As Function Of Soil Tillage Systems. 13th International Soil Conservation Organisation Conference – Brisbane, Conserving Soil and Water for Society: Sharing Solutions 777.
Danelichen, V. H. M. 2013. Soil Thermal Diffusivity of a Gleyic Solonetz Soil Estimated by Different Methods in the Brazilian Pantanal. Open Journal of Soil Science 03, 15-22.
Davis, J. C. 1986. Statistics and Data Analysis in Geology, 2nd edn. Wiley, New York, 646 pp.
De Vries, D. A. 1952. The Thermal Condictivitu of Granular Materials. Bulletin de l’Institute International du Froid, Annexe,115.
De Vries, D. A. 1963. " Thermal properties of soils. in W.R. Van Wijk, ed Physics Of Plant Environment, Chap. 7. Amsterdam."
De Vries, D. A., and Philip, J. R. 1986. Soil Heat Flux, Thermal Conductivity and The Null Agliment Method. Soil Sci. Soc. Amer. J. 50
Dec, D., Dörner, J., and Horn, R. 2009. Effect Of Soil Management On Their Thermal Properties. R.C.Suelo Nutr. Veg. 9 1 J. Soil Sc. Plant Nutr. 9 1 26-39.
Dimo, V. N. K. 1948. ısı iletkenliği ve toprak nemi arasındaki ilişki sorusu. Toprak Bilimi. 10. C. 729-733 belgesinde №. 10. C. 729-733. Rusca.
Draper, N. R., and Smith, H. 1966. Applied Regression Analysis,. John Wiley & Sons, Inc., New York.
Droulia, F., Lykoudis, S., Tsiros, I., Alvertos, N., Akylas, E., and Garofalakis, I. 2009. Ground temperature estimations using simplified analytical and semi-empirical approaches. Solar Energy 83, 211-219.
Duarte, A. P. L., De Campos, T. M. P., Arauna, J. T., and Filho, P. R. 2007. Thermal Properties for Unsaturated Soils. 4th International Conference on Unsaturated Soils, n.147, p. 1707-1718.
Ebbler, D. H. 1975. On the Probability of Correct Model Selecting Using the Maximum R-Square Choıce Criterion,. International Economic Review, 16-2, pp.516-520.
Edwards, J. T., Ford, N. J., and Roberts, J. A. 2003. Bifurcations in numerical methods for Volterra integro-differential equations. Department of Mathematics, Chester College, Parkgate Road, Chester, CH1 4BJ, UK; members of the Manchester Centre for Computational Mathematics.

Efe, E., Bek, Y., and Şahin, M. 2000. SPSS'te Çözümleri İle İstatistik Yöntemler II. Kahramanmaraş Sütçü İmam Üniversitesi Rektörlüğü Yayınları, Kahramanmaraş. 223 s.

Ekberli, İ., Gülser, C., Korkmaz, A., Özdemir, N., Aşkın, T., and Mikayilsoy, F. 2002. Su Havzalarında Toprak ve Su Kaynaklarının Korunması, Geliştirilmesi ve Yönetimi Sempozyumu. Toprak Oluşum Enerjisinin Teorik İncelenmesi. M. K. Ü. Ziraat Fak. Hatay. s. 489-494.

Ekberli, İ., Gülser, C., and Özdemir, N. 2005. Toprakların Termo-Fiziksel Özellikleri ve Isısal Yayınım Katsayısının Değerlendirilmesi. O. M. Ü Ziraat Fak. Toprak Bölümü. O. M. Ü Zir. Fak. Dergisi 20 2: 85-91, Samsun.

Ekberli, İ. 2006. Isı İletkenlik Denkleminin Çözümüne Bağlı Olarak Topraktaki Isı Taşınımına Etki Yapan Bazı Parametrelerin İncelenmesi. O. M. Ü Ziraat Fak. Toprak Bölümü. O. M. Ü Zir. Fak. Dergisi 21 2: 179-189, Samsun.

Ekberli, İ. 2008. Sistemli Yaklaşimla Ekosistemin Analizinde Matematiksel Modelleme Yöntemi. OMÜ Zir. Fak. Dergisi, J. of Fac. of Agric., OMU 233:170-182.

Ekberli, İ., and Sarılar, Y. 2014. Investigating soil temperature variability and thermal diffusivity in grass cowered and shaded areas by trees. Kazakh Journal of Soil Science Special. th 9 International Soil Science Congress on "The Soul of Soil and Civilization" Side, Antalya, Turkey 4.

Ekwue, E. I., Stone, R. J., and Bhagwat, D. 2011. Thermal Conductivities of Some Common Soils in Trinidad. The West Indian Journal of Engineering Vol.33, Nos.1/2, January 2011, pp.4-11.

Fadeev, D. K., and Fadeeva, V. N. 1963. Computational Methods ofLinear Algebra, Freeman, San Francisco, 621 p.

Filgueira, R. R., Pachepsky, Y. A., Fournier, L. L., Sarli, G. O., and Aragon, A. 1999. Comparison of fractal dimensions estimated from aggregate mass–size distribution and water retention scaling. Soil Sci. 164, 217– 223.

Filgueira, R. R., Soracco, C. G., Sarli, G., and Fournier, L. L. 2006. "Estimation of soil hydraulic properties by field measurement and use of steady -and transient-flow models."

Fırat, B. 1998. Bitki Nasıl Beslenir. Atlas Kitapevi, Konya 292.

Fisher, R. A. 1949. The Design of Experiments. . Edinburgh: Oliver & Boyd.

Fragkogiannis, G., Apostolopoulos, S., and Stamataki, S. 2010. Correlation of Thermal conductivity and electrical resistivity of soil, for near surface geothermal applications. In "72nd EAGE Conference & Exhibition incorporating SPE EUROPEC 2010. Barcelona, Spain, 14 - 17 June ".

Fritsch GmbH 2004. Manufacturers of Laboratory Instruments, User Guide Laser Particle Sizer "analysette 22".

García-Suárez, A. M., and Butler, C. J. 2006. Soil temperatures at Armagh observatory, northern Ireland, from190 to 2002. International Journal of Climatology, 26: 1075-1089.

Gasvoda, D. S., Tinus, R. W., and Burr, K. E. 2003. Monitor Tree Seedling Temperature Inexpensively With the Thermochron iButtonae Data Logger. Tree Planters' Notes 501: 14-17.

Gemant, A. 1950. The Thermal Conductivity of Soils. Jour. App. Physics, 2: 750-752.

Gerayzade, A. P. 1982. Toprak Sistemlerinde Sıcaklık ve Nem Taşınımı. Baku, Elim, 157 s. Rusça.

Gerayzade, A. P. 1989. Toprak Bitki Atmosfer Sisteminde Enerji Döngüsü. Baku. Elim, 158 s. Rusça.

Ghuman, B. S., and Lal, R. 1985. Thermal Conductivity, Thermal Diffusivity and Thermal Capacity of some Nigerian Soils. Soil Science, 139 1: 74-80.

Giakoumakis, S. G., and Tsakiris, G. P. 1991. Eliminating the effect of temperature from unsaturated soil hydraulic functions. Journal hydrology Elsevier Science Publishers B.V., Amsterdam 129, 109-125.

Gönen, N. 1978. Toprakların Islanma Isıları Üzerinde Bir Araştırma. Ankara Üniversitesi Basımevi.

Gupta, S. C., J. K. Radke, W. E. Larson, and M. J. Shaffer. 1982. Predicting temperatures of bare- and residue-covered soils from daily maximum and minimum air temperatures. Soil Sci. Soc. Am. J. 46:372-376.

Gujarati, D. 2003. "Basic Econometrics,"

Gülser, Ç., and Ekberli, İ. 2004. A Comparison of Estimated and Measured Diurnal Soil Temperature Through a Clay Soil Depht. Journal of applied Sciences, 4 3:418-423.

Hadas, A., and Fucs, M. 1973. Prediction of the Thermal Regime of Bare Soils in Physical Aspects of Soil Water and salt in Ecosystems. Spriger - Verlag.

Hadas, A. 1977. Evaloation of theoretically predited thermal conductivites of soils under field and laboratory conditions. Soil Sci. Soc.Amer. J., 41, 460 - 465.Haitovski, Y. 1969. A note on the maximization of R 2 , . 20-21. Am. Statist., 231.

Halıcı, F. 2001. "Örneklerle Isı Geçişi. Sakarya, 448 s."

Hamamoto, S., Dissanayaka, S., Kawamoto, K., and Komatsu, T. 2010. Effects of Moisture Content and Shrinkage on Soil-Thermal Properties for Peat Soils. International Conference on Sustainable Built Environment ICSBE Kandy.

Hanmam, E. J., and Quinn, B. G. 1979. The Determination of the Order of an Auturegression,. Jounal of the Royal Statistical Society, 41, pp. 190-195.

Hanson, J. L., Edil, T. B., and Yesiller, N. 2000. Thermal Properties of High Water Content Materials. Geotechnics of High Water Content Materials, ASTM STP 1374, T. B. Edil and P. J. Fox, Eds., American Society for Testing and Materials, West Conshohocken, PA.

Hartman, C. A., and Oring, L. W. 2006. An inexpensive method for remotely monitoring nest activity. J. Field Ornithol. 77, 418–424.

Hillel, D. 1980. Fundamentals of Soil Physics. Academic Press, New York. London.

Hillel, D. 1982. "Introduction to soil physics,," New York. London.

Hjorth, J. S. 1994. Computer Intensive Statistical Methods Validation Model Selection and Boostrap, . New York: Champman & Hall.

Horton, R. J. 1982. Determination and Use Of Soil Thermal Properties Near The Soil Surface. New Mexico Satate University, 151 p.

Horton, R., and Wieranga, P. J. 1983. Estimating the Soil Heat Flux From Observations of Soil Temperature Near The Surface Soil Sci. Soc. Amer. J. 47, 14 - 20.

Horton, R., Aquire-Luna, O., and Wierenga, P. J. 1984. Soil Temperature in a Row Crop with Incomplete Surface Cover. Soil Sci. Soc. Am. J. 48, 1225-1232.

Hubbart, J., Link, T., Campbell, C., and Cobos, D. 2005. Evaluation of a low-cost temperature measurement system for environmental applications. Hydrological Processes 19, 1517-1523.

Issmer, K. 2000. Optical methods in grain-size analiysis of fine-grained sediments. Geological Quarterly 44 2, 205-210.
Juri, W. A., Gardner, W. R., and Gardner, W. H. 1991. "Soil Physics."
Kakaç, S. 1998. "Örneklerle Isı Transferi. Ankara, 358 s."
Kanamaru, H., and Kanamitsu, M. 2008. Model Diagnosis of Nighttime Minimum Temperature Warming during Summer due to Irrigation in the California Central Valley. Journal of Hydrometeorology 9, 1061-1072.
Kemp, P. R., Cornelius, J. M., and F., R. J. 1992. A Simple Model For Predicting Soil Temperatures İn Desert Ecosystems, Soil Sci. 153: 280- 287.
Kertsen, M. S. 1949. "Thermal Properties of Soils. Bulletin 28. University of Minesone Agricultural Experimental Station."
Kim, D. H., Young Jin Kim, Jong-Sub Lee, and Tae Sup Yun 2011. Thermal and Electrical Response of Unsaturated Hydrophilic and Hydrophobic Granular Materials. Geotechnical Testing Journal, Vol. 34, No. 5 Paper ID GTJ103601.
Kırda, C., and Sarıyev, A. 2002. "Toprak Fiziği, Ç.Ü. Ziraat Fak. Genel Yayın No: 245, Ders Kitabı, Adana,188 s."
Kirhan, D., and Powers, W. L. 1972. "Advanced Soil Physics ".
Kluıtenberg, G. J., and Horton, R. 1990. Analytical Solution For Two Dimensional Heat Conduction Beneath A Partial Surface Mulch.
Kohnke, H., and Nakshabandi, G. A. 1964. Heat Transfer İn Soils. 8th Internetional Congres of Soil Sci. 2, 185-195.
Konert, M., and Vandenberghe, J. 1997. Comparison of laser grain size analysis with pipette and sieve analysis: a solution for the underestimation of the clay fraction Sedimentology 1, 523–535.
Koorevaar, P., Bolt, G. H., and Kamphorst, A. 1975. Basic Elements of Soil Physics. Agricultural University Wageningen.
Koorevaar, P., Menelik, G., and Dirksen, C. 1983. Elements of Soil Physics, Elsevier, Amsterdam. Oxsford.
Kowsar, A., Boersma, L., and Jarman, G. P. 1966. Effect of Petroleum Mulch On Soil Water Content And Soil. Sci. Soc. Am. Proc., 783-786.
Krarti, M., Lopez-Alonzo, C., Claridge, D. E., and Kreider, J. F. 1995. Analytical Model to Predict Annual Soil Surface Temperature Variation. Journal of Solar Energy Engineering 117, 91-99.
Krishnan, A., and Kushwaha, R. S. 1972. Analysis Of Soil Temperatures In The Arid Zone Of India By Fourier Techniques. Agricultural Meteorology 10, 55-64.
Kurtener, D. A., and Chudnovskii, A. F. 1979. Agrometeorological Basics of the Thermal Amelioration of Soils Gidrometeoizdat, Leningrad, Russian.
Lesh, R., and Doerr, H. M. 2003. " Foundations of a models and modeling perspective on mathematics teaching, learning, and problem solving.," pp. 3-33. Mahwah, NJ: Lawrence Erlbaum.
Licht, M. A., and Al-Kaisi, M. 2005. Strip-tillage effect on seedbed soil temperature and other soil physical properties. Soil and Tillage Research 80, 233-249.
Lipiec, J., Usowicz, B., and Ferrero, A. 2007. Impact of soil compaction and wetness on thermal properties of sloping vineyard soil. International Journal of Heat and Mass Transfer 50, 3837-3847.
Liu, B. C., Liu, W., and Peng, S. W. 2005. Study of heat and moisture transfer in soil with a dry surface layer. International Journal of Heat and Mass Transfer 48, 4579-4589.

Lovegrove, B. G. 2009. Modification and miniaturization of Thermochron iButtons for surgical implantation into small animals. J. Compar.Physl. B 179, 451–458.
Lowry, W. P. 1970. Weather and Life Academic Press, New York and London.
Lyman Ott, R., and Longnecker, M. 2001. "An Introduction to Statistical Methods and Data Analysis fifty Edition."
Mallows, C. L. 1973. Some Comments on Cp,. Technometrics, 15, pp. 661-675.
Mallows, C. L. 1995. More Comments on Cp,. Technometrics, 37, pp. 362-372.
Mamedov, R. G. 1989. Azerbaycan SSR topraklarının agrofiziksel özellikleri. Bakü, Elm, 244s.s.172-192, Rusça.
Marinova, T. K. 1993. On Determining the Conductivity Coefficient of the Basic Soils in Bulgaria. . Bulgarian Journal of Meteorology & Hydrology No 2 pp. 65-69.
Matthews, M. D. 1991. "The effect of pretreatment on size analysis. ," Cambridge University Press, 34–42.
Maxim-Integrated 2013. DS1921G Thermochron iButton Device. 160 Rio Robles, San Jose, CA 95134 USA 1-408-601-1000.
Mc Lean, E. O. 1982. İn Methods of Soil Analysis, Part 2, Agron. 9, AL. Page, RH. Miller, & D.R. Keeney Eds, Am. Soc. Agron., Madison, WI, pp. 199-224
McCave, I. N., Bryant, R. J., Cook, H. F., and Coughanowr, C. A. 1986. Evaluation of a laser-diffraction-size analyzer for use with natural sediments. J. Sediment. Petrol.,56:561–564.
McQuarrie, A. D., and Tsai, C. L. 1998.. Regression and Time Series Model Selection,. World Sciencetific.
Mihalakakou, G., Santamouris, M., Lewis, J. O., and Asimakopoulos, D. N. 1997. On the Application of The Energy Balance Equation to Predict The Ground Temperature Profiles. Solar Energy 60, 3/4, p: 181-190.
Mihalakakou, G. 2002. . On Estimating Soil Surface Temperature Profiles. Energy and Buildings 34, p: 251-259.
Mikayilov, F. D. 2007. Determination of Salt Transport Model Parameters for Leaching of Saturated Superficially Salted Soils. Eur. Soil Sci., 40 5, 644–654.
Mikaiylov, F. D., and Shein, E. V. 2008. Modeling and Prediction of Soil Temperature Regime in Proc. of the First All_Russia Conf. Fundamental Achievements in Soil Science, Ecology, and Agriculture on the Way to Innovations , pp. 38–45 Moskova, Russian.
Mikayilov, F. D. 2009a. About one solution of the equation of heat conductivity in soil. . InternationalConference on ‘The fifth scientific readings J.P. Bulashevicha. Deep structure.Geodynamics. Thermal field of the Earth. Interpretation of geophysical fields’.Scientific publications, pp. 319–323, Yekaterinburg, Russia Rusça.
Mikayilov, F. D. 2009b. Some Problems of Modeling the Temperature Regime of Soil. Proc. Int. Conf. “16th Winter School on Mechanics of Continuous Systems” Perm, 2009, Russian.
Mikayilov, F. D., and Shein, E. V. 2010. Theoretical principles of experimental methods for determining the thermal diffusivity of soils. Eurasian Soil Science 43, 556-564.
Mikailsoy, F. D. 2014. Modelling Of Some Soil Processes 2014.7.117.c. In "Вестник Алтайского государственного аграрного университета № 7 117, 2014", Vol. 7, pp. 59-64. Bulletin of the Altai State Agrarian University.Mirzadzhanzade, A.

H., and Shirinzade, S. A. 1986. "Improving the efficiency and quality of drilling deep wells ", Moskow.

Moerz, T., and Wolf-Welling, T. C. W. 2001. "Data report: Fine-fraction grain-size distribution data and their statistical treatment and relation to processes, Site 1095 ODP Leg 178, western Antarctic Peninsula.". Institute for Geosciences, Christian- Albrechts University Kiel, Olshausenstrasse 40, 24118 Kiel, Federal Republic of Germany.Federal Republic of Germany., GEOMAR Research Center for Marine Geoscience, Wischhofstrasse 1-3, C4, 24148 Kiel, Federal Republic of Germany.

Nabyev, Y. Y., and Guseınov, S. B. 1990. The Dependance of Soil Temperature Conductıvıtyon The Physical Clay Content and Moisture. Rusya Academy of Sciences, Soils 8.

Nabyev, E. Y. 1992. Variation of Thermal Conductivity of Soils With Low Moisture. Rassian Academy of Sciences, Pochvovedenie 2.

Nakshabandi, G. A., and Kohnke, H. 1965. Thermal Conductivity And Diffusivity Of Soils As Related To Moisture Tension And Other Physical Properties. Axricultural Meteorology - Elsevier Publishing Company 271-279.

Nassar, I. N., and Horton, R. 1990. Determination of Soil Apparent Thermal Diffusivity from Multiharmonic Temperature Analysis for Nonuniform Soils. Soil Science, 1493: 125-130.

Nassar, I. N., R., H., and Globus, A. M. 1992. Simultaneus Transfer of Heat and Solute in Porous Media: II. Experiment and Analysis. Sofi Sci. Soc. Amer. J. 56, 1357 – 1365.

Nowamooz, H., Nikoosokhan, S., Lin, J., and Chazallon, C. 2015. Finite difference modeling of heat distribution in multilayer soils with time-spatial hydrothermal properties. Renewable Energy 76, 7-15.

Otunla T. A., Oladiran E. O. 2013 Evaluation of soil thermal diffusivity algorithms at two equatorial sites in West Africa. Annals Of Geophysıcs, 56, 1, 2013, R0101; doi:10.4401/ag-6170

Ozgener, O., Ozgener, L., and Tester, J. W. 2013. A practical approach to predict soil temperature variations for geothermal ground heat exchangers applications. International Journal of Heat and Mass Transfer 62, 473-480.

Özbek, H. 1990. "Toprak Bilgisi. Çukurova Üniversitesi Ziraat Fakültesi Ders Kitabı No:34. Adana."

Özkan, İ. 1985. "Toprak Fiziği. Ankara Üniversitesi Ziraat Fakültesi Yayınları. Yayın No: 946, Ders Kitabı: 270, Ankara."

Özturk, M., Salman, Ö., and Koc, M. 2011. Artificial neural network model for estimating the soil temperature. Can. J. Soil. Sci. 91 551-562.

Pachepskii, Y. A. 1990. Mathematical Models of Physicochemical Processes in Soils, Nauka, Moscow, [in Russian].

Page, A. L., Miller, R. H., and Kccney, D. K. 1982. "Mellıods of SoiJ Analysis. Part 2. Chemical and Mierobiologieal Propenies."

Patten, H. E. 1909. Heat Transterence in Soils. Bulletin 59. United States Departmant of Agriculture Bureaus of soils.

Pearson, K. 1895. Notes on regressionand inheritance in the case of two parents//Proceedings of the Royal Societyof London, 58: 240–242.

Platonov, V. A., and Çudnovski, A. F. 1984. Modelirovaniye agrometeorologiceskix usloviy i optimizaçiya agrotexniki ASU TP v zemledelii. Leningrad, Girdometeoizdat, p. 280.

Potter, K. N., Cruse, R. M., and Horton, R. 1985. Tillage Effects on Soil Thermal Properties Soil Sci. Soc. Am. J. 49, 968-973.

Poulovassilis, A., Kerkides, P., Alexandris, S., and Rizos, S. 1998. A contribution to the study of the water and energy balances of an irrigated soil profile A. Heat flux estimates. Soil & Tillage Research 45, 189–198.

Raftery, A. E. 1995. Bayesian Model Selection in Social Researchwith Discussion by Andrew Gelman, Donald B. Rubin and Robert M. Hauser. In P.V. Marsdn Ed.,. Socialogical Methodology, pp. 111-196.

Rahimi, H., Younes Khoshkhoo, Khalili, A., and Irannejad, P. 2010. Application of numerical method in the estimation of soil thermal diffusivity and soil temperature prediction under different textures and moisture contents. Academic Journals. African Journal of Agricultural ResearchVol. 846, pp. 5764-5770, 27 november, 2013.

Rao, R. C. 1973. "Linear Statistical Inference and its Applications."

Rhoades, J. D., Shouse, P. J., Alves, W. J., Manteghi, N. A., and Lesch, S. M. 1990. . Determining soil salinity from soil electrical conductivity using different models and estimates. Soil Sci. Soc. Am. J. 54:46-54.

Robert, K. A., and Thompson, M. B. 2003. Reconstructing Thermochron iButtons to reduce size and weight as a new technique in the study of small animal thermal biology. . Herpetol. Rev. 34, 130–132.

Rollins, R. L., Spangler, M. G., and Kirkham, D. 1954. Movement of soil moisture under a thermal gradient. Proceedings of the Highway Res.Board. 33, 492–508.

Rose, C. W. 1979. Agricultural Physics. Pergaman Prees. New York, 230 p.

Roznik, E. A., and Alford, R. A. 2012. Does waterproofing Thermochron iButton dataloggers influence temperature readings? Journal of Thermal Biology 37, 260-264.

Ruan, S. 2006. Delay Differential Equations and Applications. In "Delay Dıfferentıal Equatıons in Sıngle Species Dynamics" O. A. e. al., ed.. Springer, Berlin, pp.477-517., Research was partially supported by NSF grant DMS-0412047 and a Small Grant Award from the University of Miami.

Rubio, C. M. 2011. Influence of the Hysteretic Behaviour on Silt Loam Soil Thermal Properties. Open Journal of Soil Science 01, 77-85.

Rycheva, T. A. 1994 . Temperature Conductivity of a Sod-Podzolic Soil: Moisture Movement Influence. The Russian Academy Of Sciences; Soils 8, 53-57.

Saatçı, F. 1975. “Toprak İlmi”. Ege Üniversitesi Ziraat Fakültesi Yayınları No:214 , Ege Üniversitesi Matbaası Bornova-İzmir, s. 303.

Saho, J. 1993. Linear Model Selection by Cross-Validation Journal of the American Assosiational, Vol. 88.

Sarıyev, A. L., Aydın, M., Polat, V., and Tuli, A. 1995. Toprak Rutubet Karakteristik Eğrisi ve Toprak-Kök Sistemine Su Akımının Matematiksel Modellenmesi , Ç. Ü. Z. F. Dergisi, 25. Kuruluş Yılı Özel Sayısı, Adana. Sayfa 257-268.

Sarıyev, L. A., and Gülüt, K. 1995. Agroekosistemde Bitki Gelişiminin Matematiksel Modelleri ve Bunların Temel Prensipleri. Ç.Ü. Ziraat Fakültesi Dergisi, 10, 4 : 61-66 s. Adana.

Sarıyev, A., Aydın, C., and Yusufova, M. 1998. Destekli Termoelementlerle Ölçülmesi ve Toprakta Sıcaklık Rejiminin Matematiksel Modellenmesi. M. Şefik Yeşilsoy, International Symposium on Arid Region Soils, 336-344.

Schwarz, G. 1978. Estimating the Dimensions of a Model,. The Annals of Statistical, 6, pp.461-464.

Seber, G. A. F. 1977. Linear Regression Analysis,. John Wıley & Sons, New York.

Seemann, J. 1979. Measurement Technology, Agrometeorology. Springer-Verlag, Berlin, 40-45.

Shein, E., Guber, A., and Dembovetsky, A. 2004. Key soil water contents. 30, 241-249.

Shein, E. V. 2005. A Course of Soil Physics In "Izd. Mosk. Gos. Univ., Moscow, Russian".

Shein, E. V., and Goncharov, V. M. 2006. Agrophysics Feniks, Rostov on Don [in Russian].

Shein, E. V. 2007. Toprak Fiziği Teorisi ve Metotları. Moskova, 616 s. Smith, W. O., and Byers, H. G. 1938. The Thermal Conductivity of Certain of The Great soil Groups. Soil Sci. Soc. Am. Proc., 3, pp. 13-19.

Smits, K. M., Sakaki, T., Limsuwat, A., and Illangasekare, T. H. 2009. Determination of the thermal conductivity of sands under varying moisture, drainage/wetting, and porosity conditions- applications in near-surface soil moisture distribution analysis. Center for Experimental Study of Subsurface Environmental Processes CESEP, Environmental Science and Engineering Division, Colorado School of Mines, Golden, CO, 80401, U.S.A.

Steduto, P. 2000. Determination Methods of Crop Water Consumption. ln: Kırda, C., Steduto, P. eds. Soil Water Balance and Transport Processes, Review of Theory and Field Applications. Cahiers Options Mediterraneennes 46: 1 -25.

Streck N.A., Schneider F.M., Buriol G.A. 1996.Soil Heating By Solarization Inside Plastic Greenhouse in Santa Maria, Rio Grande do Sul, Brazil Agricultural and Forest Meteorology 82, 73-82

Şımarmaz, A. 2010. Arazi Koşullarında Toprağın Isısal Özelliklerinin Araştırılması ve Matematiksel Modellemesi, Selçuk Üniversitesi Fen Bilimleri Enstitüsü.

Şirinov, N. A. 1967. Azerbaycan SSC ana toprak tipleri termal parametrelerinin deneysel olarak belirlenmesi. Yazar. cand. Dis. Tbilisi, 16, s.

Taylor, S. A., and Ashcroft, G. L. 1972. Physical Edaphology: The Physics of Irrigated and Nonirrigated Soils. W.H. Freeman and Company, San Franscisco.

Tedeschi, O. L., Fox, G. D., Saintz, D. R., Barioni, G. L., Medeiros, R. S., and Boin, C. 2005. Mathematical Models in Ruminant Nutrition. Scielo Agricalture, Brazil. 76-91.

Tenge, A. J., Kagihura, F. B. S., Lal, R., and Singh, B. R. 1998. Diurnal soil temperature fluctuations for different erosion classes of an oxisol at Mlingano, Tanzania. Soil and Tillage Research, 49, 211-217.

Theil, H. 1958. "Economic Forecasts and Policy,."

Theil, H. 1966. "Applied Economic Forecasting,."

Tikhonov, A. N., and Samarskiy, A. A. 1966. "Mathematical Physics Equation."

Tikhoravova, P. I. 1991. Heat-Physıcal Properties Of Soıls Complex Evaluatıon Of The Trans-Volga Solonetzıc. rusya bilimler akademisi topraklar 5, 56-61.

Tikhonravova, P. I., and Khitrov, N. B. 2003. Estimation of Thermal Conductivity in Vertisols of the Central Ciscaucasus Region. Russian Academy of Sciences SOILS 3, 342-351.

Ucal, M. Ş. 2006. Ekonometrik model seçim kriterleri üzerine kısa bir inceleme. C.Ü. İktisadi ve İdari Bilimler Dergisi, Cilt 7, Sayı 2.

Usowicz, B., Kossowski, J., and Baranowski, P. 1996. Spatial variability of soil thermal properties in cultivated fields. Soil & Tillage Research 39, 85- 100.

Usowicz., B., Kossowski, J., Hurtalova, T., and Matejka, F. 2001. Soil Moisture And Thermal Properties State Under Plant Crops. Acta Agrophysica 53, 189–200.

Usowicz, B., Lipiec, J., and Ferrero, A. 2006. Prediction of soil thermal conductivity based on penetration resistance and water content or air-filled porosity. International Journal of Heat and Mass Transfer 49, 5010-5017.

Usowicz, B., Lipiec, J., Usowicz, J. B., and Marczewski, W. 2013a. Effects of aggregate size on soil thermal conductivity: Comparison of Measured and model-predicted data. International Journal of Heat and Mass Transfer 57, 536-541.

Usowicz, B., Łukowski, M., Marczewski, W., Usowicz, J. B., Lipiec, J., and Stankiewicz, K. 2013b. Thermal properties of peat, marshy and mineral soils in relation to soil moisture status in Polesie and Biebrza wetlands. Geophysical Research Abstracts Vol. 15, EGU2013-8534.

Vaasma, T. 2010. Grain-Sıze Analysis of Lake Sediments: Research Methods and Applications.

Valipour, M., Mousavi, S. M., Valipour, R., and Rezaei, E. 2012. SHCP: Soil Heat Calculator Program. IOSR Journal of Applied Physics IOSR-JAP 2, 44-50.

Van Wijk, W. R., and De Vries, D. A. 1966. Periodic Temperature Variations İn a Homogeneous Soil "Physics of Plant Enviroment" Edit. W. R., Van Wijk, North- Holland Publ. Com. Amsterdam, 102-143.

Verhoef, A. 2004. Remote estimation of thermal inertia and soil heat flux for bare soil. Agricultural and Forest Meteorology 123, 221-236.

Wainwright, J., and Mulligan, M. 2004. "Environmental Modelling. Finding Simplicity in Complexity."

Wang, Z.-H., and Bou-Zeid, E. 2012. A novel approach for the estimation of soil ground heat flux. Agricultural and Forest Meteorology 154–155, 214-221.

Weasserman, L. 2000. Bayesian Model selection and Model averaging,. Jounal of Mathematical Psychology, 44, 92-107.

Willmott, C. 1981. On the validation of models. . Physical Geography 2: 184–194.

Willmott, C. 1982. Some comments on the evaluation of model performance. Bulletin of the American Meteorological Society 63:1309–1313.

Willmott, C., and Wicks, D. 1980. An empirical method for the spatial interpolation of monthly precipitation within California. . Physical Geography 1: 59–73.

Willmott, C., Ackleson, S., Davis, R., Feddema, J., Klink, K., Legates, D., O'Donnell, J., and Rowe, C. 1985. Statistics for the evaluation of model performance. . Journal of Geophysical Research 90C5: 8995–9005.

Willmott, C. J., and Matsuura, K. 2005. Advantages of the mean absolute error MAE over the root mean square error RMSE in assessing average model performance. Climate Research 30, No. 1, 79-92.

Yeşilsoy, M. Ş. 1975. Toprakların Isısal İletkenliğinin Özelliklerine Dayanarak Hesaplanması. Tübitak 5. Bilim Kongresi, Toprak-Bitki Besleme Seksiyonu, İzmir. 379- 391.

Yeşilsoy, M. Ş., and Aydın, M. 1995. "Toprak Fiziği."

Yılmaz, Ö. 2008. Toprak Kolonlarında Isısal Özelliklerin Belirlenmesi ve Modellenmesi.

Zangmeister, J. L., Haussmann, M. F., Cerchiara, J., and Mauck, R. A. 2009. Incubation failure and nest abandonment by Leach's storm-petrels detected using PIT tags and temperature loggers. J. Field Ornithol. 80, 373–379.

Zaslavskiy, B. G., and Poluektov, R. A. 1988. Upravleniye Ekologiçeskimi Sistemami. Moskow, Nauka.

Zhou, X., Persaud, N., Belesky, D. P., and Clark, R. B. 2007. Significance of Transients in Soil Temperature Series. Pedosphere 17, 766-775.

Zucchini, W. 2000. An Introduction to Model Selection,. Journal of Mathematical Psychology, 44, pp.41-61.

Appendices

Appendix 1. Measured (T_0, T_a) and calculated (ω) parameters and corresponding goodness of fit parameters calculated for plot S1 for 16 weeks of study period

		The parameters of the soil surface			**Statistical parameters for goodness of fit**							
Weeks	**Date**	T_0	T_a	ε	η	R^2	R^2_{adj}	D	$c=\eta D$	UI	HQC	$*F$
1	06.06.2013	20.75	12.6459	1.9733	0.9532	0.9086	0.8721	0.9755	0.9298	0.0625	2.6336	24.86
2	21.06.2013	22.62	12.2044	1.7283	0.9327	0.8699	0.8179	0.9643	0.8994	0.0686	2.9593	16.72
3	24.06.2013	32.06	17.2312	1.8631	0.8240	0.6790	0.5506	0.8984	0.7403	0.1204	4.8003	5.29
4	02.07.2013	25.06	17.8302	1.8931	0.8877	0.7880	0.7033	0.9382	0.8328	0.1150	4.3046	9.29
5	09.07.2013	27.69	16.2120	1.8700	0.8815	0.7770	0.6879	0.9344	0.8237	0.1014	4.1789	8.71
6	15.07.2013	19.62	2.8481	1.6770	0.8233	0.6778	0.5489	0.8945	0.7364	0.0352	1.2058	5.26
7	23.01.2013	24.56	15.8482	1.9899	0.8895	0.7912	0.7077	0.9392	0.8355	0.1054	4.0496	9.48
8	14.08.2013	26.44	15.5161	1.9658	0.8862	0.7853	0.6995	0.9374	0.8307	0.0992	4.0426	9.15
9	20.08.2013	23.00	14.1604	1.9078	0.9213	0.8487	0.7882	0.9575	0.8821	0.0837	3.4320	14.03
10	27.08.2013	24.25	15.7263	1.8933	0.9040	0.8172	0.7441	0.9476	0.8567	0.0976	3.8688	11.18
11	04.09.2013	18.81	18.1871	1.9364	0.8774	0.7699	0.6779	0.9322	0.8179	0.1507	4.4495	8.37
12	10.09.2013	21.75	18.1347	1.9479	0.8753	0.7661	0.6726	0.9310	0.8149	0.1376	4.4649	8.19
13	25.09.2013	18.50	13.7865	1.9835	0.8724	0.7610	0.6654	0.9285	0.8100	0.1285	3.9450	7.96
14	01.10.2013	6.19	3.2064	2.1055	0.7987	0.6379	0.4930	0.8811	0.7037	0.1275	1.6200	4.40
15	08.10.2013	11.94	13.7095	2.0237	0.9091	0.8264	0.7570	0.9506	0.8642	0.1416	3.5317	11.90
16	22.10.2013	12.19	17.6229	2.2070	0.9063	0.8213	0.7499	0.9490	0.8600	0.1623	4.0688	11.49

T_0: Average Temperature of Soil Surface, T_a: Wave Amplitude, ε: Phase Angle. η: Correlation coefficient, R^2: Determination coefficient, R^2_{adj}: Adjusted R^2, *D:* Agreement index, *c*: The confidence index, *UI:* Theil's Forecast Accuracy Coefficient, *HQC*; Hannan-Quinn Criteria, *F:* Fisher Criteri.
*α=0,01 for **F_{tabl}=13.27** α=0,05 for **F_{tabl}=5.79**

Appendix 2. Measured (T_0, T_a) and calculated (ω) parameters and corresponding goodness of fit parameters calculated for plot S2 for 16 weeks of study period

		The parameters of the soil surface			Statistical parameters for goodness of fit							
Weeks	**Date**	T_0	T_a	ε	η	R^2	R^2_{adj}	D	$c=\eta D$	UI	HQC	$*F$
1	06.06.2013	20.812	15.9842	2.8337	0.8581	0.7363	0.6308	0.9199	0.7893	0.1400	4.3722	6.98
2	21.06.2013	19.56	11.4479	2.3285	0.9630	0.9275	0.8984	0.9809	0.9446	0.0533	2.1833	31.96
3	24.06.2013	27.94	22.3624	2.3967	0.9443	0.8917	0.8484	0.9706	0.9166	0.0852	3.9623	20.59
4	02.07.2013	19.50	10.6443	2.4684	0.9455	0.8939	0.8515	0.9713	0.9183	0.0618	2.4548	21.06
5	09.07.2013	25.25	14.6289	2.5638	0.9734	0.9474	0.9264	0.9863	0.9601	0.0446	2.3300	45.07
6	15.07.2013	25.19	11.0311	2.7818	0.9395	0.8826	0.8357	0.9678	0.9093	0.0538	2.6398	18.80
7	23.01.2013	20.50	11.1995	2.3233	0.9599	0.9214	0.8900	0.9792	0.9399	0.0525	2.2257	29.32
8	14.08.2013	23.50	13.4111	2.2782	0.9230	0.8519	0.7927	0.9586	0.8848	0.0775	3.2985	14.38
9	20.08.2013	21.75	11.5197	2.3332	0.9336	0.8716	0.8203	0.9646	0.9005	0.0670	2.8287	16.97
10	27.08.2013	20.62	10.2932	2.2213	0.9695	0.9399	0.9159	0.9843	0.9543	0.0420	1.7682	39.13
11	04.09.2013	17.94	7.3458	2.6479	0.8996	0.8093	0.7330	0.9444	0.8495	0.0672	2.3990	10.61
12	10.09.2013	16.62	10.4235	2.4261	0.9458	0.8945	0.8522	0.9714	0.9187	0.0693	2.4069	21.19
13	25.09.2013	18.50	16.4513	2.4949	0.9451	0.8932	0.8505	0.9711	0.9178	0.0913	3.3327	20.91
14	01.10.2013	20.75	14.4821	2.6037	0.9274	0.8600	0.8040	0.9610	0.8912	0.0886	3.3865	15.36
15	08.10.2013	9.62	14.1862	2.5462	0.9429	0.8891	0.8448	0.9699	0.9146	0.1254	3.0786	20.05
16	22.10.2013	9.62	16.6522	2.5642	0.9257	0.8569	0.7997	0.9602	0.8888	0.1544	3.6911	14.97

T_0: Mean temperature at soil surface, T_a: Wave amplitude, ε: Phase angle, η: Correlation coefficient, R^2: Coefficient of determination, R^2_{adj}: Adjusted R^2 *D:* Agreement index, *c*: The confidence index, *UI:* Theil's forecast accuracy coefficient, *HQC*; Hannan-Quinn criteria, *F:* Fisher criteria
*α=0,01 for $\mathbf{F_{table}=13.27}$ α=0,05 for $\mathbf{F_{table}=5.79}$

Appendix 3. Measured (T_0, T_a) and calculated (ω) parameters and corresponding goodness of fit parameters calculated for plot S3 for 16 weeks of study period

		The parameters of the soil surface			**Statistical parameters for goodness of fit**							
Weeks	**Date**	T_0	T_a	ε	η	R^2	R^2_{adj}	D	$c=\eta D$	UI	HQC	$*F$
1	06.06.2013	20.06	11.3082	1.7606	0.9484	0.8994	0.8592	0.9728	0.9226	0.0617	2.5164	22.35
2	21.06.2013	22.00	16.3251	3.9401	0.9564	0.9147	0.8805	0.9772	0.9346	0.0706	3.0695	26.79
3	24.06.2013	27.06	18.0173	3.9568	0.9618	0.9250	0.8951	0.9802	0.9427	0.0604	3.1257	30.85
4	02.07.2013	19.44	9.3685	1.7184	0.8971	0.8048	0.7267	0.9433	0.8463	0.0789	2.9139	10.31
5	09.07.2013	23.69	13.6847	1.9649	0.9512	0.9047	0.8666	0.9743	0.9268	0.0611	2.8376	23.74
6	15.07.2013	22.62	8.1072	1.9413	0.9507	0.9038	0.8654	0.9741	0.9261	0.0400	1.8008	23.50
7	23.07.2013	18.75	6.5098	2.1059	0.9559	0.9138	0.8793	0.9772	0.9342	0.0366	1.2415	26.51
8	14.08.2013	25.50	18.0916	2.1450	0.9141	0.8355	0.7697	0.9537	0.8717	0.0985	4.0217	12.70
9	20.08.2013	23.06	16.3535	2.1203	0.8636	0.7459	0.6442	0.9232	0.7973	0.1286	4.3681	7.34
10	27.08.2013	20.94	9.6616	2.1154	0.9523	0.9069	0.8697	0.9752	0.9287	0.0496	2.1159	24.35
11	04.09.2013	15.44	5.9089	2.1568	0.9516	0.9056	0.8678	0.9749	0.9277	0.0421	1.1478	23.98
12	10.09.2013	15.94	7.7685	2.1491	0.9793	0.9590	0.9426	0.9895	0.9690	0.0337	0.8040	58.46
13	25.09.2013	14.44	9.3735	2.1850	0.9684	0.9379	0.9131	0.9838	0.9528	0.0535	1.6169	37.75
14	01.10.2013	16.06	4.7201	2.4877	0.7944	0.6311	0.4835	0.8777	0.6972	0.0773	2.4228	4.28
15	08.10.2013	7.75	8.6005	2.2586	0.9384	0.8806	0.8328	0.9674	0.9078	0.1122	2.1616	18.44
16	22.10.2013	7.19	7.7401	2.1572	0.9519	0.9061	0.8685	0.9748	0.9279	0.0966	1.6818	24.13

T_0: Mean temperature at soil surface, T_a: Wave amplitude, ε: Phase angle, η: Correlation coefficient, R^2: Coefficient of determination, R^2_{adj}: Adjusted R^2 D: Agreement index, c: The confidence index, UI: Theil's forecast accuracy coefficient, HQC; Hannan-Quinn criteria, F: Fisher criteria
*α=0,01 for $\mathbf{F_{table}=13.27}$ α=0,05 for $\mathbf{F_{table}=5.79}$

Appendix 4. Measured (T_0, T_a) and calculated (ω) parameters and corresponding goodness of fit parameters calculated for plot C1 for 16 weeks of study period

		The parameters of the soil surface			Statistical parameters for goodness of fit							
Weeks	**Date**	T_0	T_a	ε	η	R^2	R^2_{adj}	**D**	**C=ηD**	***U*1**	***HQC***	****F***
1	06.06.2013	20.19	10.4670	2.6027	0.8874	0.7875	0.7025	0.9368	0.8314	0.0887	3.2423	9.27
2	21.06.2013	21.44	12.7880	2.5951	0.8792	0.7730	0.6822	0.9325	0.8198	0.1042	3.7276	8.51
3	24.06.2013	25.25	17.3447	2.6084	0.9400	0.8835	0.8369	0.9681	0.9100	0.0788	3.5363	18.96
4	02.07.2013	18.56	6.4167	2.3999	0.9417	0.8868	0.8415	0.9692	0.9127	0.0423	1.5153	19.58
5	09.07.2013	23.50	10.7962	2.4217	0.9161	0.8393	0.7750	0.9545	0.8745	0.0673	2.9613	13.06
6	15.07.2013	24.62	8.4437	3.0105	0.7453	0.5555	0.3777	0.8350	0.6223	0.1042	3.8998	3.12
7	23.07.2013	20.37	8.5280	2.5862	0.8578	0.7358	0.6301	0.9188	0.7881	0.0844	3.1185	6.96
8	14.08.2013	22.31	9.4249	2.5170	0.9431	0.8895	0.8452	0.9699	0.9147	0.0503	2.2574	20.12
9	20.08.2013	20.87	9.5523	2.4527	0.9279	0.8611	0.8055	0.9614	0.8922	0.0616	2.5453	15.49
10	27.08.2013	20.00	7.1025	2.3541	0.9688	0.9385	0.9139	0.9839	0.9532	0.0311	1.0512	38.16
11	04.09.2013	18.12	5.7801	2.7303	0.8572	0.7348	0.6287	0.9175	0.7865	0.0658	2.3458	6.93
12	10.09.2013	15.75	8.6029	2.3665	0.9618	0.9251	0.8952	0.9802	0.9428	0.0511	1.6460	30.89
13	25.09.2013	16.19	10.7815	2.4539	0.9511	0.9047	0.8665	0.9743	0.9267	0.0688	2.3616	23.72
14	01.10.2013	18.62	8.9434	2.5517	0.9326	0.8697	0.8176	0.9639	0.8989	0.0620	2.3396	16.68
15	08.10.2013	7.19	9.1890	2.4863	0.9686	0.9383	0.9136	0.9838	0.9530	0.0854	1.5706	38.00
16	22.10.2013	7.06	10.2881	2.5418	0.9351	0.8744	0.8241	0.9654	0.9027	0.1336	2.5778	17.40

T_0: Mean temperature at soil surface, T_a: Wave amplitude, ε: Phase angle, η: Correlation coefficient, R^2: Coefficient of determination, R^2_{adj}: Adjusted R^2 *D:* Agreement index, *c*: The confidence index, *UI:* Theil's forecast accuracy coefficient, *HQC*; Hannan-Quinn criteria, *F:* Fisher criteria
*α=0,01 for $\mathbf{F_{table}=13.27}$ α=0,05 for $\mathbf{F_{table}=5.79}$

Appendix 5. Measured (T_0, T_a) and calculated (ω) parameters and corresponding goodness of fit parameters calculated for plot C2 for 16 weeks of study period

		The parameters of the soil surface			Statistical parameters for goodness of fit							
Weeks	**Date**	T_0	T_a	ε	η	R^2	R^2_{adj}	D	C=ηD	$U1$	HQC	*F
1	06.06.2013	19.37	9.2299	2.8571	0.7672	0.5887	0.4241	0.8555	0.6564	0.1311	3.9424	3.58
2	21.06.2013	20.19	10.6564	2.4893	0.9138	0.8350	0.7691	0.9533	0.8711	0.0772	2.9664	12.66
3	24.06.2013	25.69	16.1893	2.5554	0.9122	0.8321	0.7649	0.9523	0.8687	0.0907	3.8243	12.39
4	02.07.2013	18.94	7.6529	2.4992	0.8553	0.7316	0.6242	0.9172	0.7845	0.0826	2.9234	6.81
5	09.07.2013	21.25	7.7060	2.3582	0.9549	0.9118	0.8766	0.9764	0.9324	0.0386	1.6037	25.86
6	15.07.2013	21.81	3.6936	2.8982	0.8769	0.7689	0.6765	0.9310	0.8164	0.0326	1.2668	8.32
7	23.07.2013	18.62	7.4200	2.2649	0.9831	0.9664	0.9530	0.9914	0.9746	0.0252	0.5041	71.98
8	14.08.2013	21.56	8.1580	2.4347	0.9611	0.9236	0.8931	0.9798	0.9416	0.0371	1.5611	30.24
9	20.08.2013	18.75	5.4210	2.3168	0.9640	0.9292	0.9009	0.9813	0.9460	0.0276	0.6613	32.83
10	27.08.2013	19.44	5.8436	2.3536	0.9800	0.9604	0.9446	0.9898	0.9700	0.0211	0.1973	60.68
11	04.09.2013	16.94	4.1837	2.7213	0.8985	0.8074	0.7303	0.9437	0.8479	0.0419	1.2854	10.48
12	10.09.2013	15.31	7.1957	2.4308	0.9681	0.9373	0.9122	0.9836	0.9522	0.0407	1.0982	37.37
13	25.09.2013	14.94	7.0895	2.3811	0.9577	0.9171	0.8839	0.9779	0.9365	0.0477	1.3696	27.66
14	01.10.2013	16.56	5.0435	2.4688	0.9032	0.8158	0.7421	0.9467	0.8551	0.0499	1.6040	11.07
15	08.10.2013	7.69	6.2928	2.4042	0.9569	0.9157	0.8820	0.9775	0.9355	0.0755	1.1488	27.17
16	22.10.2013	7.56	6.0942	2.3707	0.9629	0.9272	0.8981	0.9808	0.9444	0.0690	0.9258	31.85

T_0: Mean temperature at soil surface, T_a: Wave amplitude, ε: Phase angle, η: Correlation coefficient, R^2: Coefficient of determination, R^2_{adj}: Adjusted R^2 *D:* Agreement index, *c*: The confidence index, *UI:* Theil's forecast accuracy coefficient, *HQC*; Hannan-Quinn criteria, *F:* Fisher criteria
*α=0,01 for $\mathbf{F_{table}=13.27}$ α=0,05 for $\mathbf{F_{table}=5.79}$

Appendix 6. Measured (T_0, T_a) and calculated (ω) parameters and corresponding goodness of fit parameters calculated for plot C3 for 16 weeks of study period

		The parameters of the soil surface			**Statistical parameters for goodness of fit**							
Weeks	**Date**	T_0	T_a	ε	η	R^2	R^2_{adj}	**D**	**C=ηD**	***U*1**	***HQC***	****F***
1	06.06.2013	22.06	16.2713	2.9223	0.8790	0.7726	0.6816	0.9326	0.8198	0.1235	4.2117	8.49
2	21.06.2013	19.81	8.9990	2.2775	0.9886	0.9773	0.9682	0.9942	0.9829	0.0233	0.4898	107.41
3	24.06.2013	23.31	11.6141	2.3517	0.9865	0.9731	0.9623	0.9931	0.9797	0.0276	1.1724	90.40
4	02.07.2013	21.00	6.3503	2.4201	0.9376	0.8790	0.8307	0.9669	0.9065	0.0387	1.5696	18.17
5	09.07.2013	23.44	6.2583	2.3879	0.9497	0.9018	0.8626	0.9735	0.9245	0.0306	1.3059	22.97
6	15.07.2013	26.62	9.1322	2.4451	0.9180	0.8427	0.7797	0.9557	0.8773	0.0508	2.6013	13.39
7	23.07.2013	20.69	6.6758	2.3617	0.9636	0.9286	0.9001	0.9811	0.9455	0.0308	1.0873	32.52
8	14.08.2013	21.19	6.6386	2.2896	0.9762	0.9531	0.9343	0.9879	0.9644	0.0240	0.6309	50.76
9	20.08.2013	20.00	5.6757	2.3003	0.9770	0.9545	0.9363	0.9882	0.9655	0.0215	0.2856	52.40
10	27.08.2013	20.69	7.6728	2.3264	0.9775	0.9555	0.9376	0.9885	0.9662	0.0274	0.8657	53.62
11	04.09.2013	17.62	3.8558	2.6465	0.8274	0.6845	0.5584	0.8971	0.7422	0.0518	1.7804	5.43
12	10.09.2013	15.69	7.0645	2.2936	0.9739	0.9485	0.9279	0.9866	0.9609	0.0353	0.8527	46.05
13	25.09.2013	15.62	8.0760	2.4200	0.9343	0.8729	0.8221	0.9649	0.9015	0.0652	2.1068	17.17
14	01.10.2013	18.69	7.5268	2.5074	0.9409	0.8853	0.8394	0.9686	0.9114	0.0492	1.8493	19.30
15	08.10.2013	7.50	7.0143	2.3636	0.9612	0.9239	0.8935	0.9798	0.9418	0.0786	1.2546	30.37
16	22.10.2013	7.12	8.1440	2.4367	0.9485	0.8997	0.8596	0.9730	0.9229	0.1038	1.8565	22.43

T_0: Mean temperature at soil surface, T_a: Wave amplitude, ε: Phase angle, η: Correlation coefficient, R^2: Coefficient of determination, R^2_{adj}: Adjusted R^2 *D:* Agreement index, *c*: The confidence index, *UI:* Theil's forecast accuracy coefficient, *HQC*; Hannan-Quinn criteria, *F:* Fisher criteria
*α=0,01 for $\mathbf{F_{table}=13.27}$ α=0,05 for $\mathbf{F_{table}=5.79}$

Appendix 7. Diurnal changes of measured (T_m) and predicted (T_p) values obtained for sugar beet plots (S1, S2, S3) on selected days in growing season

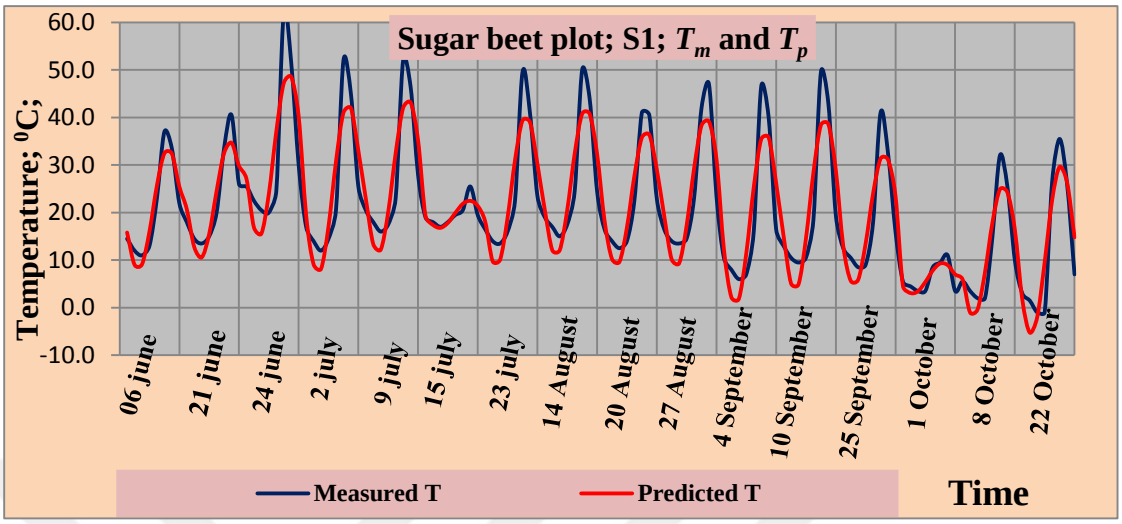

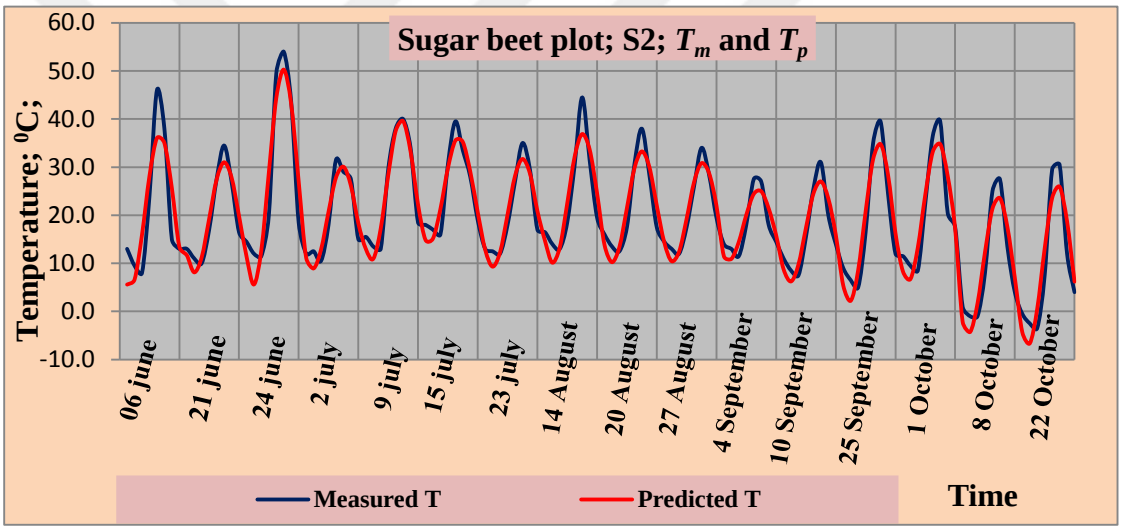

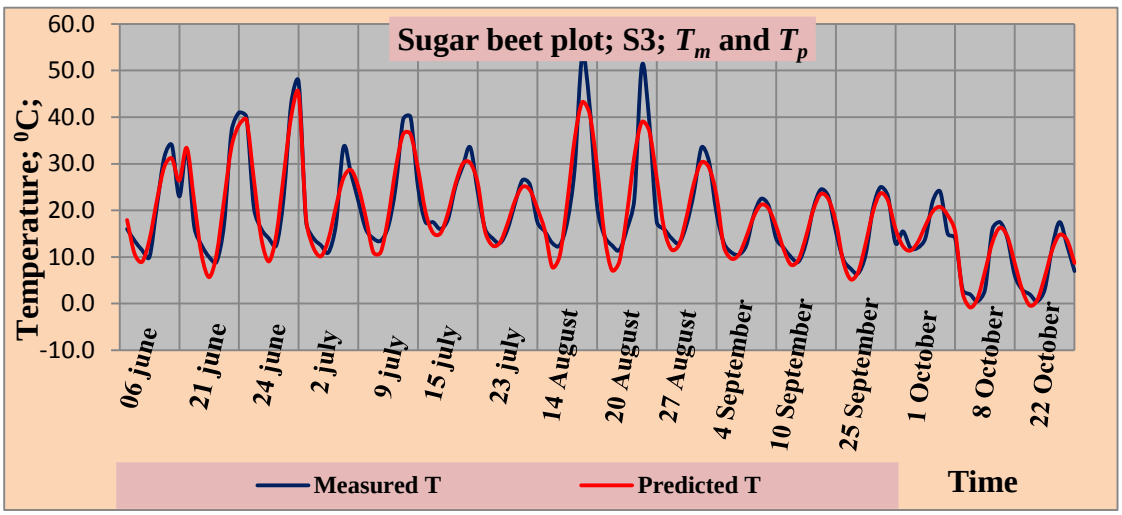

Appendix 8. Diurnal changes of measured (T_m) and predicted (T_p) values obtained for corn plots (C1, C2, C3) on selected days in growing season

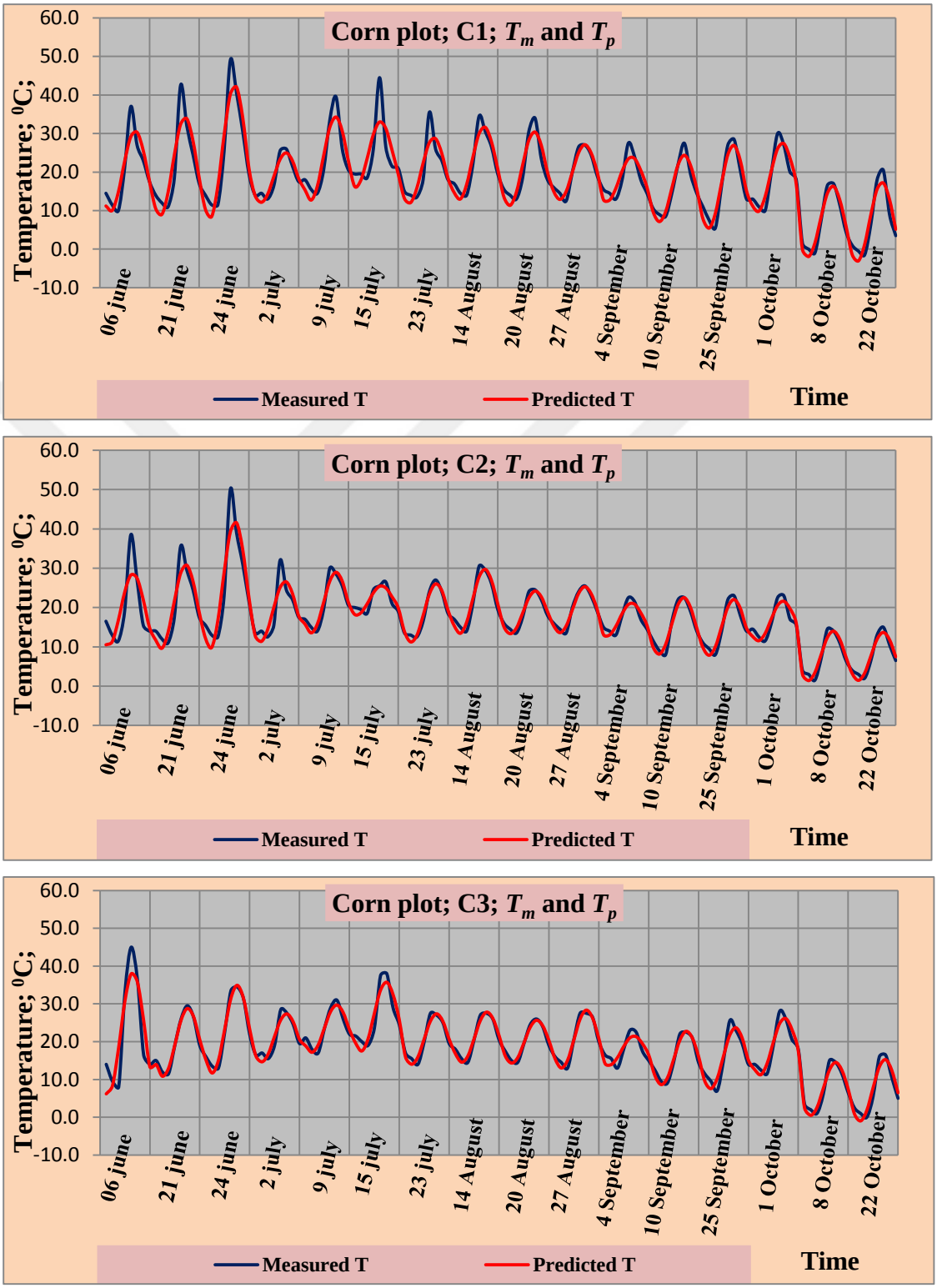

Appendix 9. Volumetric water content (θ) and calculated κ-values at sugar beet plot (S1)

Dates	6.6.13	21.6.13	24.6.13	2.7.13	9.7.13	15.7.13	23.1.13	14.8.13	20.8.13	27.8.13	4.9.13	10.9.13	25.9.13	1.10.13	8.10.13	22.10.13	Mean
Depth, m	**θ, cm^3/cm^3**																
0.05	34.60	36.81	37.73	35.81	39.73	39.73	39.30	36.17	39.40	37.26	39.91	36.20	33.60	42.47	38.19	27.83	**37.17**
0.1	37.10	40.14	40.23	38.74	40.56	40.16	41.86	40.02	41.10	39.56	40.14	38.90	36.00	39.65	41.67	29.33	**39.07**
0.2	39.60	43.47	42.73	41.67	41.39	40.59	44.41	43.86	45.44	43.00	42.18	43.02	42.40	44.41	45.14	32.52	**42.24**
0.3	39.81	40.55	41.30	39.83	40.81	41.61	42.95	42.88	42.71	40.63	43.65	39.50	38.83	41.88	43.82	35.12	**40.99**
0-0.3	**37.78**	**40.24**	**40.50**	**39.01**	**40.62**	**40.52**	**42.13**	**40.73**	**42.16**	**40.11**	**41.47**	**39.40**	**37.71**	**42.10**	**42.21**	**31.20**	**39.87**
	$\kappa.10^{-7}$ (m^2/s) (calculated by layer method)																
0.05	0.4228	0.5540	0.3562	0.2309	0.3390	1.1546	0.2575	0.3207	0.3359	0.3073	0.2280	0.3789	0.5054	5.5293	0.4730	0.3946	**0.7368**
0.1	2.7438	1.7833	1.9547	1.6218	1.6758	4.3613	1.2872	2.6928	5.4622	5.5293	2.4742	2.2474	2.2474	3.4836	2.1263	2.7459	**2.7773**
0.2	5.0648	3.0126	3.5532	3.0126	3.0126	7.5681	2.3169	5.0648	13.9345	7.5681	3.0126	5.5293	5.5293	9.3856	3.7796	7.5681	**5.5570**
0.3	3.0126	3.0126	1.8920	7.5681	22.1171	22.1171	7.5681	3.0126	22.1171	7.5681	7.5681	7.5681	1.8920	4.3308	3.0126	5.5293	**8.1179**
0-0.3	**2.8110**	**2.0907**	**1.9390**	**3.1083**	**6.7861**	**8.8003**	**2.8574**	**2.7727**	**10.4624**	**5.2432**	**3.3207**	**3.9309**	**2.5435**	**5.6823**	**2.3479**	**4.0595**	**4.2973**
	$\kappa.10^{-7}$ (m^2/s) (calculated by point 1 method)																
0.05	0.3137	0.6726	0.4835	0.2555	0.4023	0.3429	0.3019	0.3252	0.2829	0.3381	0.2308	0.4112	0.5713	0.6982	0.5335	0.3753	**0.4087**
0.1	1.6312	1.6326	1.7742	1.9826	1.7209	1.8468	1.9030	1.9250	1.6272	1.8615	1.9365	1.4855	1.6365	1.6784	1.7248	1.7734	**1.7588**
0.2	1.7488	1.7927	1.8714	2.3963	1.7419	1.9884	2.5041	2.5248	1.7469	2.5116	2.3793	1.6143	1.9551	1.7670	1.9631	2.5787	**2.0678**
0.3	2.1257	2.1647	2.1666	3.1290	2.7039	2.3436	2.9007	2.9203	2.1328	2.7518	2.7806	1.7031	2.4384	2.4726	2.4459	2.4065	**2.4741**
0-0.3	**1.4549**	**1.5657**	**1.5739**	**1.9408**	**1.6422**	**1.6304**	**1.9024**	**1.9238**	**1.4475**	**1.8658**	**1.8318**	**1.3035**	**1.6503**	**1.6540**	**1.6668**	**1.7835**	**1.6773**
	$\kappa.10^{-7}$ (m^2/s) (calculated by point 2 method)																
0.05	0.3137	0.6726	0.4835	0.2555	0.4023	0.3429	0.3019	0.3252	0.2829	0.3381	0.2308	0.4112	0.5713	0.6169	0.5335	0.3753	**0.4036**
0.1	1.6674	1.6271	1.8220	1.8446	1.7708	1.9364	1.9267	1.9497	1.6273	1.8616	1.9537	1.4855	1.6359	1.6839	1.9575	1.7735	**1.7827**
0.2	1.8210	1.8695	1.9565	2.4337	1.8133	1.9943	2.5515	2.5742	1.8189	2.5597	2.4152	1.6726	2.0491	1.8521	2.0580	1.8073	**2.0779**
0.3	2.3584	2.3560	2.5607	2.9375	2.8801	2.4070	2.9626	2.9409	2.1240	2.9080	2.8320	1.8797	2.7246	2.5030	2.7288	2.4447	**2.5968**
0-0.3	**1.5401**	**1.6313**	**1.7057**	**1.8678**	**1.7166**	**1.6701**	**1.9357**	**1.9475**	**1.4633**	**1.9169**	**1.8579**	**1.3622**	**1.7452**	**1.6640**	**1.8195**	**1.6002**	**1.3965**

Appendix 10. Volumetric water content (θ) and calculated κ-values at sugar beet plot (S2)

Dates	6.6.13	21.6.13	24.6.13	2.7.13	9.7.13	15.7.13	23.1.13	14.8.13	20.8.13	27.8.13	4.9.13	10.9.13	25.9.13	1.10.13	8.10.13	22.10.13	Mean
Depth, m	**θ, cm^3/cm^3**																
0.05	36.28	37.96	33.52	38.94	40.96	35.89	39.58	36.50	37.29	42.63	38.50	39.36	37.63	38.11	40.71	30.03	**37.74**
0.1	37.78	40.79	34.72	44.64	42.76	37.29	41.48	38.73	39.95	43.21	40.34	43.62	39.63	39.91	42.67	33.68	**40.07**
0.2	42.04	44.04	36.63	40.64	43.18	38.02	40.37	42.95	42.32	43.43	43.41	40.52	42.11	44.70	44.27	35.03	**41.48**
0.3	39.09	43.25	36.83	43.15	44.00	39.00	43.25	38.50	41.29	39.96	42.50	41.12	40.04	42.35	43.71	34.87	**40.81**
0-0.3	**38.80**	**41.51**	**35.43**	**41.84**	**42.73**	**37.55**	**41.17**	**39.17**	**40.22**	**42.31**	**41.19**	**41.16**	**39.85**	**41.26**	**42.84**	**33.40**	**40.03**
	κ.10^{-7} (m^2/s) (calculated by layer method)																
0.05	0.4054	2.0073	0.8381	1.4447	1.2479	0.9868	1.8920	0.8212	1.0374	2.1602	1.5775	1.5775	0.5928	0.4105	0.8287	0.6070	**0.4054**
0.1	3.2285	3.4836	4.3572	4.3047	3.6885	2.3464	3.6885	4.4497	3.4836	3.6885	4.4497	4.4497	4.8985	4.6565	4.8985	3.4836	**3.2285**
0.2	4.3308	3.0126	3.6468	1.8920	3.4299	6.2599	2.3169	2.3169	3.0126	3.4299	3.4299	3.4299	2.6174	3.0126	3.9826	3.0126	**4.3308**
0.3	7.5681	4.3308	5.0648	1.8920	13.9345	5.0648	7.5681	1.8920	43.9350	13.9345	13.9345	13.9345	7.5681	13.1171	13.9345	7.5681	**7.5681**
0-0.3	**3.8832**	**3.2086**	**3.4767**	**2.3834**	**5.5752**	**3.6645**	**3.8664**	**2.3699**	**12.8672**	**5.8033**	**5.8479**	**5.8479**	**3.9192**	**5.2992**	**5.9111**	**3.6678**	**3.8832**
	κ.10^{-7} (m^2/s) (calculated by point 1 method)																
0.05	0.4060	2.5616	0.8295	1.6187	1.0278	0.4964	1.2887	1.1362	1.1728	1.1610	1.4964	1.4964	0.6328	0.3991	0.9032	0.6202	**1.0779**
0.1	1.6480	3.0128	1.5393	2.5193	1.7079	1.9120	1.8306	1.9997	1.7210	2.4573	1.8282	1.8282	1.7266	1.5782	1.9878	1.6095	**1.9316**
0.2	1.7591	3.0186	2.0723	2.1515	2.0669	2.0673	2.5557	2.5830	2.2405	2.9514	2.4273	2.4273	1.9352	1.7200	2.1625	1.7101	**2.2405**
0.3	2.3261	3.5896	2.7431	2.6505	2.3763	2.5662	2.8557	3.0635	2.8559	3.1770	2.7249	2.7249	2.6813	2.3882	2.9240	1.9663	**2.7258**
0-0.3	**1.5348**	**3.0456**	**1.7961**	**2.2350**	**1.7947**	**1.7605**	**2.1327**	**2.1956**	**1.9975**	**2.4367**	**2.1192**	**2.1192**	**1.7440**	**1.5214**	**1.9944**	**1.4765**	**1.9940**
	κ.10^{-7} (m^2/s) (calculated by point 2 method)																
0.05	0.4060	2.5450	0.8295	1.6174	1.0280	0.4964	1.2767	1.1365	1.1731	1.1458	1.4808	1.4808	0.6328	0.3991	0.9033	0.6202	**1.0732**
0.1	1.6848	3.0433	1.9535	2.5177	1.9701	1.9119	1.8456	1.9910	2.2714	2.5460	1.8431	1.8431	1.7643	1.4782	2.1375	1.5948	**2.0248**
0.2	1.8324	3.1945	2.1785	2.2656	2.1726	2.2447	2.7057	2.7349	2.3634	3.1246	2.5669	2.5669	2.0271	1.7892	2.2778	1.7782	**2.3639**
0.3	2.3928	3.3749	2.9030	2.5254	2.3763	2.7662	2.9264	3.1497	2.8797	3.4851	2.9624	2.9624	2.6724	2.2986	3.0065	1.8565	**2.7836**
0-0.3	**1.5790**	**3.0394**	**1.9661**	**2.2315**	**1.8867**	**1.8548**	**2.1886**	**2.2530**	**2.1719**	**2.5754**	**2.2133**	**2.2133**	**1.7741**	**1.4913**	**2.0813**	**1.4624**	**1.3965**

Appendix 11. Volumetric water content (θ) and calculated κ-values at sugar beet plot (S3)

Dates	6.6.13	21.6.13	24.6.13	2.7.13	9.7.13	15.7.13	23.1.13	14.8.13	20.8.13	27.8.13	4.9.13	10.9.13	25.9.13	1.10.13	8.10.13	22.10.13	Mean
Depth, m	**θ, cm^3/cm^3**																
0.05	38.37	33.60	36.39	40.15	41.91	36.04	38.60	42.23	41.58	36.68	37.68	42.35	37.19	40.64	38.69	34.12	**38.51**
0.1	41.45	34.92	38.74	41.21	43.52	40.59	41.20	45.04	44.76	40.92	41.98	43.24	39.59	38.14	41.52	37.68	**40.91**
0.2	44.88	40.07	41.95	42.71	46.87	42.50	42.97	46.35	45.41	38.58	47.27	45.66	43.73	43.64	46.04	43.42	**43.88**
0.3	44.54	36.24	41.09	42.26	45.12	43.25	42.79	43.84	47.94	40.72	44.60	44.13	40.74	42.98	44.35	41.45	**42.88**
0-0.3	**42.31**	**36.21**	**39.54**	**41.58**	**44.35**	**40.60**	**41.39**	**44.36**	**44.93**	**39.22**	**42.88**	**43.84**	**40.31**	**41.35**	**42.65**	**39.17**	**41.54**
	$\kappa.10^{-7}$ (m^2/s) (calculated by layer method)																
0.05	1.4935	0.9449	1.1707	1.0827	1.9983	3.4836	3.3202	0.5351	0.3565	1.7641	1.1860	2.0780	1.5030	1.8920	1.5999	1.5999	**1.6255**
0.1	2.4742	2.4183	3.1868	5.6311	2.6311	2.1740	2.7459	1.5762	4.1150	3.4836	2.8920	2.7459	4.7969	3.1290	4.1150	4.1150	**3.2644**
0.2	1.4037	4.3308	0.9603	7.5681	7.5681	1.4037	3.0126	7.5681	4.3308	3.9345	3.0126	1.8920	1.8920	7.5681	1.8920	22.1171	**5.0284**
0.3	4.7441	3.9826	4.6184	13.9345	4.3308	5.8490	3.0126	2.6174	7.5681	4.7441	13.9345	5.5293	3.5532	11.6106	4.3308	2.5084	**6.0543**
0-0.3	**2.5289**	**2.9191**	**2.4840**	**7.0541**	**4.1321**	**3.2276**	**3.0228**	**3.0742**	**4.0926**	**3.4816**	**5.2563**	**3.0613**	**2.9363**	**6.0499**	**2.9844**	**7.5851**	**3.9932**
	$\kappa.10^{-7}$ (m^2/s) (calculated by point 1 method)																
0.05	1.1032	0.9535	1.1849	1.7851	1.8059	1.9139	1.4796	0.5252	0.4293	0.9186	0.7087	1.6723	0.9562	2.9296	1.4583	1.9422	**1.3604**
0.1	1.9320	1.5638	1.9822	2.0835	2.4724	2.2361	2.1843	1.5956	1.5848	1.9549	1.9312	2.1812	1.8476	3.3105	1.8741	2.0775	**2.0507**
0.2	2.2522	1.8738	2.1177	2.6182	2.9080	2.3351	2.0800	1.7037	1.6905	2.3317	2.2715	2.7713	2.4915	3.7909	2.3127	2.6603	**2.3881**
0.3	2.2734	2.2028	2.3536	2.6536	2.9757	2.8740	2.2721	2.1146	1.8742	2.7478	2.8339	3.1351	3.2169	4.0357	2.8586	3.6819	**2.7565**
0-0.3	**1.8902**	**1.6485**	**1.9096**	**2.2851**	**2.5405**	**2.3398**	**2.0040**	**1.4848**	**1.3947**	**1.9882**	**1.9363**	**2.4400**	**2.1281**	**3.5167**	**2.1259**	**2.5905**	**2.1389**
	$\kappa.10^{-7}$ (m^2/s) (calculated by point 2 method)																
0.05	1.1034	0.9537	1.1852	1.7819	1.8024	1.1909	1.4643	0.5252	0.4293	0.9134	0.7087	1.6704	0.9563	2.9112	1.4580	1.9367	**1.3119**
0.1	1.3179	1.5591	1.9735	2.0747	2.4694	1.9358	2.2336	1.5095	1.6848	1.9548	1.9310	2.1728	1.8398	3.3036	1.8661	2.0687	**1.9935**
0.2	2.2613	1.9798	2.2531	2.6541	2.9043	2.2363	2.0947	1.9853	1.7519	2.4509	2.7201	2.9193	2.7557	3.4824	2.9169	2.7787	**2.5090**
0.3	2.3994	2.3221	2.4869	2.8105	3.1500	2.9595	2.4536	2.1392	1.8725	2.6593	2.9151	3.3143	3.3978	4.1955	3.0276	3.8591	**2.8726**
0-0.3	**1.7705**	**1.7036**	**1.9747**	**2.3303**	**2.5815**	**2.0806**	**2.0615**	**1.5398**	**1.4346**	**1.9946**	**2.0687**	**2.5192**	**2.2374**	**3.4732**	**2.3172**	**2.6608**	**2.1718**

Appendix 12. Volumetric water content (θ) and calculated κ-values at corn plot (C1)

Dates	6.6.13	21.6.13	24.6.13	2.7.13	9.7.13	15.7.13	23.1.13	14.8.13	20.8.13	27.8.13	4.9.13	10.9.13	25.9.13	1.10.13	8.10.13	22.10.13	Mean
Depth, m	**θ, cm^3/cm^3**																
0.05	34.65	36.12	37.98	38.87	38.91	36.20	39.35	39.11	39.23	36.89	36.63	38.24	36.35	35.36	40.78	32.65	**37.33**
0.1	37.13	38.72	39.19	41.12	40.25	38.24	41.69	40.02	41.01	39.64	39.44	41.66	38.95	39.13	42.46	34.55	**39.57**
0.2	38.91	41.17	40.25	43.75	43.91	45.17	44.56	43.85	44.12	41.68	42.40	45.48	43.05	44.43	44.50	36.99	**42.76**
0.3	39.30	40.40	43.25	45.22	41.30	42.30	43.38	41.29	43.33	42.97	42.15	43.94	40.63	43.07	46.58	35.74	**42.18**
0-0.3	**37.50**	**39.10**	**40.17**	**42.24**	**41.09**	**40.48**	**42.24**	**41.07**	**41.92**	**40.29**	**40.15**	**42.33**	**39.74**	**40.50**	**43.58**	**34.98**	**40.46**
	κ.10^{-7} (m^2/s) (calculated by layer method)																
0.05	0.2832	0.2134	0.2022	0.3344	0.2352	0.1658	0.2290	0.2909	0.2007	0.4499	0.2316	0.3176	0.2564	0.2526	0.2832	0.2290	**0.2609**
0.1	1.9498	2.2352	3.6164	3.3526	2.7240	1.6621	3.5037	1.2258	4.9725	2.8314	2.2443	2.7653	1.2085	3.5155	2.5484	3.5037	**2.7412**
0.2	3.6164	4.2570	4.6430	4.1171	5.2129	3.1584	6.7784	2.1606	9.7443	5.2129	4.2570	5.2129	2.1606	6.7784	7.5681	6.7784	**5.1035**
0.3	7.5681	7.5681	6.5240	3.2500	4.0560	5.6410	7.5681	4.2560	7.5681	7.5681	5.2360	7.5681	4.2568	7.5681	3.4665	7.5681	**6.0769**
0-0.3	**3.3544**	**3.5684**	**3.7464**	**2.7635**	**3.0570**	**2.6568**	**4.5198**	**1.9833**	**5.6214**	**4.0156**	**2.9923**	**3.9660**	**1.9706**	**4.5286**	**3.4665**	**4.5198**	**3.5457**
	κ.10^{-7} (m^2/s) (calculated by point 1 method)																
0.05	0.3568	0.2860	0.2385	0.2977	0.2621	0.1816	0.2516	0.2852	0.1834	0.4028	0.2059	0.3768	0.2872	0.2395	0.2935	0.2487	**0.2748**
0.1	1.0256	0.7078	0.9597	2.2332	0.7532	0.6778	0.8436	0.8173	0.9274	1.2341	0.8402	1.1615	0.7663	0.9941	1.1196	0.9195	**0.9988**
0.2	1.6944	1.1296	1.5081	2.4945	1.2443	1.1740	1.4355	1.3494	1.6714	2.0655	1.4745	1.9463	1.2453	1.7486	1.5190	1.5903	**1.5807**
0.3	2.3464	1.6114	1.7980	2.7650	1.8308	1.6416	2.6267	2.0361	2.0114	2.9217	1.9150	2.2122	2.3097	2.5574	1.9311	1.6840	**2.1374**
0-0.3	**1.3558**	**0.9337**	**1.1261**	**1.9476**	**1.0226**	**0.9188**	**1.2894**	**1.1220**	**1.1984**	**1.6560**	**1.1089**	**1.4242**	**1.1521**	**1.3849**	**1.2158**	**1.1106**	**1.2479**
	κ.10^{-7} (m^2/s) (calculated by point 2 method)																
0.05	0.3568	0.2860	0.2385	0.2977	0.2622	0.1816	0.2517	0.2852	0.1834	0.4039	0.2059	0.3768	0.2872	0.2395	0.2935	0.2487	**0.2749**
0.1	1.0588	0.7162	0.9679	2.3553	0.7655	0.6878	0.8640	0.8339	0.9594	1.2874	0.8625	1.2080	0.7786	1.0302	1.1357	0.9474	**1.0287**
0.2	1.7608	1.1463	1.5281	2.5337	1.2689	1.1940	1.4764	1.3826	1.7355	2.1710	1.5191	2.0393	1.2700	1.8208	1.7720	1.6462	**1.6416**
0.3	2.3669	1.5281	1.8650	2.8440	1.6463	1.8442	1.8351	2.0699	2.0561	3.0053	2.0053	2.1684	1.6477	2.6420	2.0671	1.7945	**2.0866**
0-0.3	**1.3858**	**0.9192**	**1.1499**	**2.0077**	**0.9857**	**0.9769**	**1.1068**	**1.1429**	**1.2336**	**1.7169**	**1.1482**	**1.4481**	**0.9959**	**1.4331**	**1.3171**	**1.1592**	**1.2579**

Appendix 13. Volumetric water content (θ) and calculated κ-values at corn plot (C2)

Dates	6.6.13	21.6.13	24.6.13	2.7.13	9.7.13	15.7.13	23.1.13	14.8.13	20.8.13	27.8.13	4.9.13	10.9.13	25.9.13	1.10.13	8.10.13	22.10.13	Mean
Depth, m	**θ, cm^3/cm^3**																
0.05	39.51	41.26	41.79	37.96	42.18	45.09	42.51	39.24	42.37	38.34	43.69	39.69	42.80	40.25	41.43	36.45	**40.91**
0.1	42.29	41.45	42.07	39.70	43.63	42.81	43.89	40.19	42.52	41.23	45.11	40.25	44.39	44.17	43.15	37.47	**42.15**
0.2	45.06	41.63	42.36	41.45	45.09	40.54	45.27	41.14	43.78	44.11	46.52	41.69	45.97	42.68	48.89	39.97	**43.51**
0.3	44.39	45.08	42.27	40.06	45.25	47.07	44.38	40.39	42.66	41.94	45.76	41.19	44.65	43.75	45.56	38.98	**43.34**
0-0.3	**42.81**	**42.36**	**42.12**	**39.79**	**44.04**	**43.88**	**44.02**	**40.24**	**42.83**	**41.41**	**45.27**	**40.71**	**44.45**	**42.71**	**44.76**	**38.22**	**42.48**
	$\kappa.10^{-7}$ (m^2/s) (calculated by layer method)																
0.05	0.2832	0.4592	0.2960	0.2595	0.4730	0.9449	0.3662	0.3781	0.4141	0.7532	0.5101	0.4499	0.4292	0.3903	0.4228	0.3344	**0.4478**
0.1	3.9256	2.7620	2.0378	3.9138	0.9384	2.6379	1.6894	3.9731	3.9911	2.5420	11.3136	2.9027	3.9986	18.2561	1.8920	3.4836	**4.3911**
0.2	7.5681	5.0648	3.0126	7.5681	7.5681	4.3308	3.0126	7.5681	7.5681	4.3308	7.5681	43.9350	7.5681	7.5681	22.1171	3.0126	**9.3351**
0.3	3.0126	3.0126	3.7796	7.5681	1.4037	7.5681	5.0240	7.5681	22.1171	7.5681	22.1171	3.0126	7.5681	7.5681	7.5681	7.5681	**7.7515**
0-0.3	**3.6974**	**2.8247**	**2.2815**	**4.8273**	**2.5958**	**3.8704**	**2.5231**	**4.8718**	**8.5226**	**3.7985**	**10.3772**	**12.5751**	**4.8910**	**8.4456**	**8.0000**	**3.5997**	**5.4814**
	$\kappa.10^{-7}$ (m^2/s) (calculated by point 1 method)																
0.05	0.2274	0.4834	0.3953	0.3713	0.6240	0.2550	0.4110	0.3989	0.3647	0.9097	0.4827	0.4285	0.4374	0.2647	0.4765	0.3987	**0.4331**
0.1	1.4969	1.0786	0.8395	1.7163	1.9307	1.4485	1.3990	1.3761	1.2951	1.7752	1.4325	1.3361	1.0276	1.0589	1.1845	0.8284	**1.3265**
0.2	1.7110	1.6739	1.2838	1.9540	2.7843	1.6419	1.5698	1.4764	1.5366	2.6406	2.3822	1.6019	1.6178	2.7227	1.3978	1.4260	**1.8388**
0.3	2.0751	2.3241	1.8814	2.4613	2.2375	1.9513	1.7890	1.6940	2.4573	3.2946	2.8122	2.6043	2.6401	3.6327	2.1451	2.0372	**2.3773**
0-0.3	**1.3776**	**1.3900**	**1.1000**	**1.6257**	**1.8941**	**1.3242**	**1.2922**	**1.2363**	**1.4134**	**2.1550**	**1.7774**	**1.4927**	**1.4308**	**1.9197**	**1.3010**	**1.1726**	**1.4939**
	$\kappa.10^{-7}$ (m^2/s) (calculated by point 2 method)																
0.05	0.2274	0.4834	0.3953	0.3713	0.6240	0.2550	0.4110	0.3989	0.3647	0.9098	0.4827	0.4285	0.4374	0.2647	0.4765	0.3987	**0.4331**
0.1	1.5003	1.1108	0.8534	1.8210	1.7428	1.5266	1.5017	1.3960	1.2759	1.8532	1.5004	1.3364	1.0569	1.0586	1.2508	0.8286	**1.3508**
0.2	1.7793	1.7382	1.3115	2.0480	1.9265	1.7982	1.6234	1.5210	1.5871	2.7966	2.5181	1.6589	1.6764	2.8841	1.4352	1.4661	**1.8605**
0.3	2.0918	2.3656	1.8335	2.3052	2.2616	1.8560	1.8520	1.8744	2.3032	2.8139	2.6564	2.3827	2.4020	2.9163	1.7131	2.1213	**2.2343**
0-0.3	**1.3997**	**1.4245**	**1.0984**	**1.6364**	**1.6387**	**1.3589**	**1.3470**	**1.2976**	**1.3828**	**2.0934**	**1.7894**	**1.4516**	**1.3932**	**1.7809**	**1.2189**	**1.2037**	**1.4697**

Appendix 14. Volumetric water content (θ) and calculated κ-values at corn plot (C3)

Dates	6.6.13	21.6.13	24.6.13	2.7.13	9.7.13	15.7.13	23.1.13	14.8.13	20.8.13	27.8.13	4.9.13	10.9.13	25.9.13	1.10.13	8.10.13	22.10.13	Mean
Depth, m	**θ, cm^3/cm^3**																
0.05	41.14	39.53	42.35	36.91	37.62	32.86	34.59	38.72	41.71	38.85	40.63	43.37	41.57	40.61	42.86	35.82	**39.32**
0.1	43.15	41.65	43.49	37.60	39.75	36.71	35.10	39.72	42.42	42.78	43.15	45.24	43.92	42.14	44.13	38.80	**41.23**
0.2	45.15	43.77	45.16	41.30	40.53	43.37	38.06	41.68	44.13	43.01	45.68	46.00	44.72	44.67	47.27	40.75	**43.45**
0.3	44.90	42.59	43.44	40.47	39.51	42.56	37.03	40.08	43.14	42.21	43.32	44.34	43.53	43.16	43.76	40.62	**42.17**
0-0.3	**43.59**	**41.89**	**43.61**	**39.07**	**39.35**	**38.88**	**36.19**	**40.05**	**42.85**	**41.71**	**43.19**	**44.74**	**43.44**	**42.64**	**44.51**	**39.00**	**41.54**
	κ.10^{-7} (m^2/s) (calculated by layer method)																
0.05	0.4271	0.7532	0.7853	1.0378	0.9600	0.5641	0.7532	0.5527	0.8764	0.7065	0.6858	0.7532	0.5761	0.4627	0.7288	0.6324	**0.7034**
0.1	3.9976	1.3226	2.5581	22.4864	4.2640	10.0850	22.1171	7.5681	4.2222	22.1171	4.1269	3.0126	3.0126	4.0154	11.4230	3.0126	**8.0838**
0.2	7.5681	1.8920	4.3308	43.9350	7.5680	22.1171	7.5681	7.5681	7.5681	7.5681	7.5681	7.5681	7.5681	7.5681	22.1171	7.5681	**11.1026**
0.3	7.5681	7.5681	7.5681	22.1171	7.5680	7.5681	14.8426	5.4680	3.0126	14.8426	7.5681	3.7780	5.2904	7.5681	7.5681	5.2904	**8.4491**
0-0.3	**4.8902**	**2.8840**	**3.8106**	**22.3941**	**5.0900**	**10.0836**	**11.3202**	**5.2892**	**3.9198**	**11.3086**	**4.9872**	**3.7780**	**4.1118**	**4.9035**	**10.4593**	**4.1259**	**7.0847**
	κ.10^{-7} (m^2/s) (calculated by point 1 method)																
0.05	0.3200	0.7745	0.7318	0.8376	0.9680	0.4660	0.5912	0.5938	0.6769	0.7040	0.6369	0.8578	0.6733	0.5379	0.7630	0.5067	**0.6650**
0.1	1.0984	1.0813	1.1560	1.6503	1.6230	1.5724	1.3480	1.3526	2.0166	1.5358	1.2900	1.3027	1.2043	2.0185	1.4241	1.1985	**1.4295**
0.2	1.8768	1.3882	1.5802	2.4630	2.2780	1.7235	2.0329	1.9043	2.3564	1.7914	1.9431	1.6487	1.7097	3.4991	2.0851	2.3254	**2.0379**
0.3	2.1992	1.8549	1.6838	3.9230	2.4156	2.5277	2.1905	2.1979	2.4917	2.1636	2.7324	1.9364	1.9570	4.2547	2.6662	2.6197	**2.4884**
0-0.3	**1.3736**	**1.2747**	**1.2880**	**2.2185**	**1.8212**	**1.5724**	**1.5406**	**1.5122**	**1.8854**	**1.5487**	**1.6506**	**1.4364**	**1.3861**	**2.5775**	**1.7346**	**1.6626**	**1.6552**
	κ.10^{-7} (m^2/s) (calculated by point 2 method)																
0.05	0.3200	0.7746	0.7319	0.8377	0.9680	0.4660	0.5912	0.5939	0.6769	0.7040	0.6370	0.8579	0.6734	0.5379	0.7631	0.5067	**0.6650**
0.1	0.8505	1.0998	1.1835	1.7217	1.6860	1.3454	1.3810	1.3860	1.4624	1.5861	1.3364	1.3320	1.2261	1.4318	1.4778	1.2199	**1.3579**
0.2	1.3810	1.4250	1.6351	2.6056	2.4040	1.7931	1.6806	1.7300	2.2480	1.7585	2.0359	1.4067	1.5883	2.3257	2.1925	2.2311	**1.9026**
0.3	2.2206	1.7896	1.8685	3.5523	2.5137	2.7770	1.7245	2.0740	2.5378	1.9309	2.4490	1.5322	1.8555	3.2802	2.4160	2.7255	**2.3280**
0-0.3	**1.1930**	**1.2722**	**1.3547**	**2.1793**	**1.8929**	**1.5954**	**1.3443**	**1.4460**	**1.7313**	**1.4949**	**1.6146**	**1.2822**	**1.3358**	**1.8939**	**1.7124**	**1.6708**	**1.5634**

Appendix 15. Comparing values of measured (Tm) and predicted (Tp) by layer, point 1 and point 2 methods for sugar beet plots for 16 week of study period (n= 16x8 = 128) for 0.05 m depth. Each value is a mean of three plots (S1, S2, S3).

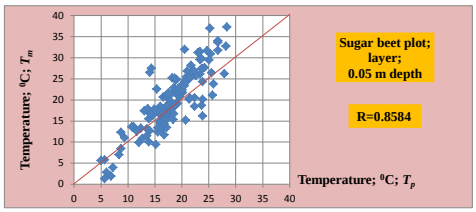

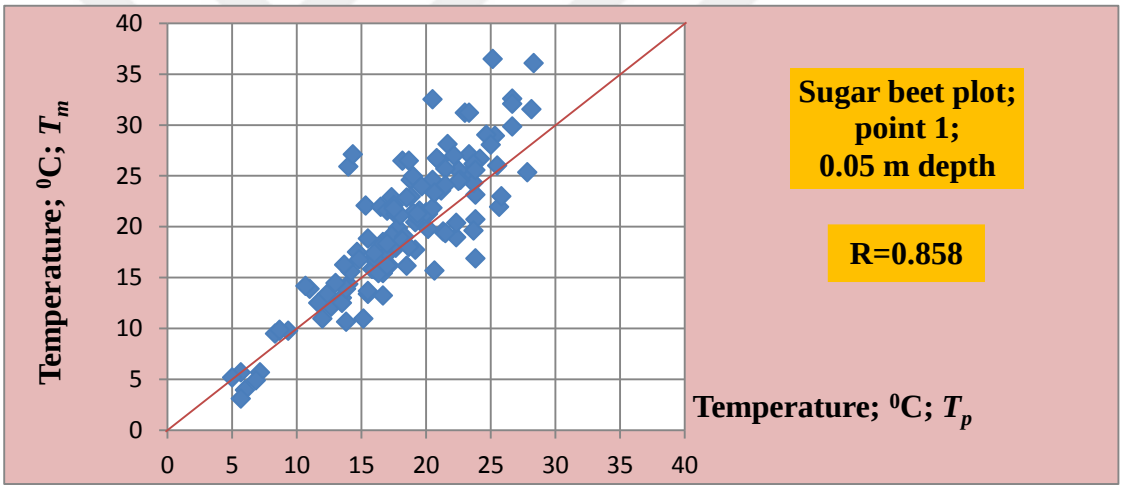

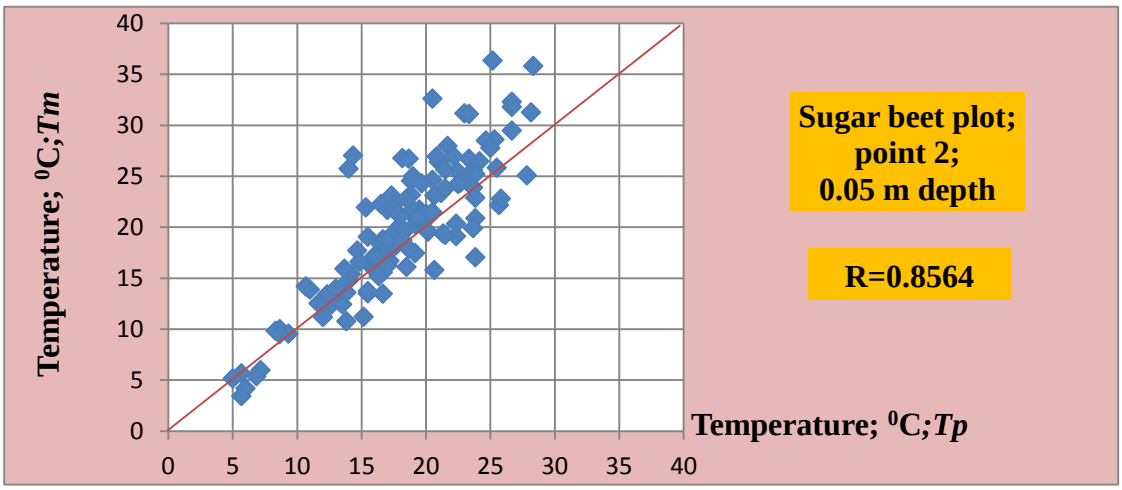

Appendix 16. Comparing values of measured (Tm) and predicted (Tp) by layer, point 1 and point 2 methods for corn plots for 16 week of study period (n= 16x8 = 128) for 0.05 m depth. Each value is a mean of three plots (C1, C2, C3).

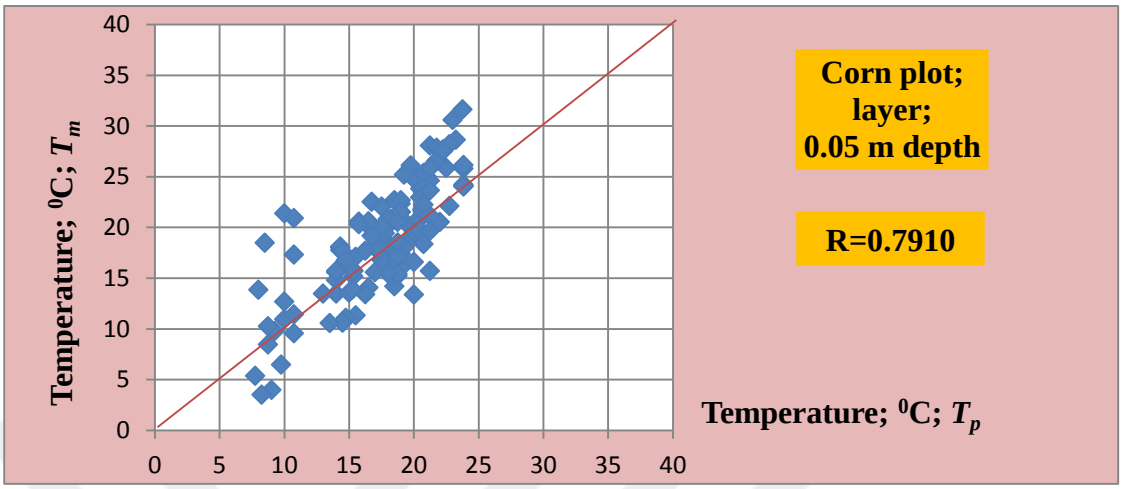

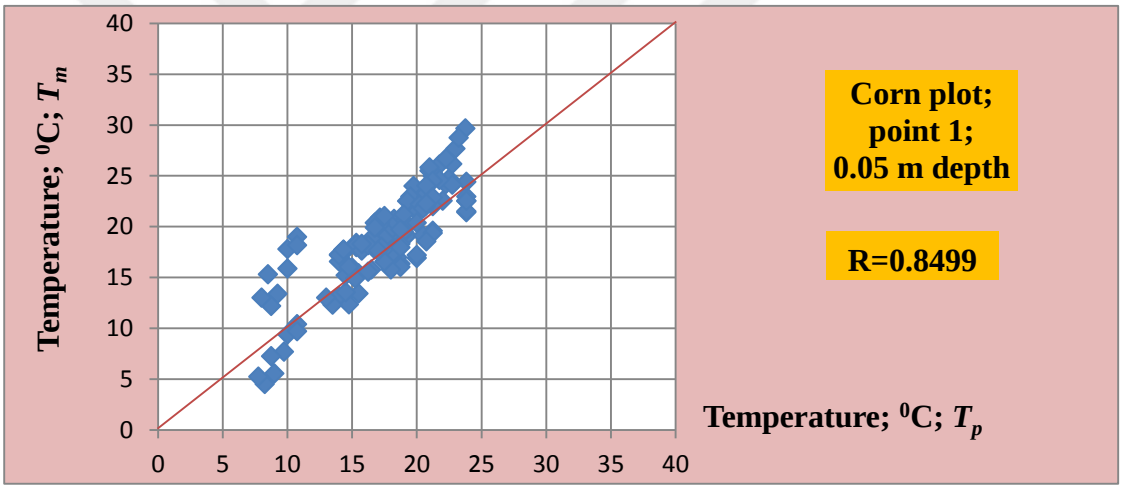

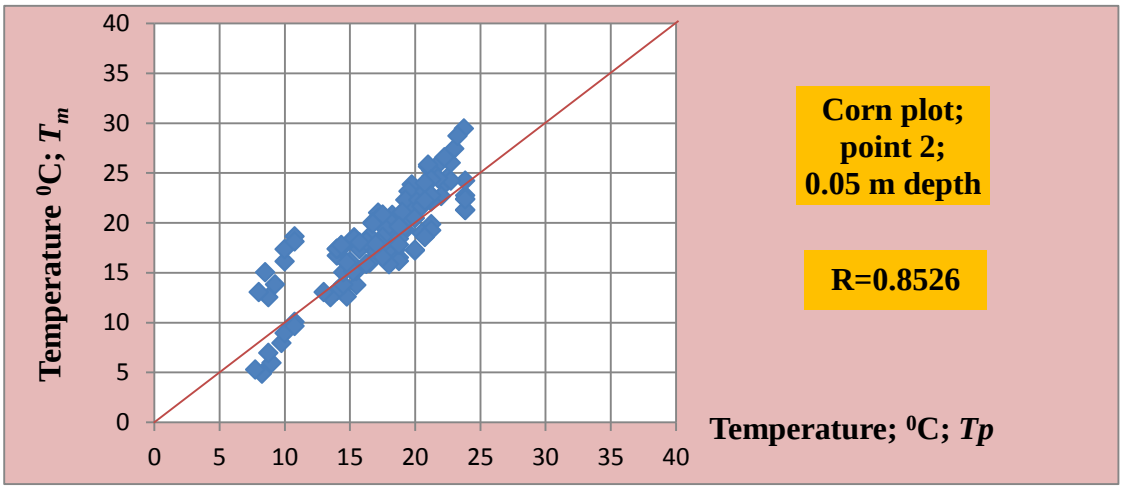

Appendix 17. Comparing values of measured (Tm) and predicted (Tp) by layer, point 1 and point 2 methods for control plot for 16 week of study period (n= 16x8 = 128) for 0.10 m depth.

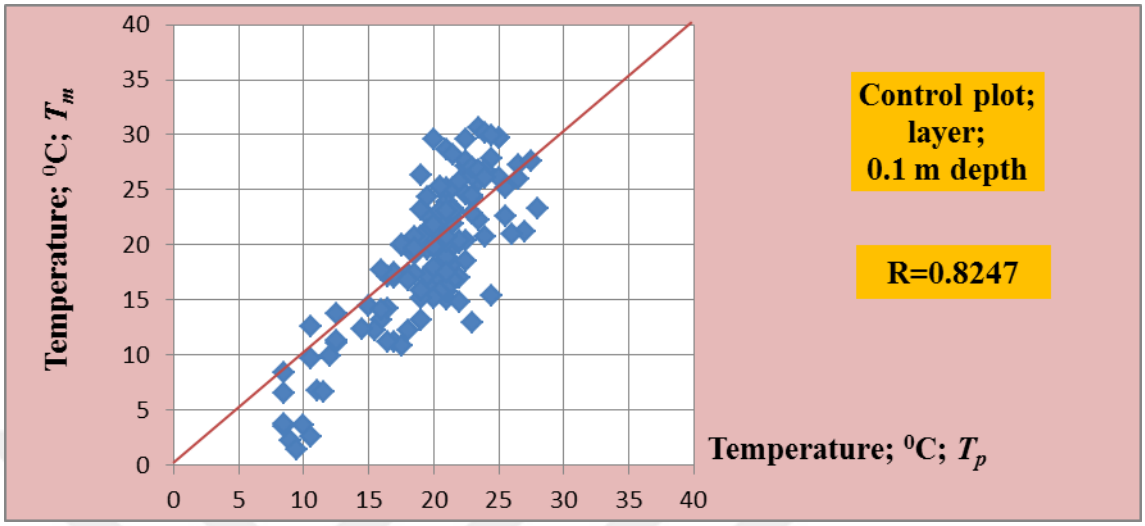

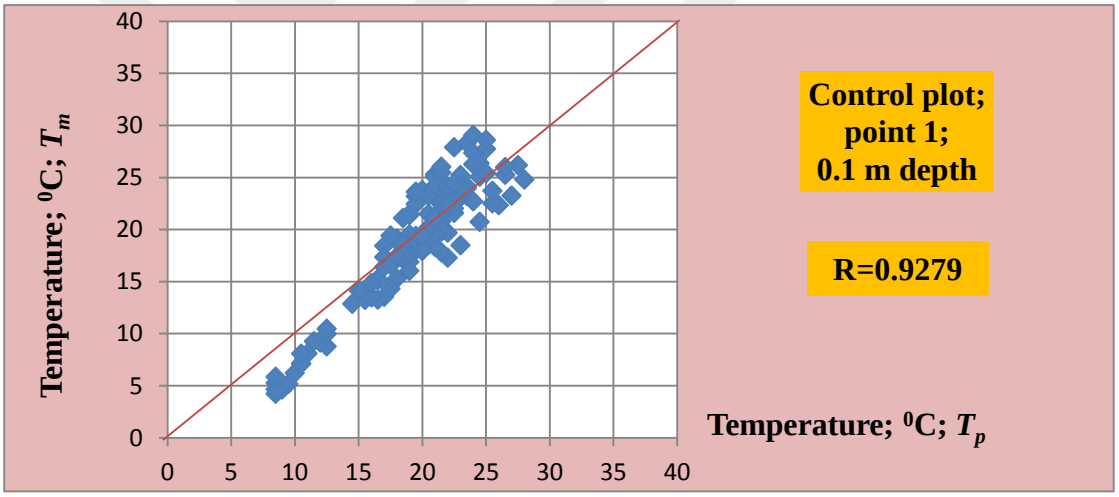

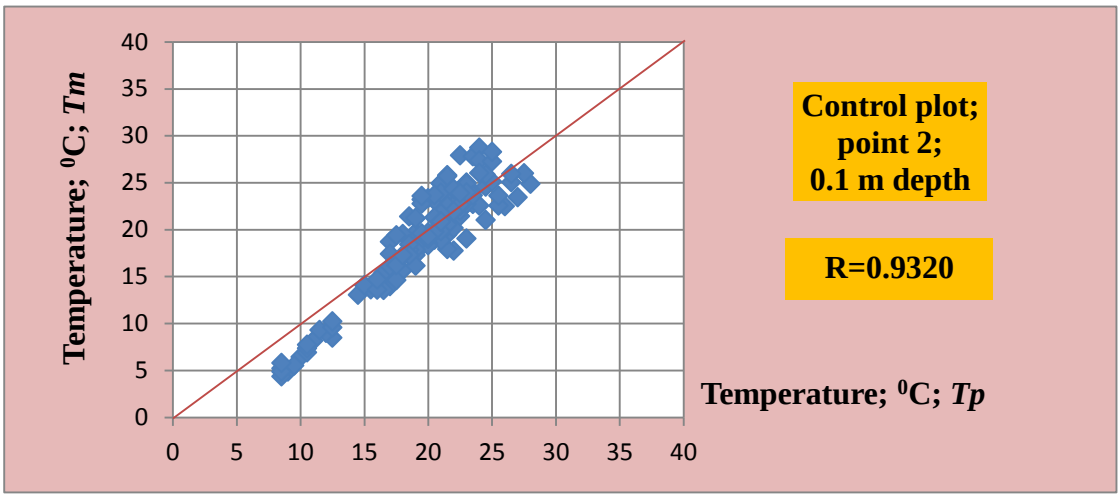

Appendix 18. Comparing values of measured (Tm) and predicted (Tp) by layer, point 1 and point 2 methods for sugar beet plots for 16 week of study period (n= 16x8 = 128) for 0.1 m depth. Each value is a mean of three plots (S1, S2, S3)

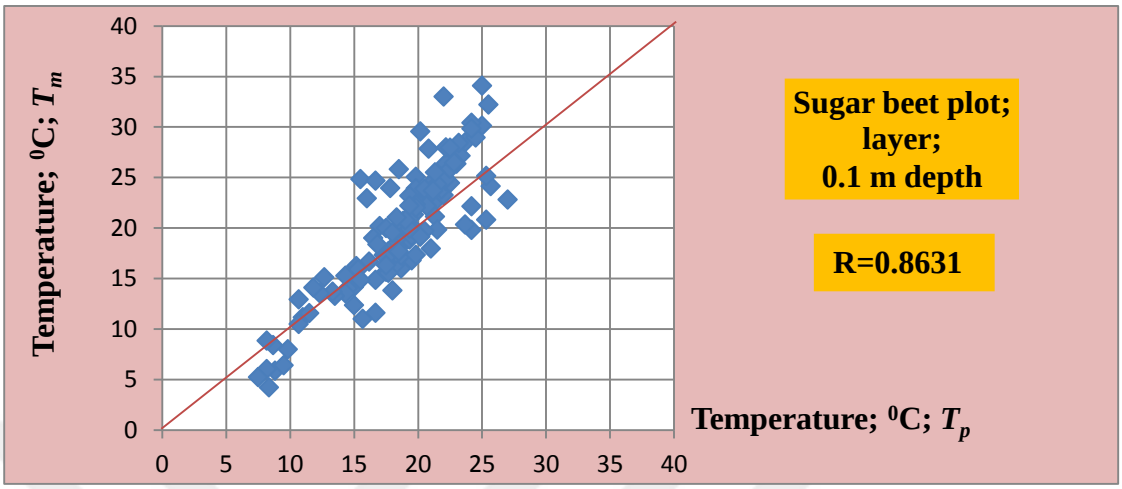

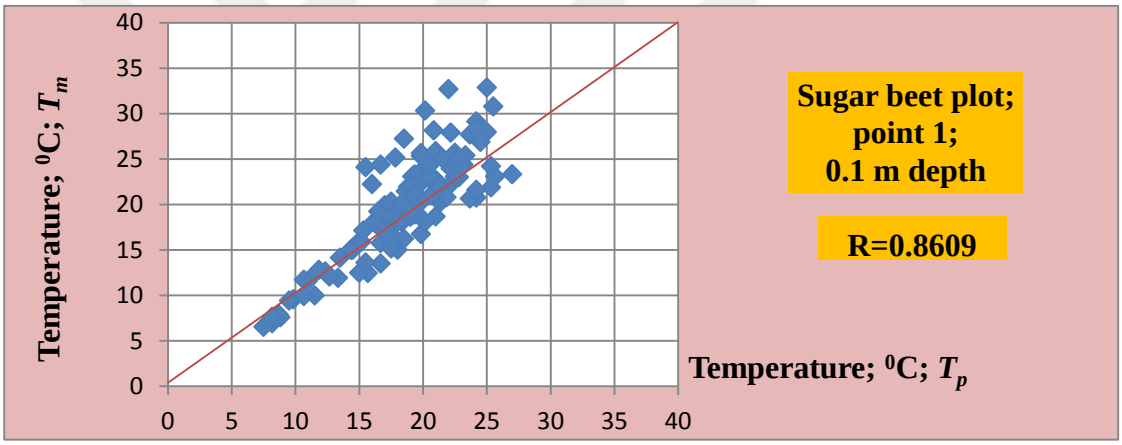

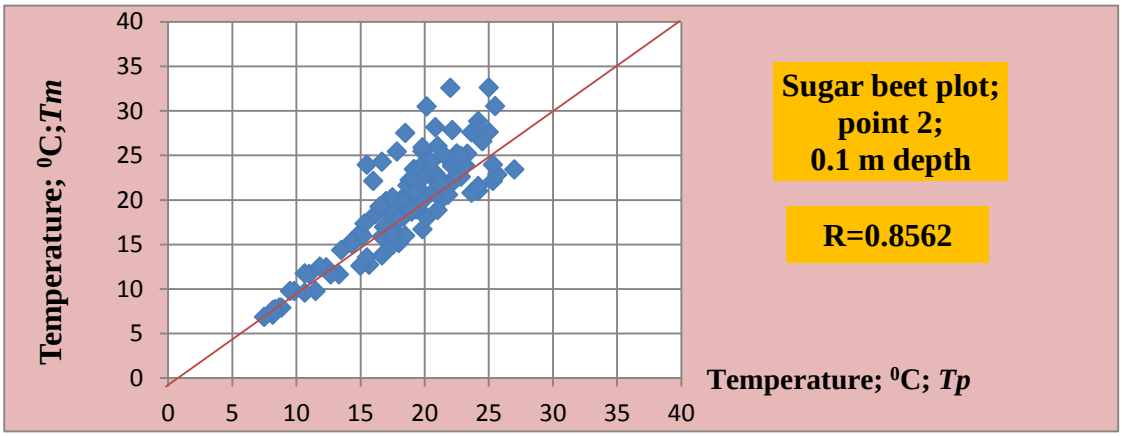

Appendix 19. Comparing values of measured (Tm) and predicted (Tp) by layer, point 1 and point 2 methods for corn plot for 16 week of study period (n= 16x8 = 128) for 0.1 m depth. Each value is a mean of three plots (C1, C2, C3)

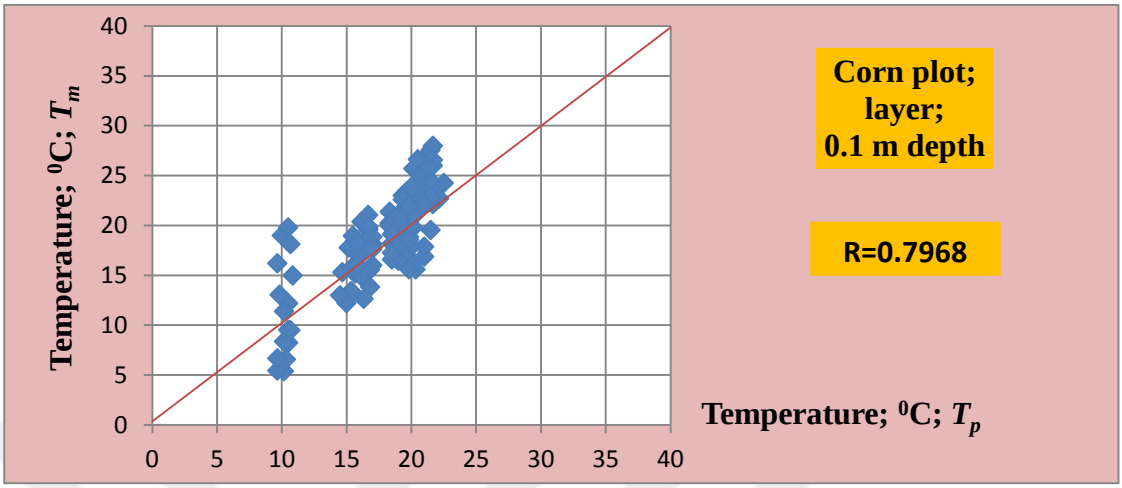

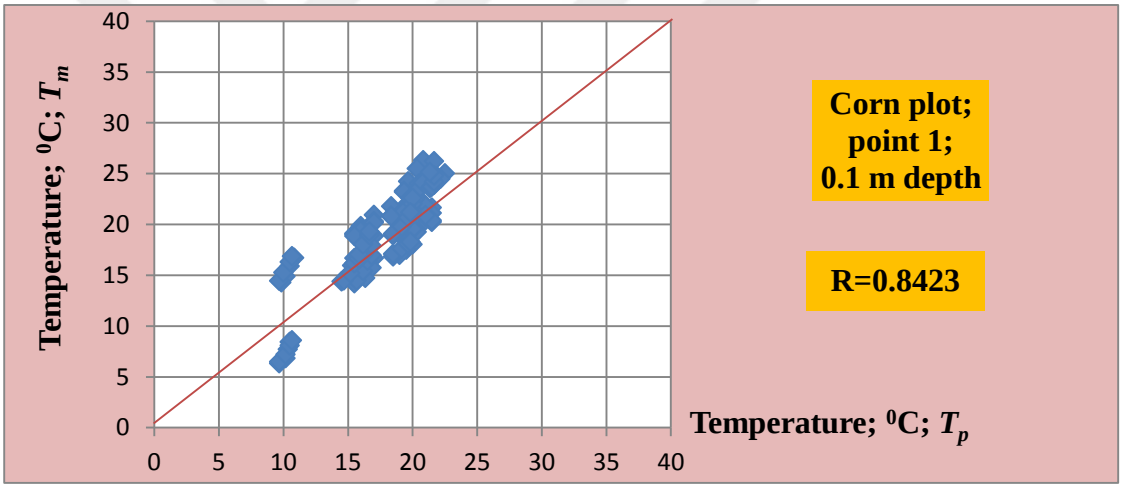

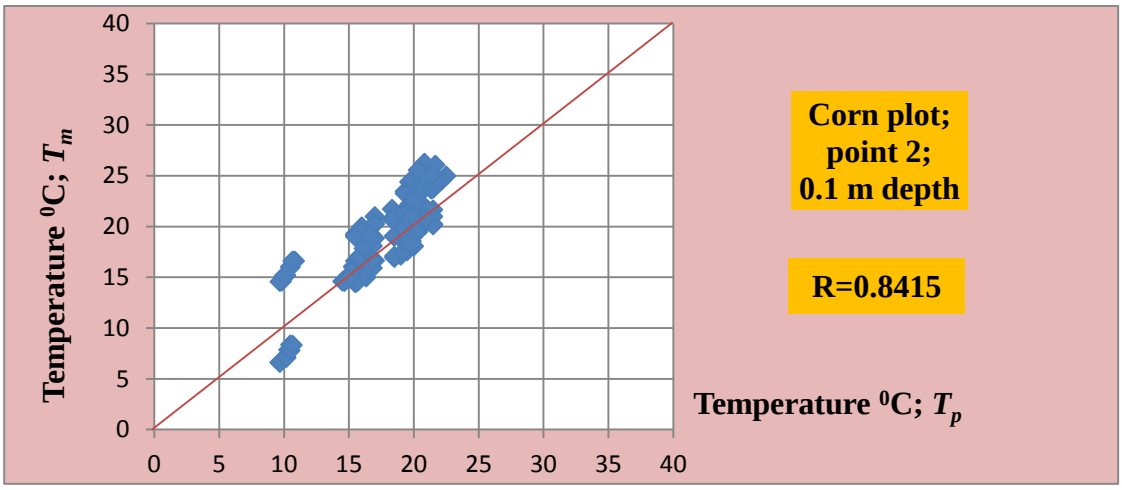

Appendix 20. Comparing values of measured (Tm) and predicted (Tp) by layer, point 1 and point 2 methods for control plot for 16 week of study period (n= 16x8 = 128) for 0.20 m depth.

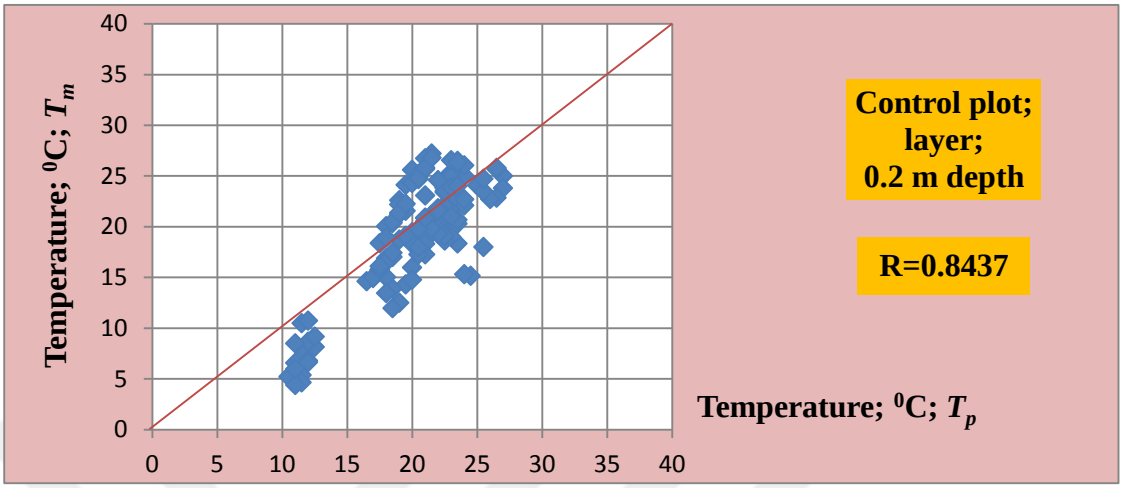

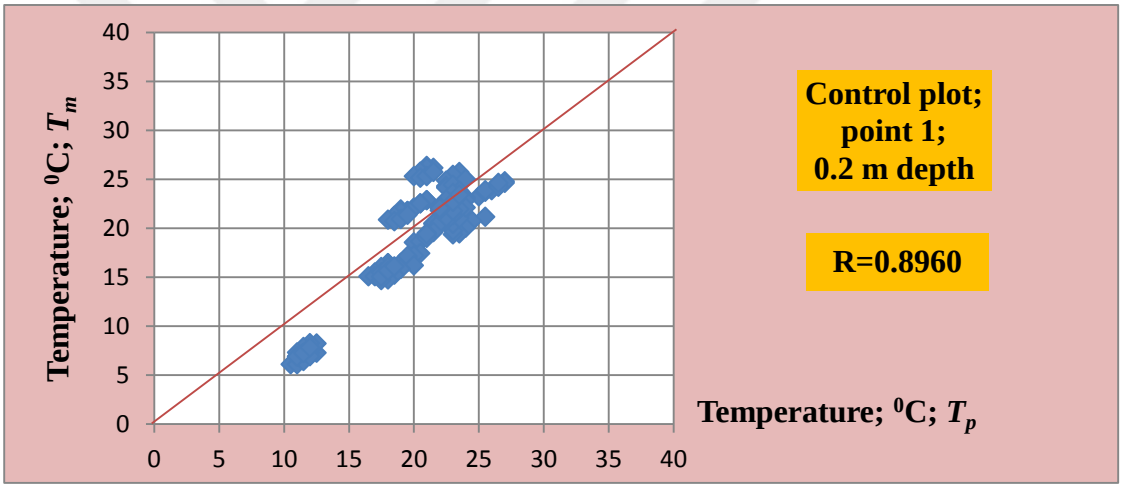

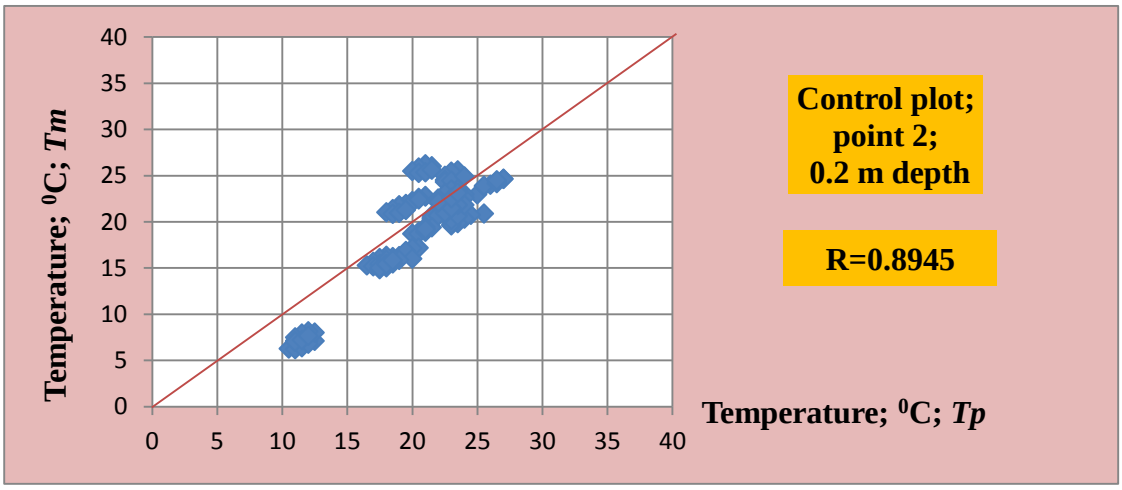

Appendix 21. Comparing values of measured (T_m) and predicted (T_p) by layer, point 1 and point 2 methods for sugar beet plots for 16 week of study period (n= 16x8 = 128) for 0.2 m depth. Each value is a mean of three plots (S1, S2, S3)

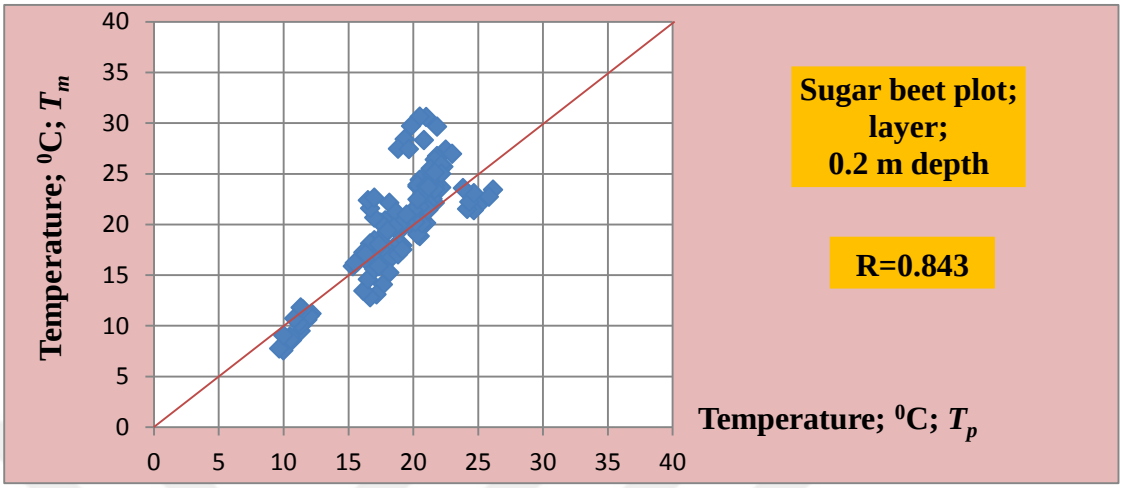

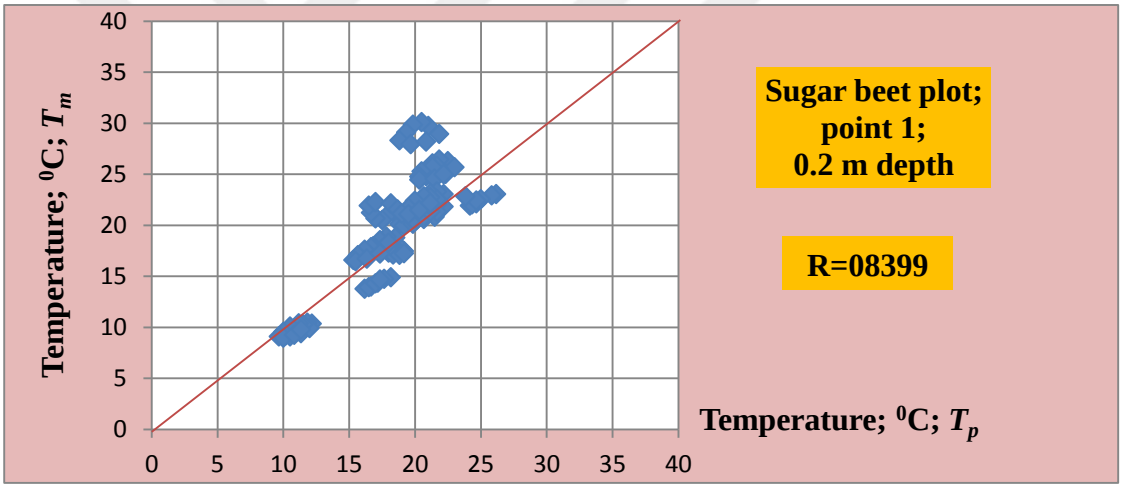

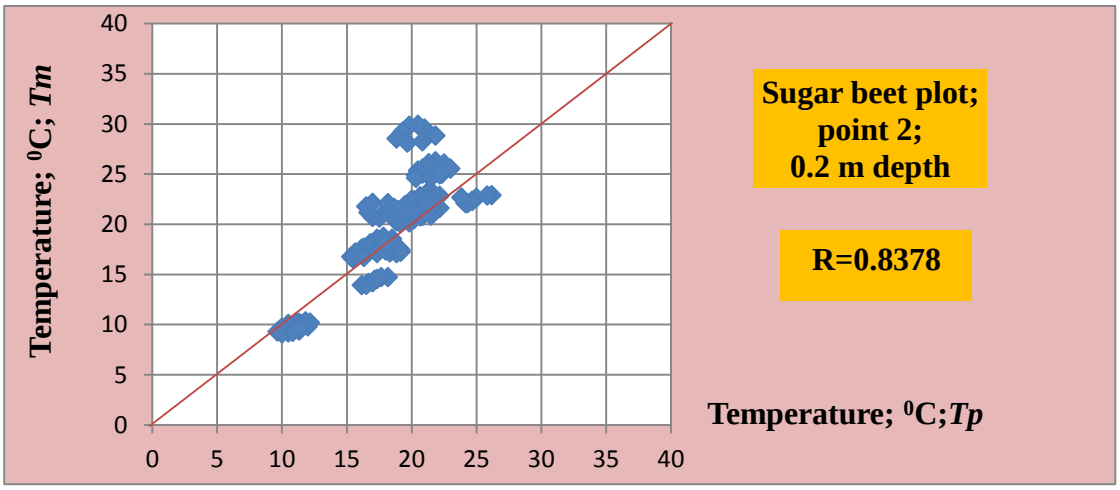

Appendix 22. Comparing values of measured (T_m) and predicted (T_p) by layer, point 1 and point 2 methods for sugar beet plots for 16 week of study period (n= 16x8 = 128) for 0.2 m depth. Each value is a mean of three plots (C1, C2, C3)

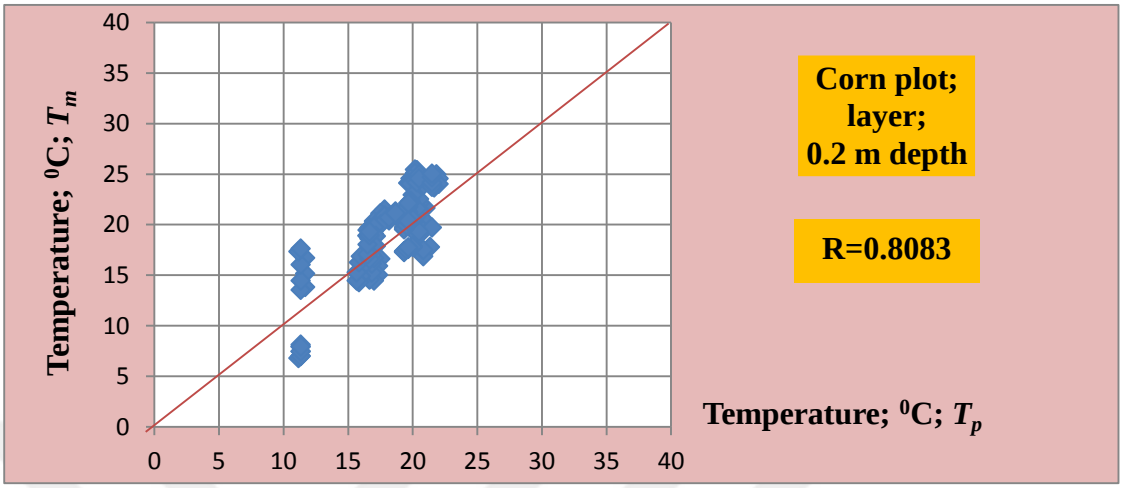

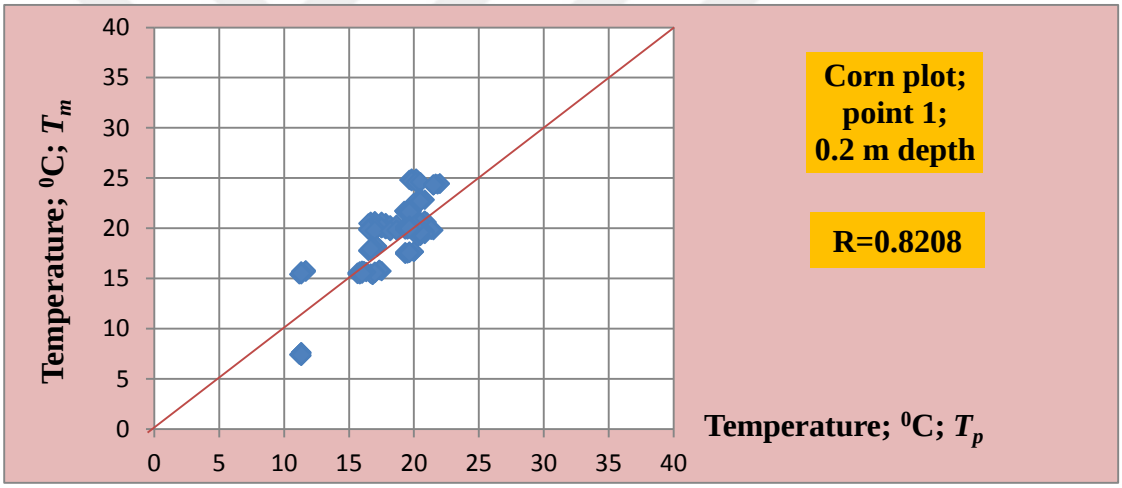

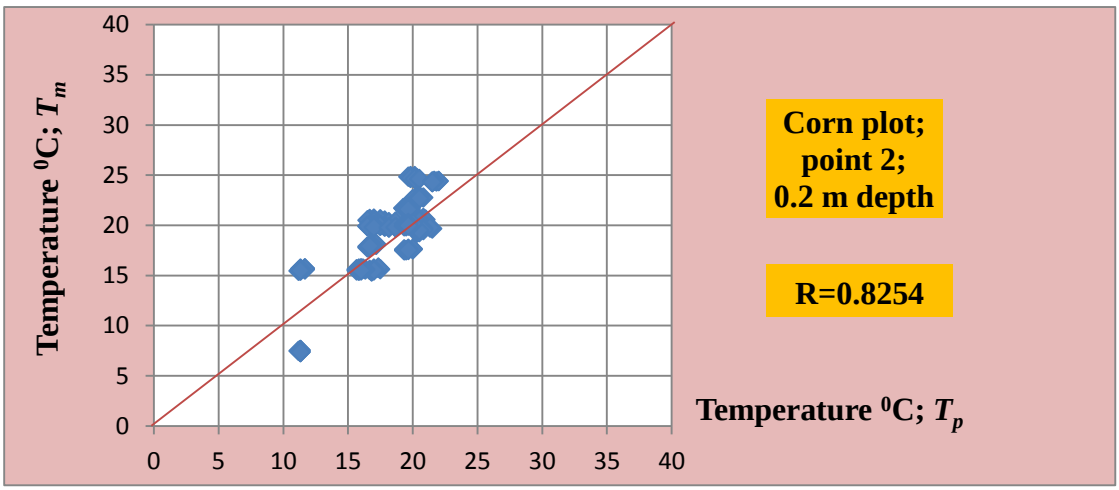

Appendix 23. Comparing values of measured (T_m) and predicted (T_p) by layer, point 1 and point 2 methods for control plot (Co) for 16 week of study period (n= 16x8 = 128) for 0.3 m depth.

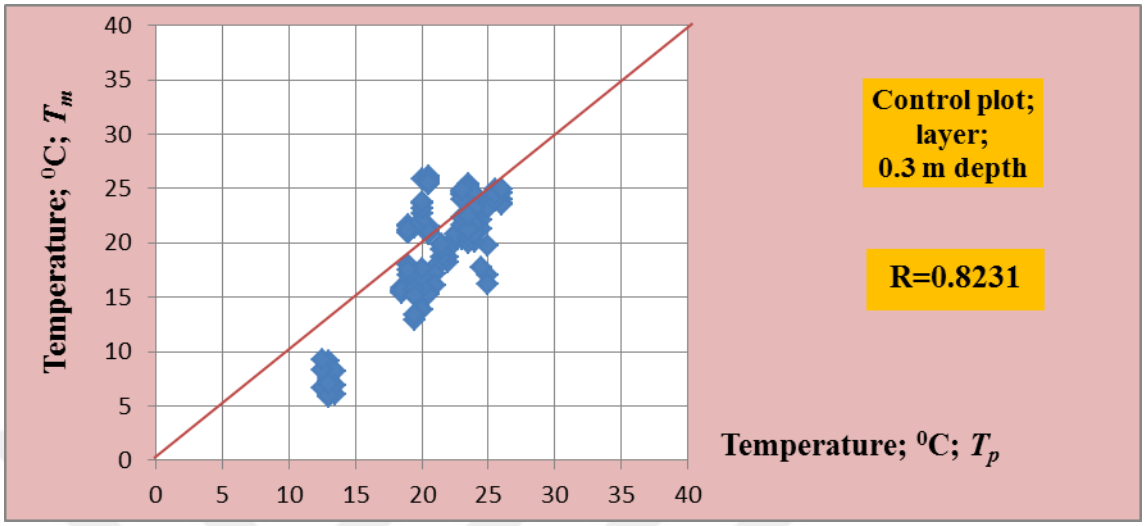

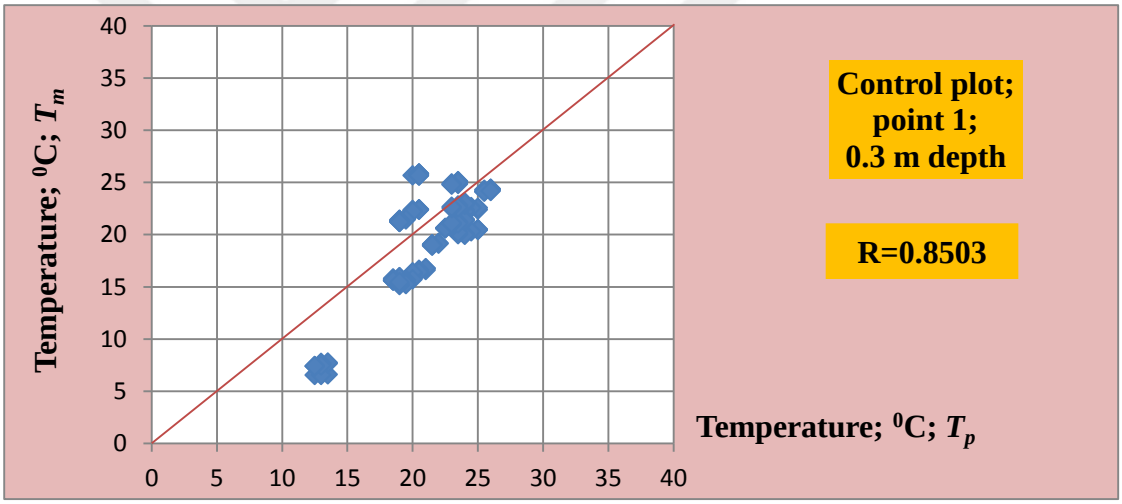

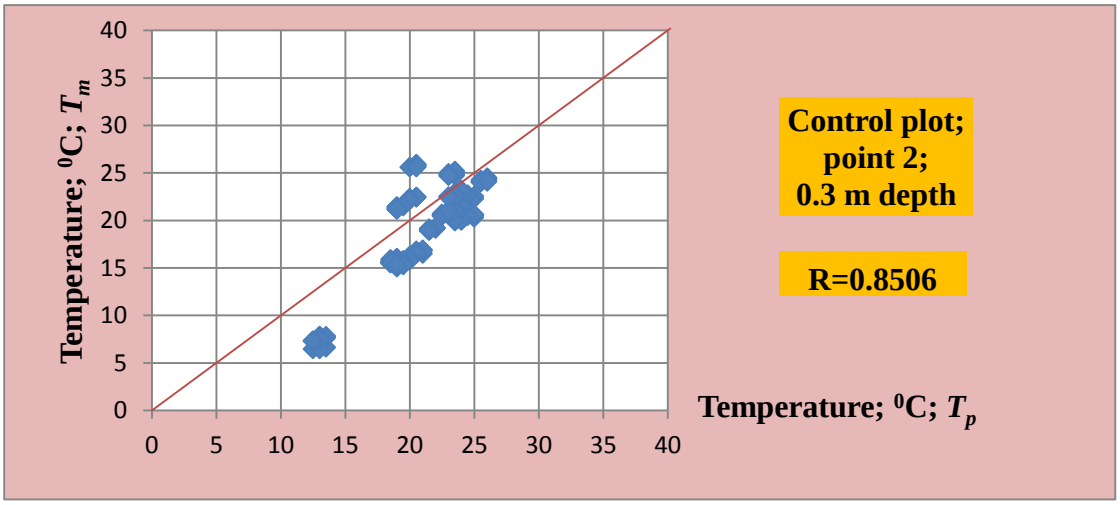

Appendix 24. Comparing values of measured (T_m) and predicted (T_p) by layer, point 1 and point 2 methods for sugar beet plots for 16 week of study period (n= 16x8 = 128) for 0.3 m depth. Each value is a mean of three plots (S1, S2, S3)

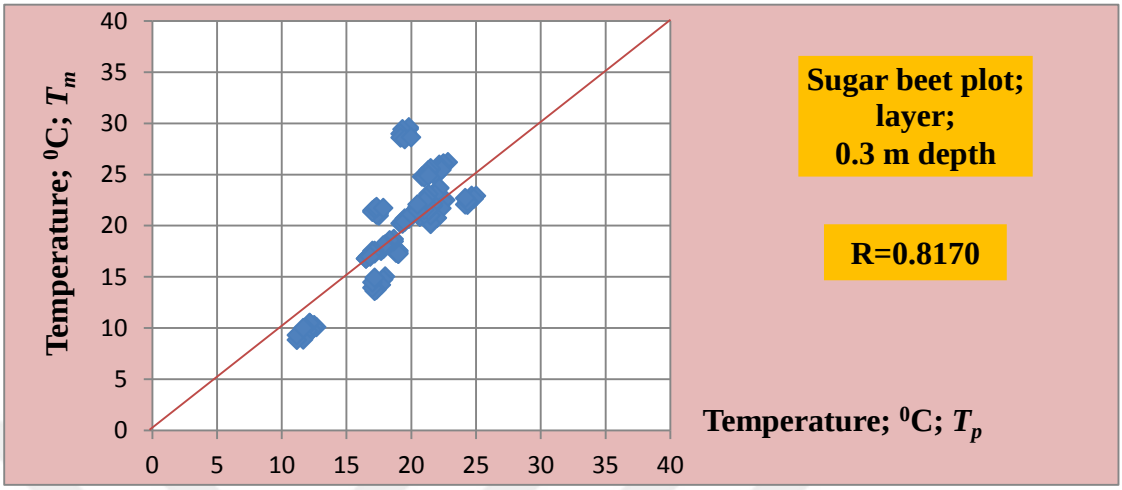

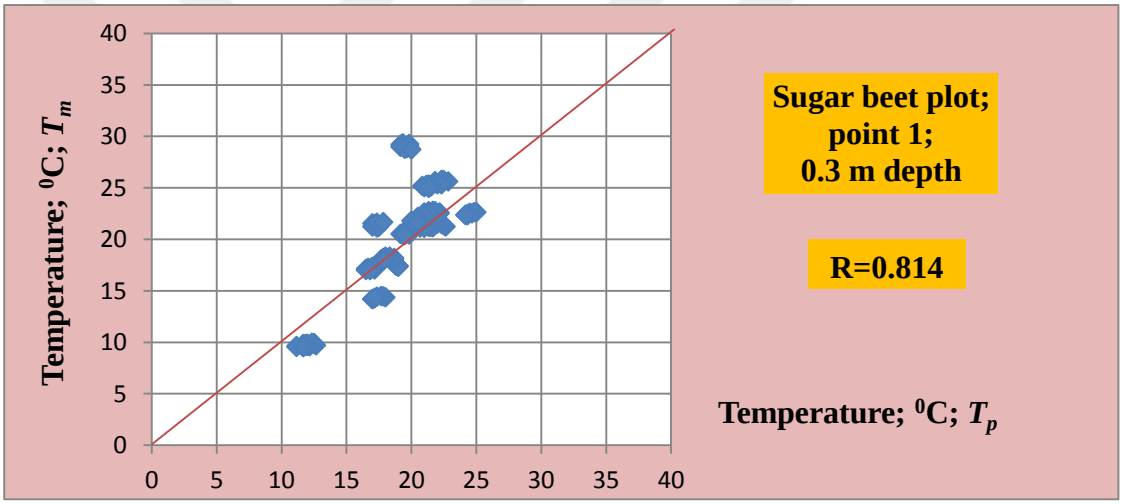

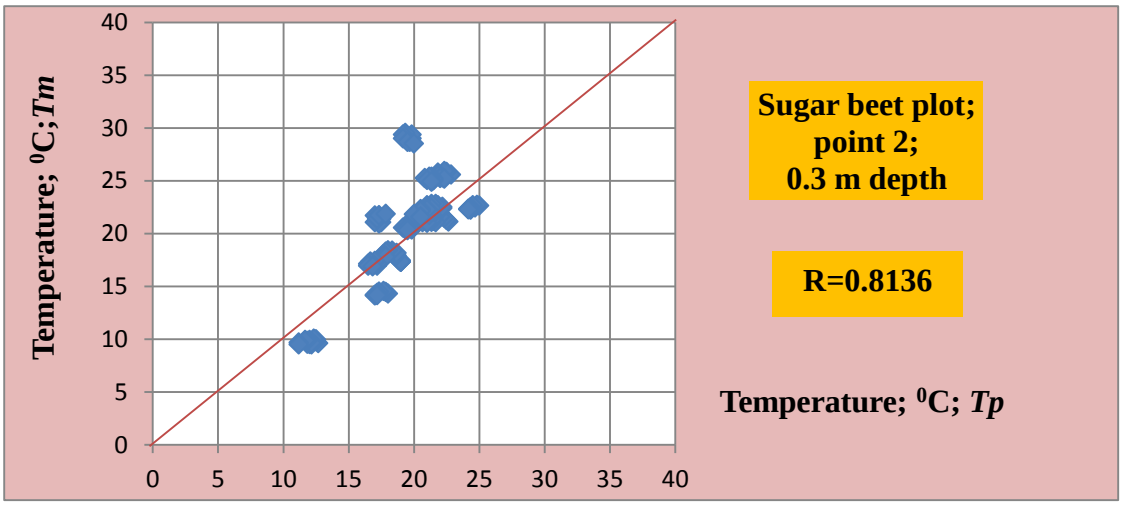

Appendix 25. Comparing values of measured (T_m) and predicted (T_p) by layer, point 1 and point 2 methods for sugar beet plots for 16 week of study period (n= 16x8 = 128) for 0.3 m depth. Each value is a mean of three plots (C1, C2, and C3)

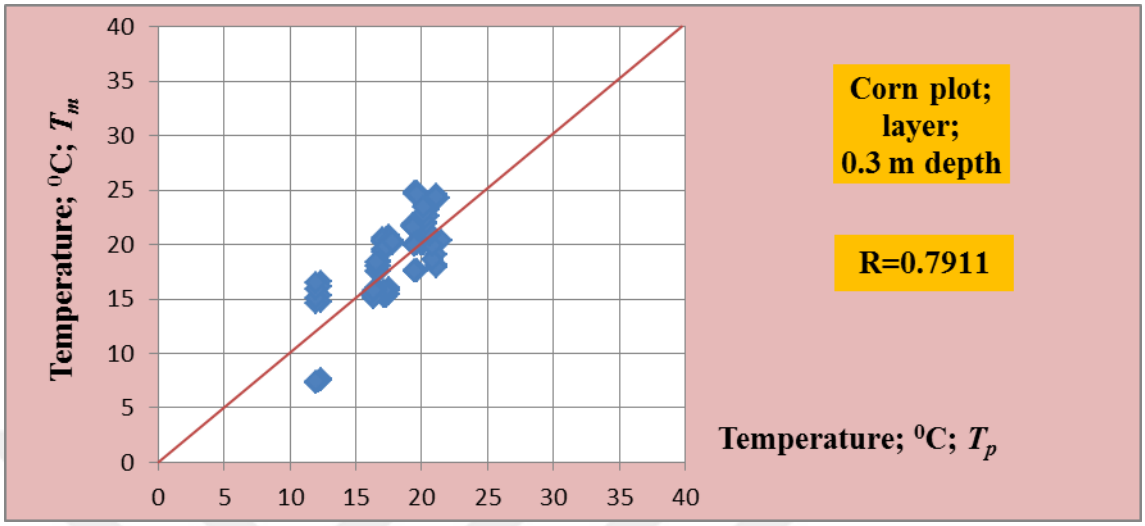

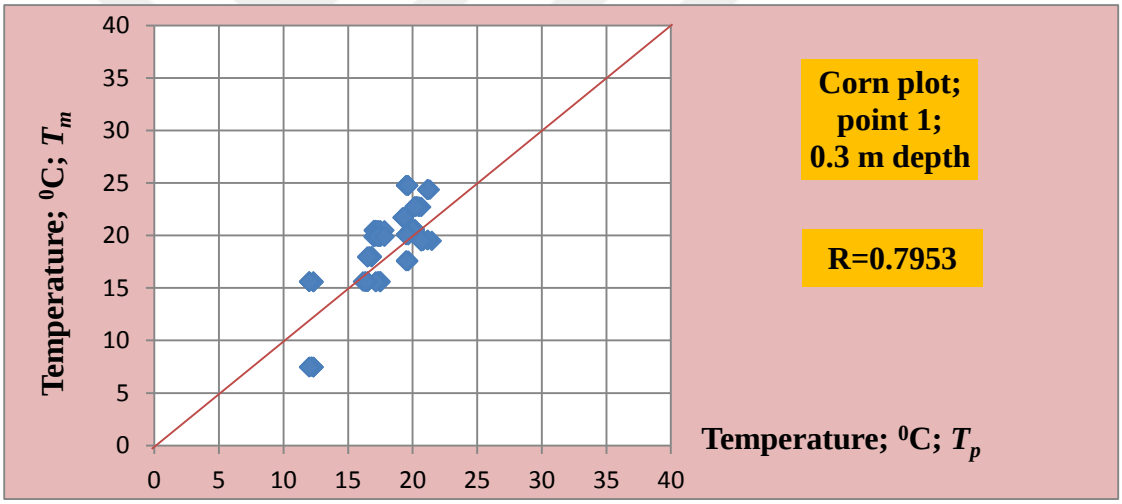

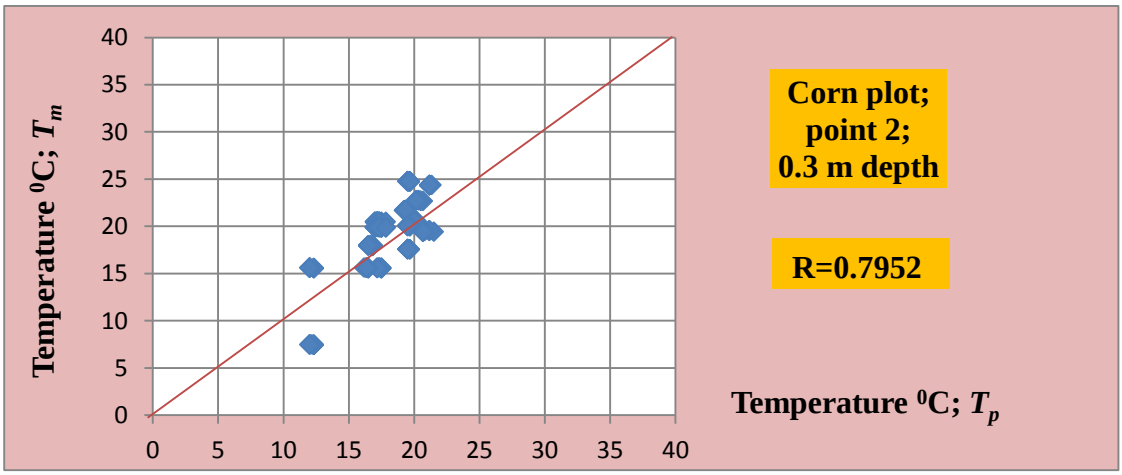

CURRICULUM VITAE

Name-Surname: Ahmet Sami EROL

Place of birth: Cumra / Konya/ TURKEY

Date of birth: 31.12.1969

Marital Status: Married

Foreign Language: English

Address: Çumra Vocational School

Telephone: +905464053300

E-mail: aserol@selcuk.edu.tr

Education

High School: Cumra Imam Hatip High School, 1988

Undergraduate: Selcuk University, Faculty of Agriculture, 1994

Master's Degree: Selcuk University, Faculty of Agriculture, 2008

Work Institution / Institution and Year

Selcuk University Cumra Vocational Schools, 2007

Publications SCI and Other

1- Erol Ahmet Sami, Erşahin Sabit, Shein Evgeny, Mikailsoy Fariz, Ceylan Durmuş Ali, Er Fatih, 2015. Examination Of Central Anatolia Region İn Terms Of Soil Structure, Product Diversity And Productivity Sample Of Konya Province -Cumra District.. Soil Science and Agrochemistry, 3, 49-55. Yayın No: 1792118

2- Mikailsoy Fariz, Erol Ahmet Sami, 2015. Dırect And Inverse Problems Of Heat Transfer In Soıl.. Soil Science and Agrochemistry, 3, 32-39. Yayın No: 1793825

3- Shein EV, Erol Ahmet Sami, Milanovskiy E Yu, Mikailsoy Fariz, Verhovtseva N V,Zinchenko S I, Er F, Erşahin Sabit, 2015. Soil Processes in Haplic Kastanozems of Central Anatolia Turkey, Ćumra Region: Bio- and Agrophysical Aspects. Biogeosystem Technique, 42, 185-188., Doi: 10.13187/bgt.2015.4.185 Yayın No: 1714645

4- Erol AS, Shein E, Milanovsky E, Mikailsoy F, Er F, Erşahin S, 2015. Physical and microbiological properties of alluvial calcareous Cumra province soils Central Anatolia, Turkey. Eurasıan Journal Of Soıl Scıence EJSS, 42, 107, Doi: 10.18393/ejss.13596 Yayın No: 1714044

5- Shein EV, Erol AS, Milanovskii EYu, Verkhovtseva NV, Mikayilov FD, Erşahin S, Er F, 2014. Agrophysical assessment of alluvial calcareous soils of the Cumra region of Central Anatolia in Turkey. Eurasian Soil Science, 477, 694-698., Atıf Sayısı: 1, Doi: 10.1134/S1064229314070114 Yayın No: 1711753

6- Özcan MM, Pedro LG, Al-Juhaimi F, Endes Z, Erol AS, Duman E, Er F, 2013. Constituents of the Essential oil of Origanum vulgare subsp. hirtum Growing Wild in Turkey. Journal of Essential Oil Bearing Plants, 154, 572-576., Doi: 10.1080/0972060X.2012.10644090 Yayın No: 1715152

7- Er F, Öğüt M, Erol AS, 2009. Path Analysis And Relatıonships Between Some Climatic Parameters And Sugar Content Of Sugar Beet. Bulgarian Journal of Agricultural Science, 153, 222-227., Atıf Sayısı: 1 Yayın No: 1714955

8- Fırat B, Mikayilsoy F, Er F, Erol, AS. 2013. Potato yield initiated with fertilizer containing NPK, its effect on existence of NPK in soil and potato lump. İnternational Agricultural Conference On "The Development And Implementation Of Modern Technologies And Farming Systems For Ensuring The Environmental Safety" . 3-6 Haziran 2013. pp. 254 Perm- Russia

9- Er F, Erol AS. 2014. Rhızospherıc Phosphate Solubılızıng Pantoea Agglomerans Lp1 Can Persısts In Non-Sterıle Materıals In Long Term. Popularisation Of Scientific Achievements İn Soil Science Of XXI Century. / 26-29 Mayıs 2014 pp.72-74. - St. Petersburg, Russsia

10- Er F, Ceylan D.A., Mıkaılsoy F, Erol A.S. 2011. Determınatıon Of Nıtrogen, Phosphorous, Potassıum, Calcıum, And Magnesıum Levels Of The Apple Gardens In Karaman Regıon. Soil Fertility And Efficient Use Of Fertilizers Materials Of The İnternational Research And Practice Conferans Devoted To The 80 Th Anniversary Of The İnstitute 5-8 july, 172-175 pp. 2011, Minks, Belaruse

11- Tuşat E, Durduran S, Er F, Özcan MM, Erol AS. 2011. Geographıc Informatıon Technologıes In Precısıon Agrıculture Applıcatıons, Soil Fertility And Efficient Use Of Fertilizers Materials Of The İnternational Research And Practice Conferans Devoted To The 80 Th Anniversary Of The İnstitute 5-8 july, 178-181 pp. 2011, Minks, Belaruse

12- Özcan MM., Pedro LG, Erol AS, Er F. 2011. Constituents of the essential oil of Origanum vulgare subsp hirtum growing wild in Turkey Türkiye'de yetişen yabani Origanum vulgare subsp. Hirtum İstanbul kekiği 'nin esansiyel yağlarının bileşimi Soil Fertility And Efficient Use Of Fertilizers Materials Of The İnternational Research And

Practice Conference Devoted To The 80 Th Anniversary Of The İnstitute 5-8 july, 175-177 pp. 2011, Minks, Belaruse

13- Tuşat E, Erol AS, Er F, Mikayilov F, Yılmaz G. 2011. GIS Application In Soil Data Analysis In Precision Agriculture Applications In Apple Gardens Grown In Karaman-Cumra Region Russian Symposium With İnternational Participation "Ecology Of Megapolises: Fundamentals And Innovation" pp. 19. 21-25 November 2011 Moskow, Russia

14- Erol AS., Er F, Mikayilov F, Brohi AR. 2012. Defınıtıon Of Soıl Organıc Matter "Toprak Organik Maddelerin Tanımları". Internatıonal Scıentıfic-Practıcal Conference on "Ratıonal Use Of Soıl Resources And Soıl Ecology", Proceedings, pp. 92-94, 15-16 November 2012 in Almaty, Republic of Kazakhstan.

15- Erol AS., Direk M. 2009. Tarım İşletmelerinin Avrupa Birliği Tarımsal Muhasebe Veri Ağı Fadn Sistemine Göre Sınıflandırılması Classıfıcatıon Of Farms On European Unıon Farm Of Agrıcultural Data Network System 1.Uluslararası 5.Ulusal Meslek Yüksekokulları Sempozyumu pp. 27-29 Mayıs 2009,

16- Er F, Erol AS. Cumra Bölgesi Topraklarının Genel Özellikleri. Cumra Sempozyumu Cilt 1 pp. 114-117

17- Erol AS, Direk M. 2012. Konya İli Cumra İlçesinde Mısır Üretimi Yapan Tarım İşletmelerinin Avrupa Birliği Tarımsal Muhasebe Veri Ağı FADN Sistemine Göre Sınıflandırılması Ve İşletme Başarı Ölçütlerinin Karşılaştırılması. 10. Ulusal Tarım Ekonomisi Kongresi cilt 2 pp. 703-712 5-7 Eylül 2012 Konya